

Hemocyanin-derived Phenoloxidase; Biochemical and Cellular Investigations of Innate Immunity

By

Christopher James Coates

A thesis submitted to the School of Natural Sciences, University of Stirling,

October 2012

In fulfilment, for the degree of

Doctor of Philosophy



**UNIVERSITY OF
STIRLING**

This research was conducted from October 2009 to October 2012, in Biological and Environmental Sciences, University of Stirling, Stirling FK9 4LA, Scotland, UK.

DECLARATION OF ORIGINALITY

I have read and understood the University's policy on plagiarism.

I declare that this thesis embodies the original work of the undersigned and has not been submitted for another purpose at any other institution of tertiary education.

Information derived from the published or unpublished work of others has been acknowledged and referenced accordingly.

Christopher J Coates, BSc, AMSB

October 2012

Principle Supervisor; *Dr. Jacqueline Nairn*

Second Supervisor: *Dr. Tim Whalley*

ABSTRACT

Hemocyanins (Hcs) and phenoloxidases (POs) are both members of the type-3 copper protein family, possessing di-cupric active sites which facilitate the binding of dioxygen. While Hcs and POs share a high degree of sequence homology, Hcs have been associated traditionally with oxygen transport whereas POs are catalytic proteins with a role in innate immunity. Evidence gathered in recent years details numerous immune functions for Hc, including an inducible PO activity. Unlike the pro-phenoloxidase activation cascade in arthropods, the endogenous mechanism(s) involved in the conversion of Hc into an immune enzyme is lacking in detail.

The overall aim of this research was to characterise the physiological circumstances in which Hc is converted into a PO-like enzyme during immune challenge. A series of biochemical, biophysical and cellular techniques were used to assess the ability of phospholipid liposomes to mimic the well-characterised induction of PO activity in Hc by SDS micelles. Incubation of Hc purified from *Limulus polyphemus*, in the presence of phosphatidylserine (PS) liposomes, yielded ~ 90% of the PO activity observed upon incubation of Hc with the non-physiological activator, SDS. Phospholipid-induced PO activity in Hc was accompanied by secondary and tertiary structural changes similar to those observed in the presence of SDS. Subsequent analysis revealed that electrostatic interactions appear to be important in the PS-Hc activation complex.

In vivo, PS-Hc interactions are assumed to be limited in quiescent cells. However, amebocytes undergoing apoptosis redistribute PS onto the outer leaflet of the plasma membrane, resulting in the potential for increased Hc-PS interactions. In the absence of a reliable culturing technique for *L. polyphemus* amebocytes, *in vitro* conditions were optimised for the short term maintenance of this labile cell type. Amebocytes retained viability and functionality in a medium that mimicked most-closely, the biochemical properties of *L. polyphemus* hemolymph. When presented with a fungal, bacterial or synthetic challenge, ~9% of amebocytes *in vitro* were found to be phagocytically active. Target internalisation was confirmed via the use of fluorescent quenchers and membrane probes. Within 4 hours of target internalisation, amebocytes underwent apoptosis, characterised by the loss of plasma and mitochondrial membrane potential, increased caspase-3 activity and extracellularisation of PS. Phagocytosis-induced cell death led to a proportional increase in the level of Hc-derived PO activity, suggesting that Hc may be interacting with PS present on terminal amebocyte membranes.

The PO activity of Hc was investigated further in order to address an economically important issue; hyperpigmentation in commercial shellfish. While PO enzymes are thought to be the cause of hyperpigmentation in *Nephrops norvegicus*, evidence presented here suggests that cellular PO is inactivated after freeze-thawing, while extracellular Hc retains stability and displays a heightened level of inducible PO activity under similar treatments. Known PO inhibitors were used successfully to reduce Hc-derived PO activity, with inhibitors assumed to bind Hc in a manner similar to PO-inhibitor complexes.

Structural and functional studies of hemocyanins and immune cells presented here provide new insights into the interactions of hemocyanin-activator complexes in invertebrates.

ACKNOWLEDGEMENTS

This thesis is dedicated to my Parents, and Grand-parents, for all their love, support and belief.

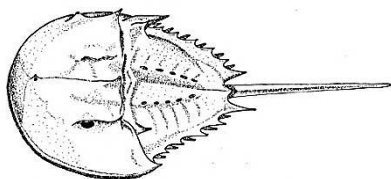
To Susan, for giving me inspiration to achieve.

I would like to take this opportunity to express my gratitude to my principle supervisor, Dr. Jacqueline Nairn, for endless guidance on this steep learning curve and without whom, this body of research would not have been possible, nor fruitful. Thanks are also in order for my secondary supervisor, Dr. Tim Whalley, for all things cellular (and comic relief).

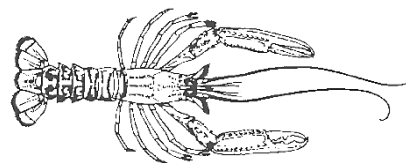
Special thanks to Dr. Sharon Kelly for guidance and training with CD experiments and friendly discussions. Thank you to Alex Mühlhölzl, CTO, Marine Biotech Limited and John Davis, Director, Xyrex for provision of beasts: *Limulus polyphemus* and *Nephrops norvegicus*, respectively.

FUNDING

This research was funded by the University of Stirling and in part, by the Scottish Funding Council Innovation Voucher Scheme, 2011-2012. Travel bursaries for conference attendance were obtained from the Biochemical Society, the International Society of Developmental and Comparative Immunology and Biological and Environmental Sciences, University of Stirling.



Limulus polyphemus



Nephrops norvegicus

ABBREVIATIONS:

<i>AMCA-X, SE</i>	6-((7-amino-4-methylcoumarin-3-acetyl)amino)hexanoic acid, succinimidyl ester (Coumarin)
<i>AMP</i>	Anti-microbial peptide
<i>BSA</i>	Bovine serum albumin
<i>Caspase</i>	Cysteine-dependent aspartate-directed proteases
<i>CD</i>	Circular dichroism
<i>CPC</i>	Cetylpyridinium chloride
<i>Cu</i>	Copper
<i>DAPI</i>	4', 6-diamidino-2-phenylindole
<i>DLS</i>	Dynamic light scattering
<i>DTT</i>	Dithiothreitol
<i>EDTA</i>	Ethylenediaminetetraacetic acid
<i>EST</i>	Expressed sequence tag
<i>FITC</i>	Fluorescein isothiocyanate
<i>Hc</i>	Hemocyanin
<i>Hc-d PO</i>	Hemocyanin-derived phenoloxidase
<i>4-HR</i>	4-hexylresorcinol
<i>HSC</i>	Horseshoe crab
<i>L-Dopa</i>	L-dihydroxyphenylalanine
<i>L-ER</i>	L-ergothioneine
<i>LPS</i>	Lipopolysaccharide
<i>L-PC</i>	Lyso-phosphatidylcholine
<i>LTA</i>	Lipoteichoic acid
<i>PAMP</i>	Pathogen associated molecular pattern
<i>PBS</i>	Phosphate buffered saline
<i>PDB</i>	Protein data bank
<i>PE</i>	Phosphatidylethanolamine
<i>PGRP-LC</i>	Peptidoglycan recognition protein-LC
<i>PI</i>	Phosphatidylinositol
<i>PICD</i>	Phagocytosis-induced cell death
<i>PO</i>	Phenoloxidase
<i>ppA</i>	Pro-phenoloxidase activating enzyme
<i>PRR</i>	Pathogen recognition receptor
<i>PS</i>	Phosphatidylserine
<i>PTU</i>	1-phenyl, 2-thiourea
<i>R18</i>	Octadecyl-Rhodamine B chloride
<i>RBCs</i>	Red blood cells
<i>Rho-Dex</i>	Tetramethylrhodamine-dextran
<i>SDS</i>	Sodium-dodecyl sulphate
<i>SUV</i>	Small unilamellar vesicle
<i>TLR</i>	Toll-like receptor
<i>TUNEL</i>	Terminal deoxynucleotidyl transferase dUTP nick-end labeling

TABLE OF CONTENTS

Declaration of Authorship.....	I
Abstract.....	II
Acknowledgements.....	III
List of abbreviations.....	IV
Table of contents.....	V
List of figures.....	XIII
List of tables.....	XVII

CHAPTER 1 - Introduction	1
1.1 Background and thesis overview	1
1.2 Innate immune responses of arthropods	5
<i>1.2.1 Physical barrier</i>	5
<i>1.2.2 Sensing, recognition and immune signalling pathways</i>	5
<i>1.2.3 Coagulation of arthropod hemolymph</i>	8
<i>1.2.4 Complement-like proteins in invertebrates</i>	9
<i>1.2.5 Arthropod immune cells</i>	12
<i>1.2.5.1 Phagocytosis</i>	13
<i>1.2.5.2 Encapsulation and nodulation</i>	14
<i>1.2.6 Humoral defences; antimicrobial peptides</i>	17
<i>1.2.7 Cell death and immunity</i>	18
1.3 Immune-functions of an ancient respiratory protein, hemocyanin	20
<i>1.3.1 Members of the type-3 copper protein family</i>	20
<i>1.3.2 On the presence of hemocyanin in invertebrates</i>	23

1.3.3 Structural characteristics and putative function	24
1.3.4 Phenoloxidase and hemocyanin-derived phenoloxidase activity	29
1.3.5 Exogenous versus endogenous activation	33
1.3.6 Mode of activation and the di-copper active site	35
1.3.7 Hemocyanin as a precursor of antimicrobial peptides	35
1.3.8 Antiviral properties of hemocyanin	38
1.3.9 Hemocyanin and the production of reactive oxygen species	42
1.3.10 Immunoglobulin-like domains and agglutination behaviour of hemocyanin	43
1.3.11 Hemolytic behaviour of shrimp hemocyanin	44
1.3.12 Hyperpigmentation in crustaceans; hemocyanin versus phenoloxidase	45
1.4 Summary	46

CHAPTER 2 – Phospholipid induced conformational changes in *Limulus polyphemus* hemocyanin; putative natural activators of hemocyanin-derived phenoloxidase activity _____ 47

2.1 **Abstract** _____ 48

2.2 **Introduction** _____ 49

2.3 **Materials and methods** _____ 50

2.3.1 Purification of *Limulus polyphemus* hemocyanin _____ 50

2.3.2 Preparation of phospholipids _____ 50

2.3.3 Dynamic light scattering _____ 51

2.3.4 Phenoloxidase assay measurements _____ 51

2.3.5 Circular dichroism _____ 52

2.3.6 Fluorescence spectroscopy _____ 53

2.3.7 Absorption spectroscopy _____ 54

2.3.8 Conductivity measurements _____ 54

2.3.9 Statistical analysis	54
2.4 Results	55
2.4.1 Purification of <i>Limulus polyphemus</i> hemocyanin	55
2.4.2 Nature of phospholipids	55
2.4.3 Phospholipid induced phenoloxidase activity	58
2.4.4 Effects of phospholipids on secondary structure	61
2.4.5 Effects of phosphatidylserine on tertiary structure	65
2.4.6 Presence of copper	69
2.4.7 Preliminary investigations on the nature of the phosphatidylserine-hemocyanin interaction	72
2.5 Discussion	77
2.6 Conclusion	86
2.7 Acknowledgements	86

CHAPTER 3 - di-Phenoloxidase activity of *Nephrops norvegicus* hemocyanin; applications for the inhibition of hyperpigmentation in shellfish **87**

3.1 Abstract	88
3.2 Introduction	89
3.3 Materials and methods	92
3.3.1 Chemicals	92
3.3.2 Maintenance of <i>Nephrops norvegicus</i>	92
3.3.3 Cellular parameters	92
3.3.4 Phenoloxidase activity of cell lysates and acellular hemolymph	94
3.3.5 Purification of <i>Nephrops norvegicus</i> hemocyanin	94
3.3.6 Dynamic light scattering	95
3.3.7 Hemocyanin-derived phenoloxidase activity	95

3.3.8 Enzyme kinetics; A) Substrate properties and B) inhibition studies	96
3.3.9 Absorption spectroscopy; A) hemocyanin stability and B) inhibitor interactions	96
3.3.10 Fluorescence spectroscopy; A) hemocyanin stability and B) inhibitor interactions	97
3.3.11 Data handling	98
3.4 Results	99
3.4.1 Effect of freeze-thawing on phenoloxidase activity from cellular and hemolymph fractions	99
3.4.2 Purification of hemocyanin from <i>Nephrops norvegicus</i>	101
3.4.3 Stability of <i>Nephrops norvegicus</i> hemocyanin	101
3.4.4 Inducible phenoloxidase activity of <i>Nephrops norvegicus</i> hemocyanin	106
3.4.5 The inhibition of hemocyanin-derived phenoloxidase activity; Inhibitor efficiency and inhibitor-hemocyanin interactions	111
3.5 Discussion	117
3.5.1 The stability of phenoloxidase and hemocyanin-derived phenoloxidase from <i>Nephrops norvegicus</i> hemolymph	117
3.5.2 Phenoloxidase activity of <i>Nephrops norvegicus</i> hemocyanin	118
3.5.3 Hyperpigmentation; inhibiting hemocyanin-derived phenoloxidase activity	121
3.6 Conclusion	123
3.7 Acknowledgements	123
CHAPTER 4 – Development of an <i>in vitro</i> phagocytosis assay for <i>Limulus polyphemus</i> amebocytes	124
4.1 Abstract	125
4.2 Introduction	126
4.3 Materials and methods	128
4.3.1 Chemicals and reagents	128

4.3.2 Maintenance of <i>Limulus polyphemus</i>	128
4.3.3 Microbial cultures	128
4.3.4 Preparation of fluorescent targets	129
4.3.5 Hemolymph extraction and total amebocyte counts	130
4.3.6 Evaluation of amebocyte viability and functionality <i>in vitro</i>	130
4.3.7 Preparation of crude <i>Limulus</i> amebocyte lysate (LAL)	131
4.3.8 <i>In vitro</i> phagocytosis assay	133
4.3.8.1 Confirmation of target internalisation	133
4.3.8.2 Phagocytic properties	134
4.3.9 Data analysis	135
4.4 Results	136
4.4.1 Amebocyte viability and vitality, <i>in vitro</i>	136
4.4.2 <i>In vitro</i> phagocytosis	142
4.5 Discussion	152
4.5.1 Maintenance of arthropod immune cells <i>in vitro</i>	152
4.5.2 Phagocytic properties of amebocytes	153
4.6 Conclusion	157
4.7 Acknowledgements	157
CHAPTER 5 - Phagocytosis-induced cell death of amebocytes: A potential mechanism for the activation of hemocyanin-derived phenoloxidase, <i>in vivo</i>	158
5.1 Abstract	159
5.2 Introduction	160
5.3 Materials and methods	162
5.3.1 Chemicals, reagents and detection kits	162

5.3.2 Maintenance of <i>Limulus polyphemus</i>	162
5.3.3 Hemolymph extraction and amebocyte properties	162
5.3.4 Microbial cultures and preparation of fluorescent targets	163
5.3.5 Phagocytosis assays	163
5.3.6 Staining amebocyte mitochondria, in vitro	164
5.3.7 Annexin V-FITC and propidium iodide staining of apoptotic amebocytes	164
5.3.8 TUNEL staining of amebocytes	165
5.3.9 Caspase-3 activity assay	166
5.3.10 Measurements of hemocyanin-derived phenoloxidase activity in vitro	166
5.3.11 Data handling	168
5.4 Results	169
5.4.1 Functional properties of amebocytes in the absence and presence of coumarin-labelled spores	169
5.4.2 Apoptotic modalities of amebocytes, in vitro	172
5.4.3 Hemocyanin activation in the presence of phagocytically active amebocytes	180
5.5 Discussion	183
5.5.1 Phagocytosis-induced cell death in invertebrates	183
5.5.2 Activation of hemocyanin into a phenoloxidase in vivo	185
5.6 Conclusion	187
CHAPTER 6 – Monitoring the effect of temperature on the health status of <i>Limulus polyphemus</i>; biochemical and cellular properties of hemolymph	188
6.1 Abstract	189
6.2 Introduction	190
6.3 Materials and methods	193
6.3.1 <i>Limulus polyphemus</i> and culture conditions	193

6.3.2 Bleeding regime_____	194
6.3.3 Estimation of hemocyanin concentration and the percentage of hemocyanin with dioxygen bound_____	196
6.3.4 Purification of <i>Limulus polyphemus</i> hemocyanin_____	196
6.3.5 Phenoloxidase assay measurements_____	196
6.3.6 Circular Dichroism_____	197
6.3.7 Fluorescence spectroscopy_____	198
6.3.8 Absorption spectroscopy_____	198
6.3.9 Determination of <i>Limulus polyphemus</i> amebocyte numbers and morphology_	198
6.3.10 Statistical analysis_____	199
6.4 Results_____	200
6.4.1 Physical evaluation; mortality and weight_____	200
6.4.2 Quantitative analysis of hemocyanin across the temperature range 8°C to 23°C_____	202
6.4.3 Hemocyanin with dioxygen bound and inducible phenoloxidase activity_____	205
6.4.4 Alterations in amebocyte numbers and morphology across the temperature range 8°C – 23°C_____	208
6.4.5 Influence of increasing temperature on inducible phenoloxidase activity of purified hemocyanin_____	212
6.4.6 Effect of temperature on the secondary structure of purified hemocyanin_____	212
6.4.7 Effect of temperature on hemocyanin tertiary structure_____	216
6.4.8 Effect of temperature on the dicopper active site_____	219
6.5 Discussion_____	222
6.5.1 Health status_____	222
6.5.2 Effect of increasing temperature on hemocyanin concentration and functionality_____	223
6.5.3 Effect of temperature on amebocyte numbers and morphology_____	226
6.6 Conclusion_____	229
6.7 Acknowledgements_____	229

CHAPTER 7 – Overall summary and general discussion	230
7.1 A pro-Hemocyanin activation cascade?	230
7.2 Applications of research	235
7.2.1 <i>Pigmentation and commercially important invertebrates</i>	235
7.2.2 <i>Biomedical applications</i>	237
BIBLIOGRAPHY	239
APPENDICES	263
A- Mass spectrometry	263
B-Dynamic light scattering	267
C-Water quality properties	269

Contributions to other research undertaken during this thesis;

Jamie Wright, William McCaskill Clark, Jennifer Anne Cain, Alan Patterson, **Christopher J. Coates** and Jacqueline Nairn. **2012**. Effects of known phenoloxidase inhibitors on hemocyanin-derived phenoloxidase from *Limulus polyphemus*. *Comparative Biochemistry and Physiology Part B*. 163, 303-308

LIST OF FIGURES

page 4	Figure 1.1 Model organisms used for research. A) <i>Limulus polyphemus</i> and B) <i>Nephrops norvegicus</i>
page 11	Figure 1.2 Schematic representation of wound healing/clot formation in arthropods
page 16	Figure 1.3 Schematic representation of microbial pathogenesis
page 21	Figure 1.4 Emphasising tyrosinase and catecholoxidase activity in the biosynthesis of the chromogen, melanin
page 22	Figure 1.5 Active sites of six representative type-3 copper proteins
page 27	Figure 1.6 Absorption spectra of 0.3 mg mL ⁻¹ <i>Limulus polyphemus</i> hemocyanin in 100 mM Tris-HCL buffer, pH 7.5.
page 28	Figure 1.7 Structure of arthropod hemocyanin and mollusc hemocyanin
page 30	Figure 1.8 The proPO activation cascade in invertebrates
page 37	Figure 1.9 View of the active site of type-3 copper proteins with placeholder residues present

page 56	Figure 2.1 Purification of hemocyanin from <i>Limulus polyphemus</i> .
page 59	Figure 2.2 Phospholipid induced phenoloxidase activity of hemocyanin from <i>Limulus polyphemus</i> .
page 60	Figure 2.3 Phosphatidylserine induced phenoloxidase activity of hemocyanin from <i>Limulus polyphemus</i> .
page 62	Figure 2.4 Far-UV CD spectra of 0.3 mg mL ⁻¹ <i>Limulus polyphemus</i> hemocyanin incubated with a range of membrane phospholipids.
page 63	Figure 2.5 Far-UV CD spectra of 0.3 mg mL ⁻¹ <i>Limulus polyphemus</i> hemocyanin following incubation with phosphatidylserine.
page 66	Figure 2.6 Fluorescence emission spectra of 0.1 mg mL ⁻¹ <i>Limulus polyphemus</i> hemocyanin in the presence of a range of phospholipids.
page 68	Figure 2.7 Near-UV CD spectra of 0.4 mg mL ⁻¹ <i>Limulus polyphemus</i> hemocyanin following incubated with phosphatidylserine.
page 70	Figure 2.8 Absorption spectra of 0.3 mg mL ⁻¹ <i>Limulus polyphemus</i> hemocyanin.
page 71	Figure 2.9 Fluorescence emission spectra of 0.1 mg mL ⁻¹ <i>Limulus polyphemus</i> hemocyanin, in the presence of phospholipids and SDS.
page 73	Figure 2.10 Conductivity measurements of 100 mM Tris-HCl, pH 7.5 were recorded in the presence of increasing concentrations of NaCl (0 – 500 mM).
page 74	Figure 2.11 Phosphatidylserine induced phenoloxidase activity of hemocyanin from <i>Limulus polyphemus</i> in the presence of increasing concentrations of NaCl (0 – 500 mM).
page 75	Figure 2.12 Fluorescence emission spectra of 0.1 mg mL ⁻¹ <i>Limulus polyphemus</i> hemocyanin with increasing concentrations of NaCl (mM).
page 81	Figure 2.13 A) Electrostatic surface potential of <i>Limulus polyphemus</i> hemocyanin (PDB ID code 1OXY). B) Location of the positively charged loop (P181 to K196) relative to the entrance of the Cu(II) centre.

page 82	Figure 2.14 Proximity of the positively charged loop to the dicopper centre of hemocyanin (PDB; 1OXY), which contains the placeholder residue, Phe 49.
page 84	Figure 2.15 Correlation of phenoloxidase activity and structural changes in <i>L. polyphemus</i> hemocyanin with increasing concentrations of phosphatidylserine.
page 85	Figure 2.16 Correlation of phenoloxidase activity and structural changes in <i>L. polyphemus</i> hemocyanin in the presence of phosphatidylserine (20 $\mu\text{g mL}^{-1}$) and increasing concentrations of NaCl.
page 91	Figure 3.1 Appearance of fresh caught prawns (A) and prawns with hyperpigmentation present (B).
page 100	Figure 3.2 Effect of freeze-thawing on cellular and hemolymph fractions from <i>Nephrops norvegicus</i> .
page 102	Figure 3.3 Purification of hemocyanin from <i>Nephrops norvegicus</i> .
page 104	Figure 3.4 Effect of freeze-thawing on the stability of purified <i>Nephrops norvegicus</i> hemocyanin.
page 105	Figure 3.5 Melting curve for purified <i>Nephrops norvegicus</i> hemocyanin across the temperature range, 0°C to 70°C.
page 107	Figure 3.6 Hemocyanin derived phenoloxidase activity of purified <i>Nephrops norvegicus</i> hemocyanin induced by a range of known phenoloxidase activators.
page 108	Figure 3.7 Stability of activated <i>N. norvegicus</i> hemocyanin in the presence of increasing concentrations of SDS.
page 109	Figure 3.8 Stability of activated hemocyanin in the presence of SDS over time.
page 110	Figure 3.9 Kinetic analysis of o-diphenoloxidase activity of <i>Nephrops norvegicus</i> hemocyanin (0.1 mg mL^{-1}) towards A) Dopamine-hydrochloride, 0 – 4 mM and B) 4-methylcatechol, 0 – 30 mM, in 100 mM Tris-HCl, pH 7.5.
page 114	Figure 3.10 Intrinsic tryptophan fluorescence of <i>Nephrops norvegicus</i> hemocyanin in the presence of phenoloxidase inhibitors.
page 116	Figure 3.11 Absorption spectra of 0.4 mg mL^{-1} <i>Nephrops norvegicus</i> hemocyanin.
page 138	Figure 4.1 Percentage viability of <i>Limulus polyphemus</i> amebocytes <i>in vitro</i> .
page 139	Figure 4.2 <i>Limulus polyphemus</i> amebocyte morphology, <i>in vitro</i> .
page 140	Figure 4.3 Degranulation of <i>Limulus polyphemus</i> amebocytes in response to LPS.
page 141	Figure 4.4 Response of crude <i>Limulus polyphemus</i> amebocyte lysates to microbial ligands and membrane phospholipids.
page 143	Figure 4.5 The appearance of <i>Limulus polyphemus</i> amebocytes following exposure to <i>E. coli</i> and 2 μm latex microspheres.
page 144	Figure 4.6 Effect of pH on the quenching properties of crystal violet, methylene blue and trypan blue in the presence of FITC-labelled <i>Saccharomyces cerevisiae</i> .
page 145	Figure 4.7 Confirmation of <i>Saccharomyces cerevisiae</i> internalisation by <i>Limulus polyphemus</i> amebocytes.
page 146	Figure 4.8 Confirmation of internalisation of 2 μm microspheres by

	<i>Limulus polyphemus</i> amoebocytes.
page 147	Figure 4.9 Confirmation of <i>Bacillus megaterium</i> internalisation by <i>Limulus polyphemus</i> amoebocytes.
page 149	Figure 4.10 Phagocytic properties of <i>Limulus polyphemus</i> amoebocytes <i>in vitro</i> .
page 150	Figure 4.11 Proportion of ‘phagocytic amoebocytes’ in the presence of fluorescent –labelled microbes, <i>in vitro</i> .
page 151	Figure 4.12 Phagocytic properties of <i>Limulus polyphemus</i> amoebocytes in the presence of hemolymph plasma, heat treated plasma (100°C for 10 min), or in the absence of plasma.
<hr/>	
page 170	Figure 5.1 Phagocytic properties of amoebocytes in the presence of coumarin-labelled microbes.
page 171	Figure 5.2 Exocytosis of amoebocyte cytosolic granules in the absence of endotoxin, <i>in vitro</i> .
page 174	Figure 5.3 MitoTracker Orange CMTMRos staining of mitochondria present in <i>Limulus polyphemus</i> amoebocytes.
page 175	Figure 5.4 Using Annexin V-FITC and propidium iodide staining to monitor amoebocyte cell death, <i>in vitro</i> .
page 176	Figure 5.5 A series of images depicting phosphatidylserine exposure and loss of plasma membrane integrity of dying amoebocytes.
page 177	Figure 5.6 Using TUNEL staining to monitor amoebocyte cell death, <i>in vitro</i> .
page 178	Figure 5.7 TUNEL staining of phagocytically active amoebocytes, <i>in vitro</i> .
page 179	Figure 5.8 Caspase-3 activity of amoebocytes in the presence and absence of spores, <i>in vitro</i> .
page 181	Figure 5.9 Inducible phenoloxidase activity of hemocyanin in the presence of dying amoebocytes.
page 182	Figure 5.10 Inducible phenoloxidase activity of <i>Limulus polyphemus</i> hemocyanin.
<hr/>	
page 192	Figure 6.1 Geographical distributions of the four extant species of horseshoe crabs.
page 195	Figure 6.2 A series of images of <i>Limulus polyphemus</i> .
page 201	Figure 6.3 Effect of temperature on mean body weight of captive horseshoe crabs.
page 203	Figure 6.4 Effect of temperature on hemocyanin concentrations (mg mL ⁻¹) present in the hemolymph of <i>L. polyphemus</i> .
page 206	Figure 6.5 Effect of temperature on the percentage of <i>L. polyphemus</i> hemocyanin with dioxygen bound.
page 207	Figure 6.6 Effect of temperature on hemocyanin-derived phenoloxidase activity.
page 210	Figure 6.7 Effect of temperature on the numbers of amoebocytes from <i>L. polyphemus</i> hemolymph.
page 211	Figure 6.8 Effect of temperature on the morphological status of amoebocytes present in <i>L. polyphemus</i> hemolymph
page 213	Figure 6.9 Phenoloxidase activity of hemocyanin from <i>Limulus polyphemus</i> upon exposure to increasing temperatures.
page 214	Figure 6.10 Far-UV CD spectra of 0.3 mg mL ⁻¹ <i>Limulus polyphemus</i>

	hemocyanin across the temperature range 5 °C to 25°C.
page 217	Figure 6.11 Effect of temperature on the tertiary structure of <i>Limulus polyphemus</i> hemocyanin.
page 218	Figure 6.12 Near-UV CD spectra of 0.4 mgmL ⁻¹ <i>Limulus polyphemus</i> hemocyanin across the temperature range 5 °C to 25°C.
page 221	Figure 6.13 Fluorescence emission spectra of 0.1 mg mL ⁻¹ <i>Limulus polyphemus</i> hemocyanin across the temperature range 8°C to 23°C.
page 228	Figure 6.14 Direct comparison of the biochemical and cellular properties of captive <i>Limulus polyphemus</i> across the temperature range, 8°C to 23°C.
page 267	Figure B1 Dynamic light scattering measurements of <i>Limulus polyphemus</i> hemocyanin and phospholipid liposomes.
page 268	Figure B2 Dynamic light scattering measurements of <i>Nephrops norvegicus</i> hemocyanin.
page 269	Figure C1 Typical tank set-up for housing horseshoe crabs, <i>Limulus polyphemus</i> .

LIST OF TABLES

page 31	Table 1.1 Known hemocyanin-derived phenoloxidase (Hc-d PO) activity in invertebrates.
page 41	Table 1.2 Hemocyanin derived immune-functionality (<i>aside from inducible phenoloxidase activity, Table 1.1</i>)
page 57	Table 2.1 Purification of hemocyanin from <i>Limulus polyphemus</i> , for 1 mL of hemolymph
page 64	Table 2.2 Percentage change in secondary structure content of hemocyanin following incubation with phospholipids
page 67	Table 2.3 Intrinsic tryptophan fluorescence peak wavelength of <i>Limulus polyphemus</i> in the absence and presence of phospholipids and SDS.
page 76	Table 2.4. Intrinsic tryptophan fluorescence peak wavelength of <i>Limulus polyphemus</i> in the presence of phosphatidylserine and increasing concentrations of NaCl.
page 103	Table 3.1 Purification of hemocyanin from <i>Nephrops norvegicus</i> , for 1 mL of hemolymph
page 113	Table 3.2 Inhibitors of hemocyanin-derived phenoloxidase
page 115	Table 3.3 Intrinsic tryptophan fluorescence peak wavelength of <i>Nephrops norvegicus</i> Hc in the presence of inhibitors and SDS.
page 120	Table 3.4 Inhibition of hemocyanin-derived phenoloxidase activity from crustaceans
page 156	Table 4.1 Phagocytic properties of selected immune cells
page 204	Table 6.1 Biochemical, immunological and cellular measurements of control and trial horseshoe crabs.
page 215	Table 6.2 Percentage change in secondary structural content of <i>L. polyphemus</i> hemocyanin across the temperature range, 5°C to 25°C
page 220	Table 6.3 Absorbance peak values for <i>Limulus polyphemus</i> hemocyanin across the temperature range 5°C – 50°C
page 263	Table A1 Data from peptide mass fingerprint analysis of proteins purified from <i>Limulus polyphemus</i> and <i>Nephrops norvegicus</i> A) <i>Limulus polyphemus</i> hemocyanin (Fig. 2.1B) B) <i>Limulus polyphemus</i> C-reactive protein (Fig. 2.1B) C) <i>Nephrops norvegicus</i> hemocyanin (Fig. 3.3B)
page 269	Table C1 Assessment of water quality

Chapter 1: Introduction

1.1 Background and thesis overview

The horseshoe crab, *Limulus polyphemus*, and the shellfish, *Nephrops norvegicus*, are members of the most diverse and successful phylum on earth, the arthropods. Predictions of arthropod species richness detail the potential existence of up to 30 million species (Mora et al., 2011). Despite constant exposure to harsh environmental conditions and a battery of pathogenic and parasitic organisms, arthropods inhabit almost every terrestrial and maritime niche on the planet. Over the past number of decades, the intricacies of arthropod immunity have been investigated; for which, the 2011 Nobel Prize in physiology or medicine was awarded to Jules A. Hoffmann and Bruce A. Beutler for their discoveries and subsequent work on Toll receptor signalling (<http://www.nobelprize.org>).

Arthropods possess a single line of inducible defence, namely innate immunity. In contrast to mammals and fish (vertebrates), arthropods (invertebrates) lack the biological machinery necessary to synthesise unique clones of lymphocytes that are

specialised to identify and proliferate in response to the presence of particular antigenic compounds. Nonetheless, this archaic, yet highly complex biological defence system can adequately eliminate infection (Rowley and Powell, 2007). Typically, invertebrate innate immunity consists of three lines of defence. The first, being of physical nature, is the sclerotised cuticle (functionally equivalent to mammalian skin) which prevents invasion of foreign entities into the hemocoel (body cavity). Once the cuticle has been breached, cellular and humoral defences constitutively present in the hemolymph (functionally equivalent to mammalian blood) work in synergy to combat sepsis, mycosis, parasitism and viremia (reviewed by Iwanaga and Lee, 2005).

Numerous immune-related signal transduction and proteolytic cascades co-operate to combat noxious invaders (reviewed by Cerenius et al., 2010). A cascade of particular importance, involved both in development and immunity, is the prophenoloxidase (proPO) activation cascade. In this, activated phenoloxidase (PO) enzymes play essential roles in the encapsulation of microbes, the generation of cytotoxic products and contribute to the formation of insoluble gel-like clots during wound healing (Cerenius et al., 2008).

PO enzymes share many sequence and functional similarities with another type-3 copper protein, hemocyanin (Hc) (Burmester, 2001). Hc, a protein considered traditionally to be involved in respiration and homeostasis in invertebrates has been characterised recently to possess numerous immune functions. Of these immune functions, the ability of Hc to be converted into a phenoloxidase (PO)-like enzyme has received most attention. Activation of PO enzymes and their respective functions *in vivo* have been well characterised in crustacean and insect systems; however, the endogenous events leading to the conversion of Hc into a PO-like enzyme are to a

greater extent unknown. Therefore, **the overall aim of this thesis was to characterise the physiological circumstances in which the respiratory protein Hc, is converted into a PO-like enzyme, *in vivo*.** To this end, the presented thesis encompasses six core objectives:

- 1) to test the ability of natural phospholipids to induce PO activity in Hc
- 2) to characterise the structural changes associated with the induction of PO activity in Hc by natural activator(s)
- 3) to isolate invertebrate immune cells and maintain them *in vitro*
- 4) to monitor phagocytic activity and apoptosis of invertebrate immune cells during immune challenge
- 5) to monitor Hc-derived PO activity in the presence of quiescent and active immune cells
- 6) to explore the role of Hc-derived PO in hyperpigmentation of shellfish

Unlike crustaceans, which possess both Hc and PO, chelicerates such as *L. polyphemus* (Fig. 1.1 A) contains Hc only, therefore, any PO activity detected is assumed to be derived from Hc alone. *L. polyphemus* proved to be an ideal system to address objectives 1 to 5 of the presented thesis. As Hc is known to display PO-like activity, the involvement of Hc in the unwanted pigmentation of commercial shellfish has been proposed in recent years. Therefore, to address an economically important issue, objective 6, Hc was purified from the langoustine, *N. norvegicus* (Fig. 1.1 B), and investigated for its contribution to the occurrence of hyperpigmentation in fresh-caught and farmed shellfish.

A)



B)



Figure 1.1 Model organisms used for research. **A)** Dorsal (top image) and ventral (bottom image) views of the Atlantic horseshoe crab, *Limulus polyphemus*. **B)** The Norway lobster, *Nephrops norvegicus*.

1.2 Innate immune responses of arthropods

1.2.1 Physical barrier

Invertebrates (including crustaceans, insects and some chelicerates) possess a chitinous external barrier consisting of three layers: a waxy epicuticle, an exocuticle and an endocuticle. Beneath the endocuticle, an epithelial layer which is in contact with the haemocoel secretes AMPs in response to cuticular damage whilst simultaneously a clotting response ensues. The sclerotised exoskeleton of horseshoe crabs consists of a series of hypodermal glands that secrete a cytolytic glycoprotein complex which prevents the attachment and colonisation by nocuous epibionts (Harrington et al., 2008, Stagner and Redmond, 1975).

Insects possess many mechanical barriers, including the chitin lining of the tracheal system and the peritrophic matrix of the mid-gut lumen (Billingsley and Lehane, 1996). The fruit fly *D. melanogaster* possesses an enzyme complex in their intestine, known as Duox (EC.1.11.1.-). Duox is analogous to the NADPH oxidase (EC.1.6.3.1) complex in mammals. In *D. melanogaster*, the Duox complex produces reactive oxygen species (ROS) in the gut, in response to the presence of invasive microorganisms (Ferrandon et al., 2007).

1.2.2 Sensing, recognition and immune signalling pathways

Invertebrates lack adaptive immunity, however, in order to withstand an infection, they have retained the ability to differentiate between classes of microorganisms via pathogen recognition receptors (PRRs) and respond accordingly (Lavine and Strand, 2002). PRRs are constitutively secreted into the hemolymph and are expressed on the hemocyte cell surface. The most studied PRRs include peptidoglycan recognition proteins (PGRP), Gram-negative binding proteins (GNBP), hemolin (a member of the

immunoglobulin (Ig) superfamily) and an abundance of insect, crustacean and horseshoe crab immune-lectins (examples: tachylectins 1 to 5, limulin and carcinoscorpins) (Kanost et al., 2004, Iwanaga, 2002, Kim et al., 2000b). PRRs function by binding to differential sugar moieties found on microbes, collectively known as pathogen associated molecular patterns (PAMPs): lipopolysaccharide (LPS) from Gram-negative bacteria, lipoteichoic acid (LTA) from Gram-positive bacteria, β -1, 3-glucan and mannan from fungi, laminarin and viral RNA (Uvell and Engstrom, 2007). Opsonisation of foreign invaders in the hemolymph allows cell derived PRRs to bind to immobilised cells and activate the appropriate immune defence. Hemolin and immunlectins such as IML-1 and IML-2 (originally isolated from *Bombyx mori*) recognise and bind to the surface of microbes and aggregate them (Koizumi et al., 1999). Cellular PRRs have been well characterised due to extensive research involving the insect model *D. melanogaster* (Silverman et al., 2009) and the availability of its fully sequenced genome (Adams et al., 2000).

The Toll receptor (first identified in *D. melanogaster*; Lemaitre et al., 1996) is considered a cellular PRR, even though it is activated via an extracellular ligand known as Spätzle. Opsonised Gram-positive bacteria and fungi are recognised by the ligand Spätzle. Spätzle binds to the Toll receptor, resulting in the oligomerization of a complex that coordinates various signal transduction cascades, the expression, synthesis and release of AMPs, and the activation/regulation of pro-PO (Cerenius et al., 2010; section 1.3.4). The Toll pathway is involved in immune recognition and plays a vital role in the development and homeostasis of an organism (Hoffmann, 2003; De Gregorio, 2001).

A *Drosophila* Toll-like receptor has been identified in horseshoe crabs (Inamori et al., 2004), shrimp (Li and Xiang, 2012) and other invertebrates. Analysis reveals that horseshoe crab Toll-like receptors maybe involved in restoring the granular content of amebocytes after exocytosis, it is postulated also, that coagulogen could act as a Toll-like ligand, given its high level of structural similarity with Spaetzle (Kurata et al., 2006).

Gram-negative bacteria are recognised by PGRPs leading to the activation of the immune deficiency (Imd) pathway. The Imd receptor initiates two cascades that result in the expression and release of AMPs. The first, involves the activation of a transforming growth factor- β kinase (dTAK1) which phosphorylates the cytosolic IKK complex. Simultaneously, a second cascade consisting of a hetero-trimeric complex (FADD/DREDD/Imd) also associates with the IKK complex (Leulier et al., 2000). Recently, dTAK1 has been observed to activate a third signal transduction cascade known as the Jun-N-terminal Kinase (JNK) pathway. The JNK pathway activates early response genes involved in wound repair and has also been associated with cell rupture and the release of PO from crystal cells in insects (Bilda et al., 2007; Tanji and Tony-Ip, 2005).

There is a fourth signal transduction cascade known as the JAK-STAT pathway. The stimulus of this pathway remains unclear; however, some evidence suggests that this pathway is involved in anti-viral defence in *Drosophila* and shrimp (Dostert et al., 2005; Li and Xiang, 2012). Furthermore, activation of this pathway is linked to development and may also be responsible for inducing the production of molecules analogous to mammalian cytokines that regulate hemocyte proliferation, differentiation and phagocytic behaviour (Lemaitre and Hoffmann, 2007; Agaisse and Perrimon, 2004; Tzou et al., 2002; Hong and Dearolf, 2001).

1.2.3 Coagulation of arthropod hemolymph

Coagulation in arthropods has been studied extensively, however, most information available has focussed on crustaceans and horseshoe crabs. Preventing the loss of vital body fluid is essential to an organism's survival. Damage to an insect's integument, whether it is created by a pathogen, parasite or herbivore, will initiate a series of reactions collectively known as the hemostatic system; this will function alongside the immune response in order to repair the wound (Theopold et al., 2002).

A number of cascades contribute to hemostasis in arthropods. The polymerisation of lipophorins and vitellogenin-like proteins is achieved via the action of a calcium dependent transglutaminase (E.C. 2.3.2.13) (Fig. 1.2) (Cerenius et al., 2010). These clotting proteins contain a cysteine rich domain homologous to the mammalian blood clotting proteins of Von Willebrand factor (Vilmos and Kurucz, 1998). Insects and crustaceans are alike in their ability to form hemolymph-clots. In both cases, transglutaminase is essential for clot formation. Conversely, horseshoe crab hemolymph clotting involves a well-characterised proteolytic cascade; in this organism, transglutaminase catalyses the cross-linking and stabilisation of existing clots (Cerenius et al., 2010). Wang et al., (2010) have demonstrated a novel function for transglutaminase in *Drosophila* (and humans). During bacterial invasion, micro-clots form (similar to nodules) and act to sequester bacteria in the hemolymph, transglutaminase anchors the bacterium to the clot matrix allowing AMPs and phagocytes to kill them.

Arguably, the most well-known invertebrate clotting cascade is that of the horseshoe crab, involving the release of clotting factors via the mass exocytosis of granules from amebocytes (Iwanaga and Lee, 2005). This phenomenon has been exploited to produce

the most sensitive test for microbial contamination in biomedicine, the Limulus amoebocyte lysate (LAL) test (Ding and Ho, 2010).

In vivo, horseshoe crab amoebocytes detect LPS (endotoxin) via a G-protein dependent exocytic pathway which depends entirely on the proteolytic activity of the serine protease, factor C (Koshiba et al., 2007). The exocytosis of the cytosolic granule-derived content into the surrounding plasma provides an endogenous feedback mechanism in which the AMP, tachyplesin, dramatically amplifies amoebocyte sensitivity to LPS (Iwanaga, 2002, Kawabata et al., 2009, Tagawa et al., 2012). Factor C (amongst other effectors) is released and is autocatalytically activated upon binding to the lipid A portion of bacterial LPS. Once factor C is activated it then subsequently activates factor B. Activated factor B converts the pro-clotting enzyme into the fully functional clotting enzyme. Clotting enzymes, in turn, promote the proteolytic conversion of coagulogen into coagulin, which aggregates spontaneously into an impermeable clot. Alternatively, factor G is released and directly cleaves the pro-clotting enzyme into the clotting enzyme in response to β -1, 3-glucans present on fungi (Kawabata et al., 2009) (Fig. 1.2). In order to ensure the newly formed clot is adequate to plug a wound, melanin is used to coat the clot (Fig. 1.2). Evidence suggests that the clotting cascade and the pro-PO cascade work synchronously during an immune response in order to deter an infection and repair wounds (Li et al., 2002; Nagai and Kawabata, 2000; Cerenius et al., 2010).

1.2.4 Complement-like proteins in invertebrates

In vertebrates, the complement cascade (also known as the hemolytic cascade) is traditionally associated with clot formation (thrombosis). A C3-convertase complex (activated by three convergent pathways: classical, lectin and alternative) cleaves C3, exposing an intramolecular thioester bond that interacts with a pathogen (Ricklin et al.,

2010). The association of C3 with pathogens serves many purposes, including: marking pathogens for phagocytosis-mediated clearance and promoting the formation of a membrane attack complex that ultimately leads to cell rupture (Nonaka, 2011). The majority of known proteases involved in mammalian complement belong to either the complement factor B (Bf) family or the mannose binding lectin associated serine proteases (MASP) or C3 proteins. C3, Bf and MASP homologues have been identified in almost all invertebrates studied thus far (reviewed by Cerenius et al., 2010).

Zhu et al., (2005) first identified complement-like proteins in the horseshoe crab *C. rotundicauda*. Proteins akin to Bf (CrBf/C2) and C3 (CrC3) were recorded having broad microbial binding properties. Subsequently, Ariki et al., (2008) and Tagawa et al., (2012) catalogued numerous complement-like proteins present in the hemolymph of *T. tridentatus*: TtC3, TtC2/Bf1 and TtC2/Bf2. Factor C, in the presence of LPS, acts as a TtC3 convertase, allowing TtC3 to recruit TtC3b deposition on Gram-negative bacterial membranes. It is thought that in order to opsonise Gram-positive bacteria and fungi, plasma and amebocyte-derived lectins such as C-reactive protein and/or tachylectin-1, form a complex with a second C3 convertase and recruit TtC2/Bf1 and TtC2/Bf2 deposition onto the respective microbial membranes (Tagawa et al., 2012). C3 proteins have been identified in a variety of invertebrates, including: horseshoe crabs, insects, sea squirts and sea urchins to name but a few (reviewed by Nonaka, 2011). However, greater understanding is needed to fully characterise complement-mediated immunity in invertebrates.

Footnote 2; This stylised diagram is constructed from information published; Kawabata et al. (2009), Iwanaga (2002) and Kurata et al. (2006)

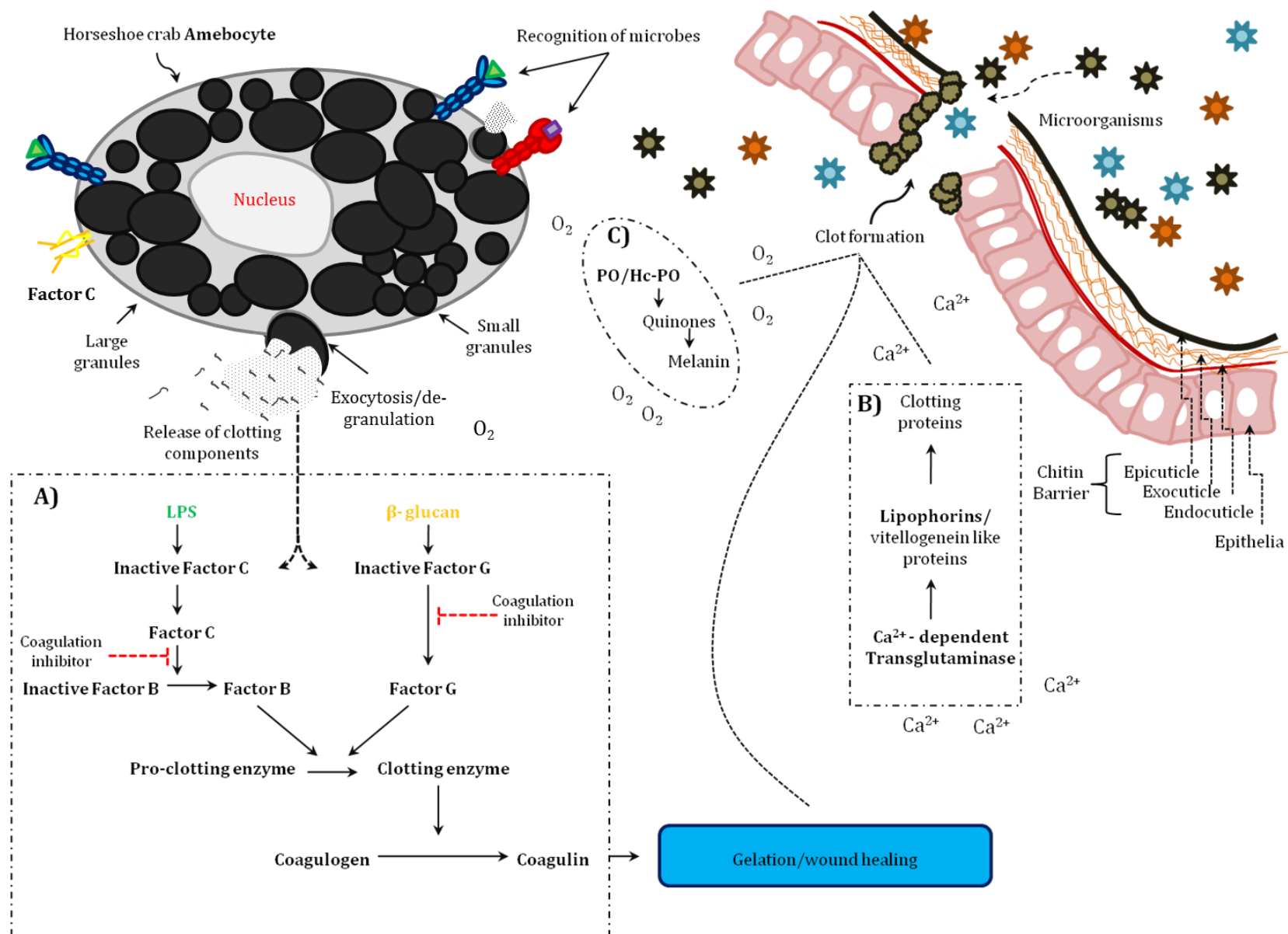


Figure 1.2 Schematic representation of wound healing/clot formation in arthropods. Cuticular damage and microbial infection activate the following cascades²; A) amebocyte-derived clotting cascade (basis for LAL) in horseshoe crabs, B) plasma-derived clotting proteins (in crustaceans and insects) and C) Phenoloxidase/Hemocyanin-derived phenoloxidase activity.

1.2.5 Arthropod immune cells

The collective name given to an immune cell found in the predominance of arthropod species is the hemocyte. The site of hemocyte generation appears to be species specific; haematopoiesis occurs in the cephalothorax of crustaceans and lymphoid glands in dipteran insects (reviewed by Smith, 2010). Amebocyte synthesis in horseshoe crabs is unknown; evidence suggests the location to be in the region of the gill flaps, or within connective tissue (Coursey et al., 2003).

Classification of hemocytes varies substantially in the literature. In lepidopteran insects (such as *Galleria mellonella*) six different classes of hemocytes have been recognised: prohemocytes, plasmatocytes, granulocytes, spherulocytes, coagulaocytes and oenocytoids (Price and Ratcliffe, 1974, Kavanagh and Reeves, 2004). A seventh class of lepidopteron hemocyte has been characterised. Known as the hyper-spreading or hyperphagocytic hemocyte, this cell only appears in the haemocoel (body cavity) of *Manduca sexta* larvae when a microbial infection reaches a critical level (Dean et al., 2004a, Dean et al., 2004b).

In Dipteran insects (such as *D. melanogaster*) there are three immune cell lineages: lamellocytes, plasmatocytes and crystal cells (or oenocytoids). These cells are involved in phagocytosis, encapsulation and PO release, respectively (Meister, 2004). Interestingly, a new hemocyte lineage known as pseudopodocytes was discovered in *Drosophila affinis* and *Drosophila obscura* (which lack lamellocytes) (Harvard et al., 2012). Evidence suggests that pseudopodocytes are essential for encapsulation in the aforementioned *Drosophila* species. In crustaceans, there are typically three mature hemocytes: granulocytes, semi-granulocytes, and hyalinocytes, and immature/undifferentiated prohemocytes (Smith, 2010; Roulston and Smith, 2011).

Often referred to as a 'living fossil', *L. polyphemus* is widely considered to possess a single immune cell type, the granular amebocyte. Other cell types observed in HSC hemolymph include cyanoblasts (Fahrenbach, 1970) and plasmatocytes (Jakobsen and Suhr-Jessen, 1990, Suhr-Jessen et al., 1989). According to Jakobsen and Suhr-Jessen (1990), the Japanese horseshoe crab *Tachypleus tridentatus* contains two different types of amebocyte: granulocytes and plasmatocytes. The latter constitutes less than one percent of the total blood cell population found in the horseshoe crab. The function of these amebocytic plasmatocytes is unknown, also, it is unclear whether plasmatocytes are simply granular amebocytes that have undergone spontaneous exocytosis of cytosolic content, or if they are pro-amebocytes. In almost all arthropods studied, a series of immune cells carry out specific functions during immune assault (Smith, 2010), however, horseshoe crab amebocytes are known to carry out multiple functions: the production and release of > 25 immune effectors from cytoplasmic stored granules (Iwanaga 2002), phagocytic behaviour (Armstrong and Levin, 1979; Gupta and Campenot, 1996; chapter 4) and hemostasis properties (Levin, 1988).

1.2.5.1 Phagocytosis

Phagocytosis is a process carried out by specialised cells in the blood of mammals and the hemolymph of invertebrates. Hemocytes can phagocytose biotic (bacteria, yeast) and abiotic targets (latex microspheres) (Jiravanichpaisal et al., 2006). In contrast to many invertebrates studied, the process of phagocytosis in *L. polyphemus* is poorly characterised (this topic is addressed in chapter 4). Phagocytosis involves the entrapment and internalisation of pathogens into a vacuole known as a phagosome (either via opsonic or direct receptor-target interactions). Thorough investigations of

the proteome of murine macrophage phagosomes were carried out by Garin et al., (2001) and Goyette et al., (2012), leading to an enhanced understanding and appreciation of the structure, complexity, maturation process and functions of phagosomes. The phagosome fuses with cytosolic granules (containing lytic enzymes: lysozyme and cathepsin) to form an intracellular acidic phagolysosome that in cooperation with reactive nitrogen and oxygen intermediates kills the pathogen (Lavine and Strand, 2002). Phagocytosis carried out by invertebrate immune cells has demonstrated mechanistic similarities with that of mammalian leukocytes, notably neutrophils (Banville et al., 2011). Cytosolic proteins in the arthropod hemocytes (homologous to mammalian neutrophil proteins) translocate to the phagolysosome membrane forming an NADPH oxidase complex (Fig. 1.3). This complex produces reactive nitrogen and oxygen species (RNS, ROS) and in co-ordination with the acidic granules, results in the destruction of engulfed pathogens (Renwick et al., 2007, Bergin et al., 2005).

1.2.5.2 Encapsulation and nodulation

During sepsis or mycosis, populations of microorganisms will be opsonised via hemolymph and hemocyte derived immune lectins and subsequently immobilised. These immobilised microbes can either be nodulated or encapsulated. Typically, a nodule is formed when a population of microorganisms are trapped in a hemocyte-derived extracellular structure and are usually found attached to internal organs, such as the fat-body/hepatopancreas (Jiravanichpaisal et al., 2006). A nodule consists of an amalgamation of viable and non-viable hemocytes, non-self particles and melanised debris (Stanley-Samuelson, 1991). Miller et al., (1994) demonstrated that microbial

populations present in the hemolymph of *M. sexta* larvae lead to the biosynthesis of eicosanoids, resulting in the hemocyte undergoing a conformational change allowing them to adhere to microorganisms, thus facilitating nodule formation.

When an infection is caused by a parasite (such as a nematode or wasp egg) rather than a microorganism, hemocytes are unable to phagocytose the parasite due to its size, therefore, the parasite is encapsulated (Lavine and Strand, 2002; Strand 2008). Upon recognition of a parasitoid, free floating granulocytes will adhere to the parasitoid and release plasmacyte spreading proteins that attract plasmacytes to the site of infection. Recruited plasmacytes secrete cytoplasmic stored adhesion molecules onto their outer membrane surface resulting in multiple layers of hemocytes attaching to the parasitoid (Strand and Clark, 1999). Finally a monolayer of granulocytes attach and apoptose on the periphery, thus ending encapsulation. Asphyxiation, production of ROS, AMP release and deposition of melanin collectively lead to the destruction of the encapsulated intruder (Lavine and Strand, 2002; Gillespie et al., 1997). The processes of encapsulation and nodulation both lead to the formation of a hemocyte-like mesh, which is ultimately melanised by PO enzymes (reviewed by Cerenius and Soderhall, 2004; Jiravanichpaisal et al., 2006)

Hemocytes can function individually (phagocytosis) or co-operatively (encapsulation, nodulation and cell signalling) to fight infections.

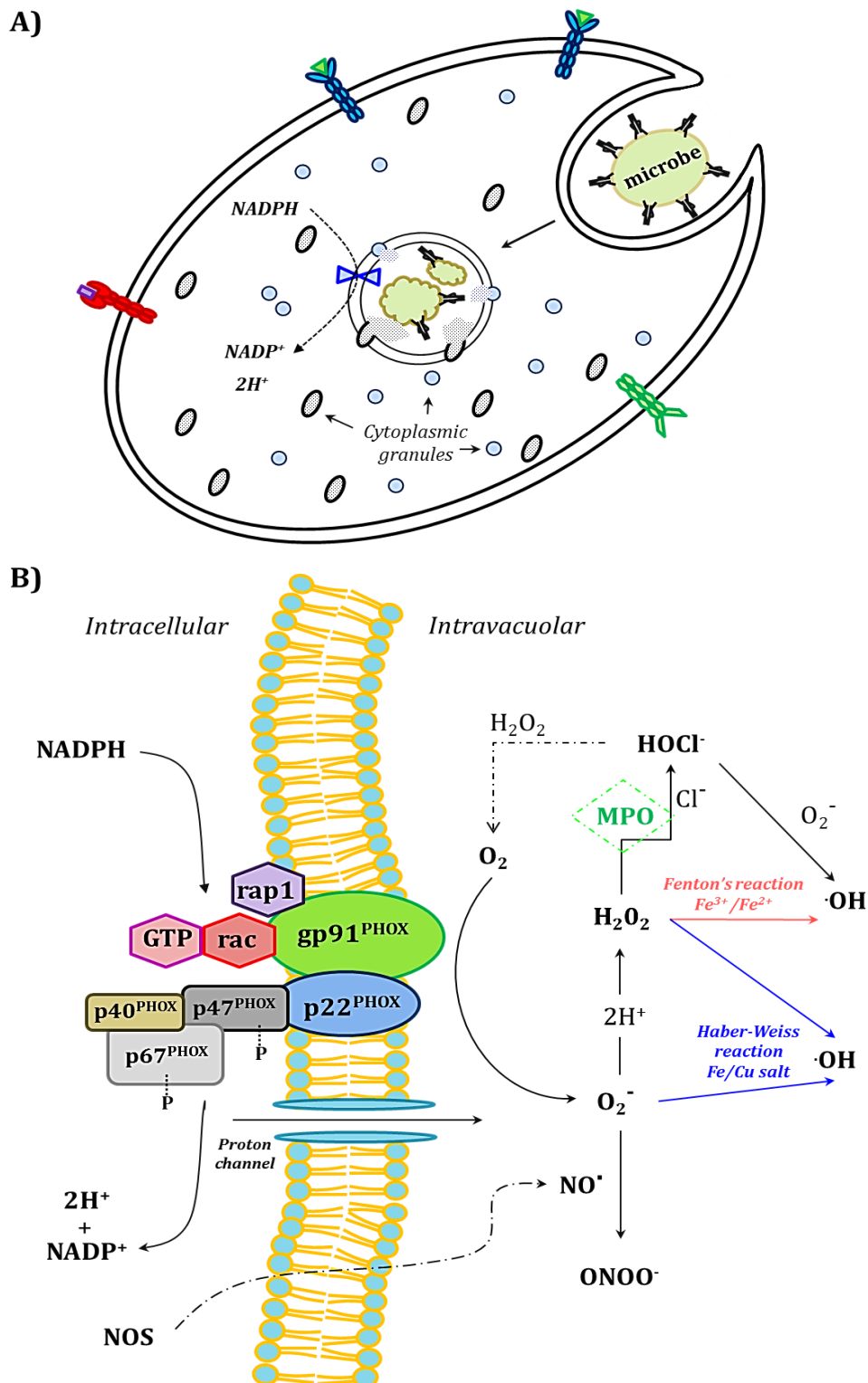


Figure 1.3 Schematic representation of microbial phagocytosis. A) An opsonised microbe is internalised into a phagosome. Microbicidal granules fuse to form a phagolysosome and the NADPH oxidase complex is activated. B) Detailed view of the NADPH oxidase complex and the components involved in respiratory burst. NADPH oxidase accepts electrons from NADPH and reduces oxygen to O₂⁻ (superoxide). Myeloperoxidase, in the presence of chlorine, uses H₂O₂ to form hypochlorous acid (HOCl). Superoxide can interact with nitric oxide (NO⁻), yielding peroxynitrite (ONOO⁻). Hydroxyl radicals (·OH) can be formed through various reactions. This figure was adapted from El-Benna et al. (2008) and Kavanagh and Reeves (2004).

1.2.6 Humoral defences; antimicrobial peptides

Arthropods do not possess antibodies; however, they are capable of synthesising a plethora of proteins that confer a degree of non-specific immunity against many pathogenic and parasitic organisms (Moret and Siva-jothy, 2003; Faulhaber and Karp, 1992). AMP synthesis is the hallmark of the humoral immune response. AMPs are synthesised in response to microbial invasion and are secreted by hemocytes, barrier epithelia, the fat body/hepatopancreas and the reproductive organs of arthropods (Nehme et al., 2007). Melanin synthesis, wound healing and proPO activation (see section 1.3.4) are considered semi-humoral responses as they can be activated via constitutively expressed PRRs in the hemolymph. Subsets of AMPs show preferential activity against particular microorganisms (Lemaitre et al., 1997). AMPs can be divided into subgroups based on their amino acid composition, molecular structure and mode of action. Not only do AMPs form membranous pores on microbes, they can translocate intracellularly and inhibit cell wall, nucleic acid and protein synthesis along with the disruption of cytoplasmic membrane integrity (Brogden, 2005). Individual organisms possess species-specific families of AMPs; for example, the horseshoe crab synthesises a series of peptides known as tachyplesins (Kawabata et al., 2009), shrimp produce penaeidins (Destoumieux et al., 1997) and the European honey bee *Apis mellifera* produces specific AMPs known as jelleines, found only in royal jelly (Fontana et al., 2004).

Research has focussed predominantly on the expression of AMPs in response to bacterial and fungal infections. Fungi present in the hemocoel elicit the expression of drosomycin and metchniokwins in insects and polyphemusins (amongst others) in horseshoe crabs (Kurata et al., 2006). Gram-positive bacteria stimulate the expression of defensin and Gram-negative bacteria induce the expression of diptericin, drosocins

(in insects) and Factor D (in horseshoe crabs) (Hoffmann, 2003; Ohta et al., 1992). Not only are AMPs synthesised dependent on which microbe is present, research conducted by Mowlds et al., (2010) demonstrated that AMP expression is influenced by the pathogen load, and not an all or nothing response.

Numerous enzymes are also synthesised to fight infection. For example, expression and activity of lysozyme has been shown to preferentially increase in the presence of a parasite, in contrast to expression levels analysed during a yeast or bacterial infection (Roxström-Lindquist et al., 2004). Recent work suggests that the release of AMPs is the last line of defence against infection. In insects, AMP synthesis is not induced until up to 99.5% of bacteria have been removed from the hemolymph, suggesting that AMPs function to kill microbes that may threaten to cause secondary infections (Haine et al., 2008)

1.2.7 Cell death and immunity

It is now well known that cell death is essential for immunomodulation, both in mammals and invertebrates (Sokolova, 2009). Depending on the circumstances, immune cell death can be achieved by pathogens, extracellular death cues, or self-induced defence mechanisms. Hemocytes in insects (oenocytoids) and crustaceans (semi-granular) and vibratile cells in echinoderms, release immune effectors via cell rupture/exocytosis, and undergo cell death in order to facilitate clot formation and pathogen encapsulation/nodulation (Smith, 2010; Sokolova, 2009; Bilda et al., 2007; Jiravanichpaisal et al., 2006). The two most well-known types of cell death are apoptosis and necrosis. Apoptosis and necrosis are considered two extremes of a continuum, because of this, numerous 'novel' cell death processes have been established recently;

Necroptosis (or programmed necrosis) and Autophagy (cellular recycling) are some examples, but will not be discussed further (Kanduc et al., 2002; Remijnen et al., 2011).

The term apoptosis was first introduced by Kerr et al., (1972). Apoptosis is considered a 'silent' pathway that serves to deter the systemic spread of pathogens, while avoiding pro-inflammatory responses. Apoptosis is an energy dependent, tightly regulated process that compartmentalises cytosolic components into membranous apoptotic bodies (micro-vesicles), preventing the release of cytotoxic and damaging substances into the surrounding environment (Elmore, 2007; Feig and Peter, 2007). Typical characteristics of a cell undergoing apoptosis include: cell shrinkage (pyknosis), the extracellularisation of PS on the plasma membrane, DNA fragmentation (karyorrhexis), vacuolisation and membrane blebbing (or blistering) (Kroemer et al., 2009). There exist a number of different apoptotic pathways that are initiated dependent on internal (intrinsic) or external (extrinsic) stimuli, such as cellular damage or death signals, respectively. A family of proteases, known as caspases, are involved in almost all apoptotic pathways; activated caspases engage in signal transduction, de-construction of the cytoskeleton and membrane packaging (Hengartner 1996, 2000; Feig and Peter, 2007).

Necrotic cell death results in the uncontrolled dissemination of harmful, pro-inflammatory molecules associated with severe stress. Necrosis is an energy independent process, categorised by an over-production of ROS, cell swelling (oncosis) and rupture of the plasma membrane (Kroemer et al., 2009). Apoptosis and necrosis have been reported in a variety of invertebrate species, notably in shrimp, possessing homologues of proteins involved in many aspects of cell death regulation (Smith, 2010).

In 2004, Brinkmann et al. described a novel form of cell death, known as NETosis (neutrophil extracellular traps). The authors observed neutrophils releasing 'microbicidal nets' consisting of a de-condensed nuclear chromatin mesh, histones and AMPs that function to entrap and kill bacteria. This cell death phenomenon is commonly known as ETosis as it has been characterised in numerous cell types (e.g. mast cells) and organisms (e.g. crustaceans/insects), not just mammalian neutrophils (Remijnsen et al., 2011; Smith et al., 2010; Robb et al., 2012). ETosis does not display stereotypical signs of apoptotic or necrotic cells, clearly distinguishing this process as an alternative cell fate, involved in innate immune defence (Remijnsen et al., 2011).

1.3 Immune-functions of an ancient respiratory protein, Hemocyanin

1.3.1 Members of the Type-3 copper protein family

Both arthropod and mollusc Hcs belong to the family of type-3 copper proteins which also include POs, insect hexamerins and cryptocyanins (Burmester, 1999; Terwilliger et al., 1999). PO commonly refers to both tyrosinases (EC 1.14.18.1) and catecholoxidases (EC 1.10.3.1), while the former can generate reactive quinonoids from the *ortho*-hydroxylation of monophenols into *o*-diphenols and their subsequent oxidation into *o*-quinones (Fig. 1.4), catecholoxidases only perform the oxidation step. Although Hcs and POs differ across all structural levels, their respective active sites share high levels of sequence homology. Two copper atoms, CuA and CuB, each coordinated by three highly conserved histidine residues, permit the binding of dioxygen. Crystal structures of bacterial, fungal, plant and insect POs all display similar di-copper centres with those of arthropod and mollusc Hcs (Fig. 1.5). Like most POs studied, Hcs incubated in the presence of detergents and/or proteinases can be activated to accommodate phenolic molecules (Decker et al., 2007a).

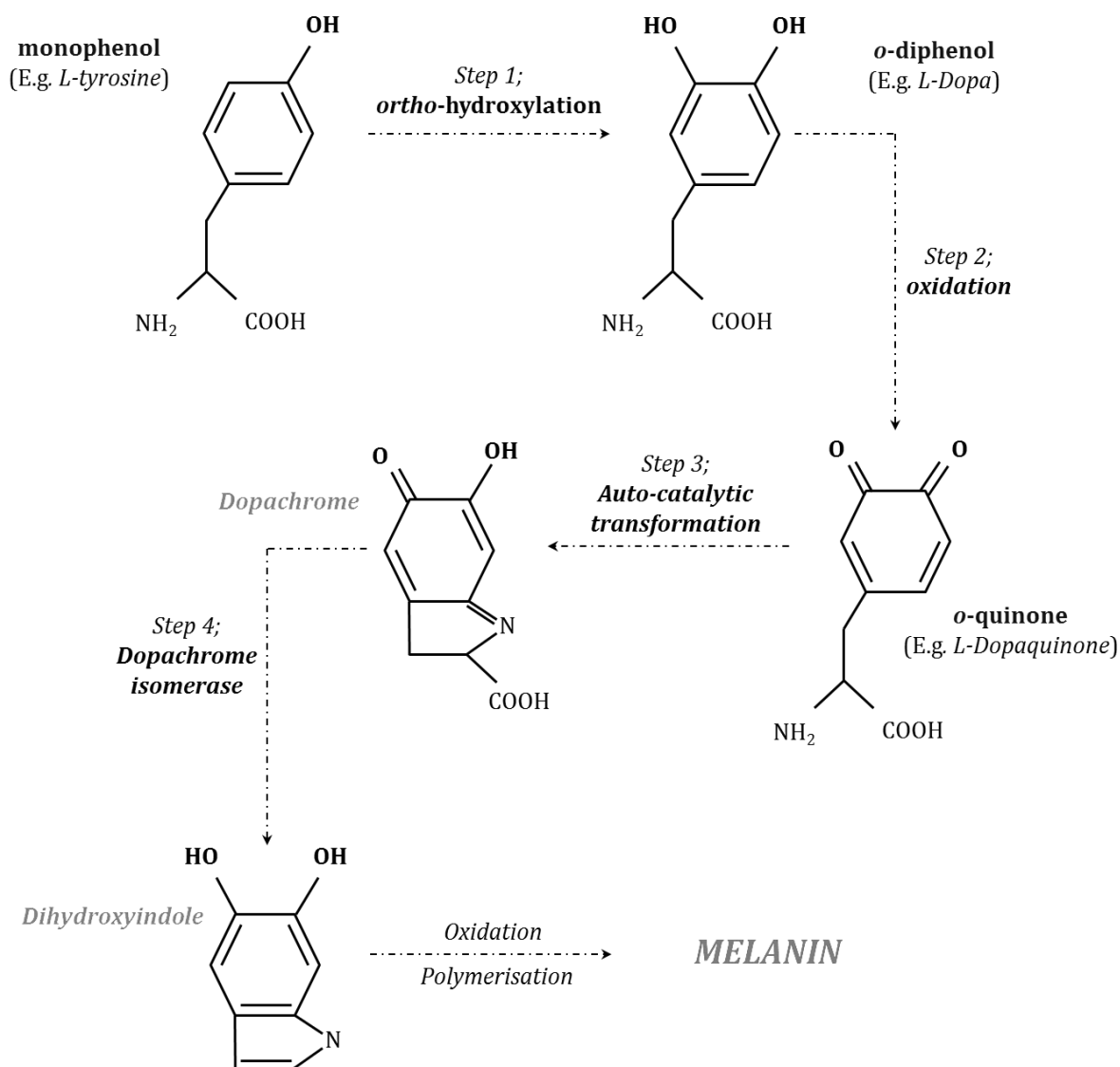


Figure 1.4 Emphasising tyrosinase and catecholoxidase activity in the biosynthesis of the chromogen, melanin. The above figure is a schematic representation of the steps associated with melanin synthesis in insects.

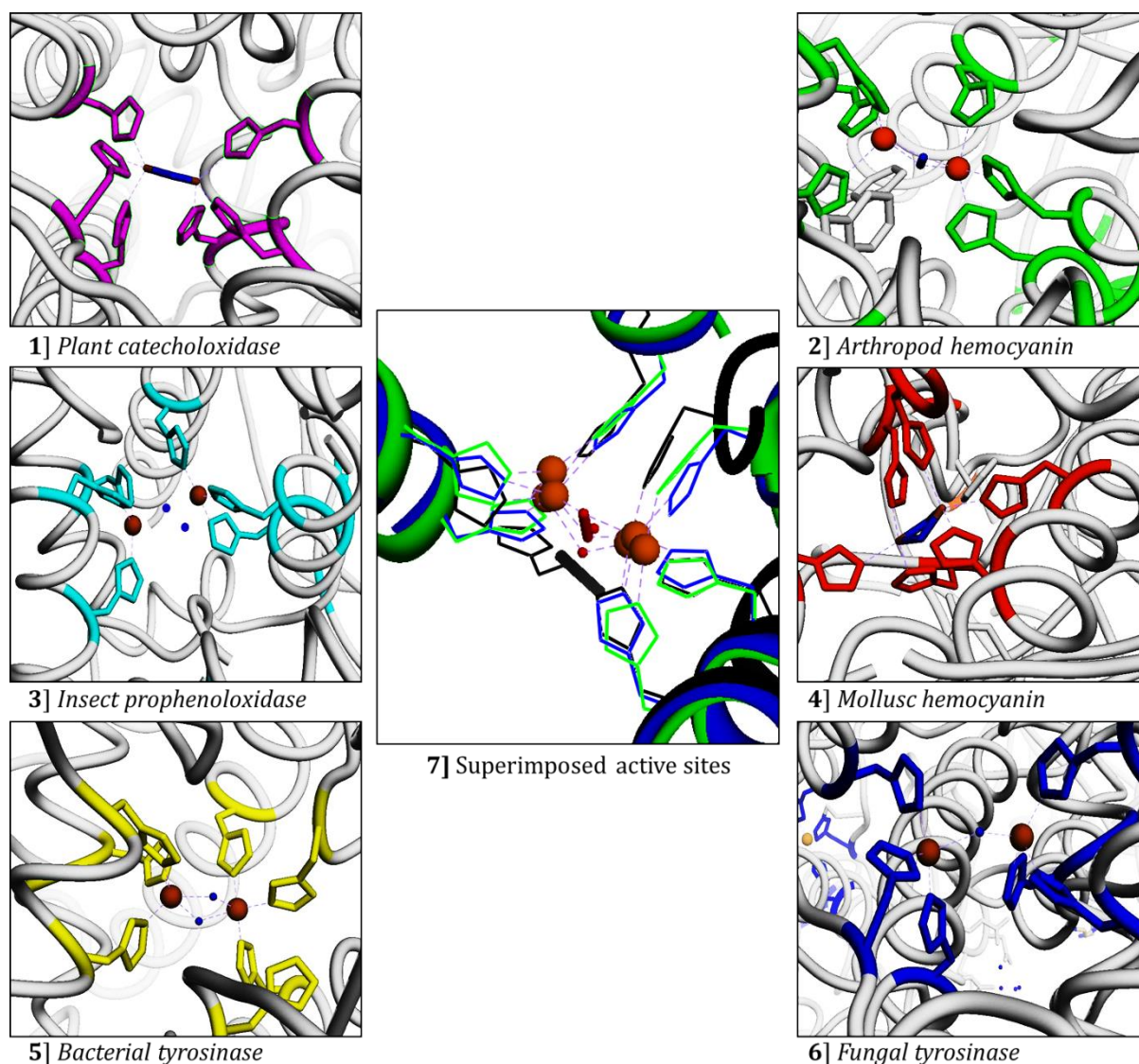


Figure 1.5 Active sites of six representative type-3 copper proteins. **1**, *Ipomoea batatas* catecholoxidase (PDB; 1BT3) **2**, *Limulus polyphemus* hemocyanin subunit II (PDB; 10XY) **3**, *Manduca sexta* prophenoloxidase (PDB; 3HHS) **4**, *Octopus dofleini* hemocyanin (PDB; 1JS8) **5**, *Streptomyces castaneoglobisporus* tyrosinase (PDB; 2ZMX) **6**, *Agaricus bisporus* tyrosinase (PDB; 2Y9W). **7**, Superimposed active sites of *L. polyphemus* hemocyanin (blue), *Manduca sexta* prophenoloxidase (green) and *Agaricus bisporus* tyrosinase (black). The dicopper atoms are depicted as orange spheres. Images were produced using UCSF Chimera molecular graphics software version 1.6.2.

1.3.2 On the presence of hemocyanin in invertebrates

Hc can be found in chelicerates, crustaceans, molluscs and larval stages of some insects (Sanchez et al., 1998). Interestingly, chelicerates possess Hc only, whereas crustaceans (and a small number of insects) possess Hc and PO. Chelicerates and crustaceans do not possess an open respiratory system (tracheal system) like insects, thus they depend almost entirely on Hc for their respiratory demands. For decades the accepted paradigm of the evolution of Hc in arthropods has entailed the loss of this particular protein in insects due to the development of a complex respiratory system, therefore, the presence of Hc is considered unnecessary (Burmester and Hankeln, 2007). Mollusc and arthropod Hcs are hypothesised to have evolved from two different ancestors, about 700-800 and 550-600 million years ago, respectively (Voit et al., 2000, Burmester, 2001, Lieb et al., 2000, van Holde et al., 2001).

Recently Pick et al., (2010) observed that the insect, *Blaptica dubia*, possesses Hc in early stages of development and stops synthesising the protein when they mature into adults. Hagner-Holler et al., (2004) observed an ancestral and functional hemocyanin in nymphs and adults of the stonefly *Perla marginata* that exhibits a high affinity for oxygen binding. The stonefly Hc consists of two subunits (Hc1 and Hc 2). Orthologous Hc subunits have been identified in the stonefly *Perla grandis*, the firebrat *Thermobia domestica* and the grasshopper *Schistocerca americana* (Fochetti et al., 2006, Pick et al., 2008, Sanchez et al., 1998). Hemocyanin present in adult stages of insects may be a remnant of early arthropod evolution and subsequent species divergence; this theory has been recently proposed by Pick et al., (2009), Amore et al., (2009) and Amore and Fochetti, (2009).

Theoretically, adult insects have no need for respiratory proteins as the open circulatory system they possess (tracheal system), provides adequate oxygen dispersion to all organs. However, insects in larval stages do not have a fully developed tracheal system, and this may be why Hc has been found in low amounts in larval and nymphal stages of development; utilised to temporarily aid gas transport. The majority of insect species that Hc has been detected in are incapable of flight. Furthermore, insects that can fly and have been shown to synthesise Hc, only possess Hc in larval stages of development. It has been suggested that Hc associated oxygen transport was an inadequate system to provide oxygen for the high demands of intense aerobic respiration needed for insect flight, leading to selection pressure that resulted in an open respiratory system.

A recent study carried out by Amore et al., (2009) investigated the functional role of hemocyanin found in the hemolymph of the stoneflies, *Dinocras cephalotes* and *Isoperla grammatica*. Using RT-PCR and bioinformatics they hypothesized that Hc may carry out a yet unknown physiological role, possibly similar to Hc-d PO activity observed in chelicerates (Amore and Fochetti, 2009). This theory remains untested.

1.3.3 Structural characteristics and putative function

Hcs are large multi-subunit enzymes, ubiquitous in crustacean, chelicerate and mollusc hemolymph. Hc is produced in the hepatopancreas (functionally equivalent to mammalian liver) and released into the hemolymph (Lee et al., 2004). Hc primarily functions as a carrier of molecular oxygen, reversibly binding peroxide in a $\mu: \eta^2-\eta^2$ side-on coordination between the two copper atoms (Cu A and Cu B) bound to a four α -helix

bundle and ligated by six highly conserved histidine residues (Decker et al., 2007a). Mammalian blood is red in colour due to the oxygenation of haemoglobin via Fe within the heme cofactor. In contrast, chelicerate and to a lesser extent crustacean hemolymph is blue in colour due to the conversion of Hc (containing a di-copper active site) from a deoxygenated (Cu I) state into an oxygenated (Cu II) state. The oxygenated state of Hc can be detected by an intense absorption peak at ~ 340 nm ($\epsilon = 20,000$ M⁻¹cm⁻¹) (Fig. 1.6) (Decker and Jaenicke, 2004). Hemocyanins are polar molecules with a predominantly negatively charged electrostatic surface. These properties improve the solubility and hydration of Hc in the hemolymph. Possessing a negatively charged surface limits Hc from associating with other negatively charged surfaces inside the organism, such as, the glycocalyx of cells bathing in hemolymph (Jaenicke and Decker, 2003).

The basic structure of arthropod Hc is hexameric in nature and is usually found as multiples of hexamers (2 x 6mer, 4 x 6mer, 6 x 6mer, and 8 x 6mer). Each arthropod Hc subunit ($\sim 70 - 75$ kDa) consists of three domains: domain I contains five to six α -helices, domain II contains a four α -helix bundle and domain III contains a seven stranded anti-parallel β -barrel. Domain II contains the di-copper active site (Decker et al., 2007a, Magnus et al., 1994, Hazes et al., 1993, Volbeda and Hol, 1989). Mollusc Hc can be found in the form of cylindrical decamers, didecamers or multiples of decamers. Each polypeptide subunit ($\sim 350 - 400$ kDa) possesses approximately seven or eight paralogous functional units (FU: FU-a – FU-h). Mollusc FUs are typically 50 kDa in size, however, the structure of FU-h is different to other FUs as it contains an additional stretch of ~ 100 amino acids located at the C-terminal end of the polypeptide, bringing the total molecular weight of FU-h to ~ 60 kDa (Lieb et al., 2000, Jaenicke et al., 2010).

Each FU is ordinarily composed of two domains, the α -domain consisting of a four α -helix bundle that includes the di-copper active site and the β -domain consisting of a seven stranded anti-parallel β -barrel. The α and β domains of mollusc Hc are functionally equivalent to domains II and III of the arthropod Hc subunit, respectively. Mollusc Hc can possess > 160 oxygen binding sites, whereas the largest known arthropod Hc (8 x6mer, from the horseshoe crab, *L. polyphemus*) contains 48 oxygen binding sites. The bi-nuclear copper active site and subsequent oxygen binding properties of both mollusc and arthropod Hcs are almost identical, however, their molecular structures differ substantially across all levels (Fig. 1.7) (Decker and van Holde, 2010, Decker et al., 2007a/b, Cuff et al., 1998).

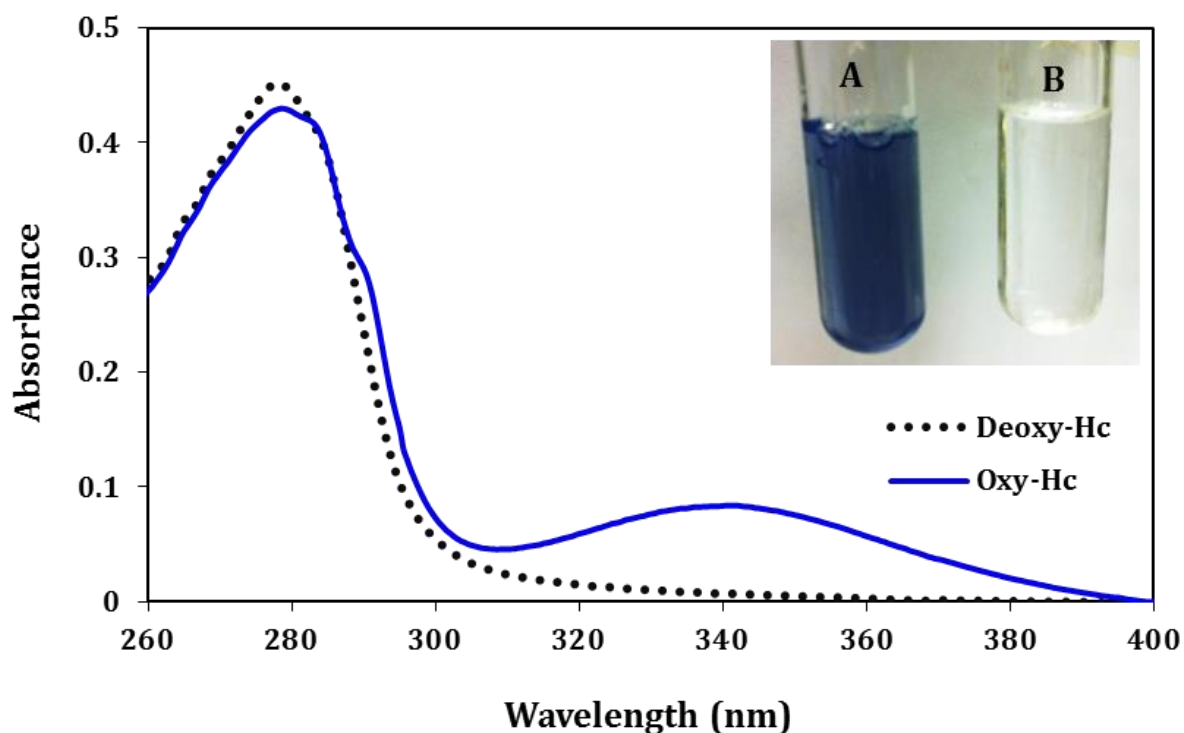


Figure 1.6 Absorption spectra of 0.3 mg mL^{-1} *Limulus polyphemus* hemocyanin in 100 mM Tris-HCl buffer, pH 7.5. The absorbance peak at $\sim 340 \text{ nm}$ observed for hemocyanin with dioxygen bound [$\text{Cu}^{\text{II}}\text{-O}_2\text{-Cu}^{\text{II}}$] is in contrast to the deoxygenated hemocyanin spectrum. Inset, A) an aliquot of oxygenated (blue) horseshoe crab hemolymph and B) an aliquot of deoxygenated (clear) horseshoe crab hemolymph. Deoxygenated hemocyanin was prepared using dialysis. Oxy-Hc in 100 mM Tris-HCl, pH 7.5 was dialysed against 100 mM Tris-HCl, pH 7.5 containing 20 mM EDTA, overnight at 4°C .

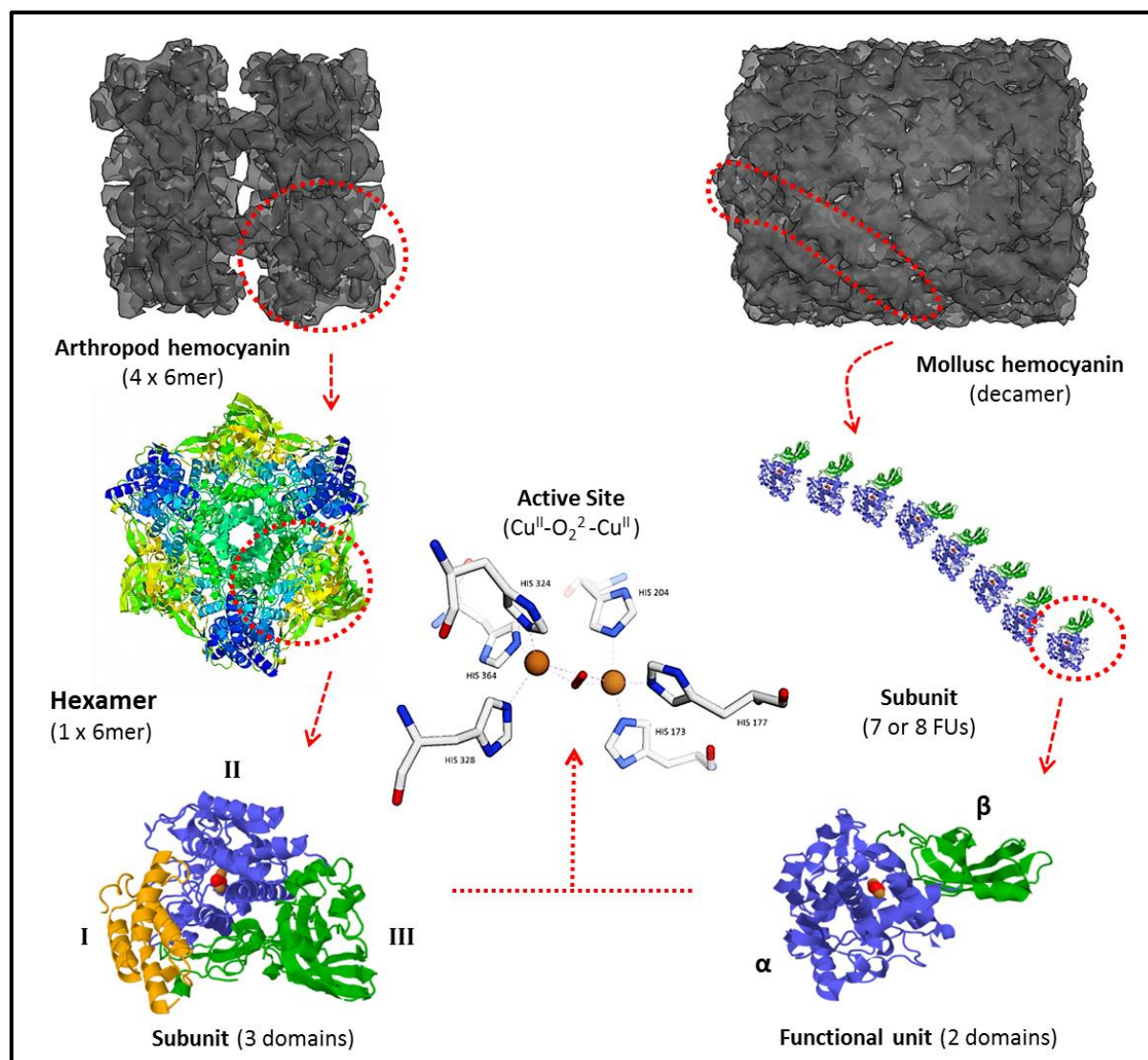


Figure 1.7 Structure of arthropod hemocyanin (PDB; 3IXV, 1LL1 and 10XY) and mollusc hemocyanin (PDB-1JS8 and EMD-1648). Also shown is the di-copper active site (with six conserved histidine residues), indicative of type three copper proteins (Copper atoms are a light brown colour and oxygen is depicted in red). Images were produced using UCSF Chimera and Jmol molecular graphics software versions 1.6.2 and 12.2.15, respectively.

1.3.4 Phenoloxidase and hemocyanin-derived phenoloxidase activity

PO enzymes are found in mammals, flora, invertebrates and microorganisms. Activated POs catalyse the initial steps in a series of enzymatic reactions of a biosynthetic pathway that will eventually lead to the formation of the pigment melanin (Cerenius and Soderhall, 2004). In insect and crustacean hemolymph, the activation of PO is coordinated by the proPO activation cascade. The proPO cascade is initiated as result of cuticular damage and/or the detection of microbes present in the hemolymph (Fig. 1.8). During a microbial or parasitic challenge, the recognition of PAMPs such as lipopolysaccharides and/or β -glucans via PRRs present in the hemolymph and on hemocyte plasma membranes, initiates a serine proteinase cascade (Cerenius and Söderhäll, 2004). Serine proteases cleave the inactive Pro-prophenoloxidase activating enzyme (pro-ppA) into an active pro-Phenoloxidase activating enzyme (ppA). Thus, ppA cleaves the inactive pro-Phenoloxidase (pro-PO) zymogen into an active PO enzyme. PO is released from specialised arthropod hemocytes (crystal cells) and deposited at the site of infection, damaged cuticle or during cell-mediated defences such as encapsulation and nodulation (Fig. 1.8). POs catalyse the oxidation of phenolic compounds into quinones. Non-enzymatic polymerisation of quinones results in the formation of melanin, which plays a vital role in the development and defence response of organisms (reviewed by Soderhall and Cerenius, 1998, Cerenius and Soderhall, 2004).

Over the last decade, a large number of publications have reported inducible PO activity of the respiratory protein Hc, *in vitro*. To date, Hc-d PO activity has been characterised in over 39 species of arthropods and molluscs (Table 1.1). It is considered that components similar to those associated with the proPO activation cascade are involved in the conversion of Hc into an immune enzyme, namely PO (Baird et al., 2007).

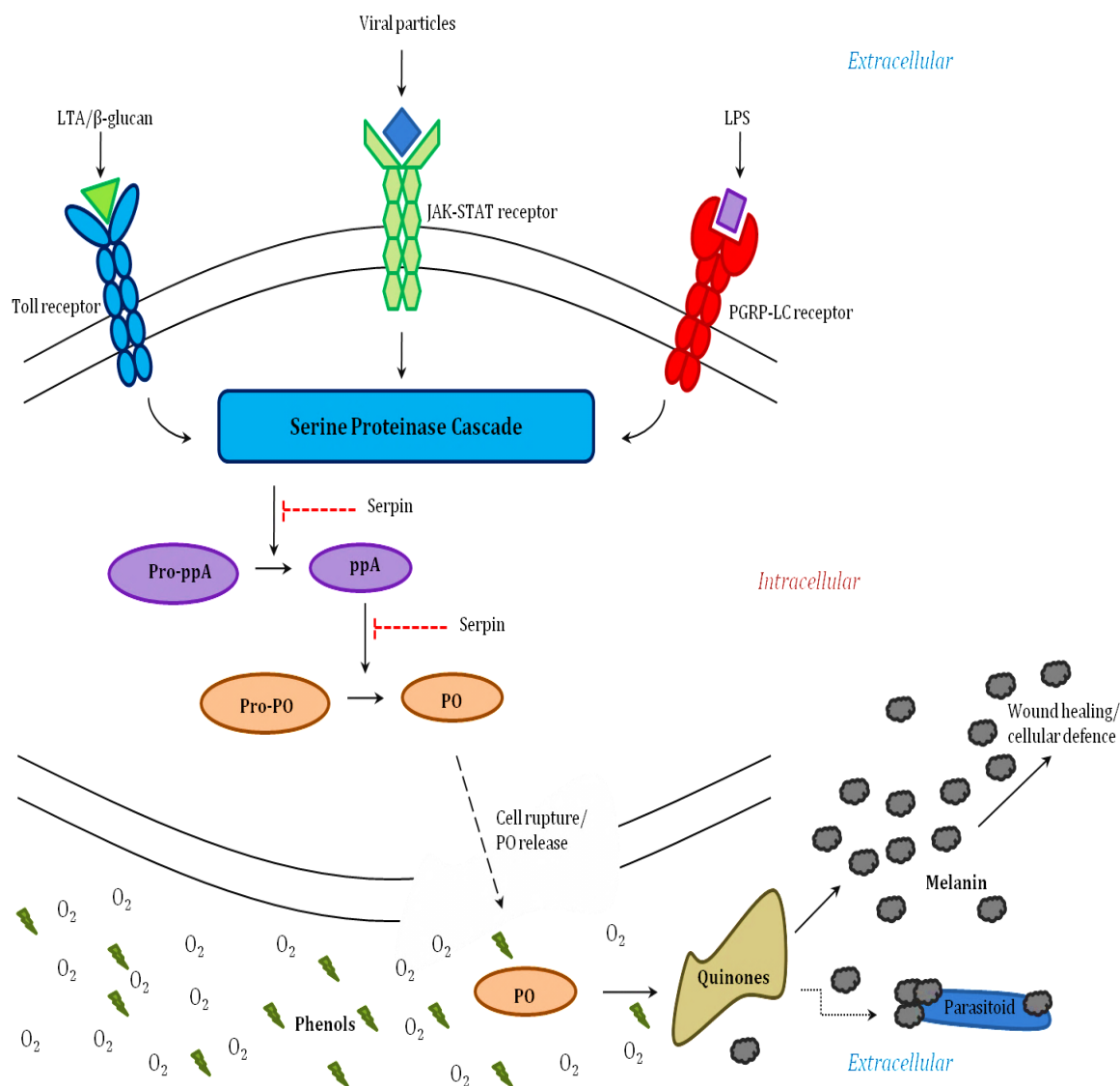


Figure 1.8 The proPO activation cascade in invertebrates. Microbial ligands are recognised by cellular receptors. A signal transduction cascade eventually leads to crystal-cell lysis and the subsequent release of activated phenoloxidase.

PO; phenoloxidase, Pro-ppA; pro-proPhenoloxidase activating enzyme, LPS; lipopolysaccharide, LTA; lipoteichoic acid and PGRP-LC; peptidoglycan recognition protein-LC.

Table 1.1 Known hemocyanin-derived phenoloxidase (Hc-d PO) activity in invertebrates

Species	Activity	Endogenous elicitors	Exogenous elicitors	References
Phylum Arthropoda				
<u>Chelicerata</u>				
<i>Carcinoscorpius rotundicauda</i>	CO	Subtilisin	LPS, LTA and microbial proteases [†]	Jiang et al., [2007]
<i>Eurypelma californicum</i>	TY & CO	Trypsin and chymotrypsin	SDS	Jaenicke and Decker, [2008], Baird et al., [2007], Decker et al., [2001], Decker and Rimke, [1998]
<i>Limulus polyphemus</i>	CO	PS, PI, L-PC, PE, PG, PC, trypsin, linoleate and linolenate	SDS and CPC	Coates et al., [2012], Coates et al., [2011], Baird et al., [2007], Decker et al., [2001], Nelliappan and Sugumaran [1996], Wright et al., [2012]
<i>Pandinus imperator</i>	TY & CO	-	SDS	Nillius et al., [2008], Baird et al., [2007]
<i>Tachyplesus tridentatus</i>	CO	Factor B, clotting enzyme, tachyplesin, PE, tachystatins [A, B, C], big defensin,	SDS	Nagai et al., [2001], Nagai and Kawabata [2000]
<u>Crustacea</u>				
<i>Astacus leptodactylus</i>	TY & CO	Trypsin	SDS	Jaenicke and Decker, [2004]
<i>Bathynomus giganteus</i>	CO	-	SDS	Terwilliger [2007], Pless et al., [2003]
<i>Calappa granulata</i>	CO	-	SDS	Jaenicke and Decker, [2004]
<i>Cancer magister</i>	CO	-	SDS	Terwilliger and Ryan, [2006] Decker et al., [2001]
<i>Cancer pagarus</i>	CO	Trypsin	SDS	Jaenicke and Decker, [2004], Bhagvat and Richter [1938]
<i>Carcinus aestuarii</i>	CO	-	-	Salvato et al., [1998]
<i>Carcinus maenas</i>	CO	Trypsin	SDS and perchlorate	Jaenicke and Decker, [2004], Zlateva et al., [1996]
<i>Cirolana harfordi</i>	CO	-	SDS	Terwilliger, [2007]
<i>Charybdis japonica</i>	TY & CO	Hemocyte lysate supernatant and trypsin	SDS and urea	Fan et al., [2009]
<i>Erimacrus isenbeckii</i>	CO	Trypsin	SDS, LPS and LTA	Kim et al., [2011]
<i>Homarus americanus</i>	CO	Trypsin	SDS and perchlorate	Jaenicke and Decker, [2004], Zlateva et al., [1996]
<i>Litopenaeus vannamei</i>	CO	Trypsin		Yan et al., [2008] [∞]
<i>Nephrops norvegicus</i>	TY & CO	-	SDS	Gimenez et al., [2010]/Chapter 3
<i>Pacifastacus leniusculus</i>	CO	Trypsin	-	Lee et al., [2004]
<i>Palinurus elephas</i>	TY & CO	Trypsin	SDS	Jaenicke and Decker, [2004,]

Table 1.1 continued...

<i>Panulirus argus</i>	CO	Trypsin and chymotrypsin	SDS	Perdomo-Morales et al., [2008]
<i>Panulirus interruptus</i>	CO	Trypsin	SDS	Jaenicke and Decker, [2004]
<i>Paralithodes camtschaticae</i>	CO	Trypsin	SDS	Jaenicke and Decker, [2004]
<i>Parapenaeus longirostris</i>	CO	-	SDS	Martinez-Alvarez et al., [2008]
<i>Penaeus japonicus</i>	TY & CO	Hemocyte lysate supernatant	SDS, Lam and isopropanol	Adachi et al., [2005a, 2003, 2001]
<i>Penaeus vannamei</i>	TY & CO	Trypsin and chymotrypsin	SDS, isopropanol, acetone and methanol	Garcia-Carreno et al., [2008]
<i>Porcellio scaber</i>	CO	Hemocyte lysate supernatant	SDS	Jaenicke et al., [2009]
<i>Portunus trituberculatus</i>	TY & CO	-	Urea	Fujieda et al., [2010a, 2010b]
<i>Potamon potamion</i>	CO	-	SDS	Jaenicke and Decker, [2004]
<i>Scylla serrata</i>	-	-	-	Chen et al., [2009] [∞]
Phylum Mollusca				
<u>Cephalopoda</u>				
<i>Octopus vulgaris</i>	TY & CO	-	Tween ₂₀ , urea and hexafluoroisopropanol	Campello et al., [2008], Suzuki et al., [2008] Morioka et al., [2006], Salvato et al., [1998, 1983]
<i>Sepia officinalis</i>	CO	Subtilisin	-	Siddiqui et al., [2006]
<i>Sepioteuthis lessoniana</i>	TY	-	-	Nakahara et al., [1983]
<u>Gastropoda</u>				
<i>Haliotis diversicolor</i>	CO	-	-	Peng et al., [2010] [∞]
<i>Helix aspersa</i>	CO	-	SDS	Decker et al., [2001]
<i>Helix pomatia</i>	TY & CO	Subtilisin	-	Siddiqui et al., [2006], Bhagvat and Richer [1938]
<i>Helix vulgaris</i>	CO	-	-	Hristova et al., [2008]
<i>Oncomelania hupensis</i>	CO	α-chymotrypsin	SDS and urea	Guo et al., [2009]
<i>Rapana thomasi</i>	CO	Subtilisin	SDS	Idakieva et al., [2009]*
<i>Rapana venosa</i>	CO	Trypsin	SDS and urea	Dolashki et al., [2011], Hristova et al., [2008]

CPC-cetylpyridinium chloride, SDS-sodium dodecylsulphate, CO-catecholoxidase, TY-tyrosinase, PS-phosphatidylserine, PI-phosphatidylinositol, PG-phosphatidylglycerol, PE-phosphatidylethanolamine, L-PC-lyso-phosphatidylcholine, PC-phosphatidylcholine, LPS-lipopolysaccharide, LTA-lipoteichoic acid and LAM-laminarin. * indicates that freeze thawing [lyophilisation] of Hemocyanin induces phenoloxidase activity. [∞] indicates the abstract is not available in English. [†] indicates microbial proteases; PAE from *Pseudomonas aeruginosa*, Proteinase K from *Tritirachium album* and type XIV protease of *Streptomyces griseus*. N.B. Subtilisins are purified from *Bacillus* species, however, they are used to represent potential endogenous inducers like trypsin and chymotrypsin).

1.3.5 Exogenous versus endogenous activation

Under certain conditions, Hc can display PO activity *in vitro*. Hc is converted into a PO-like enzyme either through proteolytic treatment (e.g. trypsin, microbial proteases) or via physical disruption of protein conformation using detergents, solvents, salts and/or phospholipids (Table 1.1). It is commonplace to use low concentrations of SDS to assess enzymatic activity of PO enzymes (Decker and Jaenicke 2004). The anionic detergent, SDS, has demonstrated on numerous occasions the ability to induce PO activity of Hc (Decker and Rimke, 1998, Decker et al., 2001, Baird et al., 2007, Decker et al., 2007a, 2007b). High concentrations of the denaturant will lead to the unfolding of the enzyme and concurrently induce PO activity in Hc for a short period of time before it is denatured completely. However, at low concentrations, SDS induces a conformational change in Hc that allows phenolic molecules access to the catalytic site for an extended period of time. A thorough study carried out by Baird et al., (2007), demonstrated that SDS micelles induce optimal PO activity in three checlicerate Hcs. Concentrations of SDS above critical micelle concentration resulted in subtle secondary and tertiary structural changes that permit substrate access to the dicopper centre and possibly mimic *in vivo* conformational changes necessary for the induction of Hc-d PO activity.

Nagai and Kawabata (2000) recorded PO activity of horseshoe crab (HSC) Hc in the presence of a clotting enzyme, with optimal activation of Hc achieved using a 1:1 stoichiometry of Hc : clotting enzyme. Subsequently in 2001, Nagai and co-workers exposed HSC Hc to chitin-binding amphiphilic anti-microbial peptides (AMPs) such as tachyplesin, and recorded PO activity. The interaction between Hc and tachyplesin seems to involve the hydrophobic side of tachyplesin, as site directed mutagenesis of tryptophan and tyrosine residues led to a severe reduction in tachyplesin affinity for Hc.

The authors postulated that *in vivo* during wound healing, AMPs bind to the internal chitin of the horseshoe crab. These chitin bound AMPs provide a platform for Hc to attach. Upon attachment to the AMPs, Hc undergoes a conformational change leading to PO activity, resulting in the formation of melanin that is subsequently used to coat the clot constructed during wound healing. This theory is supported by studies indicating Hc's involvement in wound healing and hormone transport (ecdysone binding properties) (Nagai and Kawabata, 2000, Jaenicke et al., 1999 Adachi et al., 2005b).

Even though the exposure of Hc to a number of endogenous molecules (coagulation factors, hemocyte components, etc.) can lead to PO activity *in vitro* (Table 1.1), the *in vivo* activation of Hc-d PO remains poorly characterised. Nellaiappan and Sugumaran (1996), recorded PO activity in *L. polyphemus* hemolymph in the presence of a number of phospholipids and fatty acids. They assumed the activity was derived from a PO enzyme, however, no PO has been identified in any chelicerate studied, therefore, the activity recorded is most likely derived from Hc. Furthermore, the fatty acids and phospholipids used in this study were dissolved in EtOH, making it difficult to determine the effects of these molecules on Hc activation, as EtOH is a known activator of both PO and Hc-d PO (reviewed by Decker and Jaenicke, 2004).

In vitro, SDS micelles promote optimal Hc-d PO activity; based on this information, membrane phospholipids in the form of small unilamellar vesicles (SUVs, i.e. liposomes) have been investigated as potential endogenous activators of Hc-d PO (Chapter 2). Rationally, phospholipids in liposome form share similar structural and electrostatics with SDS micelles. Moreover, phospholipids, particularly phosphatidylserine (PS), have been shown previously to induce PO activity in the fruit fly, *Drosophila melanogaster* (Bilda et al., 2009).

1.3.6 Mode of activation and the di-copper active site

Based on a vast number of publications and the recent availability of insect proPO crystal structures, it is widely considered that in true PO enzymes and in Hcs, the removal of an amino acid 'placeholder' residue from the proximity of the dicopper centre permits bulky phenolic molecules access to the active site which can be turned over and products released (Baird et al., 2007, Decker et al., 2007a, Jaenicke and Decker, 2008, Nillius et al., 2008). A phenylalanine residue in arthropod Hc (Fig. 1.9a) and a leucine residue in mollusc Hc have been identified as placeholders (Decker et al., 2007b). Proteolytic treatment of Hc appears to remove the N-terminus of arthropod Hc subunits and the C-terminus of mollusc Hc FUs, which contain the respective placeholder residues. On the other hand, treatment with detergents is thought to disrupt protein conformation, dislocating the placeholder residue, thus creating a subtle opening for substrate access (Decker et al., 2007a). With respect to proPOs, a caddie protein interacts with proPO, seemingly blocking the di-copper active site with a tryptophan or tyrosine residue (Fig 1.9b). The removal of this caddie protein is necessary for the conversion of the inactive proPO zymogen into active PO (Decker and Rimke, 1998).

1.3.7 Hemocyanin as a precursor of antimicrobial peptides

Not only can Hc-d PO activity be induced by amphiphilic antimicrobial peptides, Hc has also been observed to function as a precursor of antibacterial and antifungal peptides in crustaceans. Destoumieux-Garzón et al., (2001) isolated two peptides from the hemolymph of *Penaeus stylirostris* and a single peptide from *P. vannamei* hemolymph. The purified peptides demonstrated strict fungicidal activity. The peptides displayed up to 100 % sequence similarity with a region on the C-terminus of their respective Hcs,

and upon microbial infection, a significant increase in peptide concentrations were observed in the hemolymph. Sequence comparisons have confirmed that these peptides are products of Hc, resulting from an uncharacterised proteolytic cleavage. Similarly, Lee et al., (2003) isolated a peptide consisting of 16 amino acid residues, known as Astacidin 1, from the hemolymph of the crayfish, *Pacifastacus leniusculus*. Astacidin 1 displays potent bactericidal activity. Lee and co-workers demonstrated that the peptide is derived from the C-terminus of crayfish Hc and is present as a β -sheet structure in citric acid buffer, pH 4. Astacidin 1 concentration increased significantly in the hemolymph of shrimp exposed to microbial ligands. It is believed that a cysteine-rich proteinase, under acidic conditions, cleaves the crayfish hemocyanin in order to produce Astacidin 1 during infection.

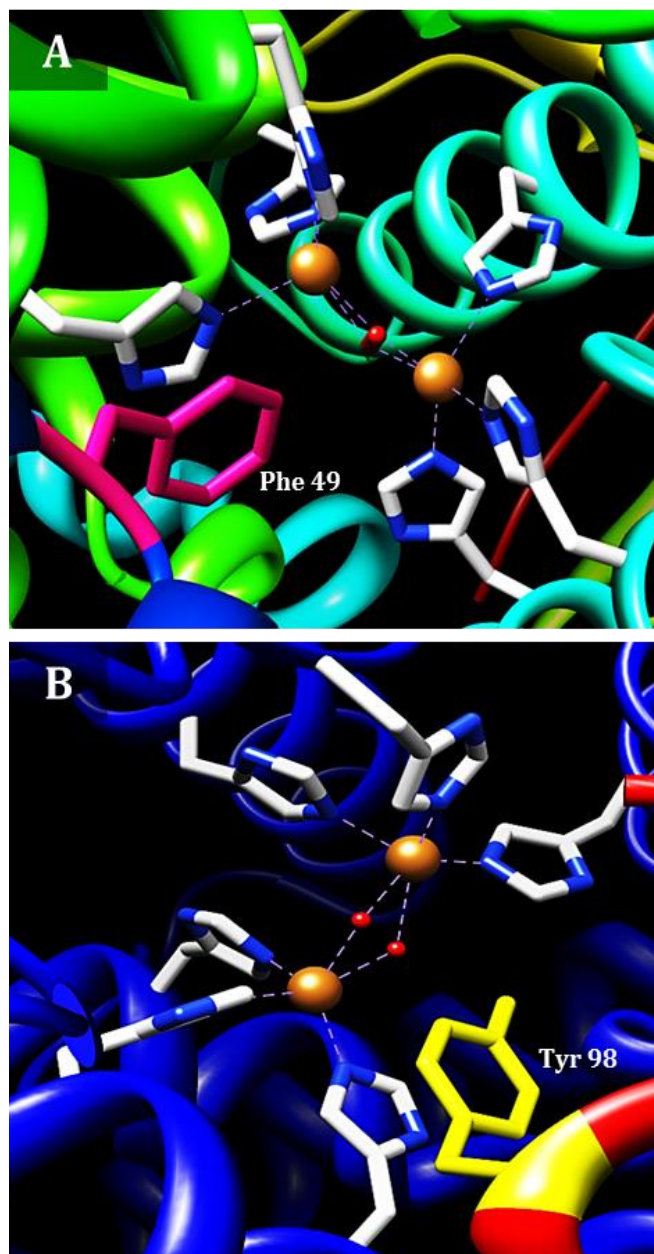


Figure 1.9 View of the active site of type-3 copper proteins with placeholder residues present. **A)** *Limulus polyphemus* hemocyanin subunit II (PDB; 10XY). The placeholder residue, Phe 49, is coloured pink. **B)** *Streptomyces castaneoglobisporus* tyrosinase (PDB; 2ZMX). The placeholder residue, Tyr 98, is coloured yellow. Histidine residues are grey and blue in colour, Cu atoms are presented as brown spheres and oxygen is coloured blue. Images were produced using UCSF Chimera molecular graphics software version 1.6.2.

1.3.8 Antiviral properties of hemocyanin

Whilst attempting to obtain novel antiviral proteins from white spot syndrome virus (WSSV) infected shrimp, *Penaeus monodon*, Zhang et al., (2004a) purified peptides (73 kDa and 75 kDa) coupled to virus particles that were subsequently identified as Hc in origin. Upon further investigation, purified Hc demonstrated non-specific antiviral properties against a range of cultured DNA and RNA fish viruses (Table 1.2), with no measureable cytotoxicity against host cells. The Hc peptides neutralised the viruses and prevented replication. Recently, Lei et al., (2008) pre-incubated white-spot syndrome virus (WSSV) particles with purified *Penaeus japonicus* Hc (PjHc) prior to infection, resulting in a ten-fold reduction in viral load present in the gills, in contrast to control shrimp that had received a non-pre-treated WSSV infection. Furthermore, upon monitoring Hc subunit transcriptional regulation during viral infection, it was demonstrated that subunit PjHcY expression remained unchanged, conversely, PjHcL expression increased significantly during viremia. This unusual difference in antiviral properties of arthropod Hc subunits has also been recorded for mollusc Hc subunits. Dolashka-Angelova et al., (2009) recorded antiviral activity of whelk (*Rapana venosa*) Hc against respiratory syncytial virus (RSV). Only glycosylated FU RvH-c was effective against RSV, whereas non-glycosylated FU RvH-b and native Hc were not. Dolashka et al., (2010) further emphasized the importance of glycosylation of *R. venosa* Hc FUs in antiviral defence, as only glycosylated FU RvH2-e demonstrated activity against HSV virus type 1. Interestingly, Dolashka et al., (2010) carried out a screen of glycans present on *R. venosa* Hc subunits and found that a number of carbohydrate chains present on FUs may associate with regions of glycoproteins found on HSV, either by interactions with specific residues or through less specific van der Waals interactions.

Differences in the oligosaccharide content of Hc subunits may be partly responsible for their varying antiviral potency and warrants further investigation.

Pan et al., (2005) carried out a genetic screen on WSSV infected shrimp, *P. japonicus*. Of eight novel immune-related genes that were observed to significantly increase in expression upon infection, Hc was the second most up-regulated (β -glucan binding protein was the first). Other studies have demonstrated similar increases in Hc mRNA expression in response to viral infection. *Macrobrachium rosenbergii* nodavirus (MrNV) and extra small virus (XSV) infected shrimp demonstrated an increase in expression of proPO and Hc mRNA (Ravi et al., 2010), similarly, exposure of red swamp crayfish *Procambarus clarkii* to WSSV led to an increase in Hc mRNA expression levels (Shi et al., 2010). The aforementioned studies did not investigate whether an increase in Hc mRNA expression correlated with a concurrent increase in Hc present in the hemolymph. An increase in mRNA expression does not necessarily lead to an increase in the synthesis of the respective protein, however, Rattanarojpong et al., (2007) and Bourchookarn et al., (2008) recorded an increase in Hc synthesis (via 2-D gel electrophoresis) in the hemolymph of *P. vannamei* and *P. monodon* in response to yellow head virus (YHV) infection, respectively. In 2009, Havanapan et al., recorded an increase in C-terminus fragments of Hc present in the hemolymph of *P. vannamei*, during Taura syndrome virus (TSV) infection, concomitantly, the N-terminus fragments of Hc were down regulated. Further analysis showed a switch in the isoelectric point of C-terminal fragments to a more acidic *pI* due to phosphorylation of serine residues.

Interestingly, extracellular regulated kinase 1/2 (ERK 1/2) was recorded to increase in expression during viral infection. Hc from TSV infected shrimp co-immunoprecipitated with ERK 1/2 (Havanapan et al., 2009). ERK enzymes are known to play a key role in

innate immunity (Garcia-Garcia et al., 2008). Motif scans of shrimp Hc revealed a potential ERK D-domain positioned at **V527**, between **R520** and **S534** on the C-terminal end of the protein. Havanapan and co-workers (2009) postulated a novel role for Hc in innate immunity, through the regulation of ERK signalling pathways during immune challenge. These findings further illustrate a broad role for Hc in anti-viral defence and highlight potential alternative strategies for enhancing cultured shrimp resistance to disease.

Table 1.2 Hemocyanin derived immune-functionality (*aside from inducible phenoloxidase activity, Table 1.1*)

Species	Immune activity	Hemocyanin aggregation state	Target	Reference
Phylum Arthropoda				
<i>Carcinoscorpius rotundicauda</i>	Production of ROS	8 x 6mer [assumed]	<i>P. aeruginosa</i> and <i>S. aureus</i>	Jiang et al., [2007]
<i>Litopenaeus setiferus</i>	Induction of ROS	Hc -like lectin [291 kDa]	<i>L. setiferus</i> hemocytes	Alpuche et al., [2009]
<i>Litopenaeus vannamei</i>	Agglutinative	Dodecamer	<i>V. parahaemolyticus</i> , <i>S. aureus</i> and mammalian RBCs	Pan et al., [2008]
<i>Litopenaeus vannamei</i>	Agglutinative	Hc-IgA like protein [~ 75 kDa]	<i>Vibrio</i> , <i>Aeromonas</i> and <i>Pseudomonas</i> sps., and mammalian erythrocytes	Zhang et al., [2006a & b]
<i>Litopenaeus vannamei</i>	Agglutinative	Multimer (<i>SNP's on C-terminus</i>)	<i>Vibrio</i> , <i>Aeromonas</i> and <i>Staphylococcus</i> sps.	Zhao et al., [2012]
<i>Litopenaeus vannamei</i>	Antibacterial?	Hc-fragment (28.5 kDa)	<i>Vibrio parahaemolyticus</i>	Zhang et al., [2008]
<i>Litopenaeus vannamei</i>	Hemolytic/Opsonising	Multimer, Hc oligomers [~ 150-230 kDa]	Mammalian erythrocytes	Zhang et al., [2009]
<i>Pacifastacus leniusculus</i>	Antibacterial	Hc derived peptide [1.945 kDa]	<i>B. megaterium</i> and <i>E.coli</i>	Lee et al., [2003]
<i>Penaeus japonicus</i>	Antiviral	Multimer and subunits [PjHc-L & PjHc-Y]	WSSV	Lei et al., [2008]
<i>Penaeus monodon</i>	Antiviral	Hc peptides [73 and 75 kDa]	SGIV, FV3, LDV, ThRV, ABV and IPNV	Zhang et al., [2004]
<i>Penaeus stylirostris</i>	Antifungal	Hc derived peptides [7.9, 8.3 kDa]	<i>F. oxysporum</i>	Destoumieux-Garzon et al., [2001]
<i>Penaeus vannamei</i>	Antifungal	Hc derived peptide [2.7 kDa]	<i>F. oxysporum</i>	Destoumieux-Garzon et al., [2001]
<i>Penaeus vannamei</i>	Agglutinative	Hc multimer	Mammalian erythrocytes	Zhang et al., [2005]
<i>Penaeus vannamei</i>	Signalling-ERK1/2	C-terminal Hc fragments	TSV	Havanapan et al., [2009]
<i>Scylla serrata</i>	Agglutinative	Hc multimer and 76 kDa subunit	<i>Vibrio</i> sps. <i>A. hydrophila</i> <i>E. coli</i> K12 and <i>S. aureus</i> .	Yan et al., [2011]
Phylum Mollusca				
<i>Octopus maya</i>	Agglutinative	Hc-like agglutinin [66 kDa]	Mammalian erythrocytes	Alpuche et al., [2010]
<i>Rapana venosa</i>	Antiviral	Subunits [glycosylated RvH2-e and RvH-c]	HSV-1 and RSV	Dolashka et al., [2010], Dolashka-Angelova [2009]

Abbreviations; angelfish birnavirus [ABV], extracellular signal regulated kinase [ERK], frog virus 3 [FV3], Herpes simplex virus type1 [HSV-1], infectious pancreatic necrosis virus [IPNV], lymphocystis virus [LDV], respiratory syncytial virus [RSV], Singapore grouper virus iridovirus [SGIV], Taura syndrome virus [TSV], threadfin reovirus [ThRV] and white spot syndrome virus [WSSV], reactive oxygen species [ROS], red blood cells [RBCs], reactive oxygen species [ROS]

1.3.9 Hemocyanin and the production of reactive oxygen species

Hc was isolated from the hemolymph of the Mangrove horseshoe crab, *Carcinoscorpius rotundicauda* and exposed to a range of microbial proteases and ligands *in vitro*, which resulted in the production of reactive oxygen species (ROS) and the simultaneous induction of Hc-d PO activity (Jiang et al., 2007). As PO enzymes catalyse the initial steps in melanin synthesis, quinone derivatives can enter enzymatic/non-enzymatic redox cycling pathways with their respective semi-quinone counterparts, leading to the production of cytotoxic ROS (Bogdan et al., 2007). ROS production by *C. rotundicauda* Hc was induced in the presence of intact microorganisms, especially pathogenic strains that secrete extracellular proteases. Both Gram-positive and Gram-negative bacteria induced Hc derived ROS, providing an instant anti-microbial assault against invading microbes. In the same study, mammalian hemoglobin treated with microbial proteases, produced ROS and displayed anti-microbial properties, also (Jiang et al., 2007). The data discussed here, hints at an evolutionary ancient mode of immune-surveillance present in invertebrates and mammals.

A Hc-like lectin purified from the hemolymph of *Litopenaeus setiferus* binds to a glycoprotein receptor on the plasma membrane of activated granular hemocytes *in vitro* and induces the production of ROS via an NADPH oxidase complex and accompanying oxidative pathways (Alpuche et al., 2009). The lectin-carbohydrate interaction appears to be mediated by carboxyl and N-acetylated groups of sugars (such as N-acetylneuraminic acid). The production of ROS is an important component of the invertebrate immune response (Bogdan, 2007) and has been used successfully as an indicator of immune competence in shrimp (Yon-Chin et al., 2008).

1.3.10 Immunoglobulin-like domains and agglutination behaviour of hemocyanin

Numerous proteins present in invertebrate hemolymph, namely opsonins and lectins, agglutinate/immobilise microbes in preparation for host cell derived defences, such as encapsulation and phagocytosis. Lacking a true adaptive immune response and therefore, the ability to produce specific antibodies, invertebrates possess proteins that belong to the Immunoglobulin superfamily (IgSF). Hc (~ 75 kDa) purified from the hemolymph of shrimp, *Litopenaeus vannamei*, was identified as an IgA like protein due to the presence of a conserved Ig domain, located at the C-terminus (Zhang et al., 2006). Using immunoblot analysis, the purified Hc cross reacted with both goat anti- human IgA and rabbit anti-shrimp Hc on independent occasions. Previously, Zhang et al., (2004b) purified Hc from *Penaeus vannamei* hemolymph and characterised an IgG like domain, consisting of ~ 252 amino acids, present at the C-terminus also. Further analysis of shrimp Hc confirmed that Hc shares four conserved regions with human Ig-heavy chain and a single conserved region on the Ig kappa chain.

Incubation of shrimp Hc with eight different species of pathogenic bacteria and animal erythrocytes, *in vitro*, resulted in the gross aggregation of the cells (Zhang et al., 2006). Hc induced agglutination of microbial and mammalian cells can be inhibited by a variety of saccharides, indicating a carbohydrate interaction between Hc and the target-cell plasma membrane. This agglutination behaviour of shrimp Hc (as well as reactivity with an Ig domain) is characteristic of IgSF molecules and further supports a role for Hc in invertebrate innate immunity. In a subsequent study, Pan et al., (2008) demonstrated that both hexameric and dodecameric oligomers of *L. vannamei* Hc could bind to bacteria and mammalian red blood cells (RBCs), however, only the Hc dodecamer could agglutinate the RBCs. Considering that a dodecamer conformation potentially offers at least two carbohydrate binding sites, whereas a hexameric conformation only contains

one, it would appear that, a dodecamer optimises the number of bacteria that can be immobilised by Hc during sepsis. More recently, Fan et al., (2011) demonstrated agglutinating activity of *Scylla serrata* Hc against seven different bacterial species. *S. serrata* Hc subunits demonstrated differential agglutinating properties (that could be inhibited by numerous saccharides), with the 75 kDa subunit showing optimal activity. Using mutant strains of *E. coli* (Δ OmpA and Δ OmpX), Fan and co-workers confirmed that ligand interactions between specific bacterial outer membrane proteins and Hc were essential for the agglutination of target cells.

Interestingly, Alpuche et al., (2010) purified a 66 kDa (3 x 22 kDa subunit) lectin from the hemolymph of *Octopus maya* that agglutinated a range of mammalian erythrocytes and demonstrated a dependence on the orientation of hydroxyl/amine groups of C2 sugars for successful agglutination to occur. The presence or absence of divalent cations (such as Ca^{2+} and Mg^{2+}) had no measureable effect on agglutination behaviour. This Octopus lectin showed no sequence identity to any known lectin, but showed partial identity to *Octopus dofleini* Hc, particularly with the tyrosinase domains and copper A and B sites.

1.3.11 Hemolytic behaviour of shrimp hemocyanin

Hc purified from the hemolymph of shrimp, *L. vannamei*, not only demonstrates agglutination behaviour (Zhang et al., 2006) but also demonstrates hemolytic activity against mammalian erythrocytes (Zhang et al., 2009). Hc subunits and oligomers induced erythrocyte cell rupture via the formation of ion permeable pores. Hemolytic activity of Hc was dependent on temperature, pH and divalent cation concentration (particularly calcium). The addition of osmoprotectants (sucrose and polyethylene glycol (PEG)) to the hemolysis assay inhibited cell rupture, providing evidence of a

colloid-osmotic lysis mechanism. There are two hallmarks of colloid-osmotic lysis of erythrocytes; 1) osmotic stabilisation of erythrocytes can be achieved in the presence of sucrose and PEG and 2) pre-lytic swelling of cells (Harris et al., 1991). Further research is needed to fully characterise the hemolytic ability of shrimp Hc.

1.3.12 Hyperpigmentation in crustaceans; hemocyanin versus phenoloxidase

Hyperpigmentation (or melanosis) in farmed and fresh caught shellfish (notably shrimp) is a non-infectious condition that causes cuticular darkening in the form of black spots; consequently, the displeasing aesthetics lead to a severe reduction in market value (Adachi et al., 2001). Traditionally, sulfiting compounds have been used to inhibit hyperpigmentation. One such sulfiting compound, sodium metabisulphite, is a known allergen, and has been linked with occurrences of occupational asthma (Steiner et al., 2008). Heeding both health concerns and shellfish sustainability issues there is a pressing need for natural, safe and effective inhibitors of shellfish hyperpigmentation.

While many inhibitors of hyperpigmentation have been used throughout the shellfish industry, the true causative agent of hyperpigmentation remains uncertain. Generally, inhibitors are considered to target PO enzymes, although, recent evidence suggests that Hc is also targeted by PO inhibitors (Garcia-Carreño et al., 2008, Martínez-Alvarez et al., 2008).

Hc is a more stable protein compared to PO, demonstrating retention in enzymatic activity upon exposure to extreme temperature and pH shifts (reviewed by Decker et al., 2007, Kim et al., 2011). The development of novel, safe and efficacious inhibitors of hyperpigmentation in shellfish would be of significant commercial importance. The stability of cellular PO and Hc-d PO of hemolymph extracted from the langoustine *Nephrops norvegicus* has been investigated (Chapter 3), in order to find the true cause of

hyperpigmentation in shellfish. A range of known PO inhibitors have been employed in order to screen for potential Hc-d PO specific inhibitors.

1.4 Summary

Once considered a primordial response, lacking complexity and sophistication, innate immunity of arthropods shares great mechanistic, biochemical and molecular similarities with those of mammals. Significant progress has been made over the last few decades, however, many aspects of arthropod immunity have been examined using favoured insect models, and to a lesser extent, crustaceans. In order to truly evaluate immune-function in arthropods, the study of a greater diversity of species is warranted.

It is now recognised widely that Hc acts as a multi-resource/function enzyme in invertebrates, being utilised for a plethora of physiological and immunological processes, when required. Even though certain advances have been made over the last decade in characterising the switch of Hc from a respiratory protein to an immune-enzyme, the *in vivo* activation and regulation of these processes are lacking in detail. Chapters 2, 3 and 6 provide new insight into the structure-function relationship of Hc-d PO from two arthropods, *L. polyphemus* and *N. norvegicus*.

Furthermore, almost six decades after Frederick Bang's initial discovery (1956) of hemolymph clotting in *L. polyphemus*, the amebocyte derived clotting cascade continues to receive substantial attention because of its economic and biomedical importance. In contrast, the alternative immune functions of amebocytes, such as phagocytosis and hemostasis, have received little attention by comparison. Chapters 4, 5 and 6 provide new insight into the maintenance of amebocytes *in vitro*, their phagocytic properties, their possible contribution towards Hc activation (*in vivo*) and their significance in monitoring captive horseshoe crabs.

Chapter 2:

Phospholipid Induced Conformational Changes in *Limulus polyphemus* Hemocyanin; Putative Natural Activators of Hemocyanin-derived Phenoloxidase Activity

A version of this chapter has been published;

Christopher J. Coates, Sharon M. Kelly* and Jacqueline Nairn. 2011. Possible role of phosphatidylserine–hemocyanin interaction in the innate immune response of *Limulus polyphemus*. *Developmental and Comparative Immunology*. 35 (2), 155-163.

*S.M. Kelly provided training with circular dichroism and performed experiments.

2.1 Abstract

Phenoloxidase enzymes and the associated pro-phenoloxidase activation cascade play an essential role in the immune response of arthropods. Phenoloxidase activity can be elicited in the oxygen carrier, hemocyanin, by the addition of the artificial inducer, SDS. There is some evidence to support hemocyanin acting as a phenoloxidase *in vivo*; however, the identity of natural activators remains unclear. This chapter explores the role of a number of phospholipids, notably phosphatidylserine, as possible natural activators of hemocyanin-derived phenoloxidase activity. Characterisation of the structural changes associated with activation of hemocyanin-derived phenoloxidase suggests that phospholipids induce similar conformational changes to those caused by the artificial inducer, SDS. Preliminary investigations on the nature of the interaction between hemocyanin and phosphatidylserine are presented also. It is proposed that anionic phospholipids, in particular phosphatidylserine, may act as natural activators of hemocyanin-derived phenoloxidase, *in vivo*.

2.2 Introduction

It is now well documented that it is possible to change the function of hemocyanin, *in vitro*, from an oxygen carrier to an enzyme activity that plays a key role in invertebrate innate immunity, namely phenoloxidase (PO) (E.C. 1.10.3.1) (Decker et al., 2007). One of the most effective activators of hemocyanin-derived PO activity, *in vitro*, is the artificial inducer, SDS. It has been demonstrated previously that SDS-induced PO activation in chelicerate hemocyanin is associated with conformational changes which enhance substrate access to the di-copper centre of this protein (Baird et al., 2007). It is assumed that the presence of SDS mimics the effects of putative natural activators present in arthropod hemolymph, such as small antimicrobial peptides (Nagai et al., 2001), fatty acids and phospholipids (Baird et al., 2007).

The phospholipid phosphatidylserine (PS) is normally located on the inner surface of the cell plasma membrane but in cells entering the apoptotic pathway, PS appears on the outer surface of the membrane. Exposure of PS on the outer membrane of the cell surface is considered a hallmark of programmed cell death in eukaryotes. It has been proposed that release of inner membrane phospholipids, including PS, during apoptosis leads to the activation of pro-phenoloxidase (proPO) in insects and crustaceans (Bilda et al., 2009, Sugumaran and Nellaiappan, 1990 and Sugumaran and Nellaiappan, 1991). Findings presented here suggest that PS may elicit PO activity in Hc, a type 3 copper protein which is structurally related to proPO (Zlateva et al., 1996 and Decker and Tucek, 2000). This chapter presents an analysis of hemocyanin-derived PO activity, and associated conformational changes, in hemocyanin from *Limulus polyphemus*, caused by the addition of the putative natural activator of PO activity, phosphatidylserine (PS).

2.3 Materials and Methods

2.3.1 Purification of *Limulus polyphemus* hemocyanin

Hemolymph was obtained via cardiac puncture (Fig. 2.1) using sterile 16 gauge needles (BD Microlance 3). Extracted hemolymph was centrifuged immediately at $500 \times g$ for 5 min at 4 °C to remove the cellular fraction. The supernatant was centrifuged at $400,000 \times g$ at 4 °C for 90 min and Hc pellets were re-suspended in stabilisation buffer (5 mM CaCl₂, 5 mM MgCl₂, 100 mM Tris-HCl, pH 7.5), yielding partially purified Hc. Partially purified Hc was applied to a Sephacryl S-500 HR (120 cm \times 1.6 cm) gel filtration column (GE Healthcare), previously equilibrated with stabilisation buffer. The gel filtration column was calibrated using Blue Dextran (2 MDa), thyroglobulin (670 kDa) and apoferritin (450 kDa). The protein concentration was determined by UV absorbance measurements at 280 nm, using the value of 1.39 for the absorbance of a 1 mg mL⁻¹ solution of Hc from *L. polyphemus*, in a quartz cuvette with pathlength 1 cm. Purified Hc was characterised by 280 nm: 350 nm absorption ratio values and by SDS-PAGE. Fractions with a 280 nm:350 nm absorption ratio value of 4.2, indicative of oxy-hemocyanin, were pooled and analysed by SDS-PAGE (4–12% NuPAGE-Novex, Bis-Tris gels (Invitrogen)). Peptide mass fingerprinting (Fingerprints Proteomics Facility, University of Dundee) was used to confirm the identity of protein species separated by SDS-PAGE.

2.3.2 Preparation of phospholipids

L- α -Phosphatidyl-L-serine from soybean (PS; P0474), L- α -phosphatidylinositol (PI; P0639) and 1-palmitoyl-sn-glycero-3-phosphocholine (L-PC; L5254) were purchased from Sigma-Aldrich Chemical Company Ltd. Phospholipid stock solutions were prepared in 100 mM Tris-HCl, pH 7.5 at concentrations of 1 mg mL⁻¹. Re-suspended

phospholipids were placed in a water bath and sonicated (Decon FS 200 frequency sweep) at room temperature for no more than 1 h. Sonicated phospholipids were stored at 4 °C under nitrogen gas. Phospholipid solutions were passed through 0.1 µm pore syringe filters (Anotop 10, Whatman) 6 times in order to remove large unilamellar vesicles. Phospholipids were added to PO assays to the following final concentrations: PS at 0–20 µg mL⁻¹ (0–25.6 µM), PI at 10 µg mL⁻¹ (11.7 µM) or LPC at 10 µg mL⁻¹ (20.2 µM).

2.3.3 Dynamic light scattering

All dynamic light scattering measurements were recorded at 20 °C on a Malvern, Zetasizer Auto Plate Reader (50 mW 830 nm Laser). A 50 µL sample of 10 µg mL⁻¹ phospholipid, in 100 mM Tris-HCl, pH 7.5, was placed in a single unit on a 384 well plate. Similar conditions were used to analyse Hc at 1 mg mL⁻¹, in 100 mM Tris-HCl, pH 7.5, in the absence and presence of phospholipids (final concentration of 10 µg mL⁻¹). Particle size measurements were recorded using 13 scans of 10 s duration over a period of approximately 10 min. Equipment was cleaned using 6 M guanidine HCl, 10% Decon, 0.1 M HCl and 0.1 M NaOH prior to use.

2.3.4 Phenoloxidase assay measurements

Spectrophotometric determination of phenoloxidase activity was carried out at 20 °C in a 96-well plate (MDS VERSA max microplate reader). Each assay (100 µL volume) consisted of 2 mM dopamine hydrochloride in 100 mM Tris-HCl, pH 7.5 and *Limulus* Hc at a final concentration of 1 mg mL⁻¹. Hc was pre-incubated for 10 min with phospholipids at concentrations ranging from 0 to 20 µg mL⁻¹ or with the anionic detergent SDS at a concentration of 3.5 mM. PO activity was initiated by the addition of

dopamine. PO activity was detected by observing an increase in absorbance at 475 nm arising from the formation of dopachrome and its derivatives. One unit is defined as 1 μmol of dopachrome formed per minute, with an absorption coefficient for dopachrome at this wavelength of $3600 \text{ M}^{-1} \text{ cm}^{-1}$. PO activity of Hc in the presence of PS and increasing concentrations of NaCl (0 – 500 mM) were monitored in order to investigate the nature of the Hc-PS interaction. Control assays consisting of Hc in the absence of activators were recorded.

2.3.5 Circular dichroism

CD spectra were recorded on a Jasco J-810 spectropolarimeter at 20 °C. 1S-(+)-10-camphorsulphonic acid was used to calibrate the spectropolarimeter. All spectral measurements were carried out using 100 mM sodium phosphate buffer, pH 7.5. In all far and near UV experiments, each measurement was corrected by the subtraction of a spectrum of buffer alone.

Spectra in the far UV region (180–260 nm) were recorded in quartz cylindrical cells of pathlength 0.02 cm at a protein concentration of either 0.3 mg mL^{-1} , or 0.4 mg mL^{-1} . Data were analysed over the wavelength range 195–240 nm with DICHROWEB, using SELCON 3 and protein reference 3 to determine the secondary structure content. Samples of Hc (0.3 mg mL^{-1}), in the presence of $10 \mu\text{g mL}^{-1}$ phospholipids or 3.5 mM SDS, were pre-incubated for 10 min before CD measurements were recorded. In each case, 4 scans were recorded (and averaged) at a scan rate of 10 nm/min with a time constant of 2 s. Samples of Hc (0.4 mg mL^{-1}) were pre-incubated for 10 min in the presence of increasing concentrations of PS (0–20 $\mu\text{g mL}^{-1}$) before CD measurements were recorded. In each case, 4 scans were recorded (and averaged) at a scan rate of 50 nm/min with a time constant of 0.5 s.

Spectra in the near UV region (250–400 nm) were recorded in a quartz rectangular cell of pathlength 1 cm using a protein concentration of 0.4 mg mL⁻¹. Samples of Hc (0.4 mg mL⁻¹) were pre-incubated for 10 min in the presence of increasing concentrations of PS (0–20 µg mL⁻¹) prior to CD measurements. In each case 1 scan was recorded at a scan rate of 10 nm min⁻¹ with a time constant of 2 s.

2.3.6 Fluorescence spectroscopy

All experiments were recorded on a Perkin Elmer LS50 spectrofluorimeter at 20 °C. Fluorescence intensity was recorded using a quartz cuvette of 1 mL capacity at a protein concentration of 0.1 mg mL⁻¹ in 100 mM sodium phosphate buffer, pH 7.5, with a 5 nm bandwidth for the excitation and emission

- I. Intrinsic tryptophan fluorescence from 300 nm – 510 nm was detected using an excitation wavelength of 290 nm. Increasing concentrations of PS (0–20 µg mL⁻¹), PI (0–10 µg mL⁻¹), LPC (0–10 µg mL⁻¹) or SDS (3.5 mM) were incubated with Hc for 10 min prior to fluorescence measurements. Fluorescence emission maxima of Hc in the presence of PS and increasing concentrations of NaCl (0 – 500 mM) were recorded to investigate the nature of the Hc-PS interaction.
- II. Histidine fluorescence (Cu(II) quenching of active site residues) from 400 nm – 510 nm was detected using an excitation wavelength of 330 nm. All phospholipids (10 µg mL⁻¹) and SDS (3.5 mM) were incubated with Hc for 10 min prior to analysis.

All scans were recorded at a rate of 50 nm min⁻¹ and corrected by the subtraction of a spectrum of buffer/activator alone. Control experiments indicated that phospholipids, SDS and NaCl made no measureable contributions to the fluorescence signals.

2.3.7 Absorption spectroscopy

Absorption spectra of Hc samples were recorded on an Ultrospec 2100 *pro* UV/Visible spectrophotometer over the range of 240–380 nm. The properties of the copper binding site of Hc were monitored via the absorption peak at 340 nm which is characteristic of type three copper proteins. The effects of increasing concentrations of PS (0–20 $\mu\text{g mL}^{-1}$), PI (10 $\mu\text{g mL}^{-1}$), LPC (10 $\mu\text{g mL}^{-1}$) and SDS (0–3.5 mM) on absorption spectra were determined by incubating 0.3 mg mL^{-1} Hc for 10 min prior to absorption spectra measurements.

2.3.8 Conductivity measurements

The conductivity of 100 mM Tris-HCl, pH 7.5 in the absence and presence of increasing concentrations of sodium chloride (0 – 500 mM) were recorded at room temperature using a Portland Electronics Conductivity meter; Model P335. The fine and coarse temperature settings were 10°C and 55°C, respectively, using a scale of 0 – 30 mmho. The electrode was placed in 5 mL of sample and left for 5 min to equilibrate before values were recorded.

2.3.9 Statistical analysis

All phenoloxidase enzyme assays were performed in triplicate on three independent occasions. Results are expressed as the mean \pm standard error. Assays were analysed using ANOVA. Differences were considered significant at $p \leq 0.05$.

2.4 Results

2.4.1 Purification of hemocyanin from *Limulus polyphemus*

The success of Hc purification was judged by the 280 nm: 350 nm absorption ratio values (Fig. 2.1A) and by SDS-PAGE (Fig. 2.1B). A 280 nm: 350 nm absorption ratio value of 4.2 was obtained, which is characteristic of type 3 copper proteins and reflects values previously obtained in similar studies (Zlateva et al., 1996). SDS-PAGE indicated the presence of Hc subunits with a molecular mass of 70 kDa and 72 kDa (identity confirmed by peptide mass fingerprinting; Appendix A), with little sign of degradation or presence of contaminants. Typically, 200 mg of Hc was purified from 10 mL of hemolymph (Table 2.1). Dynamic light scattering experiments produced a calculated radius of gyration for the purified *L. polyphemus* Hc of 7.46 nm, suggesting that Hc was present in hexameric form ($4 \times 6mer = \sim 1.68 \text{ MDa}$). This is in good agreement with the Sephacryl S-500HR gel filtration elution volume which suggested an overall native molecular mass of 1.7 MDa. The minor species, which eluted from the S-500HR gel filtration column with an apparent molecular mass of $\sim 350 \text{ kDa}$, contained both Hc and C-reactive protein.

2.4.2 Nature of phospholipids

Dynamic light scattering experiments were used to characterise the nature of the prepared phospholipids. The calculated radius of gyration of the prepared phospholipids was 10–15 nm, indicating the presence of liposomal structures (Appendix B).

SEC and SDS Purification Gel

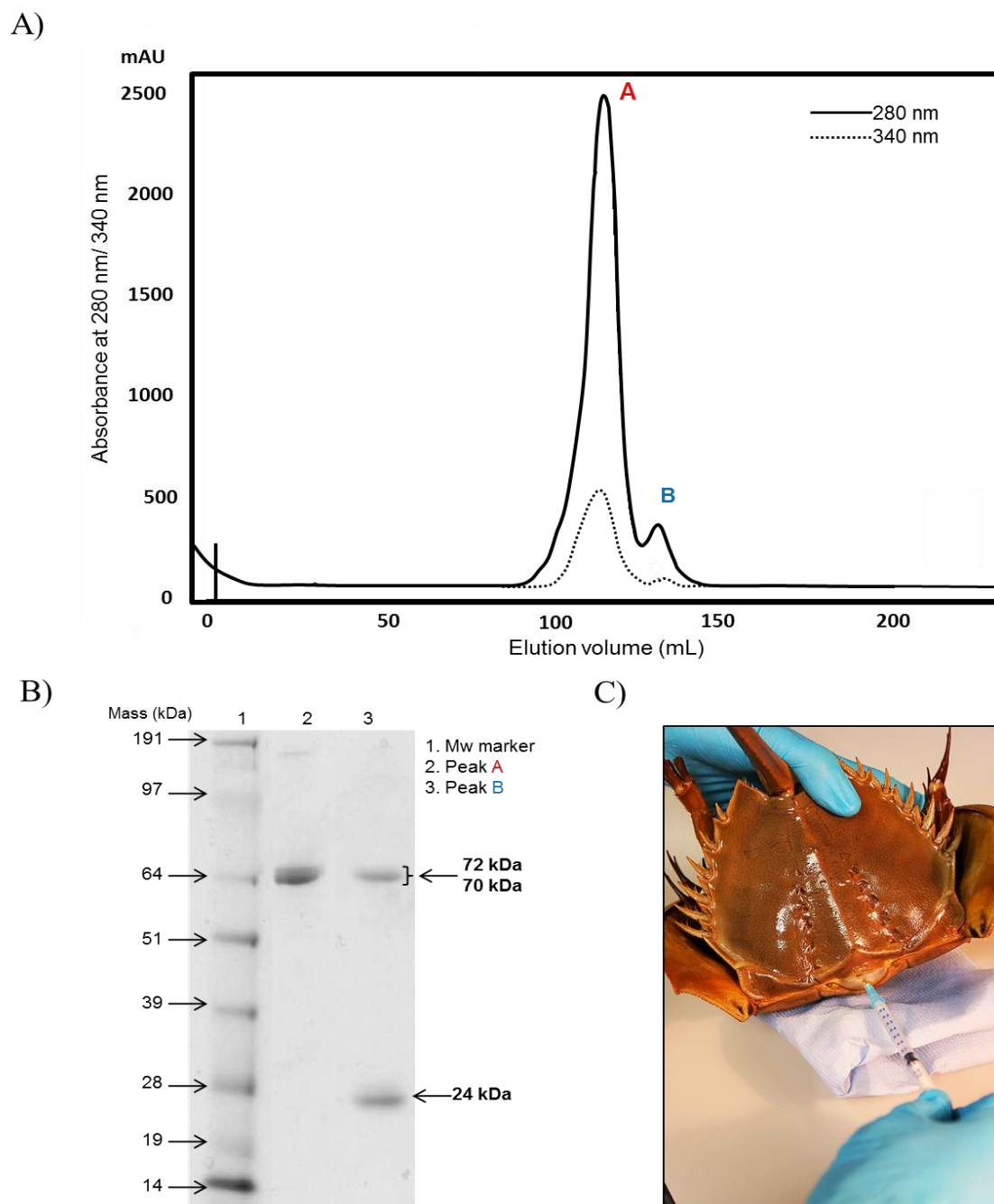


Figure 2.1 Purification of hemocyanin from *Limulus polyphemus*. **A)** Sephacryl S-500 HR size exclusion chromatogram of purified hemocyanin. There are two peaks present; peak A is hemocyanin, whereas peak B is hemocyanin and C-reactive protein. Fractions from peak A with a 280 nm: 340 nm absorption ratio value of 4.2 (hemocyanin) were pooled. **B)** SDS-PAGE analysis of purified *L. polyphemus* hemocyanin. Lane 1, molecular weight markers, lane 2, main peak (A), lane 3, minor peak (B). Each lane was loaded with 2 μ g of protein. Peptide mass fingerprinting identified subunit bands of 70 kDa and 72 kDa as hemocyanin and subunit band of 24 kDa as C-reactive protein. **(C)** Extraction of horseshoe crab hemolymph through the arthroidal membrane.

Table 2.1 Purification of hemocyanin from *Limulus polyphemus*, for 1 mL of hemolymph

	Protein conc. (mg mL ⁻¹) ^a	Percentage dioxygen bound ^b	Ratio (280 nm : 350 nm)	Total PO (U)	Specific activity (U mg ⁻¹)	Yield (%)
Hemolymph (acellular)	48	100%	4.3	133.92	2.79	100
Supernatant (centrifuged at 400,000g)	1.56	2.2%	44.6	0.84	0.54	3.25
Pellet (semi-purified)	43.3	96%	5	122.5	2.83	90.2
Peak fractions [†] (gel filtration)	4.1	100%	4.2	77.7	3.16	51.25

^a, hemocyanin concentration was determined as outlined in section 2.3.1

^b, values were calculated from the A 350 nm signal.

[†], each of the individual fractions (3 x 2 mL) had an absorbance ratio value of 4.2.

2.4.3 Phospholipid induced phenoloxidase activity

Previous data suggested that SDS induction of PO activity in Hc, which is accompanied by a conformational change, is optimal in the presence of the micellar form of SDS (Baird et al., 2007). In the search for a natural activator which would mimic SDS micelles, the ability of phospholipid liposomes to induce PO activity in Hc have been tested. PO assay measurements in the presence of phospholipids typically found in *L. polyphemus* amebocytes (MacPherson et al., 1998) indicated that they induced PO activity (Fig. 2.2). Control assay measurements indicated that phospholipids failed to oxidise dopamine in the absence of Hc. In the present study results suggest that the anionic phospholipids, phosphatidylserine (PS) and phosphatidylinositol (PI) are more effective at activating PO activity than the neutral lyso-phosphatidylcholine (PC). Under the conditions used, PS (10 µg/mL) induced 80% of the activity achieved with SDS micelles. In an attempt to determine the optimal concentration of PS required for PO activation, PO activity was monitored over a range of PS concentrations (Fig. 2.3). The PO activity increased with PS concentrations over the range 0–20 µg/mL PS; however, it proved technically challenging to explore the effects of higher concentration of PS due to the difficulties associated with PS solubilisation at concentrations in excess of 20 µg/mL in the assay. PS concentrations of 20 µg/mL induced 4.3 U of dopachrome formation, a value which represents 90% of the activation achieved with optimal micellar concentrations of SDS (3.5 mM). The structural changes associated with PS induction of PO activity in Hc were subsequently explored using a range of biophysical techniques.

Footnote 1; Images of phospholipids were obtained, and modified, from Avanti Polar lipids Inc. <http://avantilipids.com/> 2012

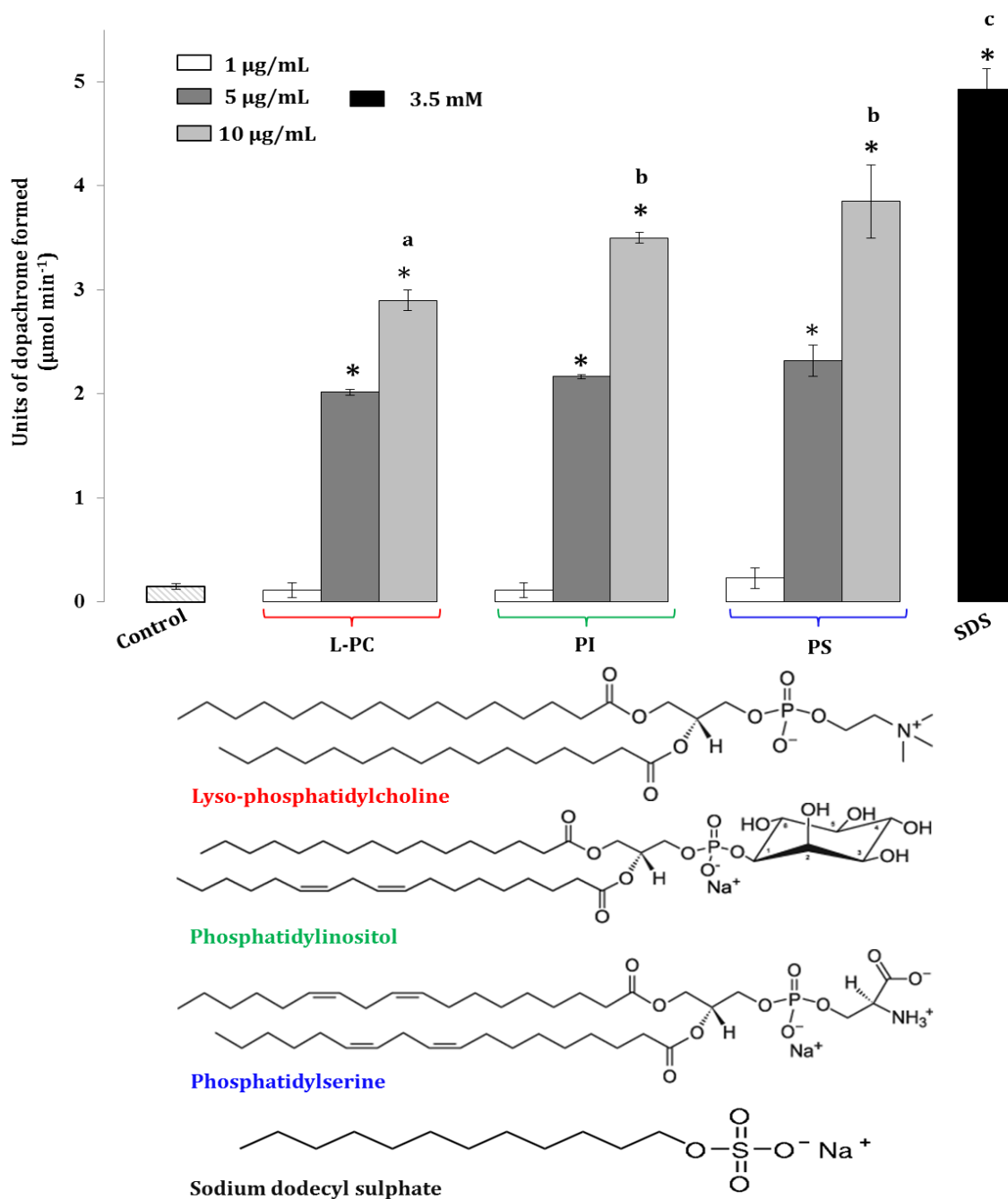


Figure 2.2 Phospholipid induced phenoloxidase activity of hemocyanin from *Limulus polyphemus*. Assays included 2 mM dopamine and 1 mg/mL hemocyanin, in 100 mM Tris-HCl, pH 7.5. Hemocyanin was pre-incubated for 10 min with either phospholipids or SDS. Phenoloxidase activity was initiated by the addition of substrate. Assays were recorded over a 6 min period. The histogram illustrates an increase in absorbance at 475 nm resulting from the formation of dopachrome and its derivatives. The control assay consisted of hemocyanin and substrate in the absence of an activator. Inset; molecular structures of phospholipids and SDS¹. A significant increase in phenoloxidase activity relative to the control at $p < 0.05$ is indicated by *. Letters common between each treatment indicate no significant difference.

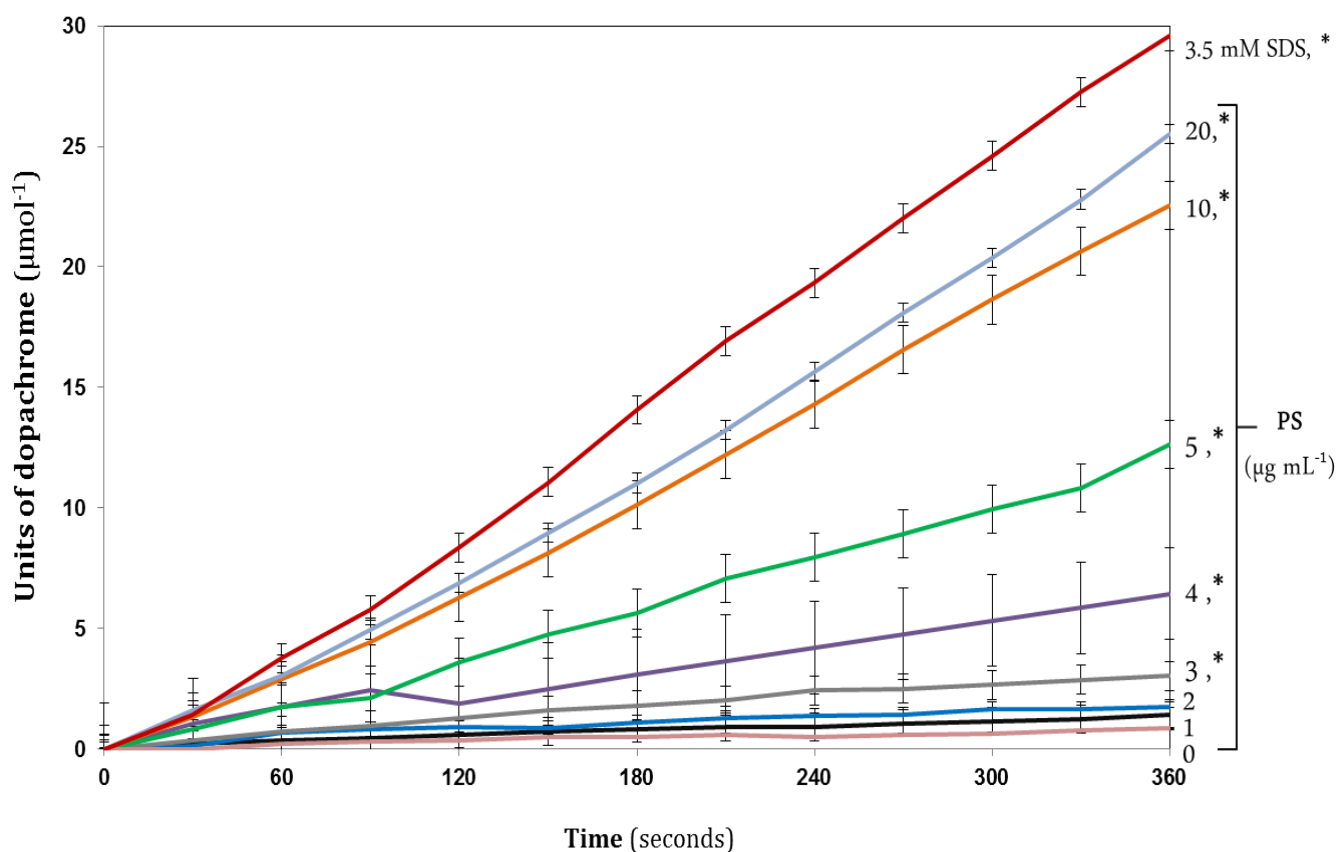


Figure 2.3 Phosphatidylserine induced phenoloxidase activity of hemocyanin from *Limulus polyphemus*. Hemocyanin was pre-incubated with increasing concentrations of phosphatidylserine ($1 \mu\text{g mL}^{-1}$ (black), $2 \mu\text{g mL}^{-1}$ (blue), $3 \mu\text{g mL}^{-1}$ (grey), $4 \mu\text{g mL}^{-1}$ (purple), $5 \mu\text{g mL}^{-1}$ (green), $10 \mu\text{g mL}^{-1}$ (orange), $20 \mu\text{g mL}^{-1}$ (light blue) and 3.5 mM SDS (red)). Typical assays consisted of 1 mg mL^{-1} hemocyanin and 2 mM dopamine in 100 mM Tris-HCl, pH 7.5. Phenoloxidase activity was initiated with the addition of substrate. The control (pink) consisted of hemocyanin and substrate in the absence of an activator. A second control was performed in the absence of hemocyanin, yielding comparable data to the control illustrated in the graph. A significant increase in phenoloxidase activity compared to the control at $p < 0.05$ is indicated by *.

2.4.4 Effect of phospholipids on secondary structure

Far-UV CD spectra (Fig. 2.4 and Fig 2.5) indicate that the presence of phospholipids induced conformational changes in Hc which are similar to the changes observed in the presence of micellar SDS (Baird et al., 2007). The anionic phospholipids, PS and PI, produced changes which were most similar to those observed with SDS; however, the change in molecular ellipticity at 205 nm was less pronounced. Analysis of the data over the wavelength range 195–240 nm using DICHROWEB suggested that, in the presence of phospholipids, the α -helical content of Hc increased, the β -sheet content decreased and the unordered structure content remained unchanged (Table 2.2). PS induced an increase in the α -helical content of Hc similar to that observed with SDS. Prolonged (2 days) incubation of Hc with the phospholipids resulted in no further change in the far-UV CD spectra indicating that the conformation associated with the activated state of Hc is stable in the presence of phospholipids. Activity measurements also indicated that prolonged incubation with PS resulted in activity retention, ~15% following 2 days incubation with PS. This is in contrast to prolonged incubation of *L. polyphemus* Hc with micellar SDS which results in denaturation and complete loss of activity (Baird et al., 2007).

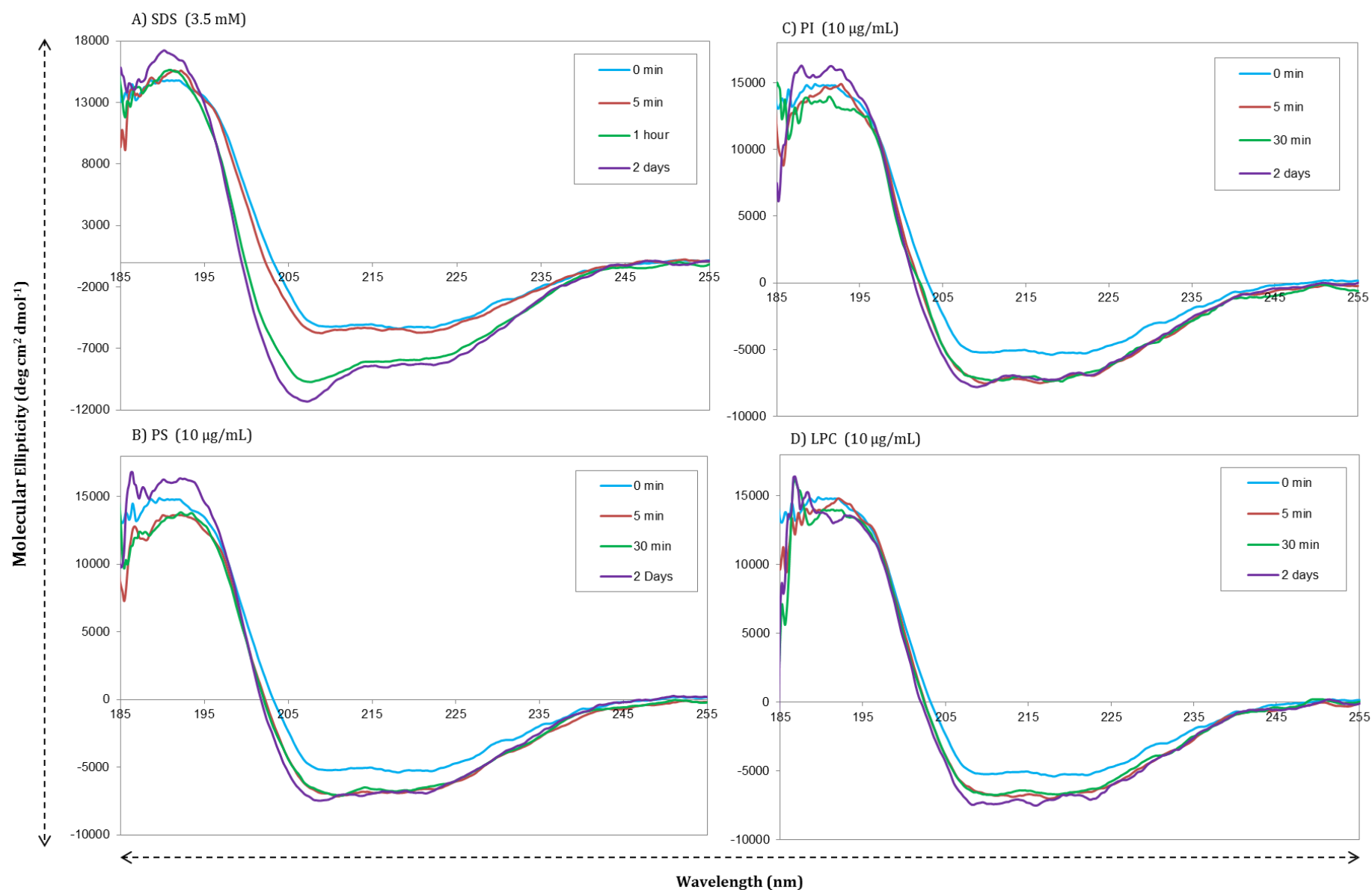


Figure 2.4 Far-UV CD spectra of 0.3 mg mL⁻¹ *Limulus polyphemus* hemocyanin incubated with a range of membrane phospholipids. Hemocyanin in 100 mM sodium phosphate buffer, pH 7.5, was incubated with (A) SDS (3.5 mM), (B) phosphatidylserine (10 μg mL⁻¹), (C) phosphatidylinositol (10 μg mL⁻¹) and (D) lyso-phosphatidylcholine (10 μg mL⁻¹) over a range of incubation periods (5min - 2days) prior to the spectral analysis.

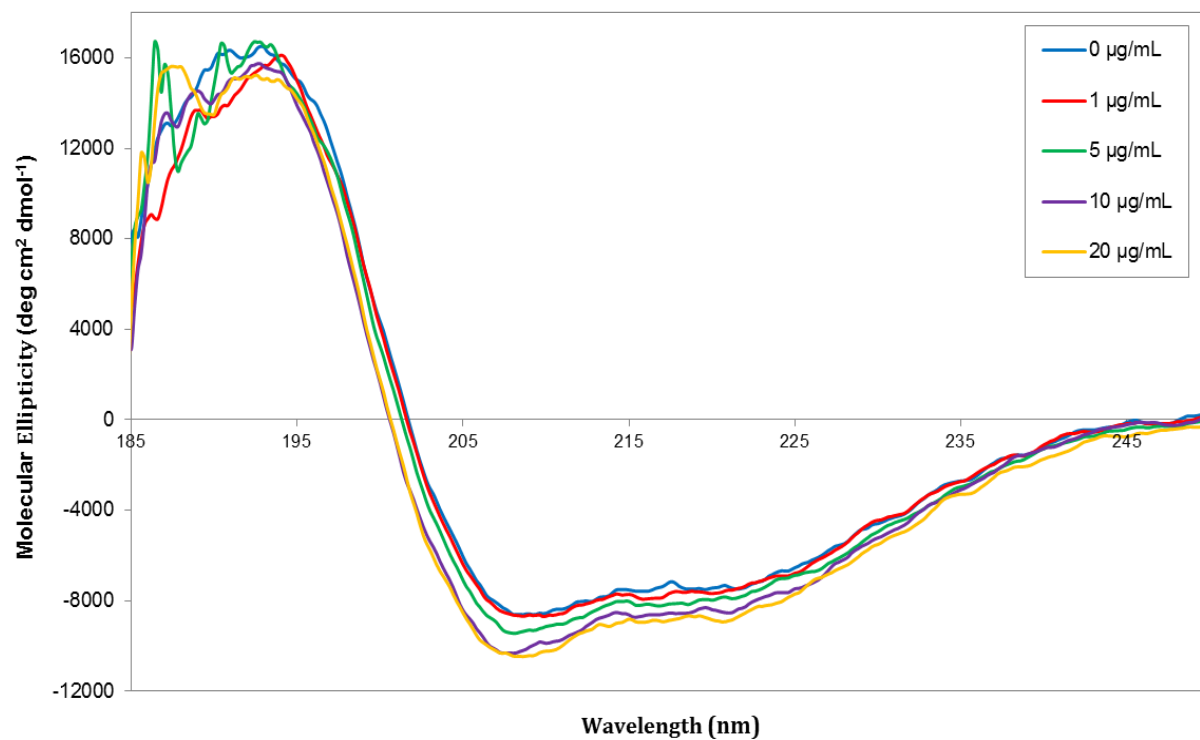


Figure 2.5 Far-UV CD spectra of 0.3 mg mL^{-1} *Limulus polyphemus* hemocyanin following incubation with phosphatidylserine. Hemocyanin in 100 mM sodium phosphate buffer, pH 7.5, was pre-incubated for 10 min with various concentrations of phosphatidylserine ($0\text{--}20 \text{ }\mu\text{g mL}^{-1}$) prior to spectral analysis.

Table 2.2 Percentage change in secondary structure content of hemocyanin following incubation with phospholipids

Activators	Limulus Hc	Experimental conditions*	Helix (%)	Sheet (%)	Turns (%)	Unordered (%)
-----	0.3 mg mL ⁻¹	Buffer alone	25.2	32.3	18.2	24.5
PS (10 µg mL ⁻¹)	0.3 mg mL ⁻¹	30 min	29.3	25.2	17.9	27.7
PI (10 µg mL ⁻¹)	0.3 mg mL ⁻¹	30 min	27.4	26.9	18.9	26.7
LPC (10 µg mL ⁻¹)	0.3 mg mL ⁻¹	30 min	27.7	23.7	19.2	29.4
SDS (3.5 mM)	0.3 mg mL ⁻¹	1 hour	31.9	20.9	30	27.2
-----	0.4 mg mL ⁻¹	Buffer alone	27.5	25.8	19.5	27.2
PS (1 µg mL ⁻¹)	0.4 mg mL ⁻¹	10 min	28.1	24.2	20.7	27
PS (5 µg mL ⁻¹)	0.4 mg mL ⁻¹	10 min	29.2	22.9	20	27.9
PS (10 µg mL ⁻¹)	0.4 mg mL ⁻¹	10 min	30.2	21.5	20.8	27.4
PS (20 µg mL ⁻¹)	0.4 mg mL ⁻¹	10 min	30.7	21.3	21.1	26.7

Secondary structure predictions were conducted on DICHROWEB, using SELCON 3 and reference set 3. * indicates the amount of time hemocyanin was incubated with each activator before the spectra were recorded.

2.4.5 Effects of phosphatidylserine on tertiary structure

Intrinsic fluorescence (Fig. 2.6) and near-UV CD (Fig. 2.7) measurements suggested that a structural change in Hc was induced by the presence of phospholipids in a manner similar to conformational change induced by micellar SDS (Baird et al., 2007), the most effective being PS. Increasing the concentration of PS from 0 to 20 $\mu\text{g mL}^{-1}$ resulted in a decrease in the wavelength of fluorescence emission maximum from 343 nm to 340 nm (Table 2.3) suggesting the presence of PS reduces solvent exposure of some or all of the tryptophan residues (Fig. 2.6A). Increasing the concentration of PS from 0 to 20 $\mu\text{g mL}^{-1}$ also led to a 4-fold increase in the intensity of fluorescence. The maximum wavelength shift and the increase in fluorescence intensity observed with Hc in the presence of 20 $\mu\text{g mL}^{-1}$ PS were very similar to the response induced by micellar concentrations of SDS. The presence of 10 $\mu\text{g/mL}$ of each phospholipid had little effect on the intrinsic fluorescence properties of the model compound N-acetyl-L-tryptophan (Fig. 2.6D), suggesting that the changes in Hc fluorescence are not a consequence of direct interactions between phospholipids and exposed tryptophan side chains. A similar control experiment with micellar SDS indicated that there are no direct SDS–tryptophan interactions.

Near-UV CD spectra of *L. polyphemus* Hc, recorded in the presence of 0–20 $\mu\text{g/mL}$ PS, revealed a conformational change in the presence of increasing PS (Fig. 2.7). The reduction in peak intensity in the region 260–320 nm suggests a change in the environment around some of the aromatic residues present in Hc. The reduction in peak intensity of the near-UV CD spectrum of Hc induced by 20 $\mu\text{g mL}^{-1}$ PS is similar to the changes induced by 3.5 mM SDS; however, the intensity of the optimum decrease was ~2.5-fold smaller with PS suggesting a less substantial change in the environment around some of the aromatic residues in Hc.

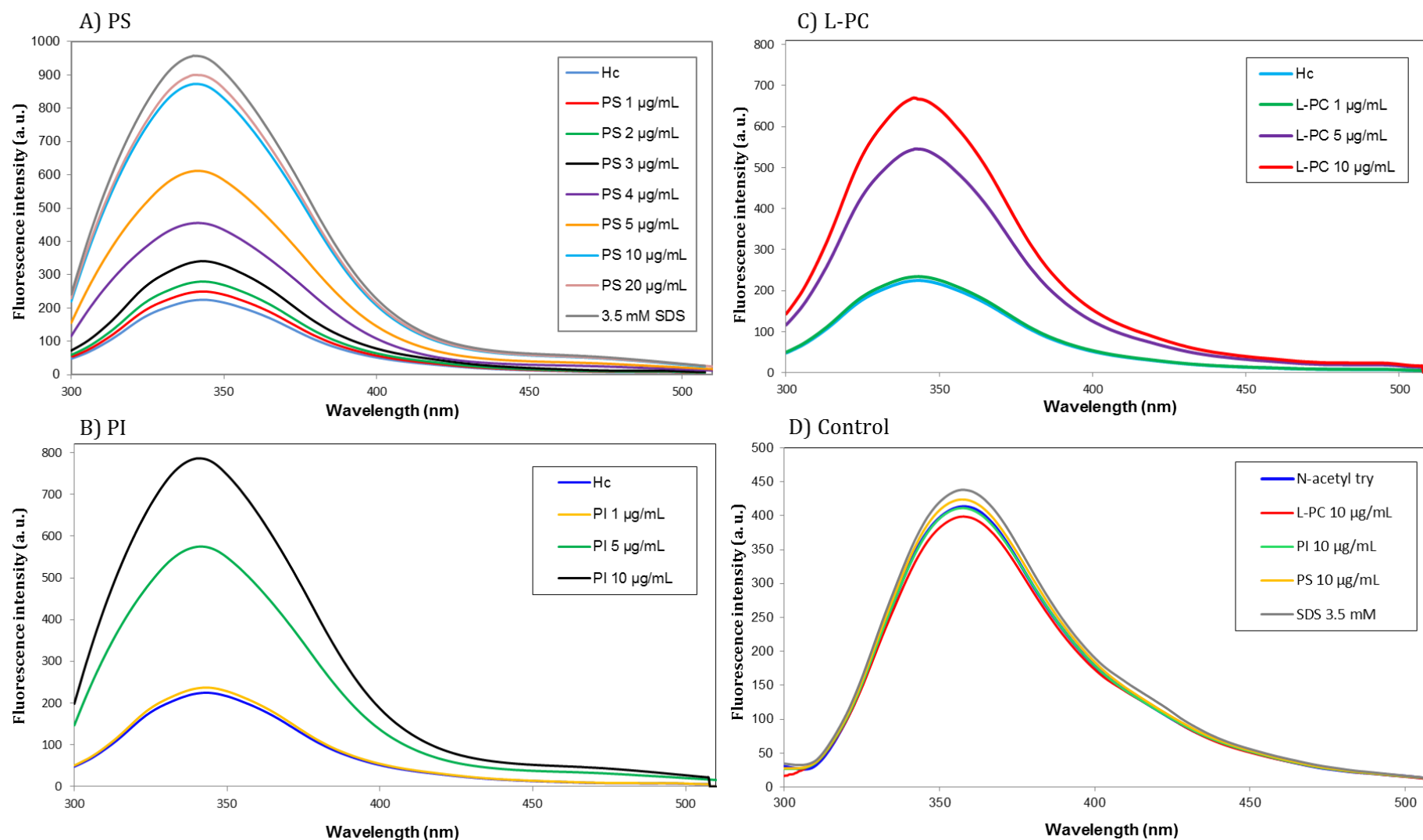


Figure 2.6 Fluorescence emission spectra of 0.1 mg mL^{-1} *Limulus polyphemus* hemocyanin, in the presence of **A)** phosphatidylserine, **B)** phosphatidylinositol and **C)** lyso-phosphatidylcholine. Hemocyanin was pre-incubated for 10 min with increasing concentrations (0 – $20 \text{ }\mu\text{g mL}^{-1}$) of phospholipids or SDS (3.5 mM). Experiments were conducted in 100mM sodium phosphate buffer, $\text{pH } 7.5$. Samples were excited at 290 nm and the subsequent fluorescent spectrum was recorded. **D)** Fluorescence emission spectrum of $2 \text{ }\mu\text{M}$ N-acetyl-L-tryptophan, in 100mM sodium phosphate buffer, $\text{pH } 7.5$, was excited at 290 nm in the absence and presence of either phospholipid ($10 \text{ }\mu\text{g mL}^{-1}$) or SDS (3.5 mM) after 10 min incubation.

Table 2.3 Intrinsic tryptophan fluorescence peak wavelength of *Limulus polyphemus* in the absence and presence of phospholipids and SDS. A blue-shift in fluorescence emission maxima occurs with 3.5 mM SDS and increasing concentrations of phospholipids, particularly phosphatidylserine.

<i>Concentration</i>	Activators			
	SDS	PS	PI	LPC
0 $\mu\text{g mL}^{-1}$ (<i>control</i>)	343 nm	343 nm	343 nm	343 nm
1 $\mu\text{g mL}^{-1}$	-	343 nm	343 nm	343 nm
2 $\mu\text{g mL}^{-1}$	-	342.5 nm	-	-
3 $\mu\text{g mL}^{-1}$	-	342.5 nm	-	-
4 $\mu\text{g mL}^{-1}$	-	341.5 nm	-	-
5 $\mu\text{g mL}^{-1}$	-	341 nm	341.5 nm	342 nm
10 $\mu\text{g mL}^{-1}$	-	340.5 nm	341 nm	341.5 nm
20 $\mu\text{g mL}^{-1}$	-	340 nm	-	-
3.5 mM	340 nm	-	-	-

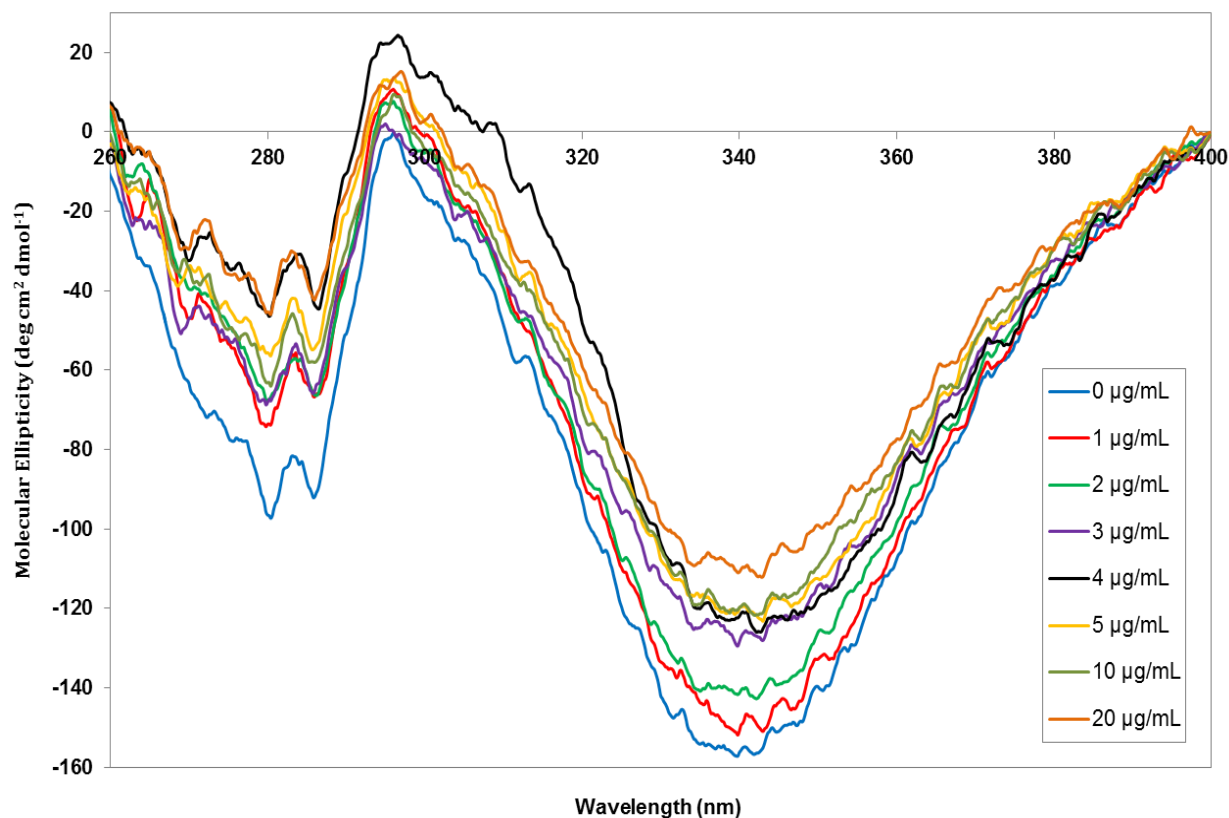


Figure 2.7 Near-UV CD spectra of 0.4 mg mL^{-1} *Limulus polyphemus* hemocyanin following incubation with phosphatidylserine. Hemocyanin in 100 mM sodium phosphate buffer, pH 7.5, was pre-incubated for 10 min with various concentrations of phosphatidylserine ($0\text{--}20 \text{ }\mu\text{g mL}^{-1}$) prior to spectral analysis.

2.4.6 Presence of copper

Type 3 copper proteins, including Hc and PO, have a characteristic absorption peak between 340 nm and 350 nm ($\epsilon \sim 20,000 \text{ M}^{-1} \text{ cm}^{-1}$) (Decker et al., 2001). The di-copper centre of type 3 copper proteins also gives rise to a characteristic near-UV CD signal at ~ 340 nm. Addition of phospholipids has little effect on the absorption band which occurs at ~ 340 nm for *L. polyphemus* Hc (Fig. 2.8) suggesting that the arrangement around the Cu(II) ions is not altered. The presence of PS at the highest concentration of $20 \mu\text{g mL}^{-1}$ reduced the near-UV CD signal at ~ 340 nm by $\sim 40^\circ \text{ cm}^2 \text{ dmol}^{-1}$ suggesting a subtle change in the nature of the Hc-copper interaction. Micellar SDS appeared to have a greater effect on the arrangement around the Cu(II) ions of *L. polyphemus* Hc; previously a reduction in the near-UV CD signal at ~ 340 nm $\times \sim 100^\circ \text{ cm}^2 \text{ dmol}^{-1}$ and a substantial reduction in the absorption band at ~ 340 nm, have been observed (Baird et al., 2007). The subtle change in Hc incubated with PS compared to the severe changes observed in Hc with SDS, infers PS may promote a more stable conformation of activated Hc-d PO.

Both Hcs and POs exhibit a characteristic histidine fluorescence signal at 415 – 430 nm when excited at 325 – 340 nm, in addition to the tryptophan fluorescence signal at ~ 340 nm (when excited at 290 nm). Histidine residues present at the active site are responsible for the fluorescence signal between 415-430 nm, however, due to the close proximity of the copper atoms (CuA and CuB), the signal is severely quenched (Bacci et al., 1983; Baird, 2007). Hc incubated in the presence of phospholipids and SDS yielded negligible changes in the histidine signal (Fig. 2.9), indicating that the dicopper centre remains intact during activation. This is unsurprising given that phospholipids do not cause alter the absorption signal at 340 – 350 nm.

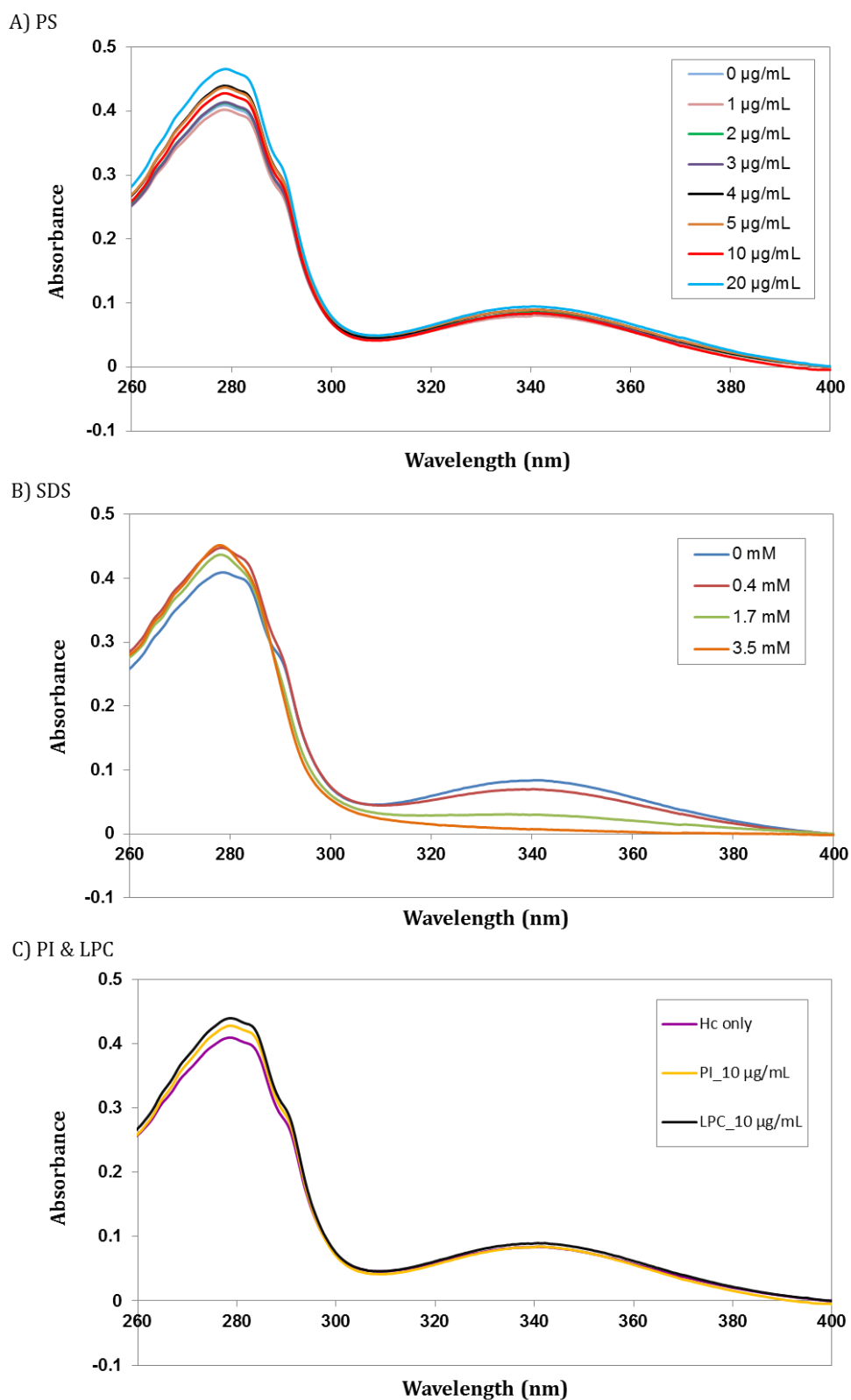


Figure 2.8 Absorption spectra of 0.3 mg mL^{-1} *Limulus polyphemus* hemocyanin. Hemocyanin in 100 mM sodium phosphate buffer, pH 7.5, was pre-incubated for 10 min with a range of concentrations of (A) phosphatidylserine ($0\text{--}20 \text{ }\mu\text{g mL}^{-1}$), (B) SDS ($0\text{--}3.5 \text{ mM}$) and (C) phosphatidylinositol and lyso-phosphatidylcholine ($10 \text{ }\mu\text{g mL}^{-1}$, respectively) prior to absorption spectrum analysis. Data was recorded over the range 260–400 nm.

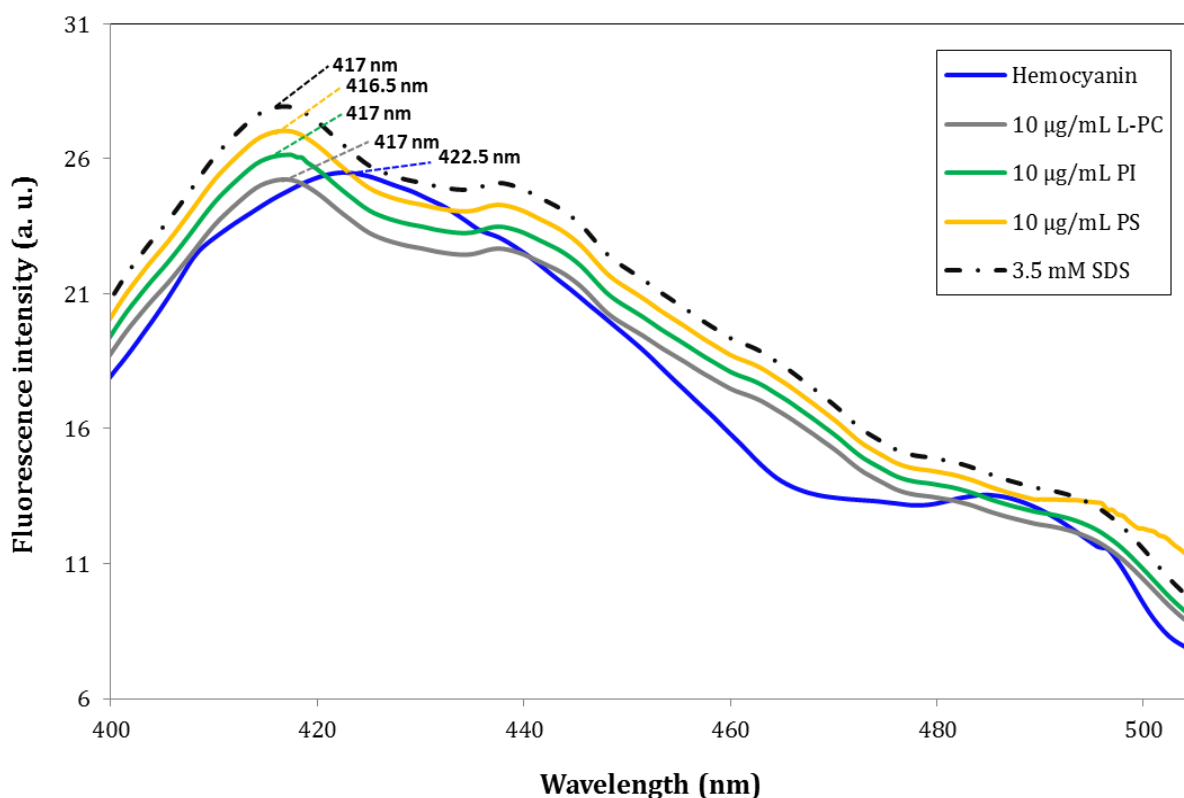


Figure 2.9 Fluorescence emission spectra of 0.1 mg mL^{-1} *Limulus polyphemus* hemocyanin, in the presence of phospholipids and SDS. Hemocyanin was pre-incubated for 10 min with $10 \text{ }\mu\text{g mL}^{-1}$ of phospholipid or SDS (3.5 mM) prior to spectral readings. Experiments were conducted in 100 mM Tris-HCl, pH 7.5. Samples were excited at 330 nm and the subsequent fluorescent spectrum was recorded. The histidine fluorescence peak wavelength of *Limulus polyphemus* in the presence of phospholipids and SDS is depicted also.

2.4.7 Preliminary investigations on the nature of the phosphatidylserine- hemocyanin interaction

In order to investigate the properties of the interaction between Hc and PS, Hc was incubated in the presence of PS and increasing concentrations of NaCl. The addition of NaCl led to a threefold increase in the conductivity of the solution (Fig 2.10), at the highest concentration of 0.5 M NaCl.

PO activity of Hc in the presence of $20 \mu\text{g mL}^{-1}$ PS and the absence of NaCl was recorded at ~ 4 U. The addition of increasing concentrations of NaCl resulted in a decrease in Hc-d PO activity, <1 U, in the presence of 0.5 M NaCl (Fig 2.11). The addition of NaCl to Hc in the presence of PS, induced a hypochromic effect and accompanying red shift in the fluorescence emission maxima of Hc (Fig. 2.12), around the 340 nm signal (Table 2.4). Control spectra indicate that increasing NaCl concentrations have no measureable effect on the model compound *N*-acetyl-L-tryptophanamide; indicating NaCl ions did not cause a change in the fluorescence spectrum due to direct interactions with exposed tryptophan side chains (Fig. 2.12B).

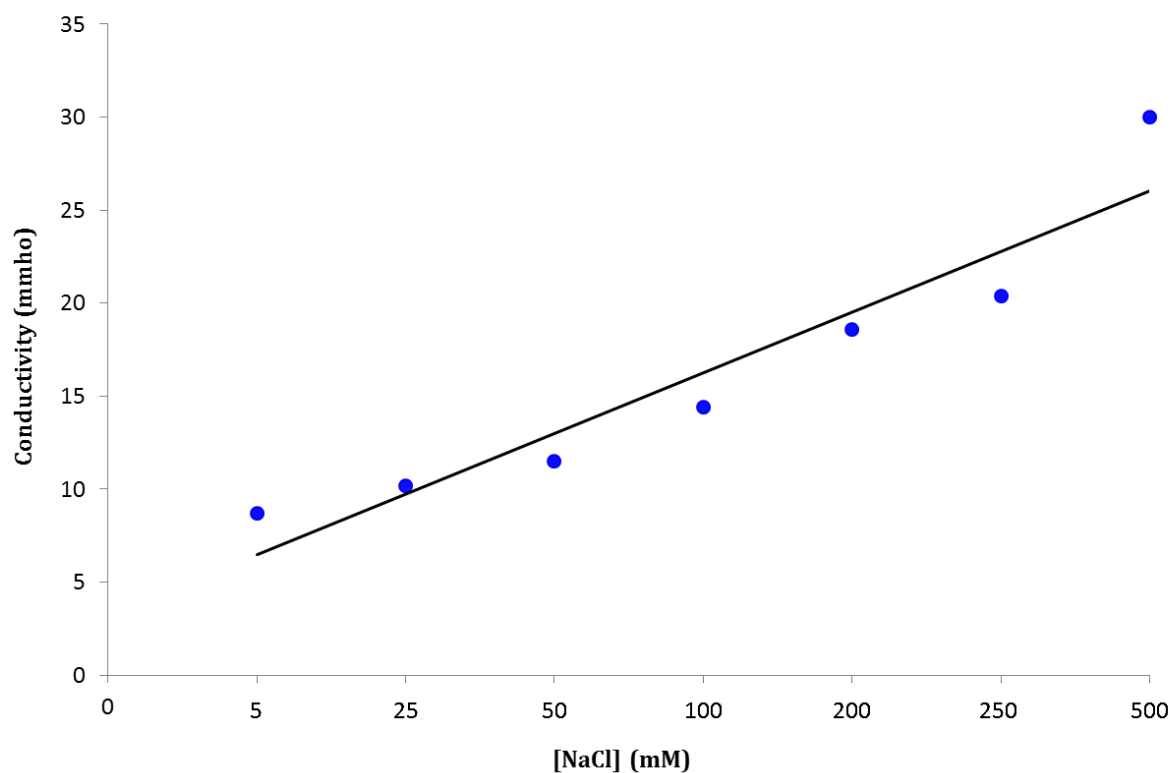


Figure 2.10 Conductivity measurements of 100 mM Tris-HCl, pH 7.5 were recorded in the presence of increasing concentrations of NaCl (0 - 500 mM). Conductivity measurements were taken at room temperature and performed in duplicate on two independent occasions.

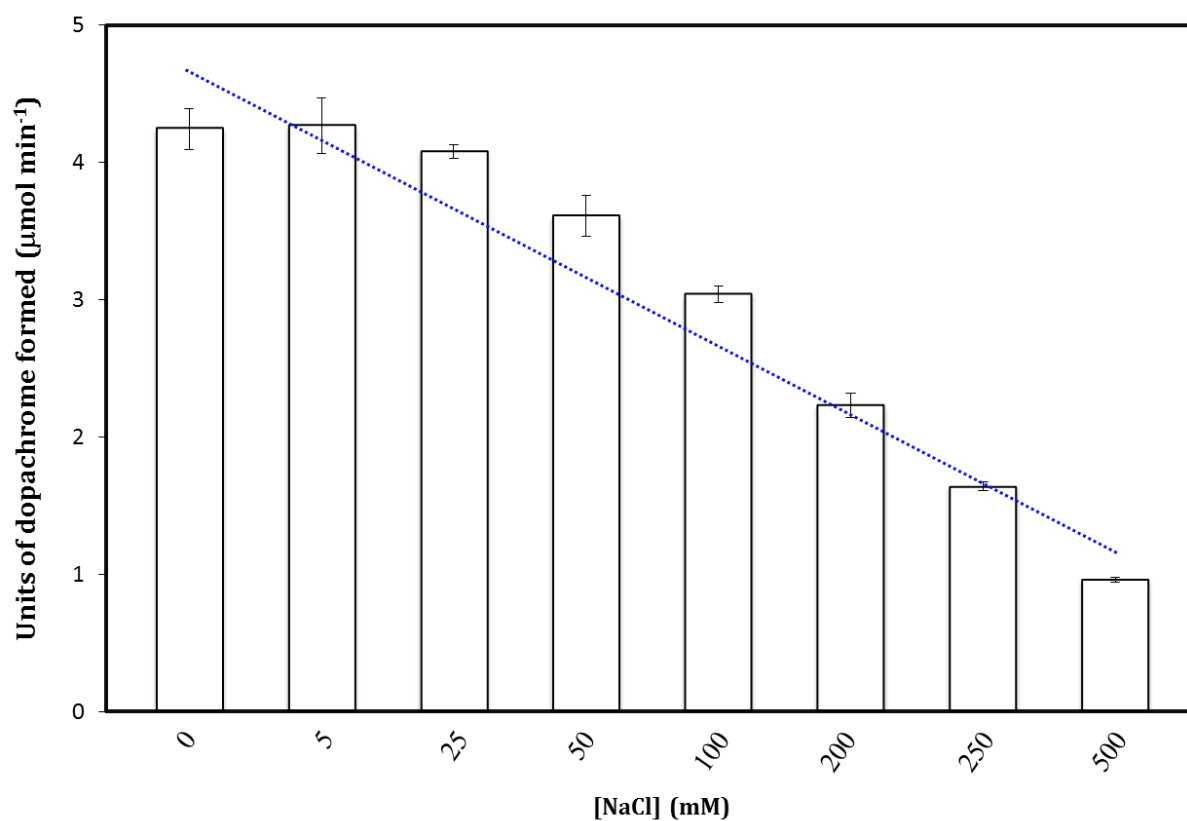


Figure 2.11 Phosphatidylserine induced phenoloxidase activity of hemocyanin from *Limulus polyphemus* in the presence of increasing concentrations of NaCl (0 – 500 mM). Hc (1 mg mL^{-1}) was pre-incubated with PS ($20 \mu\text{g mL}^{-1}$) for 10 min in 100 mM Tris-HCl, pH 7.5 in the presence of increasing salt concentrations. Phenoloxidase activity was initiated by the addition of substrate (2 mM dopamine). Assays were recorded over a 6 min period. The histogram illustrates an increase in absorbance at 475 nm resulting from the formation of dopachrome and its derivatives.

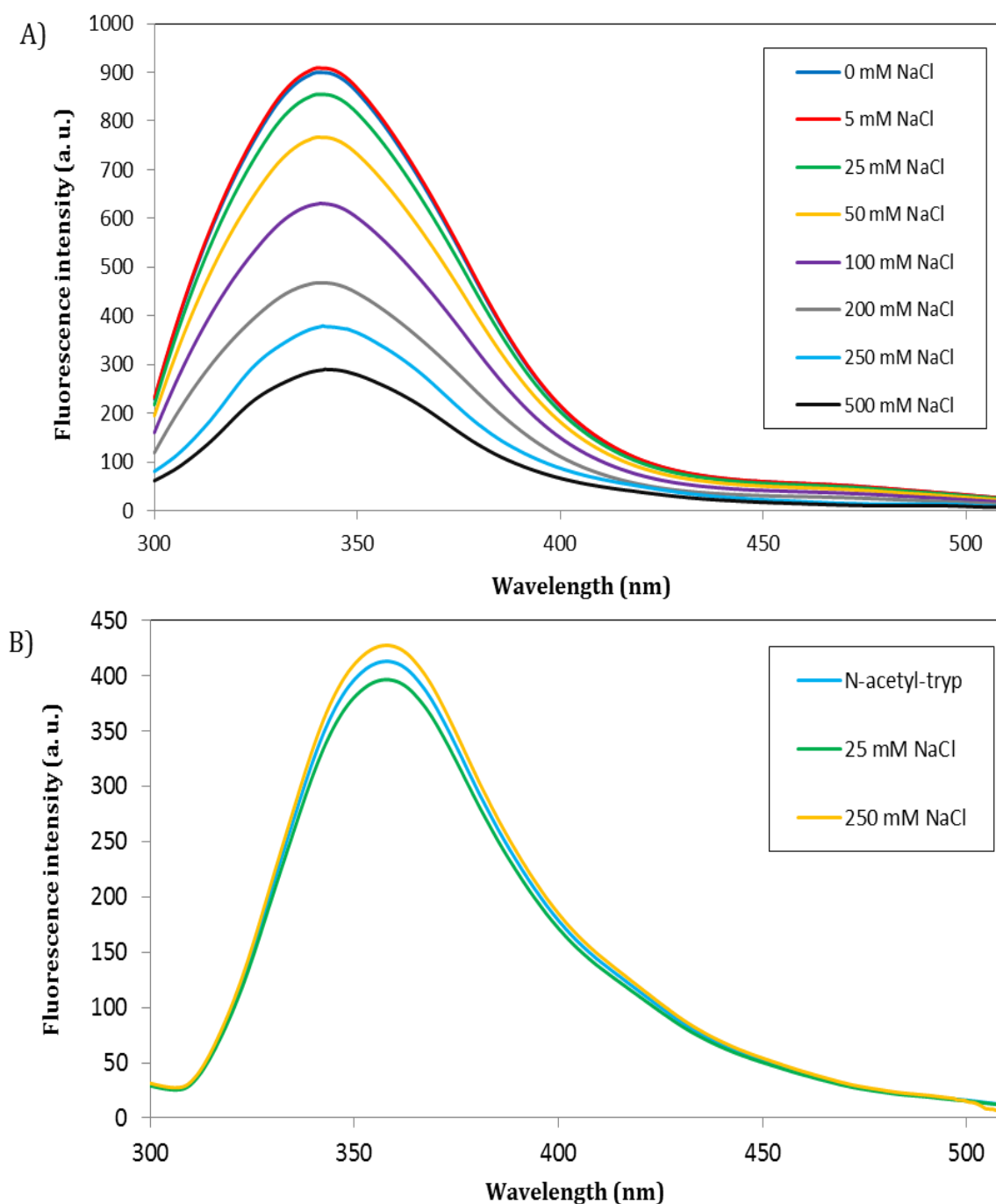


Figure 2.12 Fluorescence emission spectra of 0.1 mg mL⁻¹ *Limulus polyphemus* hemocyanin with increasing concentrations of NaCl (mM). **A)** phosphatidylserine (20 $\mu\text{g mL}^{-1}$) and increasing concentrations of NaCl (mM). Hemocyanin in the presence of PS was pre-incubated for 10 min with increasing concentrations of NaCl. Experiments were conducted in 100 mM Tris-HCl, pH 7.5. Samples were excited at 290 nm and the subsequent fluorescent spectrum was recorded. **B)** Fluorescence emission spectrum of 2 μM *N*-acetyl-*L*-tryptophan, in 100 mM Tris-HCl, pH 7.5, was excited at 290 nm in the absence and presence of 25 mM and 250 mM NaCl₂ after 10 min incubation.

Table 2.4 Intrinsic tryptophan fluorescence peak wavelength of *Limulus polyphemus* in the presence of phosphatidylserine and increasing concentrations of NaCl. Hemocyanin (0.1 mg mL^{-1}) and $20 \text{ } \mu\text{g mL}^{-1}$ PS in 100 mM Tris-HCl, pH 7.5 were pre-incubated with a range of NaCl concentrations prior to spectral analysis. A red shift in fluorescence emission maxima occurs when concentrations of NaCl increase.

[NaCl]	Sample	
	Hc only	Hc +PS
0 mM	343 nm	340 nm
5 mM	-	340 nm
25 mM	-	340 nm
50 mM	-	340.5 nm
100 mM	-	341. nm
200 mM	-	341.5 nm
250 mM	-	342 nm
500 mM	343 nm	342.5 nm

2.5 Discussion

Hc functions as an oxygen carrier in many arthropods, however, functional studies over the past decade have identified multiple roles for Hc in innate immunity (Chapter 1). The functional conversion of Hc into a PO-like enzyme has been achieved by: limited proteolysis of chelicerate and crustacean Hc (Decker and Tuczec, 2000); addition of denaturants to chelicerate, crustacean and mollusc Hc (Decker and Jaenicke, 2004); or the association of Hc from the chelicerate *Tachypleus tridentatus* with clotting cascade proteins/peptides (Nagai and Kawabata, 2000 and Nagai et al., 2001). Sequence alignments (Decker and Jaenicke, 2004) and structural comparisons (Li et al., 2009) indicate that Hc is homologous to PO, an enzyme involved predominantly in innate immunity.

In this chapter Hc-d PO activity is recorded in the presence of phospholipids, notably PS (Fig. 2.2 and Fig. 2.3). PS-induced secondary (Fig. 2.4,) and tertiary (Fig. 2.6 and Fig 2.7) structural changes in Hc are similar to those observed in the presence of SDS, in agreement with previous studies (Baird et al., 2007). Studies in *Drosophila melanogaster* have led to the proposal that PS acts as a natural inducer of proPO following injury (Bilda et al., 2007 and Bilda et al., 2009). PS is an anionic phospholipid which occurs predominantly on the cytoplasmic side of the plasma membrane in quiescent eukaryotic cells; however, PS is externalised onto the extracellular side of the plasma membrane upon damage, infection or apoptosis. The appearance of PS on the extracellular side of the membrane is required to promote protein-mediated responses to damage, infection and apoptosis (Chaurio et al., 2009). Given that PS liposomes, which activate proPO *in vivo* (Bilda et al., 2009), and that SDS micelles, which induce PO activity in Hc *in vitro* (Baird et al., 2007), share a similar charge and shape, the ability of PS to induce PO

activity in *L. polyphemus* Hc was explored. While the source of PO activity in some arthropods can be attributed to proPO, or to a combination of proPO and Hc, in the chelicerate *L. polyphemus* the PO activity appears to be due to Hc only (Terwilliger and Ryan, 2006). Thus, *L. polyphemus* presents a simple system for studying PS induction of PO activity in Hc.

In the absence of artificial or putative natural activators, purified *L. polyphemus* Hc exhibits no measurable PO activity. Addition of lyso-PC, PI and PS were capable of inducing PO activity, with PS proving almost as effective as the universal artificial activator SDS (Fig. 2.3). In mammalian systems, PS is known as the most effective anionic phospholipid capable of activating blood coagulation (Zwaal et al., 1998). PC, PE and sphingomyelin, in isolation or in combination with other phospholipids, are capable of influencing coagulation complex formation; however, PS appears to be the most effective activator. The predominant interactions between PS and coagulation proteins appear to be electrostatic, with possible membrane penetration by hydrophobic residues (Stace and Ktistakis, 2006). In general, PS-binding proteins contain short stretches of sequence rich in basic and hydrophobic residues (Stace and Ktistakis, 2006).

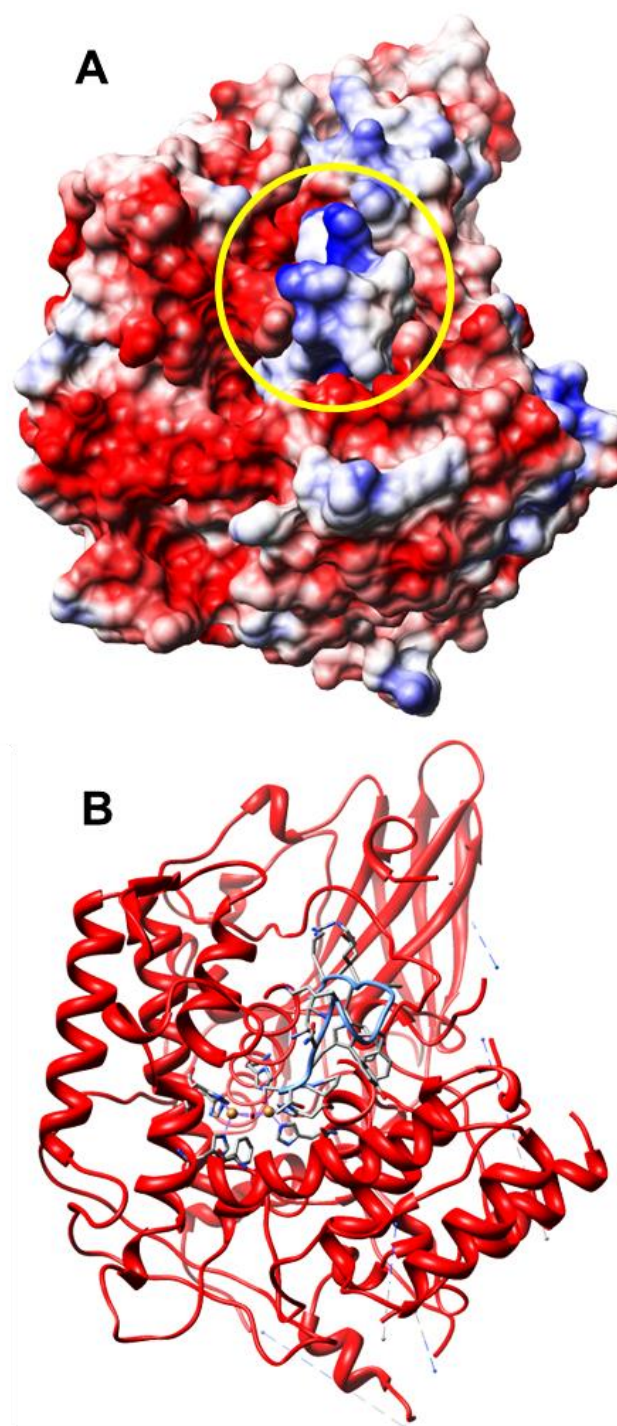
Sequence analysis of *L. polyphemus* Hc (courtesy of J. Nairn and A. Patterson; Coates et al., 2011) reveals a possible PS-binding site in the region P181 to K196, with the sequence PSTWNPKYFGKKKDRK (using *L. polyphemus* Hc subunit II, PDB; 1OXY). The identified amino acid stretch possesses a theoretical pI value of 10.3. This predominantly positively charged region is present as a loop close to the mouth of the active centre of Hc (Fig. 2.13), which contains the conserved placeholder residue, Phe 49 (Fig. 2.14). The distance between Phe 49 and Ser 182 (present on the positively charged loop) is ~ 8.3

Å. It is possible that upon binding of phospholipids to Hc, in particular PS, the removal or trans-location of this loop, could provide phenolic molecules with a direct route to the copper centre, leading to enhanced PO activity in Hc.

Preliminary investigations of Hc-PS interactions suggest that electrostatic interactions play a significant role (Fig. 2.11 and Fig. 2.12). Hc-d PO activity was reduced by ~ 75% at the highest concentration of 500 mM NaCl (concentrations above this resulted in Hc solubility issues). NaCl ions are known to influence protein stability; at low concentrations, ligand-induced ion-specific interactions of NaCl with proteins can promote conformational stability (Date and Dominy, 2013), and this may account for the most prominent changes in the fluorescence emission maxima of Hc with PS, at concentrations above 0.1 M (Fig. 2.12). On the other hand, increasing concentrations of NaCl can be correlated broadly with protein unfolding (Date and Dominy, 2013). It may be that binding of PS to Hc is dependent on a synergy of electrostatics and direct interactions with specific amino acids. In this study, NaCl may be affecting Hc and PS individually or together as a protein-lipid complex, therefore, more data is needed in order to fully characterise this interaction. Moreover, the recently crystallised structure of the zymogen proPO from *Manduca sexta* (Li et al., 2009) provided insight to the molecular mechanisms associated with proteolytic activation of PO, with a drastic change in the electrostatic surface of the enzyme accompanying the conversion of proPO to PO. The switch in electrostatic surface potential of *M. sexta* proPO upon activation may also be similar for the activation of Hc into Hc-d PO, giving credence to potential electrostatic interactions between Hc and phospholipids.

In the event of wounding and or/microbial infection, the conversion of Hc to PO may be mediated by a number of activators in a manner similar to proPO activation (Cerenius et

al., 2008). The interaction of activators with a number of specific sites on Hc would reflect the multiple roles of Hc and the regulation of its conversion to PO. Activation events may include the externalisation of PS onto the extracellular side of the cell membrane and the release of antimicrobial peptides. Antimicrobial peptides released from the S-granules of *T. tridentatus* amoebocytes form an amphipathic β -hairpin conformation which is stabilised by two disulphide bonds: one face of the β -sheet is hydrophobic and the other face is cationic. The hydrophobic side chains, together with the disulphide bonds, have been shown to be essential for the peptide–Hc interaction and the resultant conversion of Hc to PO (Nagai et al., 2001). It has been demonstrated that in the case of activation by PS, electrostatic interactions appear to be important for PS–Hc interactions and the subsequent induction of PO activity in Hc.



Seq. **PSTWNPKYFGKKKDRK**

Figure 2.13 A) Electrostatic surface potential of *Limulus polyphemus* hemocyanin (PDB ID code 1OXY). The surface of Hc is predominantly negatively charged, however, the region P181 to K196 (Hc subunit II, sequence ID code P04253) is mostly positively charged. This region may interact directly with phospholipids resulting in greater substrate access to the Cu(II) centre. B) Location of the positively charged loop (P181 to K196) relative to the entrance of the Cu(II) centre of *L. polyphemus* hemocyanin (PDB ID code 1OXY). The secondary structure elements are shown as ribbons with the positively charged loop shown in blue. The copper-coordinating His ligands are shown as sticks. The di-copper atoms are shown as spheres. Molecular graphics images were produced using the UCSF Chimera package from the Resource for Biocomputing, Visualization, and Informatics at the University of California, San Francisco (supported by NIH P41 RR-01081).

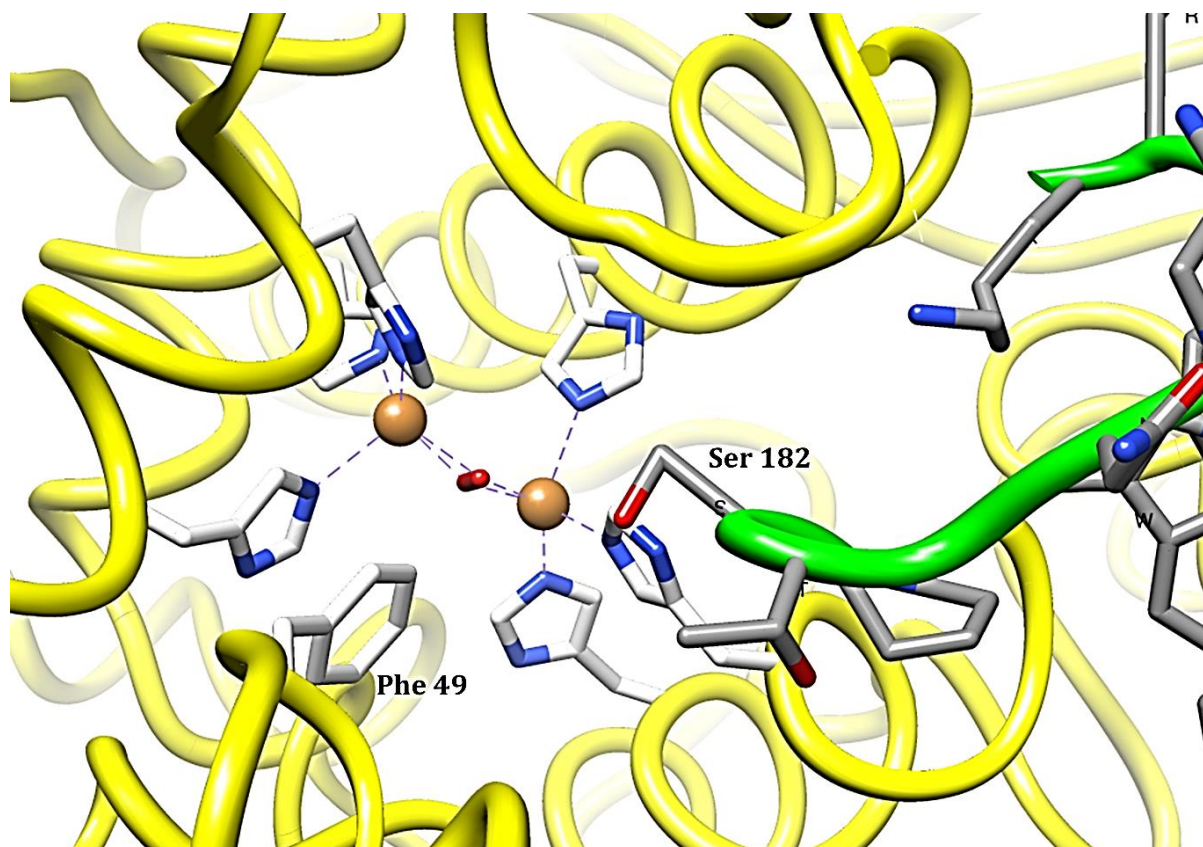


Figure 2.14 Proximity of the positively charged loop to the dicopper centre of hemocyanin (PDB; 1OXY), which contains the placeholder residue, Phe 49. The distance between Phe 49 and Ser 182 is ~ 8.3 Å. The secondary structure elements are shown as ribbons with the positively charged loop shown in green. His ligands are shown as sticks, with copper atoms represented by brown spheres. Molecular graphics images were produced using the UCSF Chimera package from the Resource for Biocomputing, Visualization, and Informatics at the University of California, San Francisco (supported by NIH P41 RR-01081).

Results presented here show clearly that PS induction of PO activity in Hc is accompanied by a structural change in the protein (Fig. 2.15) and this structural change can be reversed with the addition of NaCl (Fig. 2.16). An increase in Hc-d PO activity is correlated broadly with an increase in the fluorescence emission maximum and blue-shift; likewise, a reduction of Hc-d PO in the presence of increasing concentrations of NaCl display a hypochromic effect and accompanying red-shift in the emission maximum. The nature of this change is very similar to that observed with micellar SDS induction (Baird et al., 2007), with two subtle yet significant differences: PS induction produces a ~2.5-fold lower change in the near-UV CD spectrum and causes no change in the absorption spectrum at 340 nm. Thus PS (at 20 $\mu\text{g mL}^{-1}$) appears to induce a similar level of PO activation as micellar SDS, but PS promotes a smaller, and more stable, conformational change. The changes in both the secondary and tertiary structure of Hc which accompany induction of PO activity suggest that PO substrates can now access the Cu(II) centre, be turned over and products released.

It has been proposed that removal of a highly conserved phenylalanine (Phe 49 in *L. polyphemus* and *T. tridentatus* Hc) allows entrance to the Cu(II) centre of Hc (Decker and Tuczec, 2000; Nagai et al., 2001). Also, the crystal structure of proPO from *M. sexta* led to the proposal of a model for proPO activation in which proteolytic cleavage results in exposure of a basic region on the surface of the enzyme, promoting the formation of an activation complex involving proPO activating protease and clip-domain serine protease homolog (Li et al., 2009). The model of electrostatic interactions mediating proPO activation and the trans-location of Phe 49 may be of relevance to the induction of PO activity in Hc, caused by PS binding, and is in good agreement with data presented here.

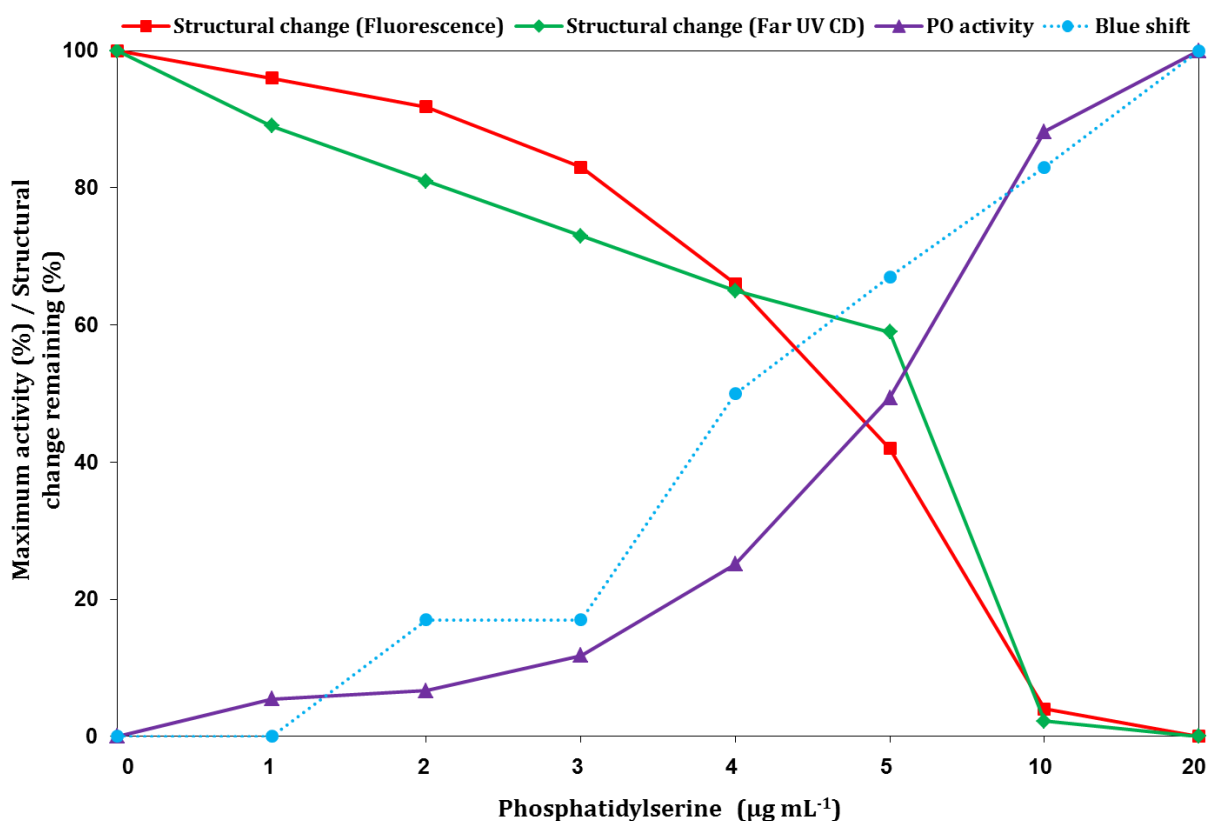


Figure 2.15 Correlation of phenoloxidase activity and structural changes in *Limulus polyphemus* hemocyanin with increasing concentrations of phosphatidylserine. The percentage of total structural change remaining (Far-UV circular dichroism spectroscopic data (at 207 nm) and intrinsic tryptophan fluorescence data (at 340 nm)) and the maximum hemocyanin-derived phenoloxidase activity are plotted against increasing concentrations of phosphatidylserine (0–20 $\mu\text{g mL}^{-1}$). The extent of the blue shift in the emission maxima of hemocyanin incubated in phosphatidylserine was also plotted against maximum phenoloxidase activity measurements. The percentage of total structural change remaining was calculated from the change in intensity in the spectra at the appropriate wavelengths, assuming 100% structure remaining in the absence of phosphatidylserine and 0% structure remaining in the presence of 20 $\mu\text{g mL}^{-1}$ phosphatidylserine.

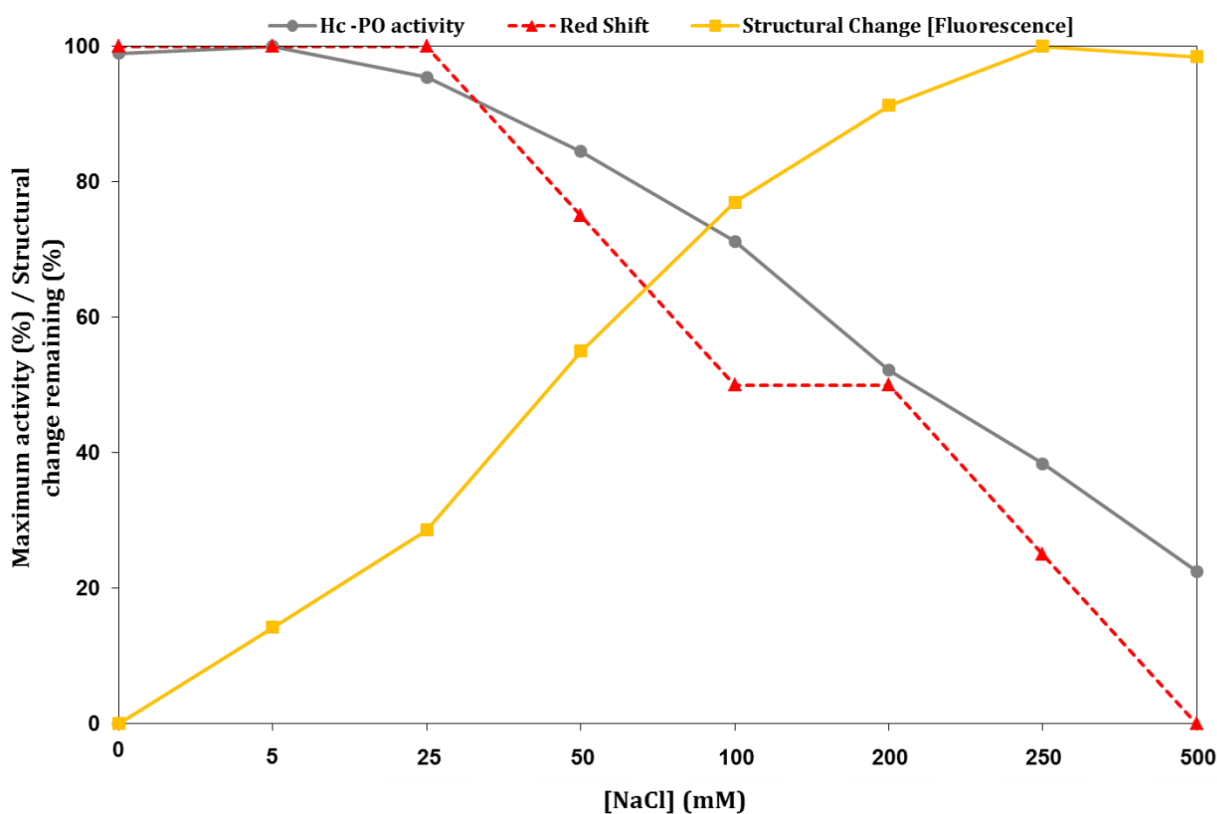


Figure 2.16 Correlation of phenoloxidase activity and structural changes in *Limulus polyphemus* hemocyanin in the presence of phosphatidylserine ($20 \mu\text{g mL}^{-1}$) and increasing concentrations of NaCl. The percentage of total structural change remaining (Intrinsic tryptophan fluorescence data (at 340 nm)) and the maximum hemocyanin-derived phenoloxidase activity are plotted against increasing concentrations of NaCl (0 – 500 mM). The extent of the red-shift in the emission maxima of hemocyanin in the presence of PS with increasing NaCl concentrations was also plotted against phenoloxidase activity measurements. The percentage of total structural change remaining was calculated from the change in intensity in the spectra at the appropriate wavelength ($\sim 340 \text{ nm}$) assuming 100 % structure remaining in the presence of 500 mM NaCl, and 0 % structure remaining in the absence of 500 mM NaCl.

2.6 Conclusions

Anionic phospholipids, in particular phosphatidylserine, induce phenoloxidase activity in Hc from *L. polyphemus*. This change in function is accompanied by a structural change which mimics the activity and structural changes observed in chelicerate hemocyanins in presence of the artificial activator SDS. A direct interaction between PS and Hc, possibly via a PS-binding site, or a less specific electrostatic interaction is suggested. These findings suggest a novel role for PS in activating innate immunity following its exposure on the cell surface and subsequent interaction with Hc.

2.7 Acknowledgements

Thanks to Douglas Lamont, University of Dundee, for obtaining and interpreting mass spectrometry data and Dr Liz Blackburn, Biophysical Characterisation Centre, University of Edinburgh, for assistance with dynamic light scatter experiments and Alex Mühlhölzl, Managing Director, Marine Biotech Limited for providing the hemolymph from *L. polyphemus*. Special thanks to Alan Patterson for his help with producing the images of the Hc structures (*Fig. 2.13*) and Professor Nicholas C. Price for helpful discussions and suggestions.

Chapter 3:

di-Phenoloxidase Activity of *Nephrops norvegicus* Hemocyanin; Applications for the Inhibition of Hyperpigmentation in Shellfish

A version of this chapter has been published;

Christopher J. Coates and Jacqueline Nairn. 2013. Hemocyanin-derived phenoloxidase activity; a contributing factor to hyperpigmentation in *Nephrops norvegicus*. *Food Chemistry*. 140, 361-369.

3.1 Abstract

The phenomenon of hyperpigmentation (melanosis) in shellfish has long been attributed to phenoloxidase enzymes. Over the last number of years, the oxygen carrier hemocyanin, has demonstrated multiple immune- and physiological functionalities, most notably, inducible phenoloxidase activity. In this chapter, hemocyanin purified from the hemolymph of *Nephrops norvegicus* displays diphenoloxidase activity in the presence of a number of elicitors and retains structural and functional integrity throughout the process of freeze-thawing (at -25°C). Conversely, cellular phenoloxidase activity (present in crude cell-lysates), demonstrates > 98% reduction in activity after freeze-thawing. Evidence suggests that hemocyanin may act as a causative agent of hyperpigmentation in *N. norvegicus*. The inhibition of hemocyanin-derived phenoloxidase activity is discussed in this chapter, and for the first time, the biophysical interactions of shellfish hemocyanin with known phenoloxidase inhibitors are presented.

3.2 Introduction

Hyperpigmentation (or melanosis) is a non-infectious condition of shellfish which has deleterious impacts on shellfish aquaculture/fisheries and is associated with food spoilage (Kim et al., 2000a). Although this cuticular darkening is not a health hazard (Fig. 3.1), the displeasing aesthetic appearance of the shellfish ultimately leads to a reduction in market value (Garcia-Carreno et al., 2008). Phenoloxidase (PO) enzymes, both tyrosinases (E.C. 1.14.18.1) and catecholoxidases (E.C. 1.10.3.1), catalyse the initial steps in a series of enzymatic reactions that leads to the synthesis of the chromogen, melanin (Cerenius & Soderhall, 2004). PO enzymes and the associated proPO activation cascade play an essential role in invertebrate immunity, however, it is thought that PO enzymes are the primary cause of hyperpigmentation, post mortem (Martinez-Alvarez et al., 2008). Consequently, concerted efforts have been made to prevent and/or inhibit hyperpigmentation, by targeting PO enzyme activity (Nirmal & Benjakul, 2009; Montero et al., 2001). Recent reports suggest that the extracellular PO derived from Hc, and not cellular PO, is the likely cause of hyperpigmentation in crustaceans (Adachi et al., 2001; Garcia-Carreno et al., 2008; Martinez-Alvarez et al., 2008). Furthermore, Hc not only demonstrates PO activity, but is also inhibited by known PO inhibitors (Jaenicke & Decker, 2008; Wright, et al., 2012).

Hc is abundant in the hemolymph of invertebrates, comprising > 90% of total protein content, and is known to retain structural and functional integrity across a wide temperature range, -20°C to 70°C (Decker, et al., 2007a). Conversely, PO is less abundant within the cells of hemolymph and is more sensitive to thermal denaturation (Cong et al., 2005; Garcia-Carreno et al., 2008; Liu et al., 2006). Cellular PO activity (cell lysates) and extracellular hemocyanin-derived phenoloxidase activity (Hc-d PO) of *N.*

norvegicus hemolymph, pre- and post-freezing, mimicking the *in situ* handling of harvested shellfish, have been investigated with a view to characterising the true cause of hyperpigmentation. *N. norvegicus* is of significant commercial importance in the North-east Atlantic and Mediterranean areas, with an average of 20-30 metric tonnes caught per port annually, in the Spanish Mediterranean alone (Gimenez, et al., 2010). This chapter details the purification of Hc from *N. norvegicus*. The kinetic properties of Hc-d PO activity are presented and the efficacy of known PO inhibitors against Hc-d PO activity has been determined.

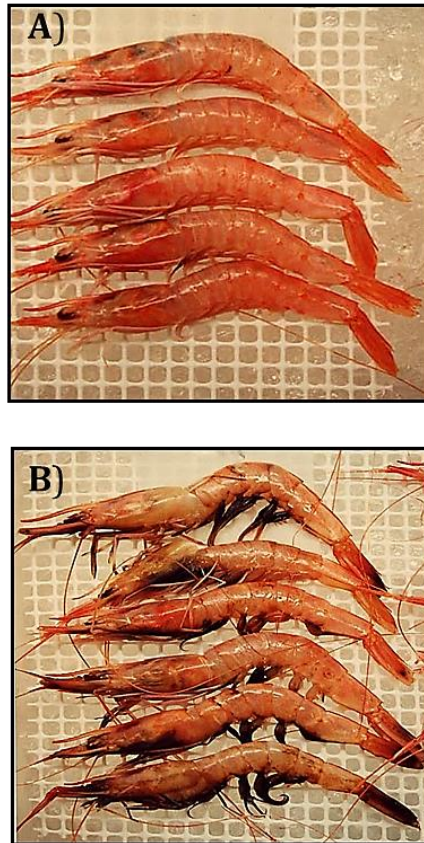


Figure 3.1 Appearance of fresh caught prawns (A) and prawns with hyperpigmentation present (B). Melanin appears to accumulate on the ventral surfaces of the prawns. Modified from <http://www.inrb.pt/fotos/editor2/guidebook.pdf>.

3.3 Materials and Methods

3.3.1 Chemicals

All chemicals and reagents used in this study were of the highest quality, purchased from Sigma Aldrich Chemical Company, Dorset UK, unless stated otherwise. Inhibitors: L-ergothioneine (L-ER), mimosine and 4-hexylresorcinol (4HR) were purchased from BIOMOL International, Acros Organics and Santa Cruz Biotechnology Inc., respectively. Tropolone, kojic acid and 1-phenyl 2-thiourea (PTU) were purchased from Sigma.

3.3.2 Maintenance of *Nephrops norvegicus*

N. norvegicus specimens were kindly provided by John Davis, Xyrex. Specimens were maintained in a closed circulation tank (at $16^{\circ}\text{C} \pm 2^{\circ}\text{C}$) containing natural seawater and fed three times a week on squid and/or mussels. Approximately 50% of seawater was exchanged per week, in addition to using an internal submerged filter pump (Hailea-BT1000) and siphoning of faeces/particulates. Water quality assessments (including salinity, ammonia, nitrites, nitrates, phosphates, pH and calcium) were performed regularly using a Hagen Master Test Kit (Aquatic Warehouse).

3.3.3 Cellular parameters

Hemolymph was extracted using a 23 gauge hypodermic needle attached to a sterile syringe. The needle was inserted into the membrane between the pincher cheliped and cephalothorax (Fig. 3.3). The membrane was cleaned with 70% ethanol pre- and post-extraction to avoid sepsis. A maximum of 200 μL of hemolymph was extracted per specimen.

A) Hemocyte numbers and viability

Extracted hemolymph was diluted immediately in a ratio of 1:1 (v/v) in marine anti-coagulant (3% NaCl, 100 mM dextrose, 47 mM citric acid and 10 mM EDTA, pH 4.6), adapted from Söderhäll & Smith (1983). Serial dilutions were carried out in LPS-free saline (3% NaCl, 10 mM NaHCO₃, pH 7.5) and hemocyte concentrations were calculated using an improved Neubauer hemocytometer.

Viability of extracted hemocytes was determined by the trypan-blue exclusion method (Altman et al., 1993). Hemocytes were washed in LPS-free saline and re-suspended in 3% NaCl-20 mM HEPES, pH 7.5 containing 0.2 % (w/v) trypan-blue. Hemocytes were incubated for ~ 3 min at room temperature, with stained vs. unstained hemocyte counts used to determine percentage viability.

B) Phenoloxidase staining

Approximately 5×10^4 hemocytes were added to culture wells (final volume, 500 μ L) containing 3% NaCl, 20 mM HEPES, pH 7.5, 10 mM CaCl₂, 10 mM MgCl₂, 5 mM KCl₂ and 10 mM NaHCO₃. Hemocytes were allowed to settle to the bottom of the well (~ 30 min) before half of the buffer (~ 250 μ L) was removed and replaced with an equal volume of PO stain (3% NaCl - 20 mM HEPES, pH 7.5, 20 μ g mL⁻¹ lipopolysaccharide (LPS), 5 mM dopamine, 5 mM 4-methoxyphenol, 5 mM 3-methyl-2-benzothiazolinone hydrazine (MBTH) and 2.5% EtOH), adapted from Aladaileh, Nair & Raftos (2007). Hemocytes were incubated for 30 min at room temperature in the presence of the PO stain and then fixed with 2.5 % neutral formaldehyde. Cells were viewed and quantified using brightfield optics of an Olympus M081 inverted microscope. Randomly chosen fields of view were selected until ~ 300 individual cells had been observed per well.

3.3.4 Phenoloxidase activity of cell lysates and acellular hemolymph

Approximately 200 μL of hemolymph were withdrawn per specimen (*N. norvegicus*). Extracted hemolymph was centrifuged immediately at 1000 x *g* for 5 min at room temperature. The supernatant (containing Hc) was removed and stored on ice or frozen at -25°C . Cell pellets were washed, and either; **(A)** re-suspended in Lysis buffer (100 mM Tris-HCl, pH 7.5, 10 mM CaCl_2 , 10 mM sodium cacodylate, 1% (v/v) nonidet P-40, 50 μM phenylmethylsulfonylfluoride (PMSF) and 20 μM E-64) and sonicated for 5 min at 30 Amp and subsequently frozen at -25°C , or **(B)** re-suspended in 3% NaCl - 20 mM HEPES, pH 7.5 and frozen. Following incubation at -25°C for 24, 72 and 120 h, cell-free hemolymph and cell extracts were incubated on ice for 2 h prior to PO activity measurements. The PO assays contained 1 mg mL^{-1} hemolymph protein or 50 $\mu\text{g mL}^{-1}$ cell lysate proteins in 100 mM Tris-HCl, pH 7.5 containing 2 mM dopamine hydrochloride as substrate and 0.1% (3.5 mM) SDS. Protein samples were pre-incubated with SDS for 5 min prior to activity measurements. PO activity was initiated with the addition of substrate and was monitored by an increase in absorbance at 475 nm, detecting the products of dopamine oxidation.

Protein concentrations of the cell lysates and hemolymph-supernatant were determined using 0.06% Coomassie G250 dye reagent, with bovine serum albumin as standard (Sedmak & Grossberg, 1977).

3.3.5 Purification of *Nephrops norvegicus* hemocyanin

The purification of Hc from the hemolymph of *N. norvegicus* was adapted from Coates et al. (2011). Hemolymph from 5 individuals (5 x 200 μL) was pooled together. Extracted

hemolymph was centrifuged immediately and the acellular supernatant was collected and stored on ice. The supernatant was treated further as outlined in section 2.3.1. The concentration of purified Hc was determined by UV absorbance measurements at 280 nm, using the value of 1.43 for the absorbance of a 1 mg mL⁻¹ solution of Hc (Brouwer, Whaling, & Engel, 1986) in a quartz cuvette of 1cm pathlength. Hc fractions with a 280 nm: 350 nm absorbance ratio value of 4.2 (oxy-hemocyanin) were pooled and analysed by SDS PAGE (4 – 12%, NuPAGE-Novex Bis-Tris Gels, Invitrogen). The proteins with an apparent molecular weight of 72-74 kDa were identified by peptide mass fingerprinting (Fingerprints Proteomics Facility, University of Dundee). Purified Hc was stored at 4°C.

3.3.6 Dynamic light scattering

All measurements were recorded at 5°C on a Malvern, Zetasizer Auto Plate Reader (50mW 830nm Laser). A 50 µL sample of a 2.5 mg mL⁻¹ solution of purified *N. norvegicus* Hc in 100 mM Tris-HCl, pH 7.5 was placed in a single unit on a 384 well plate. Particle size measurements were recorded using 13 scans of 10 s duration over a period of ~ 10 min; the estimated size represents an average of 3 repeats. For the melting curve experiments, single measurements were taken from 5°C to 90°C in 2°C increments. Equipment was cleaned using 6M Guanidine HCl, 10% Decon, 0.1M HCl and 0.1M NaOH prior to use.

3.3.7 Hemocyanin derived phenoloxidase activity

Phenoloxidase activity was measured at 20°C in a 96 well plate (MDS VERSA max microplate reader). Assays (100 µL volume) consisted of 2 mM dopamine hydrochloride in 100 mM Tris-HCl, pH 7.5 and *N. norvegicus* Hc at a final concentration of 1 mg mL⁻¹. Hc was either pre-incubated for 5 minutes with 0.1 % SDS, CPC or 20 % (v/v)

isopropanol, or for 30 mins with 1 M Urea and/or 200 mM NaClO₄. PO activity was monitored as outlined in section 2.3.4. Values for the auto-oxidation of substrate were deducted from the Hc-d PO activity values to generate absorbance changes which could be attributed to Hc-d PO only.

3.3.8 Enzyme Kinetics

A) Substrate properties

Stock solutions of dopamine and 4-methylcatechol were prepared in 100 mM Tris-HCl, pH 7.5. Hc was pre-incubated with 3.5 mM SDS for 5 min. Assays were initiated by the addition of substrate. Dopamine and 4-methylcatechol were assessed over the ranges 0 – 4 mM and 0 – 30 mM, respectively. Hc failed to display monooxygenase activity in the presence of L-tyrosine at concentrations between 0 – 20 mM.

B) Inhibition studies

Stock solutions of kojic acid, PTU, tropolone, L-ER and mimosine were prepared in 100 mM Tris, pH 7.5. Stock solutions of 4-HR were prepared in 100 mM Tris, pH 7.5, containing 25% ethanol. Inhibition studies were carried out by pre-incubating *N. norvegicus* Hc with SDS for 5 min and subsequently with an inhibitor for a further 5 min. The assays were initiated by the addition of 2 mM dopamine. Each assay was conducted in triplicate and average rates were calculated.

3.3.9 Absorption Spectroscopy

The absorption spectra of purified Hc samples were recorded on an Ultrospec 2100 pro UV/Visible spectrophotometer over the range of 240–400 nm. The properties of the

copper binding site of Hc were monitored via the absorption peak at ~ 350 nm which is characteristic of type three copper proteins with dioxygen bound.

A) Hemocyanin stability; freeze-thawing

The absorption spectra of 0.3 mg mL⁻¹ *N. norvegicus* Hc, in 100 mM Tris-HCl, pH 7.5, were recorded prior to incubation at -25°C and following incubation at -25°C for 24 h with subsequent thawing on ice for 2 h.

B) Inhibitor interactions

The absorption spectra of 0.4 mg mL⁻¹ Hc were recorded in the presence of SDS and inhibitors. Hc, in 100 mM Tris-HCl, pH 7.5, was pre-incubated with 1.4 mM SDS for 5 min and subsequently incubated in the presence of an inhibitor (4-HR, 60 µM, L-ergothioneine, 220 µM and/or mimosine, 250 µM) for a further 5 min. A control spectrum, with no inhibitor, was recorded to note any changes caused by a further 5 min incubation with SDS.

3.3.10 Fluorescence Spectroscopy

All experiments were recorded on a Perkin Elmer LS50 spectrofluorimeter at 20°C over the range 300-510 nm. Intrinsic tryptophan fluorescence was recorded using a quartz cuvette of 1 mL capacity at a protein concentration of 0.1 mg mL⁻¹ in 100 mM Tris-HCl, pH 7.5. The excitation wavelength used was 290 nm with a 5 nm bandwidth for the excitation and emission. All scans were recorded at a rate of 50 nm/min and corrected by the subtraction of a spectrum of SDS/inhibitor only. Control experiments were conducted to note the contribution that inhibitors and SDS made to the fluorescence signals.

A) Hemocyanin stability; freeze-thawing

Fluorescence emission spectra of 0.1 mg mL⁻¹ *N. norvegicus* Hc, in 100 mM Tris-HCl, pH 7.5, were recorded prior to incubation at -25°C and following incubation at -25°C for 24 h with subsequent thawing on ice for 2 h.

B) Inhibitor interactions

Fluorescence emission spectra of 0.05 mg mL⁻¹ Hc were recorded in the presence of SDS and inhibitors. Hc, in 100 mM Tris-HCl, pH 7.5, was pre-incubated with 1.4 mM SDS for 5 min and subsequently incubated in the presence of an inhibitor (4-HR, 30 µM, L-ergothioneine, 110 µM and/or Mimosine, 125 µM) for a further 5 mins. A control spectrum, with no inhibitor, was recorded to note any changes caused by a further 5 min incubation with SDS.

3.3.11 Data handling

Substrate kinetic data was fitted to a Michaelis-Menten equation using Sigma Plot 12, yielding V_{\max} and K_m values. IC_{50} inhibition values were calculated using a range of inhibitor concentrations; 4-HR (0 – 0.5 mM), L-ER (0 – 1 mM), Mimosine (0 – 1 mM), Kojic acid (0 – 1 mM), Tropolone (0 – 1 mM) and PTU (0 – 0.05 mM). Inhibition data was fitted to a standard curve using a four parameter logistic equation (minimum, maximum, EC_{50} and slope of the curve). Data presented here, represents the mean \pm standard error.

3.4 Results

3.4.1 Effect of freeze-thawing on phenoloxidase activity from cellular and hemolymph fractions

The relative amounts of inducible PO activity from extracellular Hc-d PO and cellular PO were calculated as ~ 50 U and ~ 969 U (prepared from 1 mL of hemolymph), respectively. Cellular PO activity is reduced by $> 98\%$ after incubating at -25°C for 120 h and subsequently thawing for 2 h, whereas extracellular Hc-d PO retains 100% activity following a similar treatment (Fig. 3.2A). Interestingly, it appears that the freeze-thawing process increases PO activity recorded in the hemolymph fraction (Hc-d PO activity) by $\sim 20\%$ following incubation at -25°C for 72 h.

Extracted hemocytes of *N. norvegicus* were stained for viability (using trypan-blue) and the presence of PO (Fig. 3.2B), to ensure functionality prior to lysis, and to confirm the presence of cellular proPO. Between 5 to 6×10^6 hemocytes per mL were enumerated, $> 98\%$ were viable and $\sim 11\%$ stained positive for PO, under the conditions used.

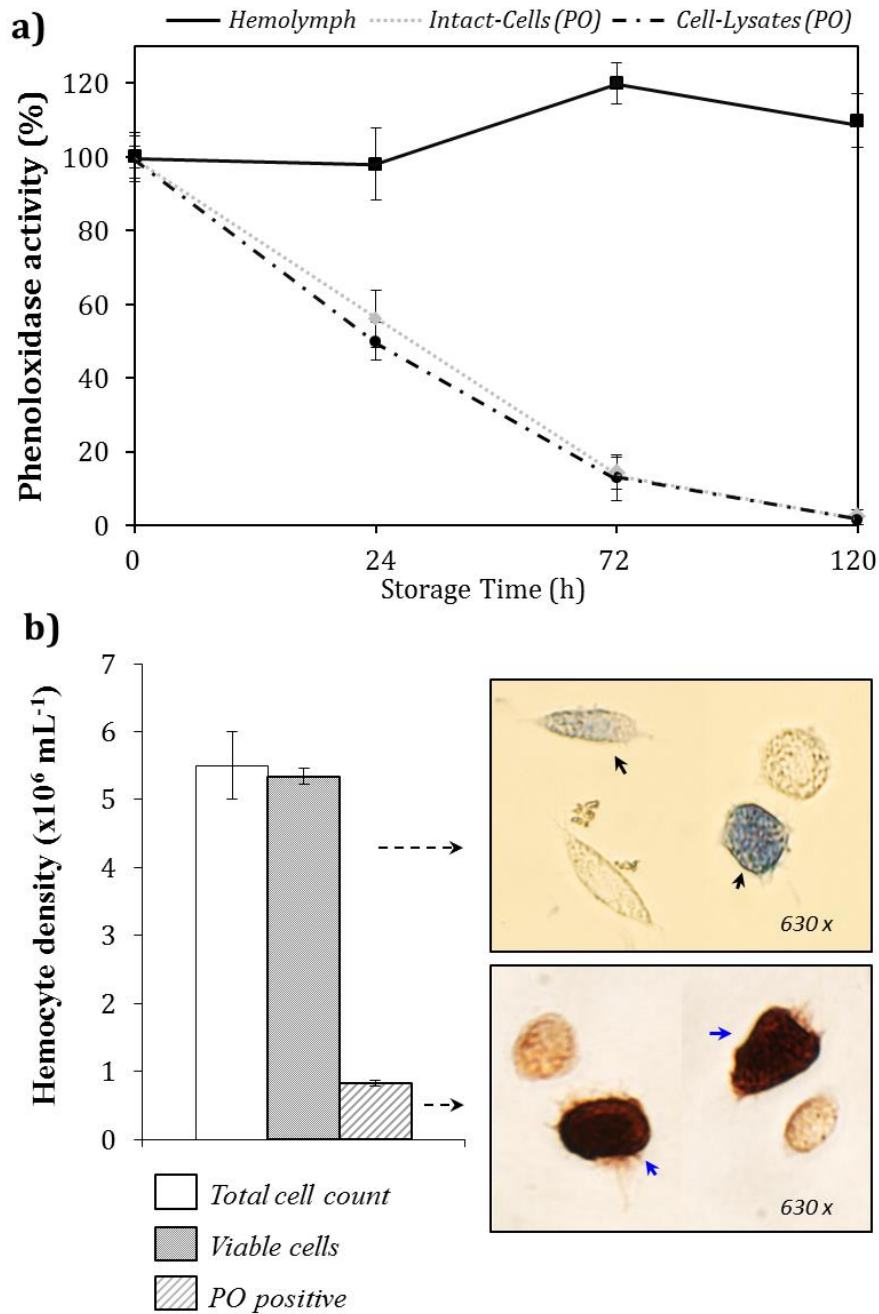


Figure 3.2 Effect of freeze-thawing on cellular and hemolymph fractions from *Nephrops norvegicus*. **A)** Phenoloxidase activity of freeze-thawed crude cell lysates and cell-free hemolymph (i.e. Hc-d PO) from *N. norvegicus*. At time 0, hemocytes were lysed via lysis buffer and sonicated. At time points; 24 – 120 h, hemocyte lysis was achieved via the freeze-thawing process. **B)** Properties of hemocytes extracted from *N. norvegicus*. Images; non-viable hemocytes stain blue due to loss of plasma membrane integrity (black arrows). Viable cells are unstained. Hemocytes that stain positive for PO appear an intense dark brown/red colour (blue arrows). Unstained cells appear a faint brown due to the presence of the chromogenic substance, MBTH, in the stain. Values are represented by the mean \pm standard error, $n = 7$.

3.4.2 Purification of hemocyanin from *Nephrops norvegicus*

The success of Hc purification from *N. norvegicus* hemolymph was determined by the 280 nm: 350 nm absorption ratio values and SDS-PAGE (Fig. 3.3). A 280 nm: 350 nm absorption ratio value of 4.2 was achieved, which is characteristic of type three copper proteins with dioxygen bound, and in good agreement with Hcs purified previously (Coates et al., 2011). Hc subunits with a molecular mass of ~ 72 kDa and ~ 74 kDa were identified using SDS-PAGE (Fig. 3.3B), and confirmed by peptide mass fingerprinting (Appendix 10.1). Typically, ~ 10.5 mg of Hc was purified from 1 mL of *N. norvegicus* hemolymph (Table 3.1). Dynamic light scattering measurements produced a calculated radius of gyration of 8.3 ± 0.2 nm for purified *N. norvegicus* Hc, suggesting Hc was present as a hexamer (Appendix 10.2).

3.4.3 Stability of *Nephrops norvegicus* hemocyanin

Purified Hc from *N. norvegicus* hemolymph was incubated at -25°C for 24 h and thawed subsequently on ice for 2 h. The resultant absorption spectra (Fig. 3.4A) and fluorescence spectra (Fig. 3.4B), pre- and post-freezing, demonstrated retention of Hc structural integrity. Using DLS, Hc displayed a melting point at ~ 55°C (Fig. 3.5), characterised by high levels of protein aggregation.

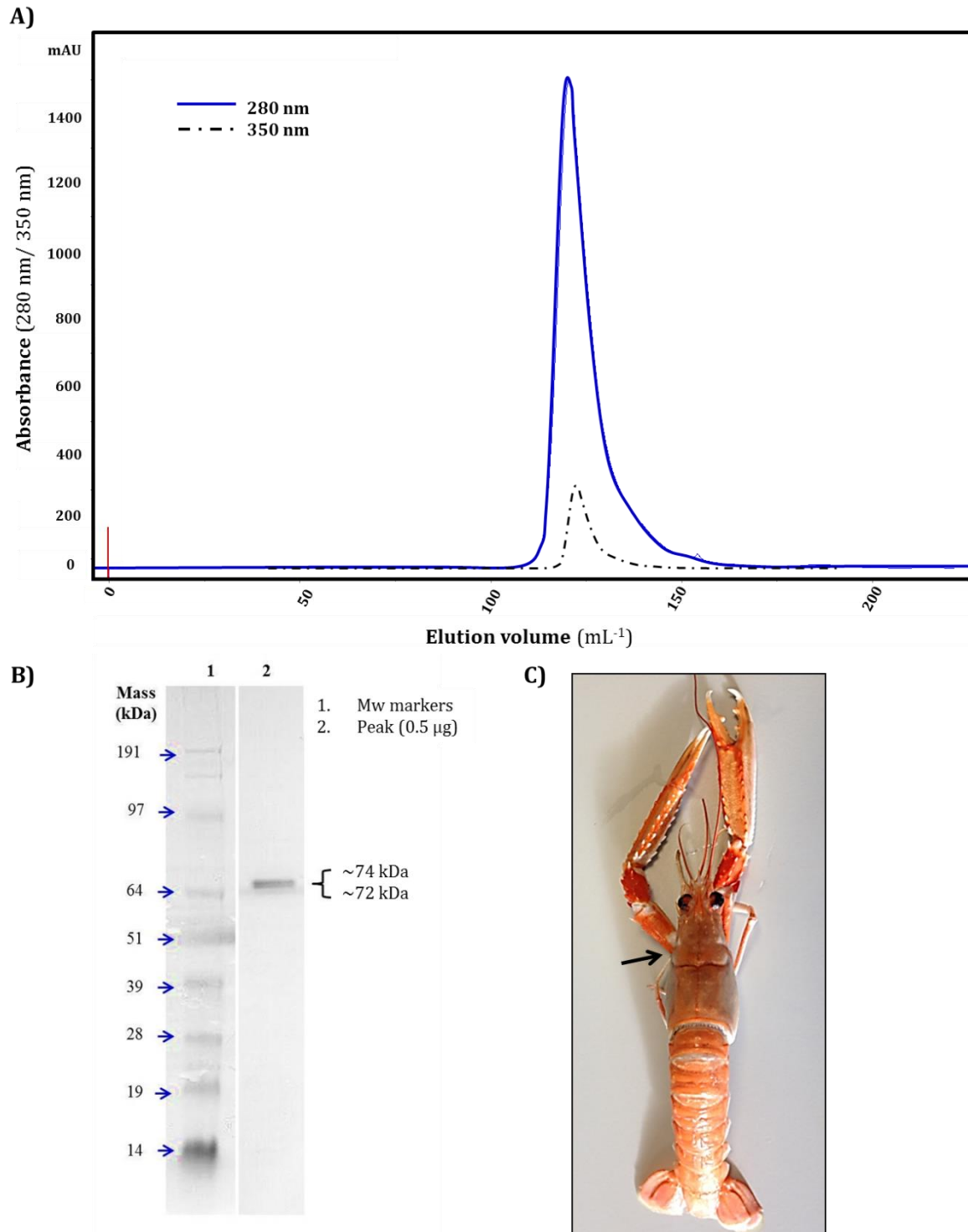


Figure 3.3 Purification of hemocyanin from *Nephrops norvegicus*. **A)** Sephacryl-500 HR size exclusion chromatogram displaying a single peak. Peak fractions with a 280 nm: 350 nm absorption ratio value of 4.2 (oxy-hemocyanin) were pooled. **B)** SDS PAGE analysis of purified *N. norvegicus* hemocyanin. Lane 1, molecular weight markers and Lane 2, represents the peak (lane was loaded with 0.5 μg protein). **C)** Hemolymph is extracted from *N. norvegicus* between the pincher cheliped and cephalothorax (black arrow).

Table 3.1 Purification of hemocyanin from *Nephrops norvegicus*, for 1 mL of hemolymph

	Protein conc. (mg mL ⁻¹) ^a	Percentage dioxygen bound ^b	Ratio (280 nm : 350 nm)	Total PO (U)	Specific activity (U mg ⁻¹)	Yield (%)
Whole hemolymph (acellular)	22.1	100 %	4.7	47.5	2.15	100
Supernatant (centrifuged at 400,000 g)	2.2	10.5 %	47.4	1.12	0.51	9.95
Pellet (Semi-purified)	19.3	96 %	5	41.3	2.14	87.3
Peak fractions † (Gel filtration)	1.77	100 %	4.2	23.7	2.23	48

^a, hemocyanin concentration was determined as outlined in section 3.3.5

^b, values were calculated from the A 350 nm signal.

†, each of the individual fractions (3 x 2 mL) had an absorbance ratio value of 4.2.

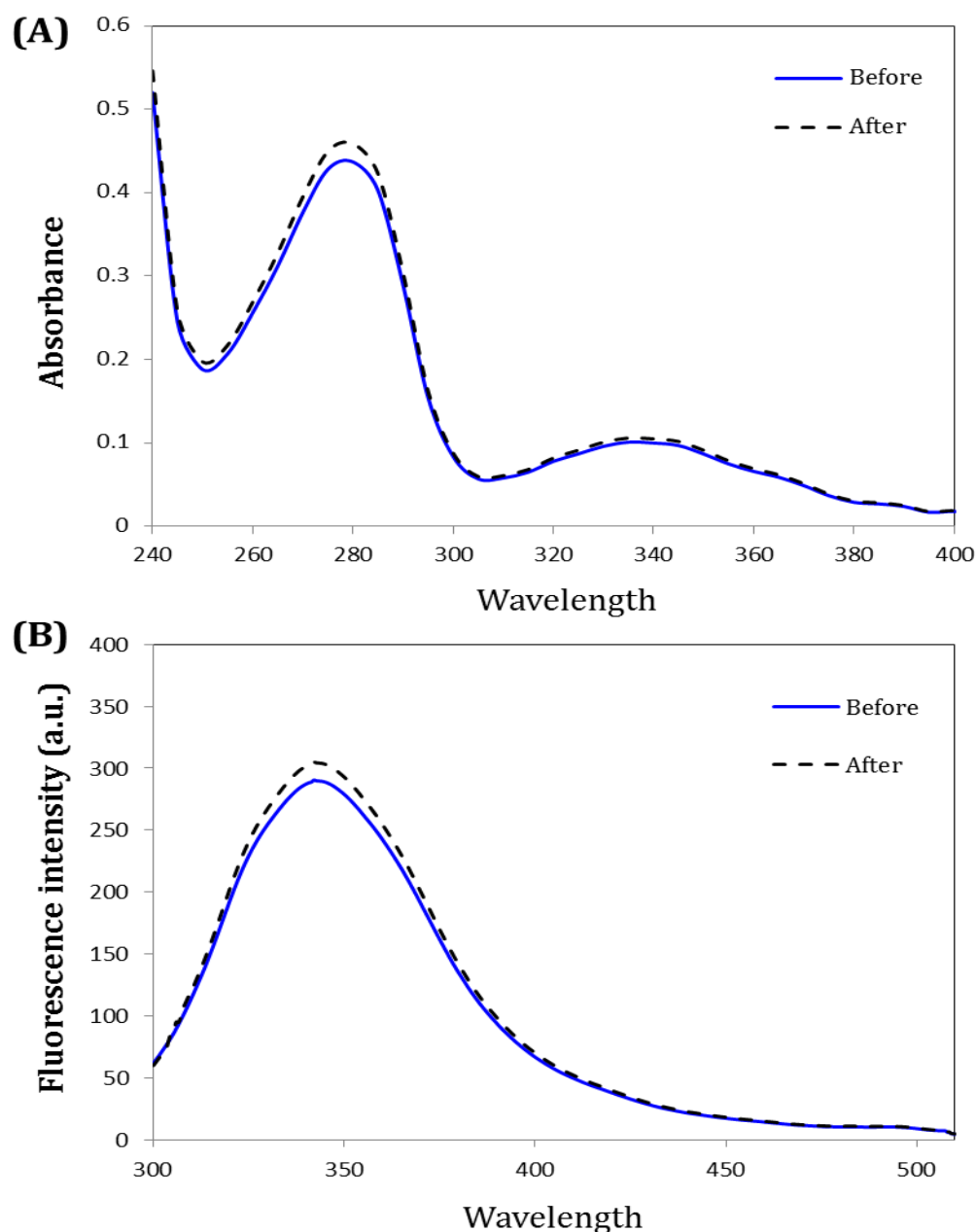


Figure 3.4 Effect of freeze-thawing on the stability of purified *Nephrops norvegicus* hemocyanin. **A)** Absorption spectra of 0.3 mg mL^{-1} *N. norvegicus* hemocyanin (in 100 mM Tris-HCl, pH 7.5) before and after freeze-thawing. **B)** Fluorescence emission spectra of 0.1 mg mL^{-1} *N. norvegicus* hemocyanin (in 100 mM Tris-HCl, pH 7.5) before and after freeze-thawing. Purified hemocyanin was frozen at -25°C for 24 h and subsequently thawed on ice for 2 h before spectral measurements.

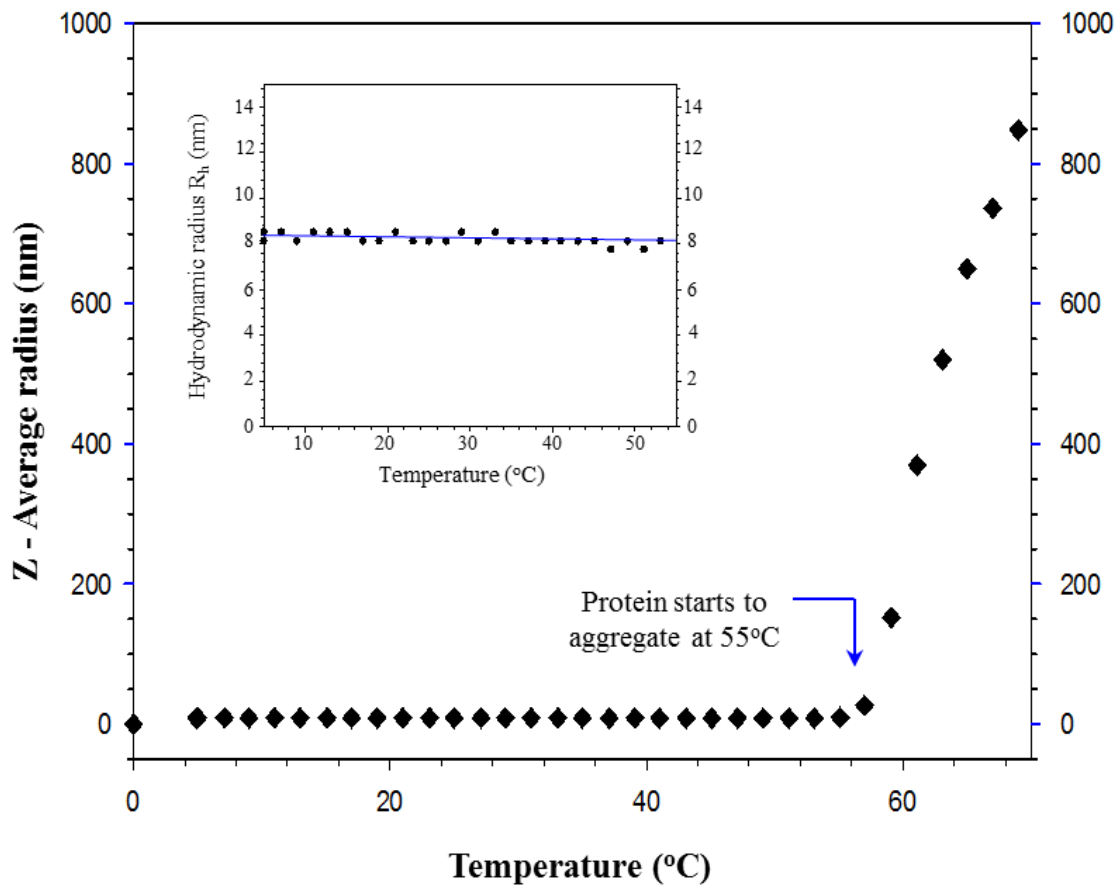


Figure 3.5 Melting curve for purified *Nephrops norvegicus* hemocyanin across the temperature range, 0°C to 70°C. Inset; the hydrodynamic radius of the major species (Hemocyanin) in the solution is depicted, before aggregation (0°C - 55°C).

3.4.4 Inducible phenoloxidase activity of *Nephrops norvegicus* hemocyanin

Effect of elicitors

PO activity of *N. norvegicus* Hc was assessed in the presence of known PO elicitors (Fig. 3.6) (using conditions similar to those in Perdomo-Morales et al., 2008 and Fan et al., 2009). Hc-d PO activity was highest in the presence of the anionic detergent, SDS, at a concentration of 3.5 mM, conditions which would ensure the micelle form of SDS. However, incubation of Hc in the presence of SDS concentrations > 4 mM appeared to have a deleterious effect on enzyme activity (Fig. 3.7). Incubation of Hc in the presence of the cationic detergent, CPC, yielded high levels of PO activity, but overall CPC was not as effective as SDS. Urea and isopropanol also induced PO activity. Hc failed to display PO activity in the absence of an elicitor.

Extended incubation of *N. norvegicus* Hc in the presence of 3.5 mM SDS, over a period of 2 h, led to a significant decrease in enzymatic activity (Fig. 3.8). Maximum activity of ~ 2.23 U was achieved after 5 minutes pre-incubation with SDS.

Substrate Kinetics

The PO activity of *N. norvegicus* Hc was not detected in the presence of the monophenol tyrosine, but was evident using the di-phenolic substrates, dopamine hydrochloride and 4-methylcatechol (Fig. 3.9). Data was fitted to the Michaelis-Menten equation in order to determine the kinetic parameters: V_{max} and K_m . Analysis indicates that while 4-methylcatechol elicits a higher rate of activity; $V_{max} = 5.84 \pm 0.235 \text{ U}$, $K_m = 9.85 \text{ mM} \pm 0.894$ ($R^2 = 0.973$), dopamine appears to bind more efficiently; $V_{max} = 2.4 \pm 0.067 \text{ U}$, $K_m = 0.431 \text{ mM} \pm 0.043$ ($R^2 = 0.956$).

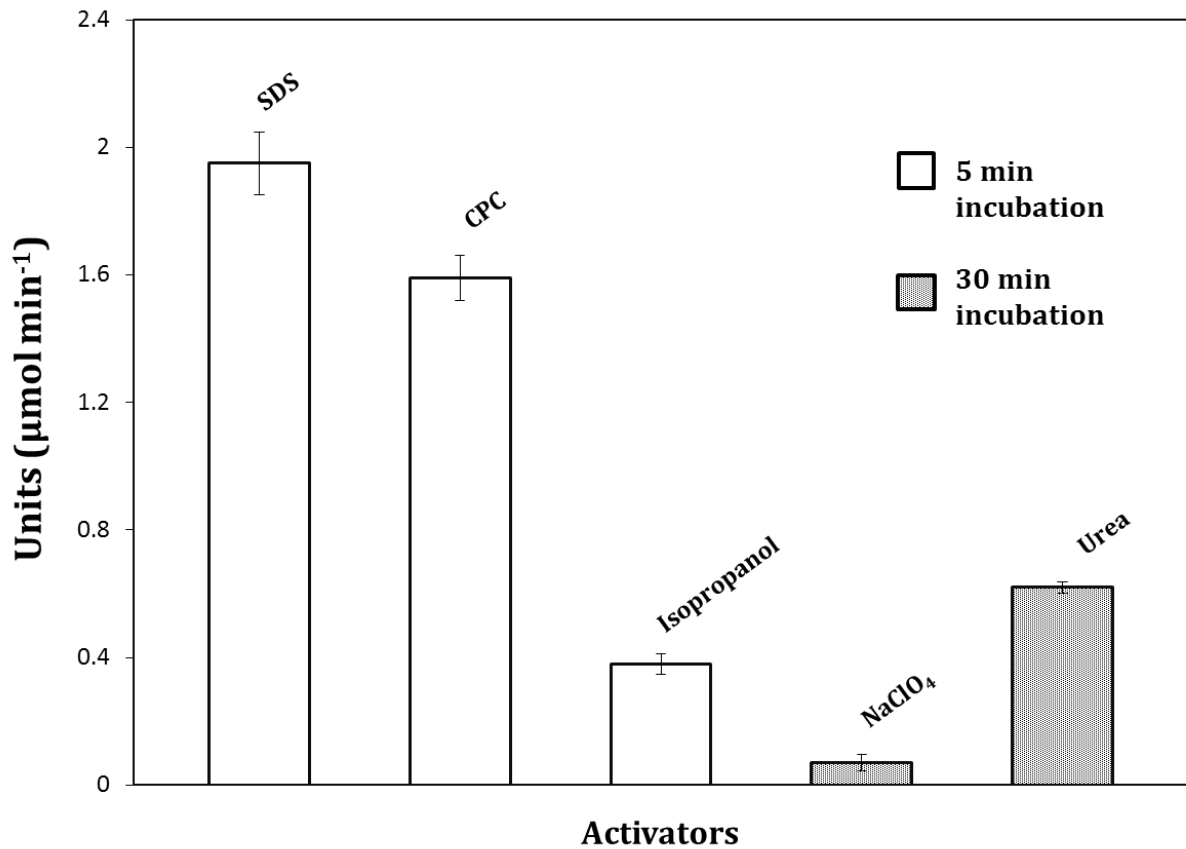


Figure 3.6 Hemocyanin derived phenoloxidase activity of purified *Nephrops norvegicus* hemocyanin induced by a range of known phenoloxidase activators. Assays included 2 mM dopamine and 1 mg mL⁻¹ hemocyanin in 100 mM Tris-HCl, pH 7.5. Hemocyanin was pre-incubated in either SDS (3.5 mM), CPC (2.8 mM) or isopropanol (20%, v/v) for 5 min or for 30 min in sodium perchlorate (200 mM) or Urea (1M) before activity measurements were recorded. Assays were initiated with the addition of substrate and recorded over a 10 min period. Control assays consisted of hemocyanin and substrate in the absence of an activator. Values are represented by the mean \pm standard error.

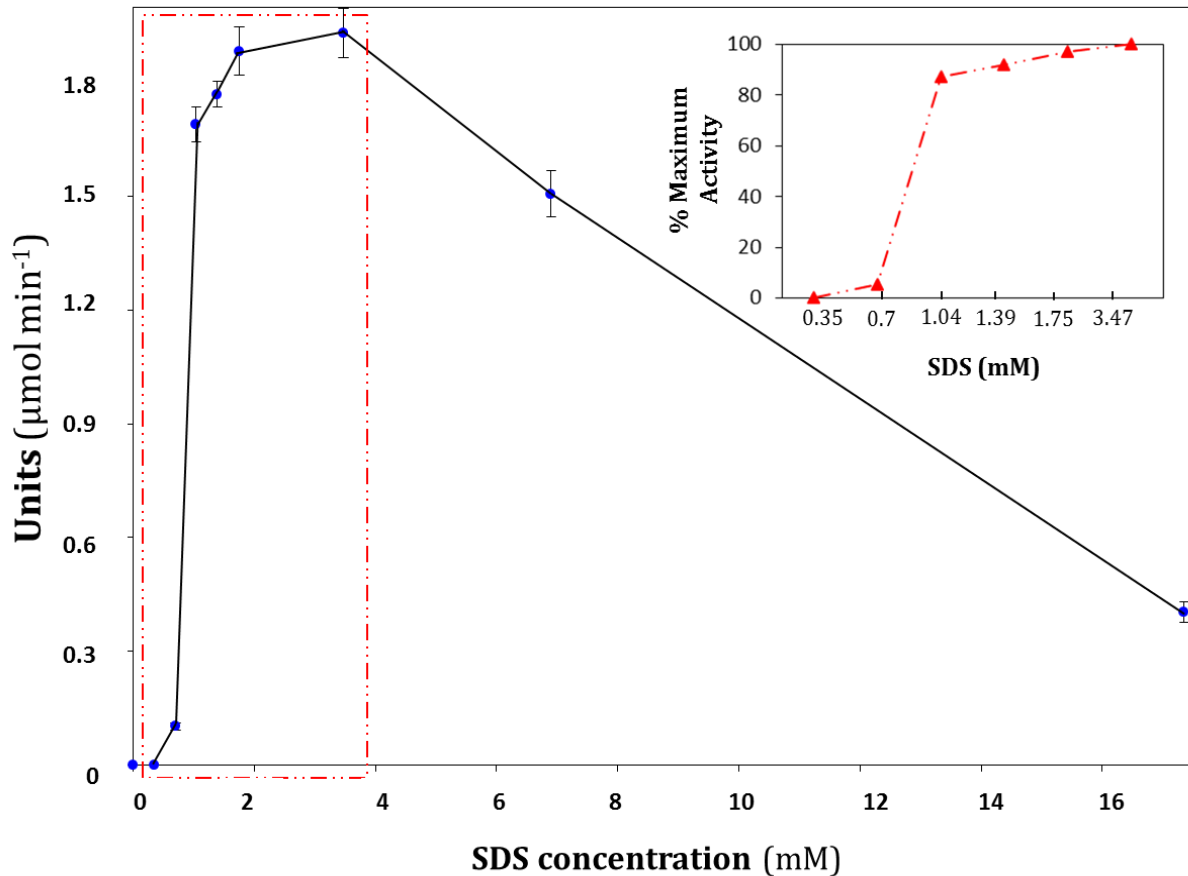


Figure 3.7 Stability of activated *Nephrops norvegicus* hemocyanin in the presence of increasing concentrations of SDS. Hc was pre-incubated in each concentration of SDS, for 5 mins. Assays were initiated by the addition of substrate. The inset provides clearer detail of the region of the main plot contained within the red box and shows phenoloxidase activity expressed as a percentage of the maximum activity. Values are represented by the mean \pm standard error

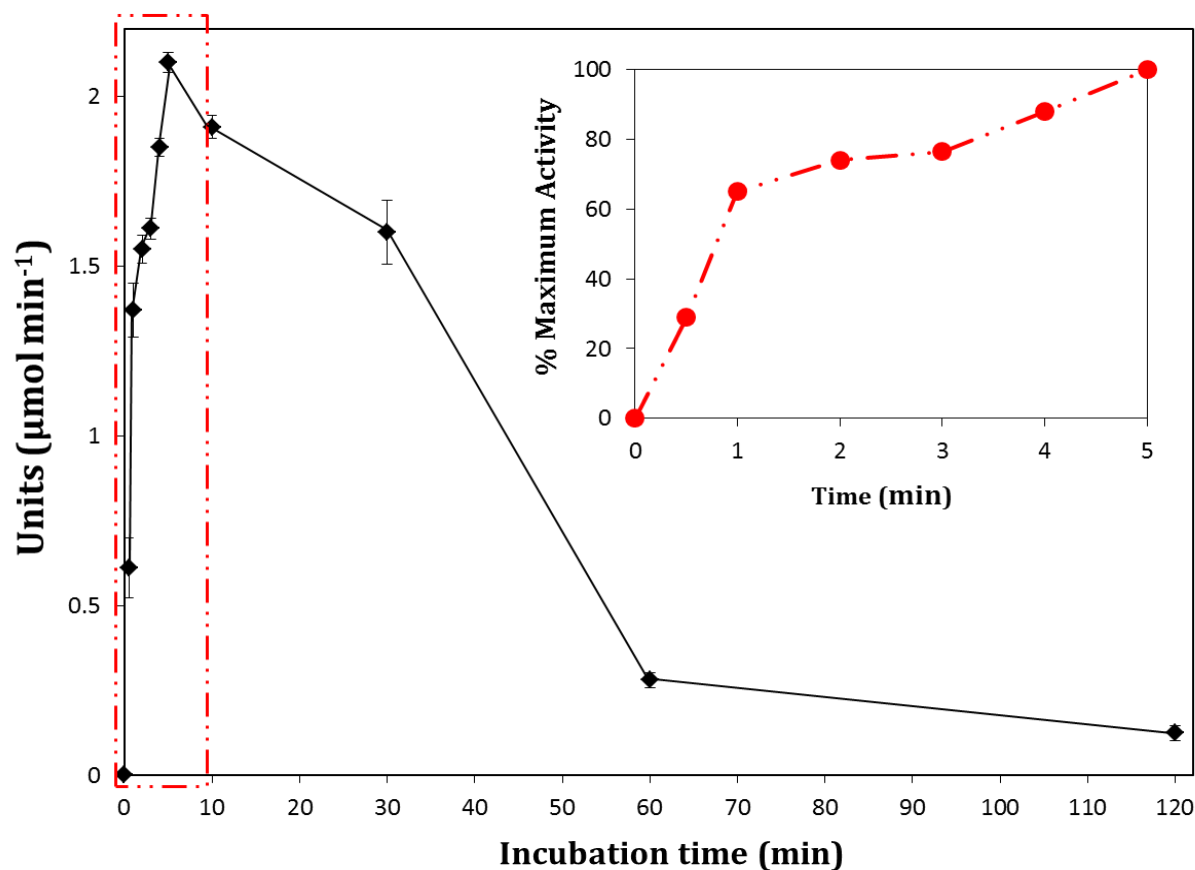


Figure 3.8 Stability of activated hemocyanin in the presence of SDS over time. Hemocyanin was pre-incubated with 3.5 mM SDS for periods between 0 and 120 min. The inset provides clearer detail of the region of the main plot contained within the red box and shows phenoloxidase activity expressed as a percentage of the maximum activity. Control assays consisted of hemocyanin and substrate in the absence of an activator. Values are represented by the mean \pm standard error.

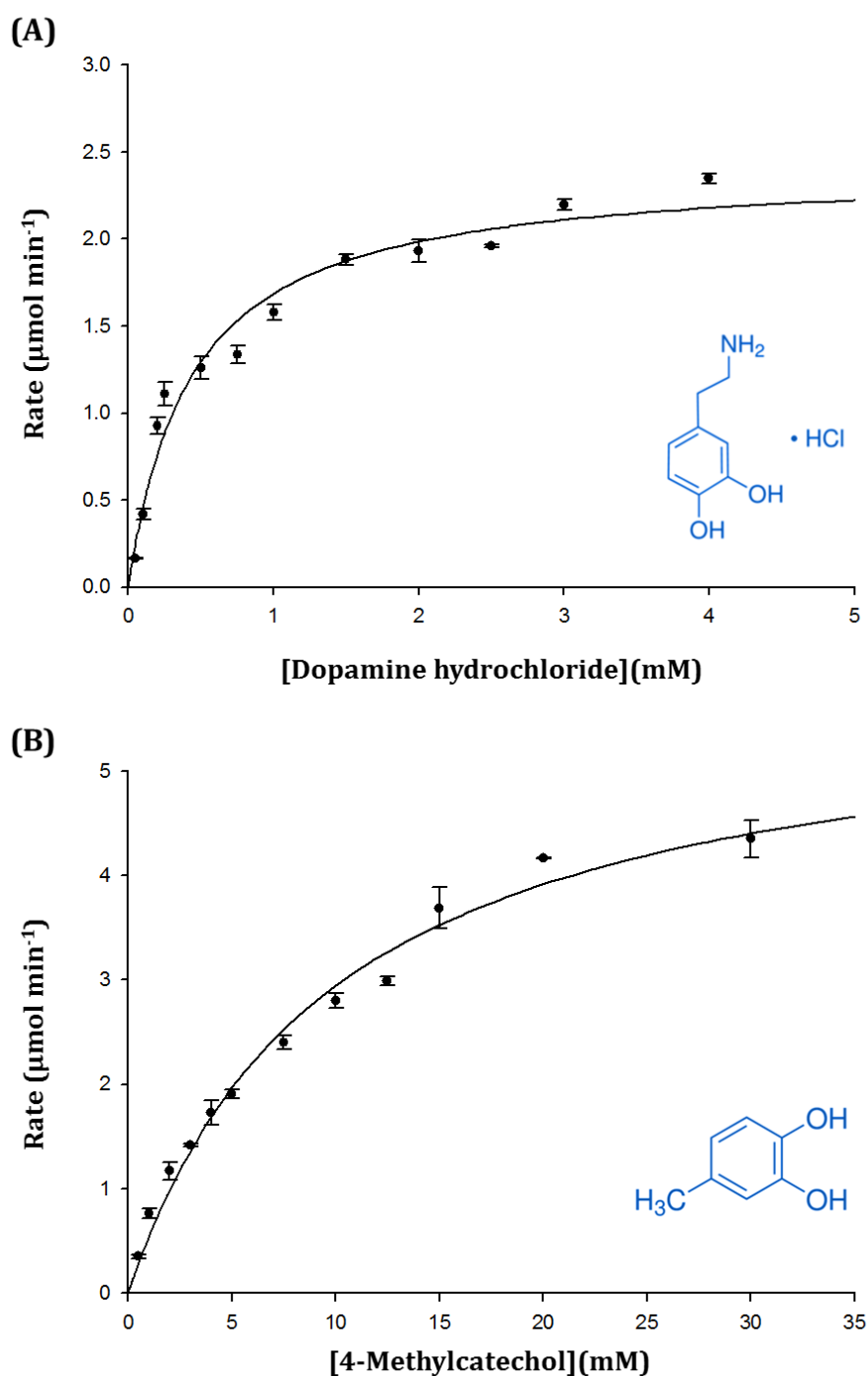


Figure 3.9 Kinetic analysis of o-diphenoloxidase activity of *Nephrops norvegicus* hemocyanin (0.1 mg mL^{-1}) towards A) Dopamine-hydrochloride, 0 – 4 mM and B) 4-methylcatechol, 0 – 30 mM, in 100 mM Tris-HCl, pH 7.5. Kinetic data was fitted to the Michaelis-Menten equation using SigmaPlot 12 and the subsequent V_{max} and K_{m} values for each substrate were recorded. Inset; chemical structures of each substrate.

3.4.5. The inhibition of hemocyanin derived phenoloxidase activity

Inhibitor efficiency

The effects of a range of known PO inhibitors (Table 3.2), were tested on Hc-d PO activity from *N. norvegicus*, using dopamine as substrate. IC₅₀ values were calculated for each inhibitor. While all six inhibitors affected the catecholoxidase activity of *N. norvegicus* Hc, the teratogenic compound PTU, demonstrated the most effective inhibition; IC₅₀ = 0.57 μM ± 0.11. In this study, the order of inhibitor efficiency is PTU > 4-HR > tropolone > L-ER > kojic acid > mimosine (Table 3.2). The second most effective inhibitor, 4-HR, displayed an IC₅₀ value of 56 μM ± 5.5, which is ~ 4-fold lower than L-ER, kojic acid, mimosine and tropolone.

Inhibitor-hemocyanin interactions

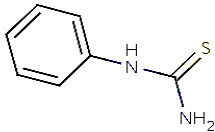
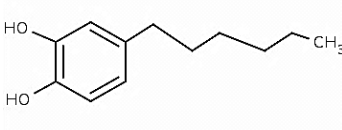
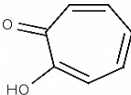
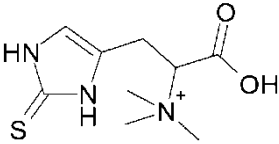
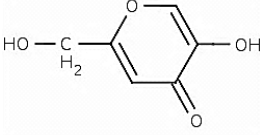
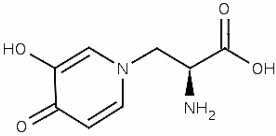
Inhibitor induced changes in the tertiary structure of Hc were recorded using intrinsic tryptophan fluorescence intensities (Fig. 3.10). Incubation of Hc in the presence of inhibitors, 4-HR, L-ER and mimosine, led to an increase in fluorescence intensity, which is indicative of a reduction of internal quenching. Hc in the presence of 4-HR and L-ER resulted in a decrease (6.5 nm) in the wavelength of the fluorescence emission maximum, suggesting that tryptophan residues present in the Hc subunit become less exposed to the solvent. The tyrosinase substrate analogue, mimosine, also caused an increase in fluorescence intensity, but was accompanied by a red shift in the emission maximum (Table 3.3). While incubating Hc in the presence of SDS micelles yields an increase in intrinsic fluorescence intensity, the increase is at least ~ 2 fold greater in the presence of SDS plus an inhibitor (Fig. 3.10A). Fluorometric assessment of Hc in the presence of inhibitors suggests significant structural changes may accompany the

inhibition of PO activity. Control experiments in which each inhibitor was added to the model compound *N*-acetyl-L-tryptophanamide confirmed that the inhibitor-induced conformational changes in Hc fluorescence were not the result of direct interactions between the inhibitor and exposed tryptophan side chains (Fig. 3.10B).

The effects of 4-HR, L-ER and mimosine on the di-copper centre of *N. norvegicus* Hc were monitored by UV-absorption spectroscopy (Fig. 3.11). Incubation of Hc with the inhibitors resulted in a decrease in the absorption peak at ~ 350 nm. This peak is typical of type 3 copper enzymes with di-oxygen bound and is due to the peroxide which is present in a $\mu\text{-}\eta^2\text{:}\eta^2$ side-on coordination and acts as a strong σ -donor ligand to the Cu(II) ions. This hypochromic effect, at ~ 350 nm, in the presence of inhibitors, suggests a distortion of the dicopper centre via inhibitor-active site interactions or changes induced by inhibitor binding in close proximity to the active site.

The spectral properties of tropolone and kojic acid prevented the determination of the effects of these inhibitors on the 350 nm absorption peak and fluorescence emission maximum of Hc.

Table 3.2 Inhibitors of hemocyanin-derived phenoloxidase

Inhibitor (order of efficacy)	IC ₅₀ value (μ M)	Inhibitor Structure
<i>1-phenyl 2-thiourea</i>	0.57 \pm 0.11	
<i>4-Hexylresorcinol</i>	56 \pm 5.5	
<i>Tropolone</i>	188 \pm 3.57	
<i>L-Ergothioneine</i>	217 \pm 20.1	
<i>Kojic Acid</i>	247 \pm 23	
<i>Mimosine</i>	277 \pm 12.3	

IC₅₀ inhibition values were calculated using a range of inhibitor concentrations.

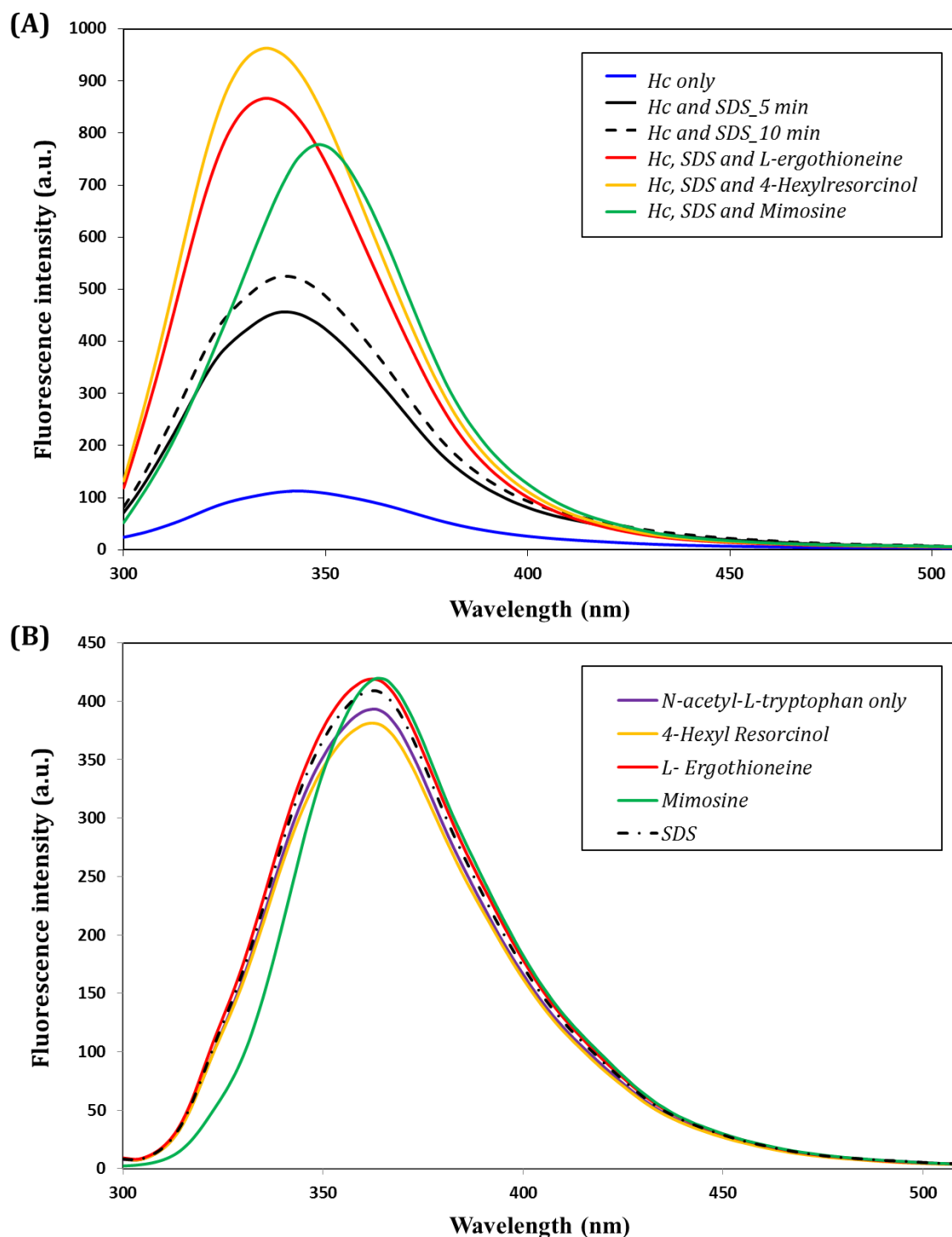


Figure 3.10 Intrinsic tryptophan fluorescence of *Nephrops norvegicus* hemocyanin in the presence of phenoxidase inhibitors. **A)** Fluorescent emission spectra of 0.05 mg mL^{-1} *Nephrops norvegicus* hemocyanin. Hemocyanin (in 100 mM Tris-HCl, pH 7.5) was pre-incubated with 1.4 mM SDS for 5 min and subsequently incubated in the presence of an inhibitor for a further 5 mins. Samples were excited at 290 nm and the subsequent spectrum was recorded. **B)** Fluorescent emission spectra of $2 \mu\text{M}$ *N*-acetyl-*L*-tryptophan, in 100 mM Tris-HCl, pH 7.5 was excited at 290 nm in the presence and absence of SDS and/or inhibitors after a 5 min incubation period. Inhibitor concentrations used for both **A** and **B** were as follows; 4-HR, $30 \mu\text{M}$, *L*-Ergothioneine, $110 \mu\text{M}$ and Mimosine, $125 \mu\text{M}$. Data was recorded over the range 300 nm – 510 nm.

Table 3.3 Intrinsic tryptophan fluorescence peak wavelength of *Nephrops norvegicus* Hc in the presence of inhibitors and SDS.

^ASpectral properties prevented the determination of the effects of inhibitor on the dicopper active site of Hc, as the inhibitor displayed peaks around the fluorescence emission maxima (and the absorption spectrum). Inhibitors were in the presence of both Hc (0.05 mg mL⁻¹) and SDS (1.4 mM).

	Inhibitor	Tryptophan fluorescent emission maxima
Hc only (0.05 mg mL ⁻¹)	-	342 nm
Hc & SDS_5 min	-	340 nm
Hc & SDS_10 min	-	340 nm
-	<i>1-phenyl 2-thiourea</i>	-
Hc & SDS_5 min	<i>4-Hexylresorcinol</i>	335.5 nm
-	<i>Tropolone^A</i>	-
Hc & SDS_5 min	<i>L-Ergothioneine</i>	335.5 nm
-	<i>Kojic Acid^A</i>	-
Hc & SDS_5 min	<i>Mimosine</i>	348.5 nm

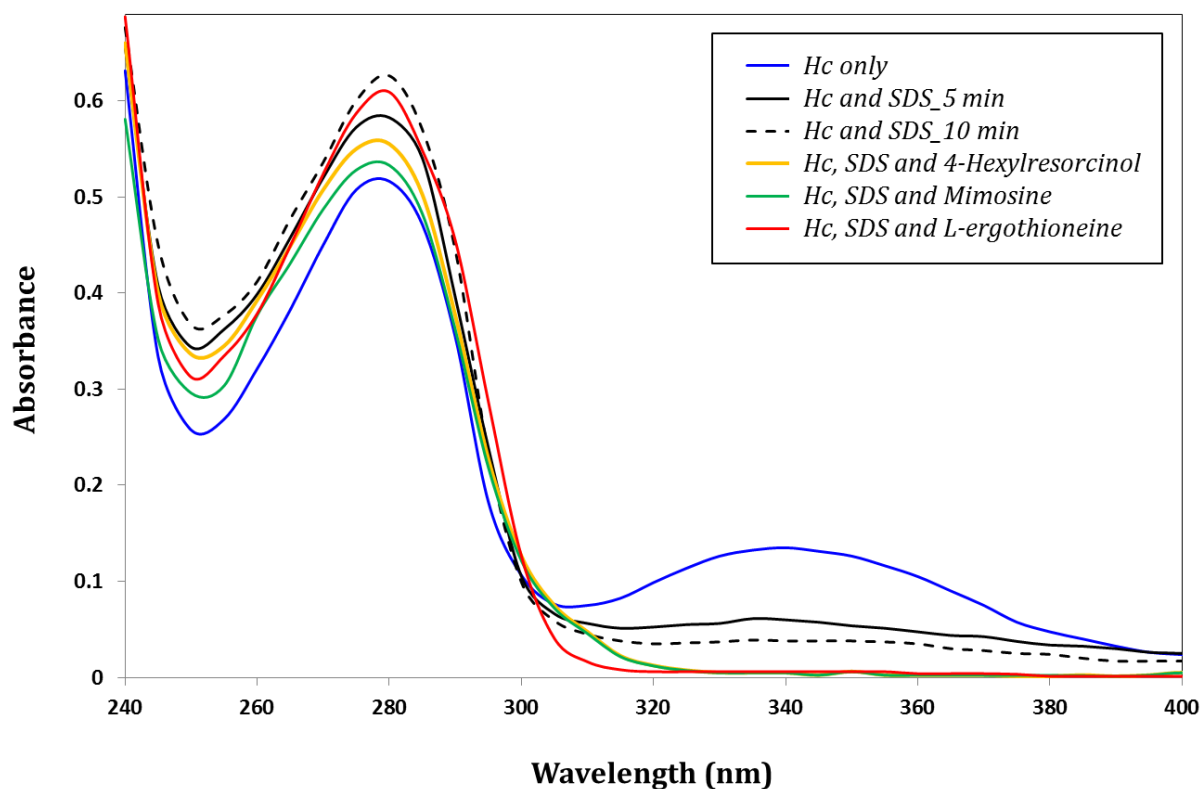


Figure 3.11 Absorption spectra of 0.4 mg mL^{-1} *Nephrops norvegicus* hemocyanin. Hemocyanin (in 100 mM Tris-HCl, pH 7.5) was pre-incubated with 1.4 mM SDS for 5 min and subsequently incubated in the presence of an inhibitor (4-HR, 60 μM , L-ergothioneine, 220 μM and/or Mimosine, 250 μM) for a further 5 mins. Data was recorded over the range 240 nm – 400 nm.

3.5 Discussion

3.5.1 The stability of phenoloxidase and hemocyanin derived phenoloxidase from *Nephrops norvegicus* hemolymph

The onset of hyperpigmentation occurs when fresh-caught or harvested shellfish are thawed after frozen storage (Adachi et al., 2001). Both cellular and supernatant fractions of *N. norvegicus* hemolymph were incubated at -25°C for a period between 0 to 120 h, subsequently thawed, and assessed for PO activity. Cell-derived PO activity was almost completely inactivated following this treatment (Fig. 3.2). Conversely, the supernatant fraction containing Hc, not only retained activity under similar conditions, but Hc-d PO activity levels increased by ~ 20 % at 72 h. Interestingly, mollusc Hc purified from *Rapana thomasiana*, displays an increase in PO levels, from ~ 1 U to 9 U (with catechol as substrate), after freeze-drying (lyophilisation) (Idakieva, Islam-Siddiqui, Meersman, De Maeyer, Chakarska & Gielena, 2009). By freezing intact cells and cell lysates, and subsequently monitoring PO activity after thawing, we have confirmed that PO activity is susceptible to hypothermic induced de-activation (Fig. 3.2).

Hc from *N. norvegicus* was purified from the acellular hemolymph fraction by size exclusion chromatography. The elution profile of purified Hc (Fig. 3.3A), along with the optical density ratio values (A 280 nm: A 350 nm, Table 3.1), the SDS-PAGE profile (Fig. 3.3B) and mass spectrometry data, indicates Hc is present without cell-derived PO contamination.

The abundance of Hc present in hemolymph (> 90 % of total protein content) and the high resistance of Hc to adverse temperatures (Fig 3.4, Fig. 3.5), suggests that Hc-d PO may contribute to hyperpigmentation. Similar studies performed in *Penaeus japonicus*

(Adachi et al., 2001), *Parapenaeus longirostris* (Martinez- Alvarez et al., 2008) and *Penaeus vannamei* (Garcia-Carreno et al., 2008) also exhibit inducible PO activity of purified Hc and noted tolerances to extreme pH and temperature conditions.

Hemocyte lysate supernatants and clotting factors/antimicrobial peptides are capable of inducing PO activity of *P. vannamei* Hc (Garcia-Carreno et al., 2008) and *Tachypleus tridentatus* Hc (Nagai & Kawabata, 2000; Nagai, Osaki & Kawabata, 2001), respectively. Post mortem, tissue and cellular integrity is compromised, leading to the systemic release of endogenous activators of Hc-d PO, such as: proteinases from the digestive gland, immune effectors (Adachi, Hirata, Nagai, Fujisawa, Kinoshita & Sakaguchi, 1999) and phospholipids from hemocytes/amebocytes (Nellaiappan & Sugumaran, 1996; Coates, et al., 2011). Furthermore, substantial levels of Hc have been shown to reside throughout the cuticle layers of shrimp exoskeleton (Adachi et al., 2005a); while these findings suggest a role for Hc in the sclerotisation of cuticle during moulting, this reservoir of Hc may also contribute to the progression of hyperpigmentation, post mortem.

3.5.2. Phenoloxidase activity of *Nephrops norvegicus* hemocyanin

In vivo, the native precursor prophenoloxidase (proPO) does not possess enzymatic activity, but is processed by serine proteinases into an active PO enzyme, in the presence of pathogens (Cerenius and Soderhall, 2004). Similarly, native Hc does not possess PO activity, but may be converted *in vitro* into a PO-like enzyme in the presence of denaturants and/or proteinases (Decker and Jaenicke, 2004; Jiang et al., 2007). The universal *in vitro* activator of PO activity, SDS, also causes optimal activation of Hc-d PO activity of *N. norvegicus* Hc (Fig. 3.6 and Fig. 3.7). The activation of PO activity in Hc from *L. polyphemus* has been shown to be accompanied by secondary and tertiary

structural changes induced by SDS micelles (assumed to mimic the *in vivo* mode of activation) which allows substrate access to the di-copper centre, be turned over, and products released (Baird et al., 2007). Evidence presented in chapter 2 suggests that liposomal phospholipids, principally phosphatidylserine, sharing similar structural and electrostatic surface properties with SDS micelles, are putative activators of Hc-d PO activity, *in vivo* (Coates et al., 2011).

Hc purified from the hemolymph of over 20 different species of Crustacea demonstrate inducible PO activity, *in vitro* (Table 3.4). In contrast to chelicerate and mollusc Hcs, the kinetic properties of crustacean Hc-d PO activity are poorly understood. Purified crustacean Hc appears relatively more susceptible to denaturation in comparison to chelicerate Hc-d PO, especially in the presence of SDS (Jaenicke and Decker, 2004; Jaenicke and Decker, 2008). Incubation of *N. norvegicus* Hc in SDS (3.5 mM) over a period of 2h led to a substantial loss of PO activity, > 96% (Fig. 3.8).

Considering the two di-phenolic substrates tested here, *N. norvegicus* Hc displayed a 20-fold higher affinity for dopamine hydrochloride over 4-methylcatechol. A K_m value of 0.431 ± 0.043 mM for dopamine is similar to that determined for *Agaricus bisporus* tyrosinase ($K_m = 0.72 \pm 0.08$ mM) (Fenoll, et al., 2002). Hc purified from *Panulirus argus* demonstrates a higher affinity for dopamine with a K_m value of 0.181 ± 0.0011 mM (Perdomo-Morales et al., 2008). The high affinity of Hcs for the phenolic substrate, dopamine, emphasises the similar catalytic properties of Hcs and POs.

Table 3.4 Inhibition of hemocyanin-derived phenoloxidase activity from crustaceans

Species	Activity	Exogenous elicitors	Inhibition ($\geq 50\%$)	References
<i>Bathynomus giganteus</i>	CO	SDS	PTU; ~ 2.5 mM, DETC; 0.1 mM EDTA; 1 mM	Terwilliger, (2007), Pless et al., (2003)
<i>Calappa granulata</i>	CO	SDS	-	Jaenicke and Decker (2004)
<i>Cancer magister</i>	CO	SDS	-	Terwilliger and Ryan, (2006), Decker et al., (2001)
<i>Cancer pagurus</i>	CO	SDS and trypsin	HCN; ~ 0.28 mM, NaF; ~ 0.18 mM, cupferron; ~ 0.05 mM, Na_2S ; ~ 0.1 mM	Jaenicke and Decker, (2004) Bhagvat and Richter, (1938)
<i>Carcinus aestuarii</i>	CO	-	-	Salvato et al., (1998)
<i>Carcinus maenas</i>	CO	SDS, perchlorate and trypsin	-	Jaenicke and Decker, (2004), Zlateva et al., (1996)
<i>Cirolana harfordi</i>	CO	SDS	-	Terwilliger, (2007)
<i>Charybdis japonica</i>	TY & CO	SDS, urea, HLS and trypsin	PTU; 5 mM, Cysteine; 10 mM, Ascorbic acid; 10 mM, Sodium sulphite; 10 mM, EDTA; 10 mM, DETC; 20 mM, Benzoic acid; 10 mM, Zn^{2+} ; 5 mM, Cu^{2+} ; 5 mM PTU; 29.3 μM , DETC; 29.3 μM , EDTA; 37.5 μM	Fan et al., (2009)
<i>Erimacrus isenbeckii</i>	CO	SDS, LPS, LTA and trypsin	-	Kim et al., (2011)
<i>Homarus americanus</i>	CO	SDS, perchlorate and trypsin	-	Jaenicke and Decker, (2004), Zlateva et al., (1996)
<i>Nephrops norvegicus</i>	CO	SDS, CPC, urea, isopropanol, sodium perchlorate	4-HR; 56 μM , L-ER; 217 μM , Kojic acid; 247 μM , mimosine; 277 μM , tropolone; 188 μM , PTU; 0.57 μM	Gimenez et al., (2010),*
<i>Pacifastacus leniusculus</i>	CO	Trypsin	-	Lee et al., (2004)
<i>Palinurus elephas</i>	TY & CO	SDS and trypsin	-	Jaenicke and Decker, (2004)
<i>Panulirus argus</i>	CO	SDS, trypsin and chymotrypsin	-	Perdomo-Morales et al., (2008)
<i>Panulirus interruptus</i>	CO	SDS and trypsin	-	Jaenicke and Decker, (2004)
<i>Paralithodes camtschaticae</i>	CO	SDS and trypsin	-	Jaenicke and Decker, (2004)
<i>Parapenaeus longirostris</i>	CO	SDS	4-HR; 0.01-1 mM, Tropolone; 9 mM, Ascorbic acid; 0.01-1 mM, $\text{Na}_2\text{S}_2\text{O}_5$; 0.025-0.5 mM	Martinez-Alvarez et al., (2008)
<i>Penaeus japonicus</i>	TY & CO	SDS, Lam, isopropanol and HLS	4-HR; 0.01 mM, Hinokitiol; 0.01 mM, PTU; 0.1 mM, Kojic acid; 0.1 mM, DETC; 1 mM, Cysteine; 1 mM	Adachi et al., (2001), Adachi et al., (2005a & b), Adachi et al., (2003)
<i>Penaeus vannamei</i>	TY & CO	SDS, isopropanol, acetone, methanol, trypsin and chymotrypsin	-	Garcia-Carreño et al., (2008)
<i>Porcellio scaber</i>	CO	SDS and HLS	-	Jaenicke et al., (2009)
<i>Portunus trituberculatus</i>	TY & CO	Urea	-	Fujieda et al., (2010a & b),
<i>Potamon potamion</i>	CO	SDS	-	Jaenicke and Decker, (2004)
<i>Scylla serrata</i>	CO	-	EDTA	Chen et al., (2009) [∞]

SDS-sodium dodecylsulphate, CO-catecholoxidase, TY-tyrosinase, LPS-lipopolysaccharide, LTA-lipoteichoic acid, LAM-laminarin and HLS-hemocyt lysate supernatant, PTU, 1-phenyl, 2-thiourea, DETC, diethyldithiocarbamic acid, EDTA, ethylenediaminetetraacetic acid, HCN, hydrogen cyanide, NaF, sodium fluoride, Na_2S , sodium sulphide, 4-HR, 4-hexylresorcinol, L-ER, L-ergothioneine, $\text{Na}_2\text{S}_2\text{O}_5$ - sodium metabisulphite. [∞] indicates the entire manuscript is not available in English, * represents data presented in this study.

3.5.3 Hyperpigmentation; inhibiting hemocyanin derived phenoloxidase activity

The inhibition of PO activity has been well studied; the prevention of hyperpigmentation of human skin, browning of fruits and mushrooms (Khan, 2012). The occurrence of hyperpigmentation post harvesting, in fresh-caught and cultured shellfish is also a major concern, however, the cause and subsequent inhibition of the abnormal accumulation of melanin in shellfish is lacking in detail. Data presented here, not only establishes Hc as a possible cause of hyperpigmentation in *N. norvegicus*, but also provides information on the kinetic and biophysical interactions of PO inhibitors with shellfish Hc.

A biophysical assessment of chelicerate Hc conformational changes in the presence of SDS, concurrent with the induction of PO activity, reveals a decrease in the absorption spectra of Hc at 350 nm and an increase in the fluorescence emission maxima, indicative of changes in the di-copper active site and the tertiary structure of the protein (Baird et al., 2007). Inhibition data presented here (Table 3.2, Fig. 3.8 and Fig. 3.9), suggest that 4-HR, L-ER and mimosine inhibit Hc-d PO activity; biophysical studies indicate that these inhibitors either mimic a phenolic substrate and occupy the di-copper active site, or bind close to the active site. The observed collapse in the absorption spectrum around the 350 nm signal in the presence of an inhibitor has also been recorded for *L. polyphemus* Hc in the presence of PTU and 4-HR (Wright et al., 2012).

Recently, the crystal structures of *Bacillus megaterium* (Sendovski et al., 2011) tyrosinase with kojic acid bound and *A. bisporus* tyrosinase with tropolone bound (Ismaya et al., 2011) have provided valuable insight into the mechanisms of PO inhibition. Kojic acid interacts strongly with residues at the entrance of the binuclear

active site, Phe197, Pro201, Asn205, and Arg209. Bound kojic acid binds in an identical position in both tyrosinase subunits and is orientated similarly to the placeholder residue Tyr 98, of the caddie protein associated with the inactive proPO zymogen. On the other hand, the *A. bisporus* Hc-tropolone complex reveals that tropolone binds in a less specific manner, binding in different positions with each subunit, but appearing to block phenolic entrance to the active site nonetheless.

Tropolone and kojic acid have been shown to inhibit Hc-d PO from *L. polyphemus* (Wright et al., 2012) with modelling studies suggesting that tropolone and kojic acid may bind *L. polyphemus* Hc in a similar manner to the PO-inhibitor complexes. PTU and 4HR were also reported as efficient inhibitors of *L. polyphemus* Hc-d PO. Our results suggest that *N. norvegicus* Hc-d PO is inhibited by PTU, 4HR, tropolone and kojic acid in a manner similar to Hc-d PO from *L. polyphemus* (Wright et al., 2012). Data presented here are consistent with inhibition studies performed previously on other arthropod Hcs, namely *Eurypelma californicum* (Jaenicke and Decker, 2008) and *Parapenaeus longirostris* (Martinez-Alvarez et al., 2008).

Chang (2009) discussed the relative success of different classes of PO inhibitors based on their biochemical structures; it appears that compounds containing a 4-rescorinol moiety or a 5-resorcinol moiety are the most effective inhibitors of PO, with novel inhibitor design focussed predominantly on this structural criterion. Even though PTU was found to be the most potent inhibitor of Hc-d PO activity in *N. norvegicus* (Table 3.2) and other invertebrates (*L. polyphemus* (Wright et al., 2012), *E. californicum* (Jaenicke and Decker, 2008) and *Charybdis japonica* (Fan et al., 2009)), due to its toxic nature and restricted use, PTU is not a viable option for commercial application. 4-HR, a well characterised inhibitor of PO activity (reviewed by Chang, 2009), has proven to be

a potent inhibitor of Hc-d PO from *N. norvegicus*. Derivatives of 4-HR may prove to be more effective inhibitors of Hc-d PO and should be investigated further.

3.6 Conclusion

The presented data reports the loss of *N. norvegicus* cellular PO activity and the retention of acellular Hc-d PO activity, after freeze-thawing, emphasising the need for future studies on Hc-d PO inhibition and a new approach to the treatment of hyperpigmentation. Known PO inhibitors were effective at inhibiting Hc-d PO activity from *N. norvegicus*, with 4HR proving the most promising candidate of the compounds tested here (considering both health and safety concerns). While PO and Hc share some similarities at their copper centres, subtle structural differences occur. The development and characterisation of Hc-d PO specific inhibitors is key to the safe and efficient prevention of hyperpigmentation in commercial shellfish.

3.7 Acknowledgements

This work was financially supported by the Scottish Funding Council Innovation Voucher Scheme, 2011-2012, and the University of Stirling. Many thanks to John Davis, Director, Xyrex Ltd., for provision of *N. norvegicus* specimens and helpful discussions, to Dr. Liz Blackburn, Biophysical Characterisation Centre, University of Edinburgh, for assistance with dynamic light scattering measurements and Douglas Lamont (University of Dundee) for performing mass spectrometry experiments.

Chapter 4:

Development of an *in vitro* phagocytosis assay for *Limulus polyphemus* amebocytes

A version of this chapter has been published;

Christopher J. Coates, Tim Whalley* and Jacqueline Nairn. 2012. Phagocytic activity of *Limulus polyphemus* amebocytes *in vitro*. *Journal of Invertebrate Pathology*. 111, 205-210.

*T. Whalley (co-supervisor) provided membrane probes and aided experimental design.

4.1 Abstract

Phagocytosis of invading microorganisms is a fundamental component of innate immune defense. The Atlantic horseshoe crab, *Limulus polyphemus*, possesses a single immune cell type, the granular amebocyte. Amebocytes release a repertoire of potent immune effectors in the presence of pathogens, and function in hemostasis. In contrast to other arthropod hemocytes, phagocytosis by *L. polyphemus* amebocytes remains poorly characterised, partly due to the technical challenges associated with handling these labile cells. These challenges have been addressed and the internalisation of microbial and synthetic targets by amebocytes *in vitro* were observed. Confirmation of target internalisation was achieved using a combination of fluorescent quenching and lipophilic membrane probes: R18, FM 1-43. Viability, morphological integrity and functionality of extracted amebocytes appeared to be retained *in vitro*. The phagocytic properties of *L. polyphemus* amebocytes described here, in the absence of endotoxin, are similar to those observed for arthropod hemocytes and mammalian neutrophils.

4.2 Introduction

The Atlantic horseshoe crab (HSC), *L. polyphemus*, is unique among arthropods in that it appears to contain a morphologically distinct cell type, the granular amebocyte. Granular amebocytes comprise approximately 99 % of circulating blood cells (Suhr-Jessen et al., 1989) and upon infection, release a battery of immune effectors, including: components necessary for coagulation to occur, anti-microbial peptides (AMPs), lectins and transglutaminases (Akbar-John et al., 2010; Iwanaga and Lee, 2005; chapter 1). The remaining 1% consists of plasmatocytes-like cells. Amebocytes respond differentially to microorganism surface polysaccharides, enlisting a suite of complement proteins, which enable the recognition and conditional clearance of invading microorganisms (Gupta et al., 1991; Kawabata et al., 2009; Kurata et al., 2006; Tagawa et al., 2012). It is the exceptional sensitivity of amebocytes to lipopolysaccharides (LPS) that has led to the commercial exploitation of HSCs to provide the LAL test (Ding and Ho, 2001).

Phagocytosis of pathogens is an essential process required for combating infection and is indicative of immune competence in invertebrates (Iwanaga, 2002, Le Moullac and Haffner, 2000). The biochemical and molecular processes involved from the recognition of opsonised pathogens via specific receptor-ligand interactions (complement/TLR), to subsequent ingestion and eventual destruction by superoxide and microbicidal granules have been well characterised in mammalian and invertebrate model host systems (Chapter 4; Garin et al., 2001, Rosales, 2011, Vazquez et al., 2009, Lavine and Strand, 2002, Ratner and Vinson, 1983). In HSCs, however, relatively few studies have detailed the phagocytic properties of amebocytes, possibly due to the technical challenges associated with this labile cell type, including, high sensitivity to endotoxins, demonstrating a lack of proliferation *in vitro* and proving recalcitrant to molecular manipulation and standard culturing methods (Armstrong, 1985, Copeland and Levin,

1985, Sherman, 1981). Armstrong and Levin (1979) described the internalisation of carbonyl iron particles by amebocytes, *in vitro*. Although later studies have attempted to detail the phagocytic capacity of HSC amebocytes (Gupta and Campenot, 1996, Gupta, 1997), a standardised assay does not exist, hence, amebocyte phagocytosis remains poorly understood.

In many phagocytosis assays, crystal violet (CV), methylene blue (MB) and trypan blue (TB) are used routinely to quench fluorescence of non-internalised targets (Serda et al., 2009, Xue et al., 2001, Van Amersfoort and Van Strijp, 1994). Here, the quenching effectiveness of each quencher mentioned above has been assessed across the range pH 4.5 – pH 7.0. Commercial fluorescent-labelled microspheres were not sensitive to quenching in this study, therefore lipophilic membrane probes, FM1-43 and R18, along with the fluid phase marker, Rho-dextran, were used to confirm microsphere internalisation. Lipophilic membranes probes have been utilised previously in studies to investigate various cellular phenomena (Cochilla et al., 1999, Whalley et al., 1995), particularly respiratory burst associated with phagocytosis in mammalian leukocytes (Yeung et al., 2006, Emmendörffer et al., 1990).

In this chapter, the conditions necessary for the short term maintenance (≤ 24 h) of amebocytes *in vitro* have been optimised, permitting evaluation of amebocyte phagocytosis in the presence of microbial and synthetic targets. Confirmation of target internalisation was achieved using a combination of fluorescent quenching and lipophilic membrane probes.

4.3 Materials and methods

4.3.1 Chemicals and reagents

All chemicals and reagents used were of the highest purity and quality, purchased from Sigma Aldrich Chemical Company (Dorset, UK) unless stated otherwise. All consumables such as falcon tubes, culture plates and hypodermic needles were purchased pyrogen-free. All glassware was baked at 180°C for no less than 4 h and all solutions were autoclaved to ensure sterility.

4.3.2 Maintenance of *Limulus polyphemus*

Intermolt Atlantic horseshoe crabs (HSCs) (kindly provided by Alex Mühlhölzl, Marine Biotech Limited) were housed in a closed circulation tank (200 L) at 13°C ± 2°C, containing artificial seawater (Red Sea Salt) with a stocking density of no more than three HSCs per 1 m² floor space. HSCs were fed approximately 2 % of their body weight in mussels/shrimp, three to four times per week. Approximately 35 % of water was exchanged per week, in addition to using an external filtration pump (Eheim Classic External Filter, 2213) and daily siphoning of faeces, to maintain water quality. Assessments of water quality properties (NH₃, PO₄, NO₃⁻, NO₂, pH, Ca²⁺ and carbonate hardness) were performed routinely, using a Hagen Master Test Kit (Aquatics Warehouse) (Appendix C).

4.3.3 Microbial cultures

Escherichia coli M15 (cultured in Lysogeny Broth) and *Bacillus megaterium* (cultured in Nutrient Broth) were grown overnight at 37°C in an orbital shaker at 200 rpm. *Saccharomyces cerevisiae* AH22 were grown to stationary phase (~ 1 x10⁸ cells mL⁻¹) in 25 mL YEPD broth (2 % w/v, bactopectone (Oxoid Ltd.), 1 % w/v, yeast extract (Oxoid

Ltd.) and 2 % w/v, glucose) in an orbital shaker (200 rpm) at 30°C. *Beauveria bassiana* were grown for two weeks on potato dextrose agar containing chloramphenicol (0.05 mg mL⁻¹) and subsequently left to sporulate and dry at room temperature for a further two weeks. Fungal spores were harvested and stored at 4°C in a 50 mL pyrogen-free falcon tube containing silica beads (for desiccation). Optical density readings at 600 nm were used to calculate microbial cell concentrations, an OD₆₀₀ value of 1.0 corresponds to ~ 1.2 x10⁹ cells/mL for bacteria (*E.coli* and *B. megaterium*) and ~ 3 x10⁷ cells/mL for *S. cerevisiae*, using previously established growth curves (Novaspec-4049 Spectrophotometer). *B. bassiana* spores were enumerated using an Improved Neubauer haemocytometer.

4.3.4 Preparation of fluorescent targets

Microorganisms were cultured as stated previously. 1 mL of microbial culture was pelleted at room temperature (10,000 x *g* for 5 min) and subsequently washed four times in 100 mM NaHCO₃, pH 9. The final pellet was re-suspended in 100 mM NaHCO₃, pH 9 containing either 0.5 mg mL⁻¹ fluorescein isothiocyanate (FITC, Sigma-Aldrich; F2502) or 0.1 mg mL⁻¹ Lissamine Rhodamine B Sulfonyl Chloride (Molecular Probes, Invitrogen; L1908) and incubated in the dark for 1 h at room temperature or 4°C, respectively. After incubation, microbes were pelleted and washed in the same manner until a clear supernatant was observed. The final pellet containing the fluorescent-labelled microbes was re-suspended in 1 mL PBS, pH 7.3 and stored in the dark at 4°C for no longer than five days. Dried *B. bassiana* spores, ~ 10 mg, were suspended in 1 mL 100 mM NaHCO₃, pH 9 and labelled as above. 2 µm FITC labelled (Fluoresbrite®, Polysciences; 18338-5) and Rhodamine labelled (Sigma-Aldrich; L3030) 2 µm

(diameter) carboxylate-modified latex microspheres were also used as targets for phagocytosis.

4.3.5 Hemolymph extraction and total amebocyte counts

All salts and glassware used were rendered endotoxin free by baking at 180°C for a period no less than 4 h. HSC hemolymph (500 µL) was extracted via cardiac puncture using a 26-gauge hypodermic needle (BD Microlance 3) attached to a syringe containing an equal volume of pre-chilled marine anti-coagulant (3% NaCl, 100 mM dextrose, 47 mM citric Acid and 10 mM EDTA, pH 4.6), adapted from Söderhäll and Smith (1983). The arthroidal membrane was cleaned with 70 % ethanol before and after hemolymph withdrawal to prevent sepsis. Serial dilutions of hemolymph were carried out in LPS-free saline (3% NaCl, 10 mM NaHCO₃, pH 7.5) and amebocyte counts were estimated using an improved Neubauer haemocytometer.

4.3.6 Evaluation of amebocyte viability and functionality *in vitro*

Extracted cells were washed in LPS-free saline (500 x *g* for 5 min at 4°C) before being seeded into wells of a 24-well pyrogen-free culture plate containing Grace's Modified Insect Medium (GMIM)(no salt supplement) or 3 % NaCl- 20 mM HEPES, pH 7.5, 10 mM CaCl₂, 10 mM MgCl₂, 5 mM KCl₂, and 10 mM NaHCO₃ (NaHEP), or Shields and Sang Insect medium (SSIM, supplemented to 3% NaCl). Each well contained 500 µL of culture media (supplemented with 5 % v/v HSC plasma) and ~ 1 x10⁵ amebocytes. Amebocytes were left to settle for 20 min to form a monolayer before the media was exchanged by aspiration. Viability of amebocytes, *in vitro*, was determined by the trypan-blue exclusion method; see section 3.3.3.

The morphology of amebocytes *in vitro* was observed using brightfield optics of an Olympus M081 inverted microscope and categorised. At each time point amebocytes were fixed using 2.5 % formaldehyde and assessed immediately. Amebocyte morphology categories were identified using characteristics outlined previously (Hurton et al., 2005, Coates et al., 2012). Namely, granular spherical (GS) amebocytes are dense and highly refractile. Granular flat (GF) amebocytes are identified by a visible nucleus. Dendritic-Like (D-L) amebocytes lose refractility due to exocytosis of cytosolic granules. Large vacuoles and pseudopodia are also visible in D-L amebocytes.

Exposure of amebocytes to LPS in this study served as an indicator of immune-functionality (adapted from Armstrong and Rickles, 1982). Amebocytes were deemed functionally compromised when < 50% of (GS and GF) amebocyte cytosolic granules were released in response to the presence of LPS (20 $\mu\text{g mL}^{-1}$). All *in vitro* experiments were performed at 18°C, unless otherwise stated.

4.3.7 Preparation of crude *Limulus* amebocyte lysate (LAL)

LAL from freshly isolated amebocytes

Hemolymph was extracted (5 mL) using a 16-gauge hypodermic needle attached to a syringe containing an equal volume of 3 % NaCl, pH 7.5 and 10 mM N-ethylmaleimide. Amebocytes were washed immediately in LPS-free saline and lysed in sterile, pyrogen free distilled water. Debris was removed by centrifugation, 10,000 $\times g$ for 5 min at 4°C. Crude lysate was lyophilized (Christ Alpha 1-4 freeze-dryer) overnight and reconstituted in pyrogen free water (Sigma).

LAL from amebocytes maintained in vitro

Amebocytes maintained *in vitro* (NaHEP) for 24 hours were dissociated from the substratum of culture wells by trypsinization (0.1 mM trypsin, prepared in PBS, pH 7.3), pelleted, re-suspended in 3 % NaCl, pH 7.5 containing 10 mM N-ethylmaleimide and lysed as stated above.

Estimates of protein concentrations present in cell lysates were performed using 0.06% Coomassie G250 dye reagent and bovine serum albumin as standard (Sedmak and Grossberg, 1977). The reactivity of 0.5 mg mL⁻¹ crude lysate from freshly extracted and *in vitro* amebocytes was tested using microbial ligands and phospholipids.

- I. Ligands: LPS (5 µgmL⁻¹) from *E. coli*, mannan (20 µgmL⁻¹) from *S. cerevisiae*, lipoteichoic acid (LTA, 20 µgmL⁻¹) from *Streptococcus pyogenes* and laminarin (20 µgmL⁻¹) from *Laminaria digitata*.
- II. Phospholipids: PS (50 µgmL⁻¹), PI (50 µgmL⁻¹), L-PC (50 µgmL⁻¹), PC (50 µgmL⁻¹) and phosphatidylethanolamine (PE, 50 µgmL⁻¹) (adapted from Kurata et al., 2006)

Reaction mixtures were monitored continuously over a 3 h period using an Ultrospec 2100 pro UV/Visible spectrophotometer. An increase in absorbance at 470 nm upon incubation of cell lysate with ligands is indicative of flocculation and an increase in sample viscosity, due to coagulation/gelation (Adapted from Young et al., 1972). Control spectra of lysates were recorded in the absence of a ligand/phospholipid.

4.3.8 *In vitro* phagocytosis assay

4.3.8.1 Confirmation of target internalisation

To confirm internalisation of fluorescent targets and to eliminate non-phagocytic target-amebocyte associations, two methods were developed:

- I. Quenching of fluorescence; the quenching properties of CV, MB and TB were assessed by monitoring fluorescence intensity of labelled microbes (FITC-labelled *S. cerevisiae* presented here), pre- and post-quenching, over the range, pH 4.5- pH 7. Quenchers were used at a final concentration of 0.2 % (w/v).
- II. Commercial 2 μm fluorescent -labelled microspheres were not sensitive to quenching, therefore lipophilic membrane probes, R18 and FM 1-43 (Molecular probes, Invitrogen; O246 and T3163) and the fluid-phase marker Rhodamine-dextran (D3308) were used to confirm microsphere internalisation. Amebocytes were applied to pre-prepared culture wells containing fluorescent microspheres and R18, FM 1-43 or Rho-Dex (depending on the concurrent target fluorophore) at final concentrations of 2 μM , 6 μM and 10 μM , respectively. Upon assay completion, samples were also treated with CV (0.2%), in order to quench non-internalised membrane probe.

Amebocytes were washed and re-suspended in 3% NaCl-20 mM HEPES, pH 7.5 containing 2.5 % neutral formaldehyde and subsequently analysed. N.B. microbial target sizes: *S. cerevisiae*; 3-4 μm , *B. bassiana* spores; 2-4 μm and *B. megaterium*; ~2.5 μm .

4.3.8.2 Phagocytic properties

Microbes and/or fluorescent microspheres were applied to culture wells containing 500 μ L NaHEP. Targets were centrifuged at 500 x *g* for 10 min at 4°C to promote monolayer formation. Extracted amebocytes were applied to pre-prepared culture wells containing fluorescent targets with the final ratio of amebocytes: targets of 1:20. Amebocytes were allowed to settle to the bottom of the well for 20 min before the assay was recorded. Phagocytic activity was monitored over a 1 h period and then stopped by the addition of 2.5 % formaldehyde. Samples were assessed for phagocytosis using fluorescent filters on an Axiovert 135 inverted microscope. GFP/FITC filter-set (excitation 450-490 nm, emission 515-560 nm) to view FITC (green) labelling and red filter-set (excitation 546 nm, emission 590 nm) to view rhodamine B labelling. Images and videos were captured using a Moticam Pro 282B camera. Image analysis/preparation was achieved using Image J software. Approximately 300 amebocytes were scored per culture well. The rate of phagocytosis was recorded as the percentage of phagocytically active amebocytes. The phagocytic index was recorded as the number of internalised targets per phagocytically active amebocyte.

Some phagocytosis assays were conducted in the absence and presence of either, normal HSC plasma (5 % v/v) or heat treated (100°C for 10 min) HSC plasma, to investigate whether hemolymph-derived components influence amebocyte phagocytosis.

4.3.9 Data analysis

A total of 7 HSCs were used in this study: each HSC was bled on 3-4 independent occasions, with no less than a week between each extraction. The Ryan-Joiner test for normality and Levene's test for equal variances were employed to assess data sets. Amebocyte viability, morphology and functionality were analysed using a two-way analysis of variance with culture media and time as designated factors. Time was treated as a nested factor within the main effect of culture medium. Bonferroni *post hoc* tests were applied when necessary. Percentage data sets were transformed successfully using arcsine square-root or exponential square-root functions. Rates of phagocytosis and PIs were also analysed using 2-way ANOVA, with target and fluorophore as factors. A one way analysis of variance was used to analyse quenching of fluorescence at pH 4.5 and amebocyte lysate gelation at the 1h time point. Differences were considered significant at $p \leq 0.05$. Statistical analysis was performed using Minitab version 16 analytical software. Values are represented by the mean \pm standard error.

4.4 Results

4.4.1 Amebocyte viability and vitality, *in vitro*

Previous attempts to maintain HSC amebocytes *in vitro* yielded limited success. In the data presented here, HSC amebocytes retained viability levels of 83.1% in GMIM, 55% in SSIM and 84% in NaHEP, after 24 h *in vitro* (Fig. 4.1). Amebocytes maintained *in vitro* in either GMIM or NaHEP exhibited > 60% GS, 16-25% granular-flat (GF) and 10-15% dendritic-like (D-L) morphologies, after 24 h (Fig. 4.2 B and C). A significant decrease ($p < 0.05$) in GS morphology was recorded using SSIM, accompanied by a significant increase in the proportions of GF and D-L morphologies ($p < 0.01$, $p < 0.05$, respectively), over the course of the experiment (Fig. 4.2D).

LPS-induced granule exocytosis was used as a proxy for amebocyte immune-functionality. Irrespective of the culture media used, a decreasing trend was observed in the proportion of GS and GF amebocytes degranulating in the presence of LPS (Fig. 4.3) over time. After 24 h *in vitro*, ~ 65% of amebocytes present in NaHEP, fully degranulated upon exposure to LPS, whereas only 42% and 19% of amebocytes responded to LPS in GMIM and SSIM, respectively (Fig. 4.3). While amebocytes maintained *in vitro* in GMIM and NaHEP exhibited similar levels of viability and GS morphology (Fig. 4.1 and 4.2), amebocytes in GMIM demonstrated a significant reduction in immune-functionality ($p < 0.05$, $n = 7$).

Based on these observations, the functional state of amebocytes in NaHEP was further assessed. *In vivo*, granules released from amebocytes, in response to microbes, contain all the components necessary for coagulation to occur (Akbar-John et al., 2010, Iwanaga and Lee, 2005). The efficacy of lysates from freshly isolated amebocytes and

amebocytes maintained *in vitro* for 24 h was monitored upon exposure to microbial ligands (LPS, LTA, mannan and laminarin) and phospholipids (PS, PI, L-PC and PE). Spectrophotometric analysis of the freshly withdrawn and isolated amebocyte lysates in the presence of ligands/phospholipids yielded almost identical results, with no significant differences detected (Fig. 4.4A and B). Lysates in the absence of ligands or phospholipids did not show any measureable increase in flocculation/gelation (Fig. 4.4). These measurements further emphasise the effective immune-functionality of *ex vivo* amebocyte populations, preserved in NaHEP.

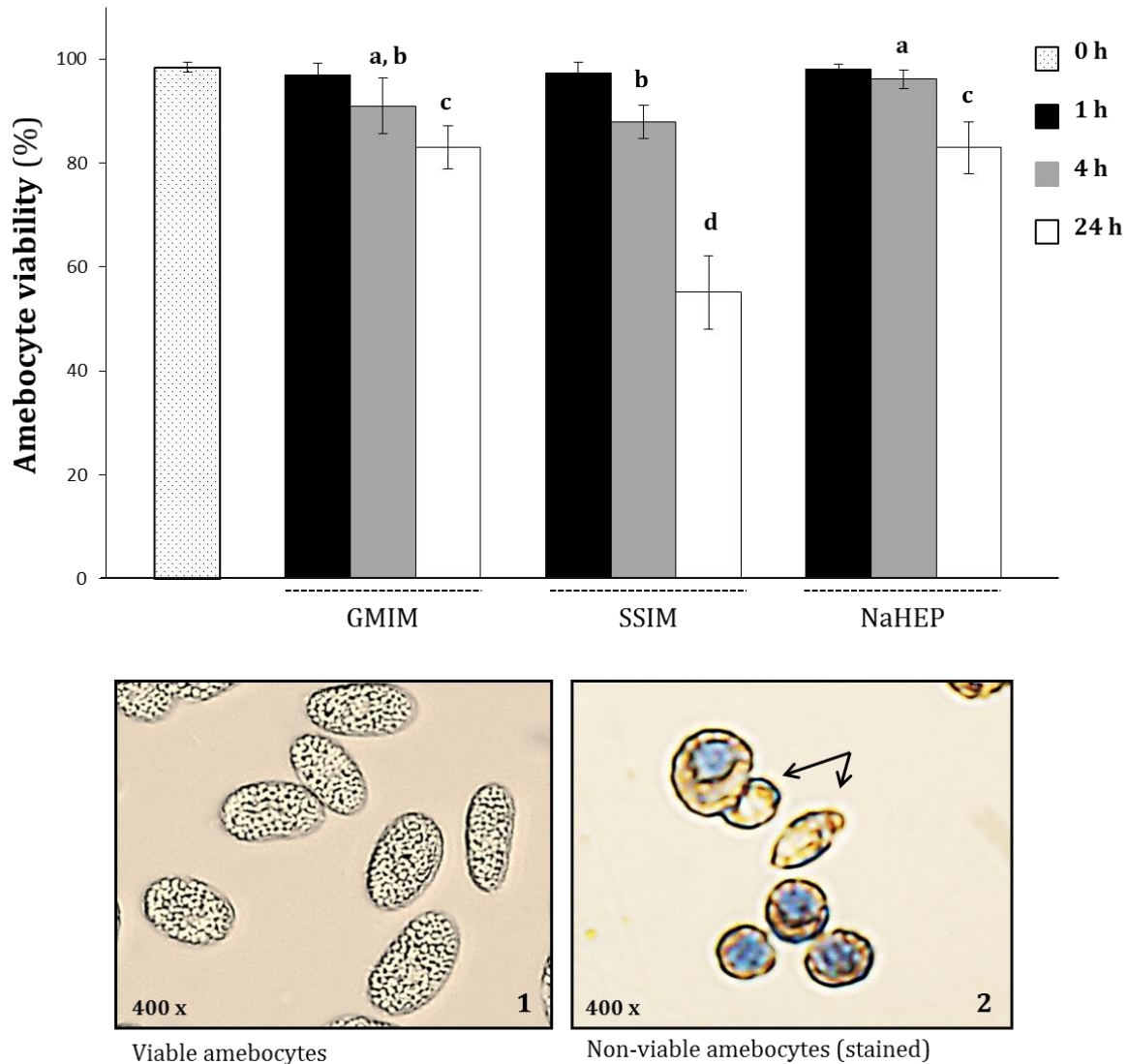


Figure 4.1 Percentage viability of *Limulus polyphemus* amebocytes *in vitro*. Amebocytes were extracted from *L. polyphemus* and seeded into culture wells containing SSIM or GMIM or NaHEP, pH7.5. Viability was assessed over 24 h using trypan blue to distinguish between viable and non-viable amebocytes. Inset; (1) viable amebocytes remain unstained, (2) non-viable amebocytes stain blue due to the loss of plasma membrane integrity (arrows represent viable amebocytes). A significant decrease in amebocyte viability between different culture media at $p \leq 0.05$ ($n = 7$) are represented by a & b at 4 h and c & d at 24 h. Letters common between treatments indicate no significant difference.

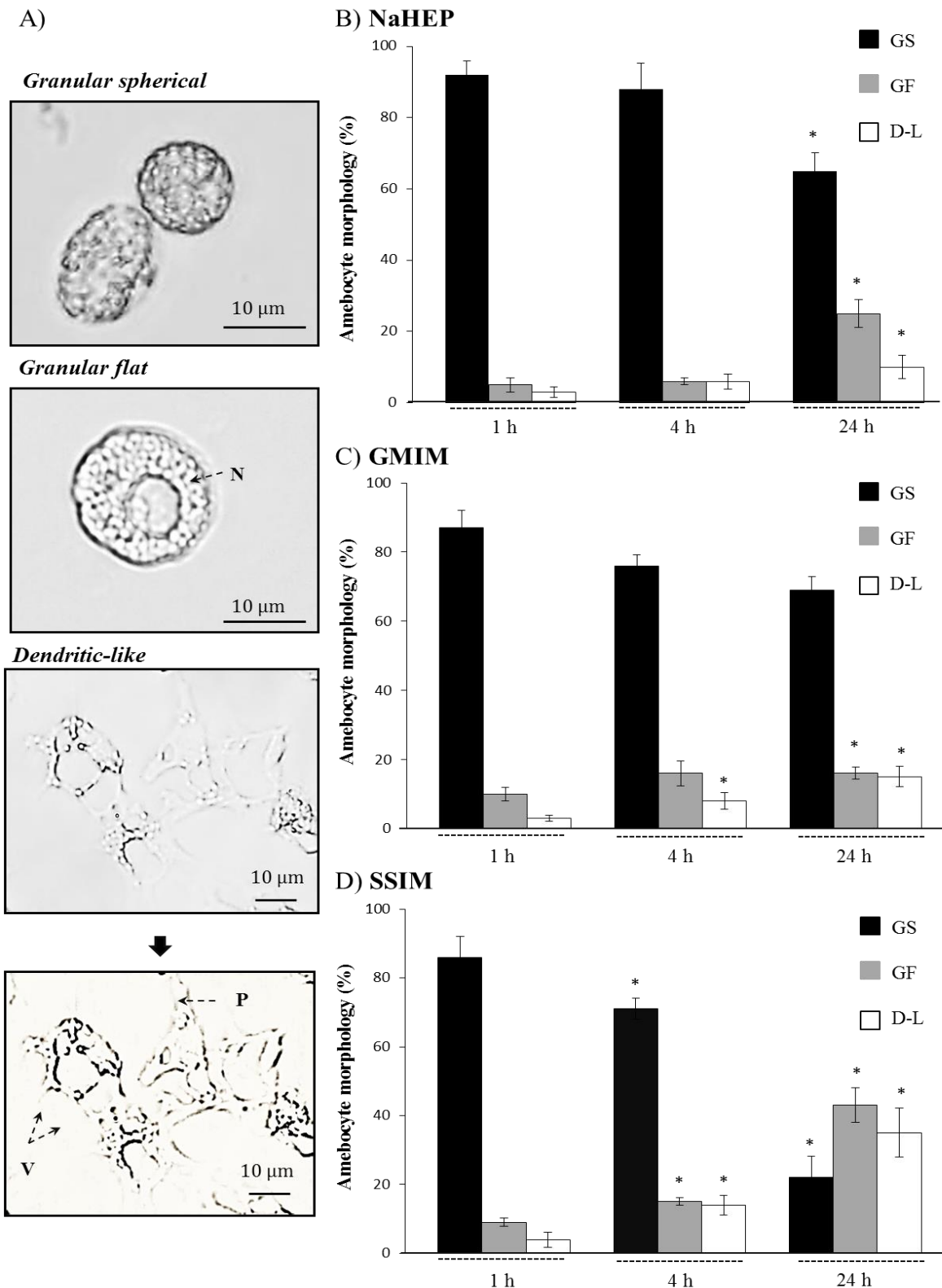


Figure 4.2 *Limulus polyphemus* amebocyte morphology, *in vitro*. **A)** Appearance of different amebocyte morphologies present *in vitro*. Granular spherical (GS) amebocytes are dense and highly refractile. Granular flat (GF) amebocytes are identified by a visible nucleus (N). Dendritic-Like (D-L) amebocytes lose refractility due to the loss of cytosolic granules. Large vacuoles (V) and pseudopodia (P) are also visible. The scale bar represents 10 μm . **B), C)** and **D)** represent the percentage morphologies of amebocytes maintained *in vitro* over a period of 24 h, with either, NaHEP, GMIM or SSIM, respectively. A significant decrease in amebocyte morphology representation compared to 1 h samples at $p \leq 0.05$ is represented by * ($n = 7$).

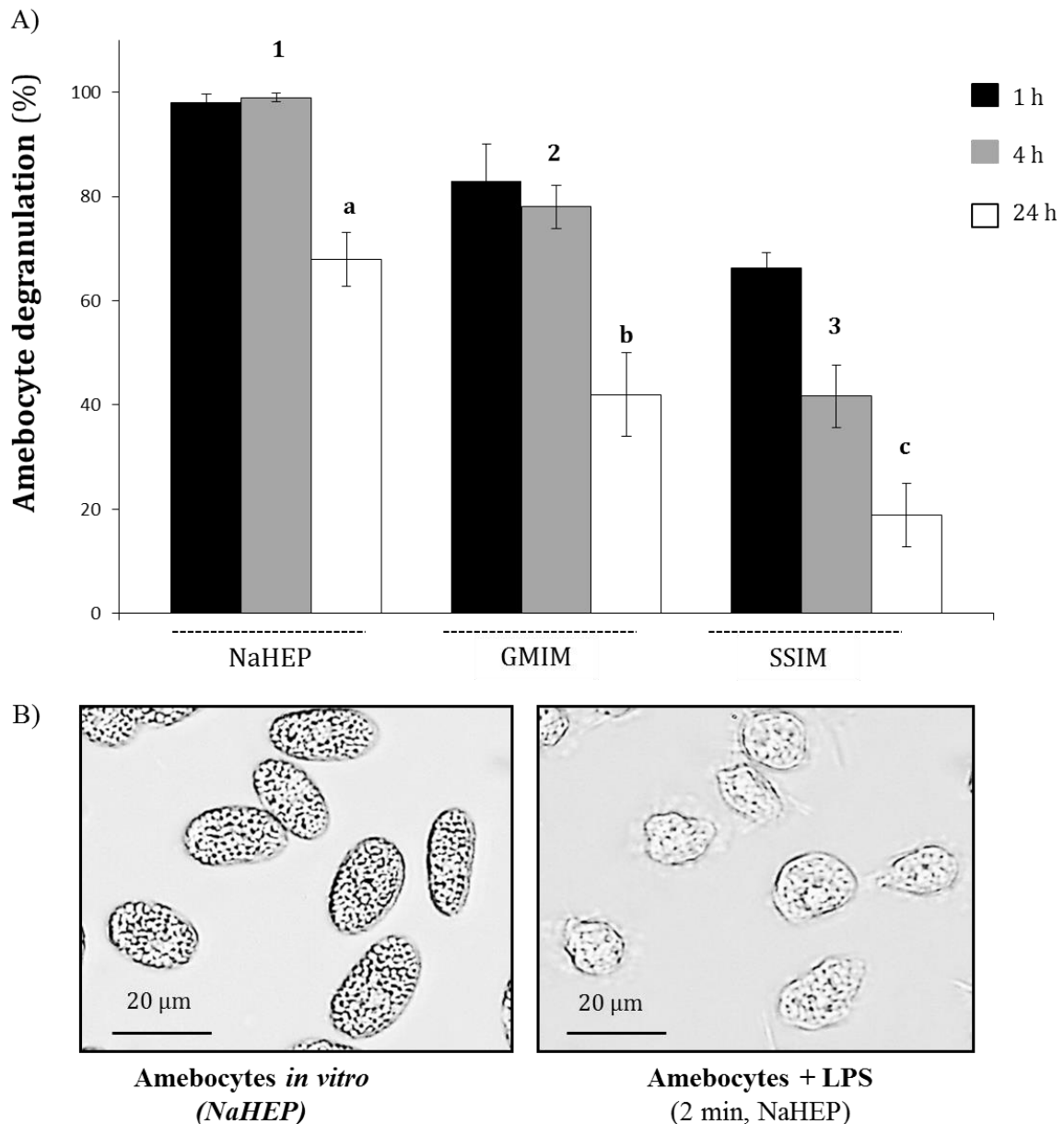


Figure 4.3 Degranulation of *Limulus polyphemus* amebocytes in response to LPS. **A)** Percentage degranulation of *in vitro* amebocytes in response to the presence of $20 \mu\text{g mL}^{-1}$ lipopolysaccharide (LPS). Extracted amebocytes were maintained in one of three media and subsequently exposed to LPS at 1 h, 4 h and 24 h time points. Amebocytes were considered functionally active when $> 50\%$ of cytosolic granules were released in response to LPS exposure. **B)** Viable amebocytes in the absence and presence of LPS. De-granulation was completed within 2 min. A significant decrease in amebocyte functionality between different culture media at $p \leq 0.05$ is represented by * ($n = 7$) numbers 1-3 for 4 h and letters a-b for 24 h. Treatments sharing either the same letters or numbers are not significantly different.

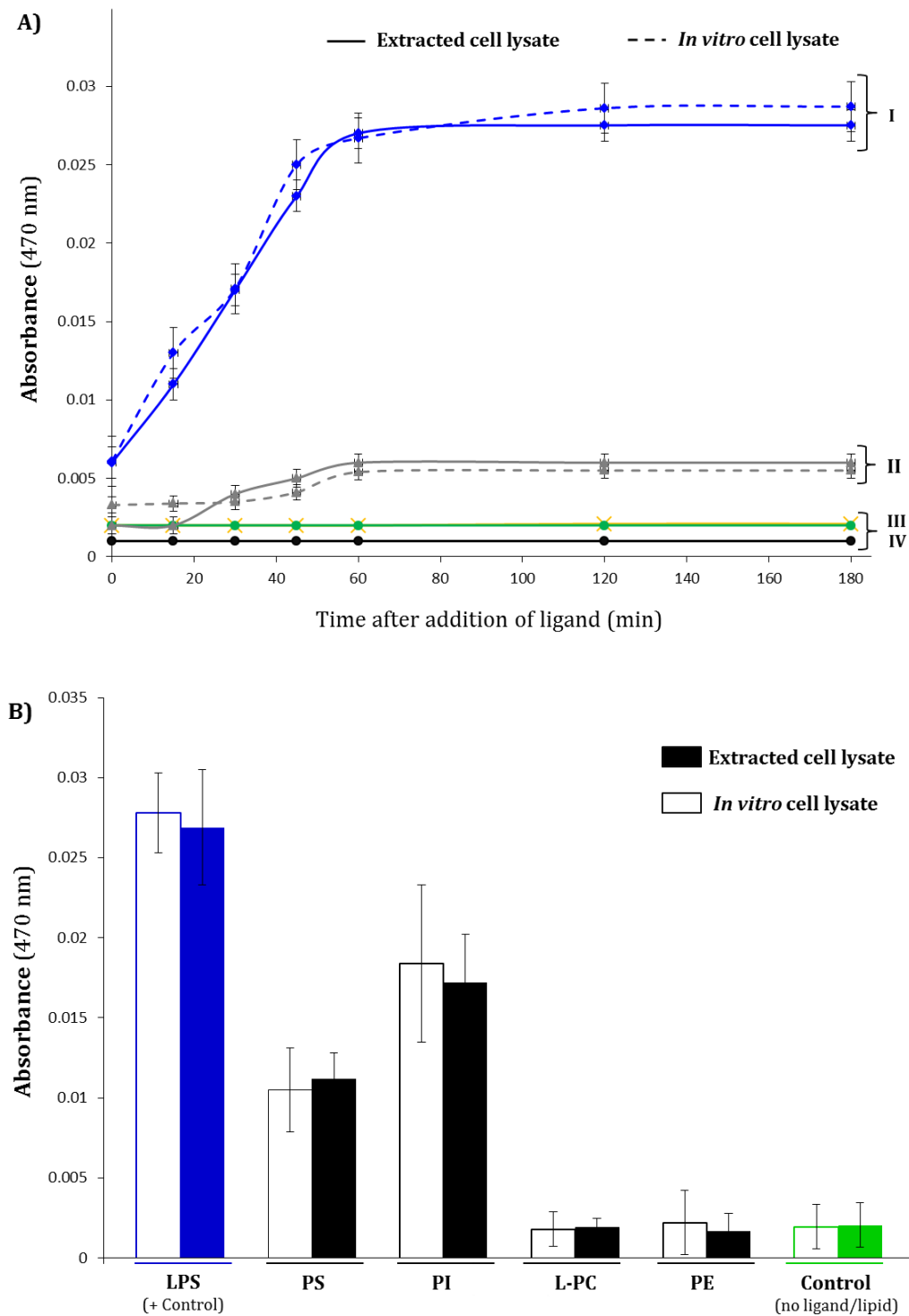


Figure 4.4 Response of crude *Limulus polyphemus* amebocyte lysates to microbial ligands and membrane phospholipids. Lysates were prepared from freshly extracted amebocytes and from amebocytes which had been *in vitro* (NaHEP) for 24 h. **A)** Spectrophotometric analysis of 0.5 mg mL^{-1} lysate in the presence of I) $5 \text{ } \mu\text{g mL}^{-1}$ LPS, II) $20 \text{ } \mu\text{g mL}^{-1}$ laminarin, III) $20 \text{ } \mu\text{g mL}^{-1}$ LTA or mannan was measured over a period of 3 h. IV) Control spectra consisted of lysates only. **B)** Absorbance readings at 1 h post incubation of 0.5 mg mL^{-1} lysate in the presence of $50 \text{ } \mu\text{g mL}^{-1}$ phospholipid (PS, PI L-PC and PE), and $5 \text{ } \mu\text{g mL}^{-1}$ LPS as a positive control. An increase in absorbance at 470 nm is indicative of lysate gelation. Data is represented by the mean \pm standard error ($n = 4$).

4.4.2 In vitro phagocytosis; confirming target internalisation

The sensitivity of amebocytes *in vitro* to Gram-negative bacteria led to mass degranulation and severe clotting upon exposure to *E. coli* (Fig. 4.5 A). Previous reports have also highlighted this technical difficulty and commented on the inability of amebocytes to perform phagocytosis in the presence of endotoxin (Gupta and Campenot, 1996, Armstrong and Levin, 1979). For this reason, fluorescent (FITC/Rhodamine B) carboxylate modified 2 μm latex microspheres were used to mimic the approximate size and electrostatic properties of *E.coli*, for phagocytosis assays (Fig. 4.5B).

Using FITC-labelled *S. cerevisiae*, the quenching effectiveness of CV, MB and TB were assessed across the range pH 4.5 to pH 7. In each case, quenching at pH 4.5 resulted in the largest decrease in *S. cerevisiae* fluorescence (Fig. 4.6A). CV yielded the largest decrease in fluorescence, 84%, followed by MB with 72% and lastly by TB with a 54% reduction (Fig. 4.6A and B). As the fluorescent latex microspheres used in this study were not sensitive to quenching, a method was developed to distinguish between ingested and non-internalised microspheres. Labelling the amebocytes with fluorescent lipophilic (styryl) membrane probes, R18 and FM 1-43, and the fluid -phase marker Rho-Dex enabled the visualisation and counting of phagocytosed microspheres. FM 1-43 (green/yellow) was used in conjunction with Rhodamine B (red) labelled targets (Fig. 4.7), R-18/Rho-Dex were used alongside FITC- labelled targets (Fig. 4.8 and 4.9). While this method was developed to permit the use of latex microspheres, the technique was effective in distinguishing phagocytosed from non-phagocytosed fluorescent microbes.

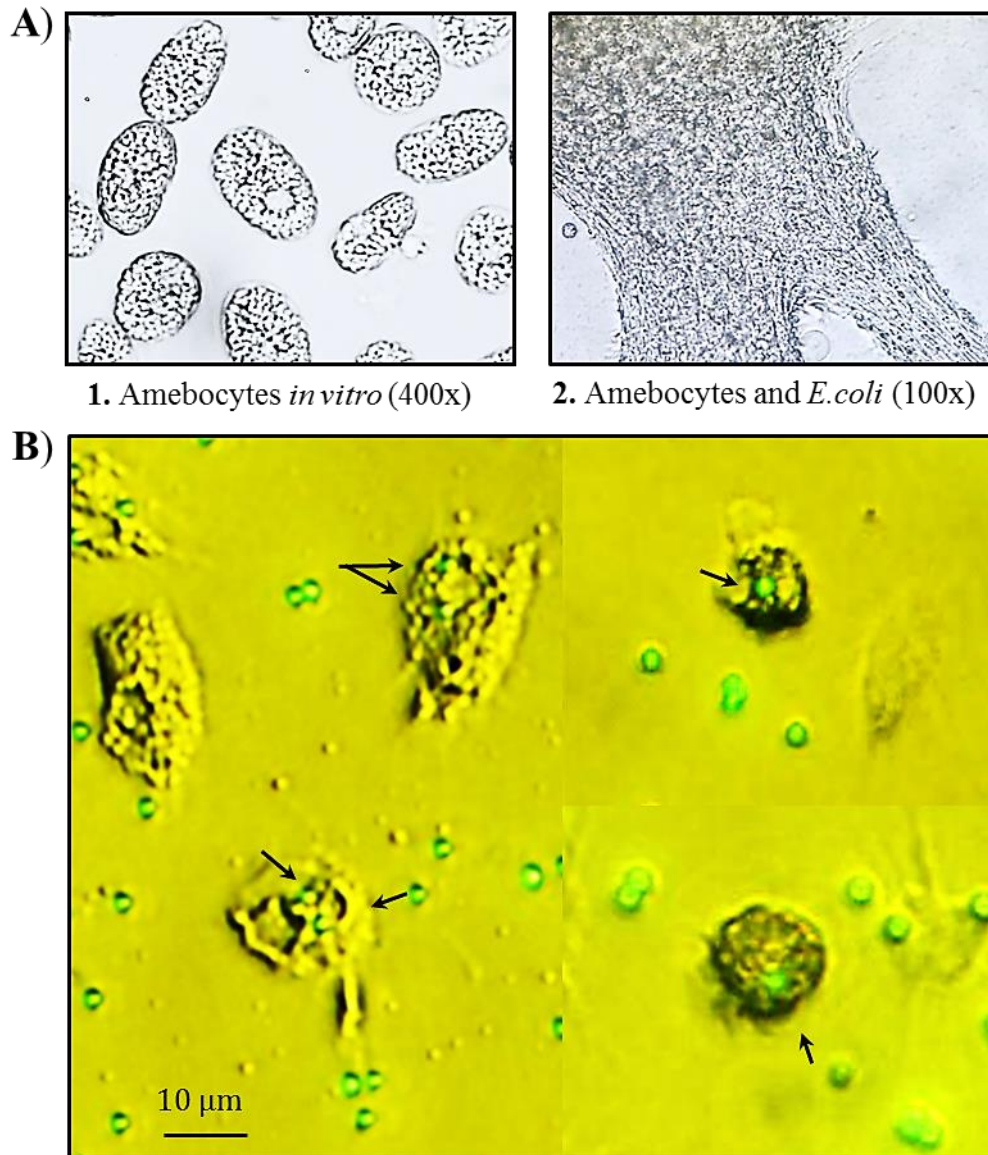


Figure 4.5 The appearance of *Limulus polyphemus* ameobocytes following exposure to *E. coli* and 2µm latex microspheres. **A)** *L. polyphemus* ameobocytes *in vitro* (NaHEP), 1) in the absence of *E. coli* and 2), in the presence of *E. coli*. Image 2 shows the clotting (gelation) of ameobocytes in the presence of *E. coli*. **B)** *L. polyphemus* ameobocytes in the presence of FITC-labelled 2 µm latex microspheres. Black arrows indicate internalised microspheres.

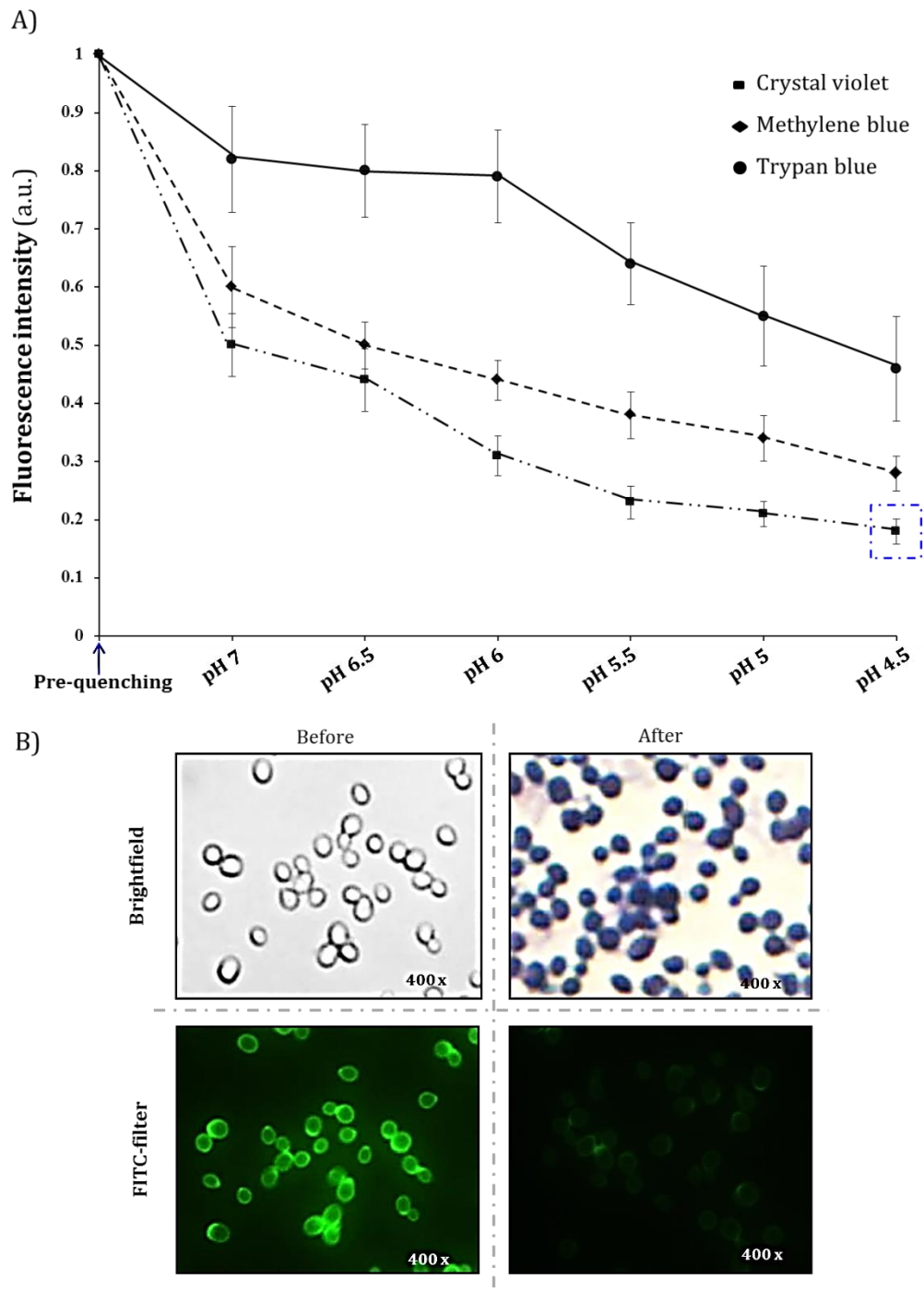


Figure 4.6 Effect of pH on the quenching properties of crystal violet, methylene blue or trypan blue in the presence of FITC-labelled *Saccharomyces cerevisiae*. **A)** *S. cerevisiae* were incubated (for 20 mins) in each quencher (0.2%, w/v) over the range pH 4.5 to pH 7.0. Changes in fluorescent intensity due to quenching are presented above. **B)** Fluorescent and brightfield images, taken before and after quenching using crystal violet (0.2%, w/v in 3% NaCl-20 mM HEPES, pH 4.5 [blue square]).

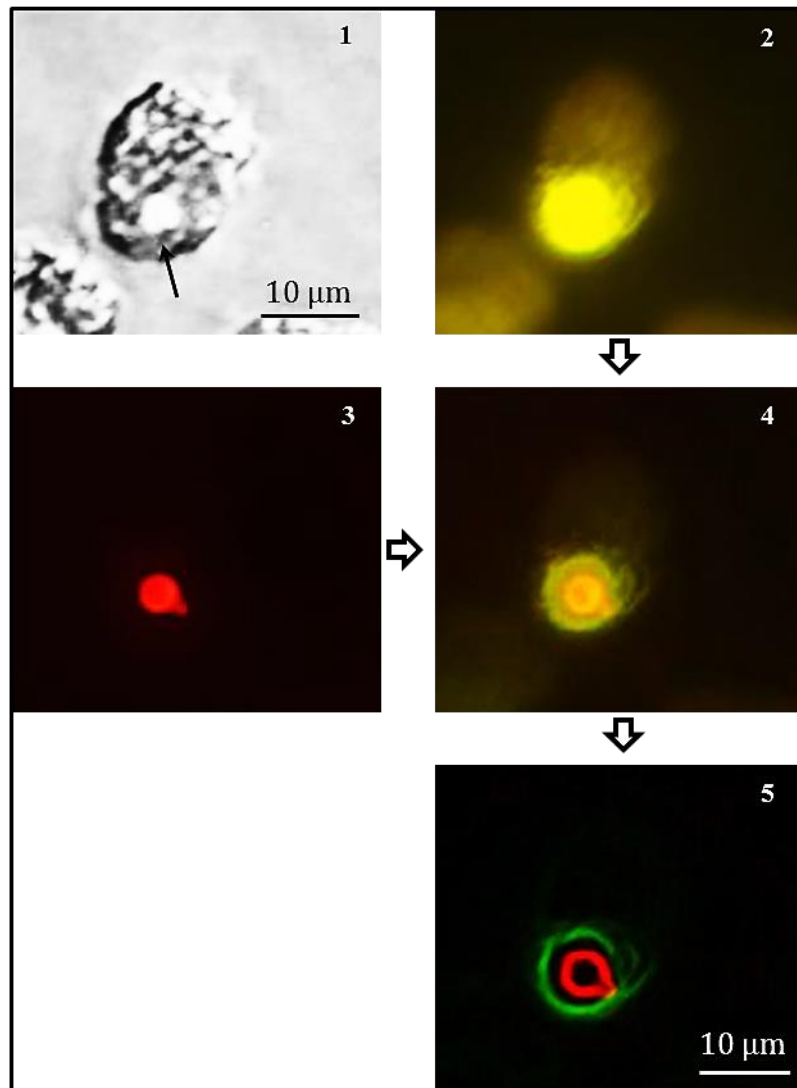
Rho-*S. cerevisiae* and FM 1-43

Figure 4.7 Confirmation of *Saccharomyces cerevisiae* internalisation by *Limulus polyphemus* amebocytes. Amebocytes were labelled with FM 1-43 and yeast were labelled with Rhodamine B. 1) Brightfield image of an *L. polyphemus* amebocyte *in vitro* (black arrow is showing an internalised yeast cell). 2) Green/yellow fluorescent filter showing the amebocyte labelled with the membrane probe, FM 1-43, post quenching. 3) Red fluorescent filter showing the Rhodamine-labelled yeast cell. 4) A merging of images 2 and 3. 5) The edges of the internalised yeast cell and the amebocyte phagosome are highlighted from image 4.

FITC-microspheres and R-18

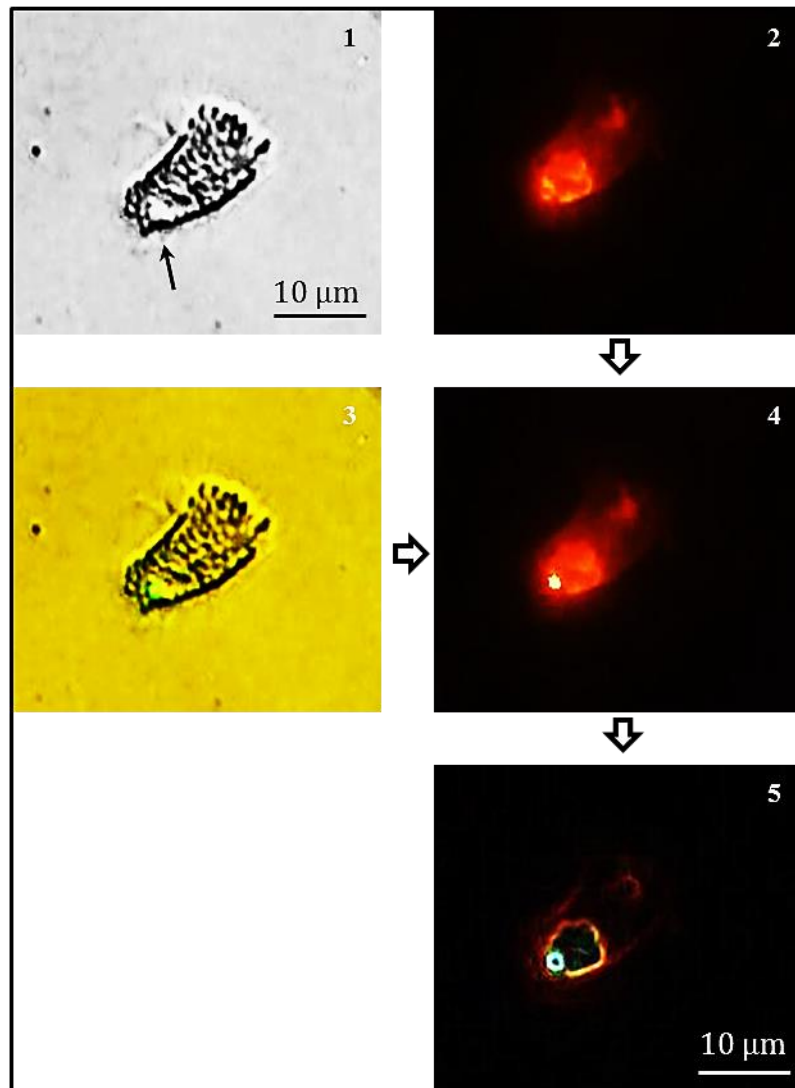


Figure 4.8 Confirmation of internalisation of 2 µm microspheres by *Limulus polyphemus* amebocytes. Amebocytes were labelled with R18 and 2 µm latex microspheres were purchased pre-labelled. 1) Brightfield image of a *L. polyphemus* amebocyte *in vitro* (black arrow is showing an internalised microsphere). 2) Red fluorescent filter showing the amebocyte labelled with the R18 membrane probe. 3) Green/yellow fluorescent filter showing the FITC-labelled microsphere. 4) A merging of images 2 and 3. 5) The edges of the microsphere inside the amebocyte phagosome are highlighted from image 4. Image J software was used to prepare images 4 and 5.

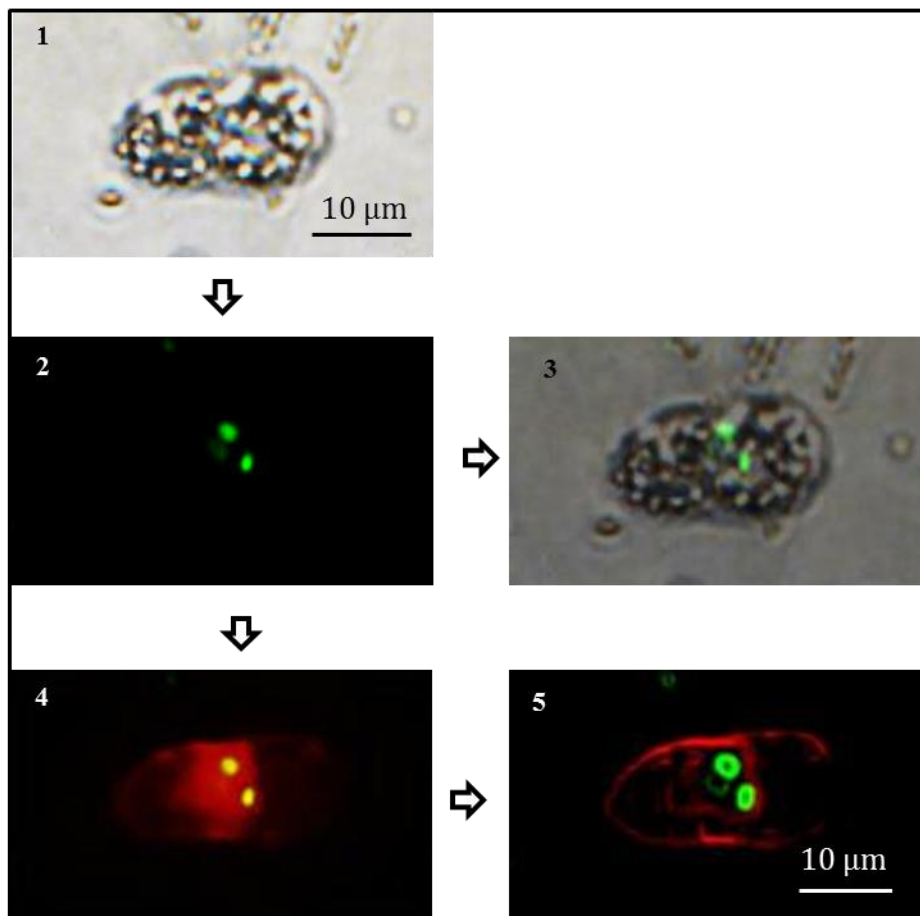
FITC-*B. megaterium* and Rho-dextran

Figure 4.9 Confirmation of *Bacillus megaterium* internalisation by *Limulus polyphemus* amebocytes. Amebocytes were incubated with the fluid phase marker, Rhodamine-dextran and FITC-labelled *B. megaterium*. 1) Brightfield image of a *L. polyphemus* amebocyte, 2) Crystal violet quenching demonstrating *B. megaterium* internalisation, 3) merging of images 1 and 2, 4) Image showing internalisation of targets and fluid-phase marker (Rho-Dex). 5) The edges of the three bacterial cells inside the amebocyte phagosome are highlighted from image 4.

4.4.2. continued...

On average, 9 % of the total amebocyte population displayed phagocytic properties in this study (Fig 4.10); however, if non-internalised (externally attached) amebocyte-target interactions are included, the proportion of potentially active increase to ~ 21 % (Fig. 4.11). No differences were observed in the rate of phagocytosis between amebocytes assayed with fungal (*S. cerevisiae*, *B. bassiana*), bacterial (*B. megaterium*) or synthetic (latex microspheres) targets (Fig. 4.10). The number of targets internalised per amebocyte (phagocytic index) was determined for each of the microbial and synthetic targets used, with no differences observed. Amebocytes that phagocytosed *S. cerevisiae* (3-4 μm) and/or *B. bassiana* spores (2-4 μm) displayed a phagocytic index between 1.26 and 1.43, while phagocytic indices for *B. megaterium* (~ 2.5 μm) and synthetic microspheres (2 μm) were between 1.61-1.7 and 1.69-1.71, respectively (Fig. 4.10). No significant differences were detected between rates of phagocytosis (Fig. 4.10A) and phagocytic indices (Fig. 4.10B) using either FITC (green) or Rhodamine B (red) labelled targets; suggesting that neither fluorophore used had any measurable effect on the phagocytic properties of amebocytes.

Moreover, a preliminary study was conducted in order to investigate whether hemolymph components influenced amebocyte phagocytosis. Amebocytes in the presence of spores and bacteria demonstrated reduced rates of phagocytosis in the absence of hemolymph plasma ($p < 0.01$) and in the presence of heat-treated plasma ($p < 0.05$) (100°C for 10 min) (Fig. 4.12).

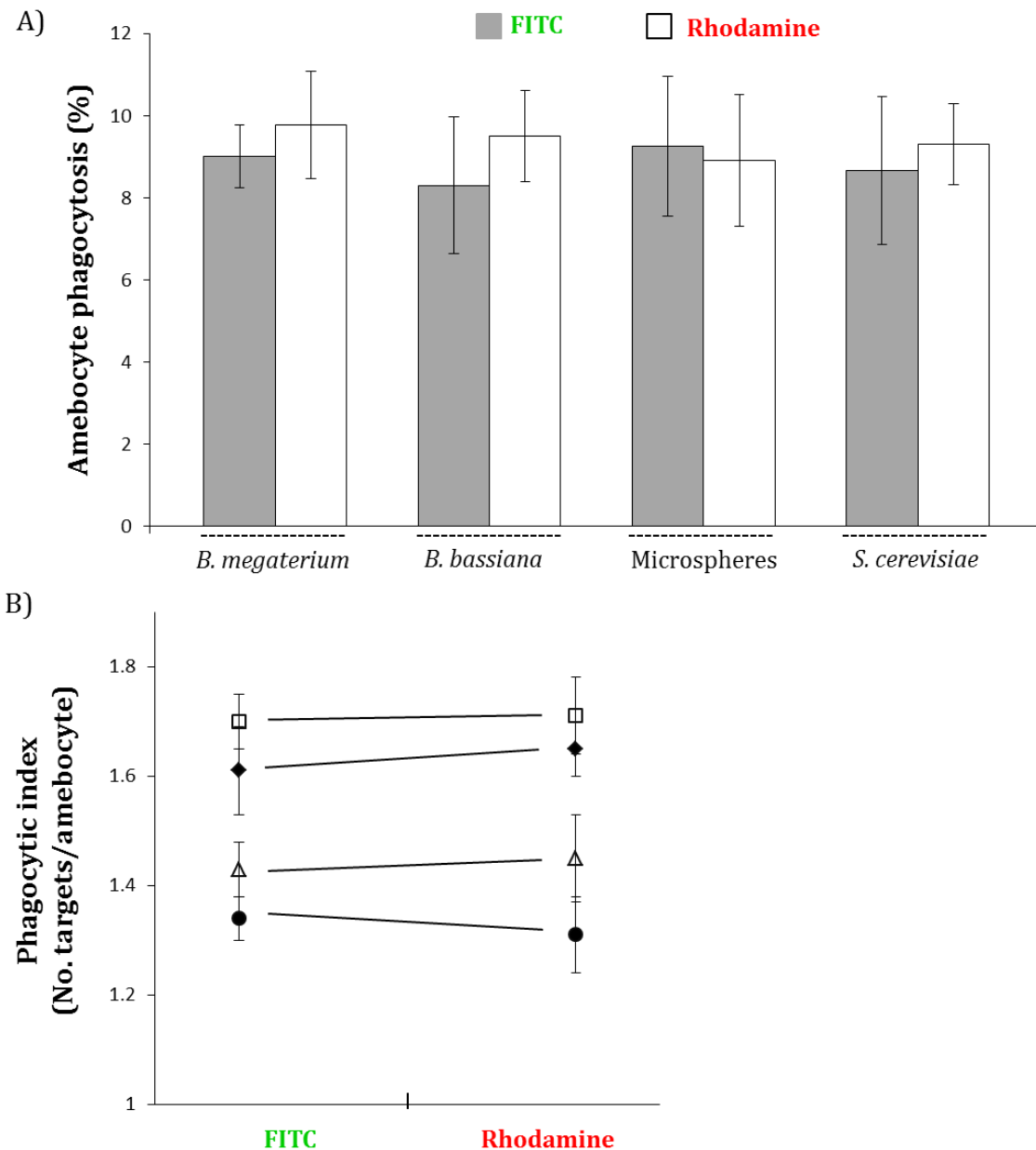


Figure 4.10 Phagocytic properties of *Limulus polyphemus* amebocytes *in vitro*. **A)** Ratio of *L. polyphemus* amebocytes phagocytosing in the presence of fluorescent microbial targets and/or synthetic microspheres after 1 h *in vitro*. Assays were stopped by the addition of 2.5% neutral formaldehyde. **B)** The phagocytic indices (number of targets internalised per amebocyte) were observed for targets labelled with each fluorophore; FITC-green and Rhodamine B-red. Symbols; ● *S. cerevisiae*, Δ *B. bassiana*, ◆ *B. megaterium* and □ latex microspheres. included. Data is represented by the mean ± standard error. No significant differences were detected between microbial/synthetic targets (n = 5).

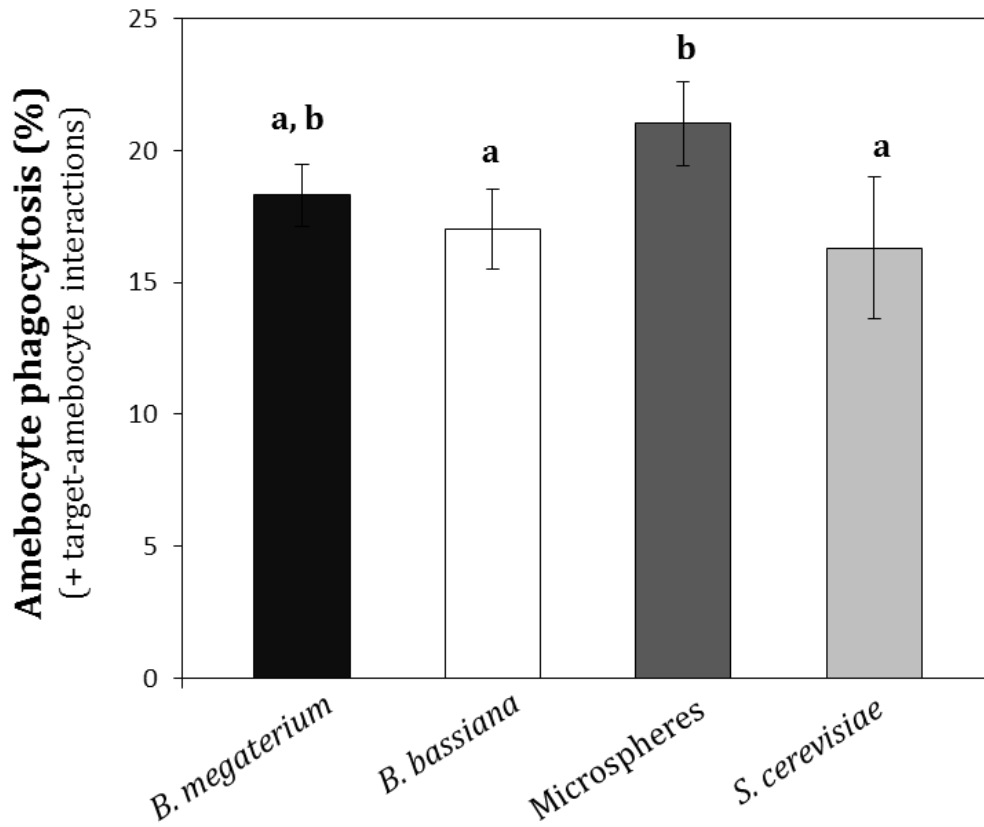


Figure 4.11 Proportion of amebocytes having internalised and/or associated with fluorescent-labelled microbes, *in vitro*. Phagocytosed microbes and extracellular amebocyte-target associations have been included. Values are represented by the mean \pm standard error. Significant differences ($p \leq 0.05$) between targets are represented by letters that are not shared. Data is represented by the mean \pm standard error ($n = 5$).

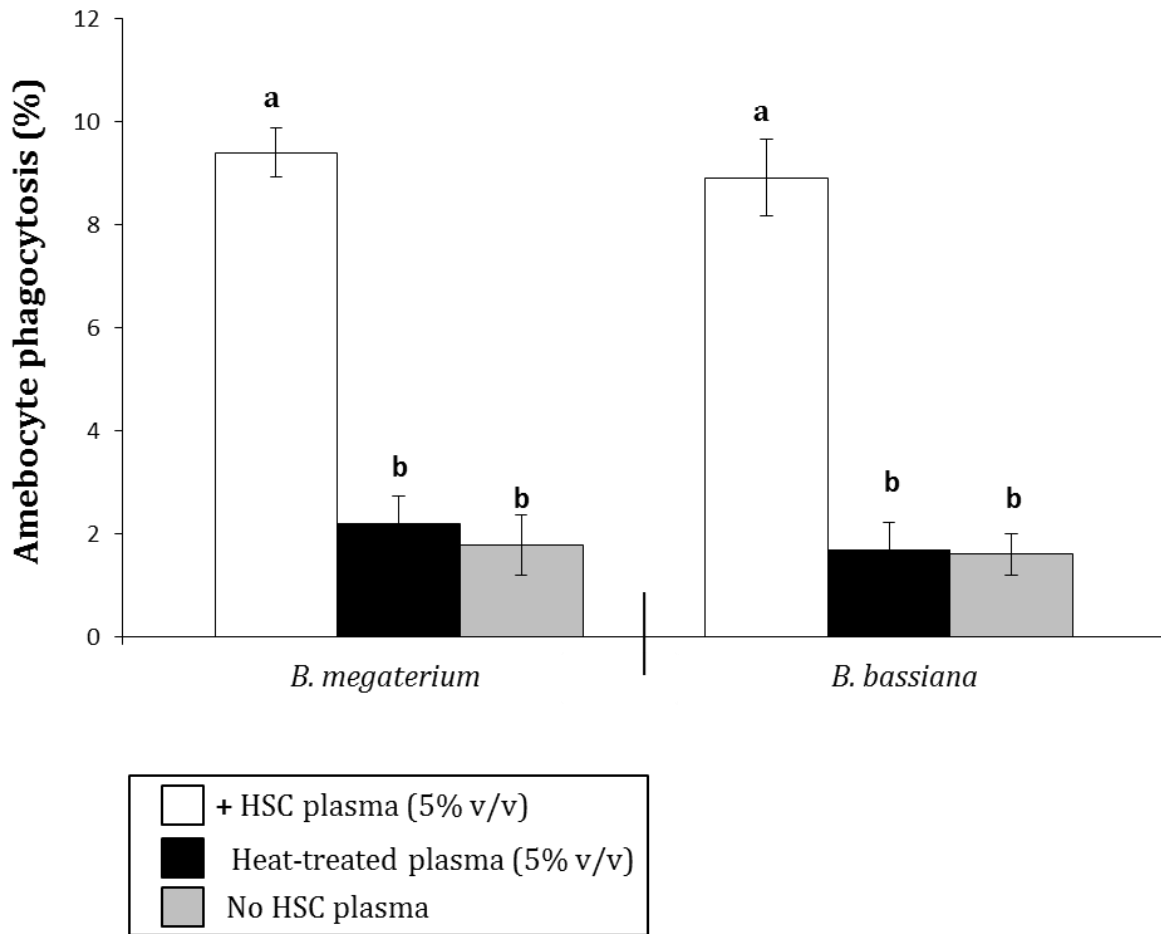


Figure 4.12 Phagocytic properties of *Limulus polyphemus* amebocytes in the presence of hemolymph plasma, heat treated plasma (100°C for 10 min), or in the absence of plasma. NaHEP was supplemented with 5% (v/v) plasma in experiments. A one-way ANOVA was used to confirm differences in amebocyte phagocytosis (using FITC-labelled microbes), in the absence and presence of either normal plasma or heat-treated plasma. Data is represented by the mean \pm standard error. A significant decrease in amebocyte functionality between different conditions at $p \leq 0.05$ is represented by * (n = 4). Letters common between each treatment indicate no significant differences.

4.5 Discussion

4.5.1 Maintenance of arthropod immune cells *in vitro*

Given the biomedical and economic importance of HSC amebocytes (Ding and Ho, 2001, Walls et al., 2002), significant investment has been made in attempts to produce amebocytes *in vitro*. Although a number of patents, including those issued in 1980 to Pearson and 1992 to Gibson and Hilly, have claimed to culture successfully HSC crab amebocytes using excised gill lamellae and high levels of L-arginine; to date, these efforts have proved largely unsuccessful. Indeed, a similar outcome has been noted for attempts to maintain hemocytes from other marine invertebrates (Rinkevich, 2011). Limited success has been achieved in establishing long-term cultures and/or hemocyte cell lines derived from arthropods, notably marine organisms (Rinkevich, 2005, 2011). Crustacean hemocytes remain viable (~ 70% for hyalinocytes) for up to 14 days *in vitro* (Walton and Smith, 1999). Recent advancements in understanding *Pacifastacus leniusculus* haematopoiesis may aid the design of more robust methods (Noonin et al., 2012). In contrast, insect cell lines have been successfully maintained *in vitro*, with over 500 insect lines in use (Ikonomou et al., 2003, Smagghe et al., 2009).

In this study, GMIM (recommended by Hurton et al., 2005) and NaHEP, assumed to imitate the ionic strength of HSC hemolymph (section 4.3.6) were tested for their ability to sustain HSC amebocytes *in vitro*. While viability and GS states of amebocyte morphology remained high in both GMIM and NaHEP (Fig 4.1 and Fig. 4.2), the functionality of amebocytes present in GMIM (at 24 h) appeared compromised (Fig. 4.3). Overall, amebocytes exhibited the highest levels of viability, morphological integrity and functionality, when maintained in NaHEP. Moreover, upon testing crude amebocyte lysates from *in vitro* and freshly withdrawn samples, no deterioration in the

ability of *in vitro* amebocyte lysates to gelate in the presence of microbial ligands and/or membrane phospholipids was observed (Fig. 4.4). PI and PS are known to bind and subsequently activate protease activity in Factor C, almost as efficiently as bacterial LPS (Ariki et al., 2004; Kurata et al., 2006). However, neither L-PC nor PE have demonstrated affinities for Factor C, therefore, it is unsurprising that upon incubation of L-PC and PE with amebocyte lysates, no measurable increase in lysate gelation is recorded (Fig. 4.4B). Amebocytes extracted, and preserved for 24 h in NaHEP, are capable of responding to the presence of ligands via degranulation, with their exocytosed granular content appearing to gelate in a manner similar to the assumed amebocyte response *in vivo*. These findings are not only relevant to phagocytosis studies but could also enhance development of the commercial-scale maintenance of amebocytes, reducing the need for the bi-annual harvest of HSC blood by biomedical companies.

4.5.2 Phagocytic properties of amebocytes

Phagocytosis by HSC amebocytes was first reported by Ruediger and Davis (1907) and later by Stagner and Redmond (1975); amebocytes were observed ingesting Gram-positive bacteria. Armstrong and Levin (1979), characterised HSC amebocytes phagocytising carbonyl iron particles *in vitro*, however, amebocytes failed to demonstrate phagocytic behaviour in the presence of bacterial endotoxin. Gupta and Campenot (1996) monitored the phagocytic behaviour of HSC amebocytes in the presence of 1 μ m FITC-labelled microspheres and observed up to 55% of amebocytes exhibited phagocytic properties. This is a significantly greater percentage of phagocytosis than the 9% observed in data presented here, using 2 μ m FITC-labelled microspheres (Fig. 4.10). Inclusion of the non-internalised amebocyte-target

interactions, in a manner similar to the studies of Gupta and Campenot (1996), results in the 'phagocytic' proportion of amebocytes increasing to ~ 21 % (Fig. 4.11). The discrepancy between results may be due to system differences; Gupta and Campenot (1996) did not confirm target internalisation, used different sized microspheres and carried out their phagocytosis assay in a marine anti-coagulant, pH 4.6, lacking divalent cations and supplemented with 10 mM EDTA. The physiology of the amebocytes in Gupta and Campenot's assay may differ from that of the amebocytes used here with NaHEP, pH 7.5, containing similar levels of CaCl₂, MgCl₂ and KCl₂ to those found in HSC hemolymph (Robertson, 1970).

More recently, Zhu et al., (2005), recorded what appeared to be phagocytosis of *Staphylococcus aureus* by *Carcinoscorpius rotundicauda* amebocytes, *in vitro* and *in vivo*; however, due to excessive clumping there remains a possibility that the bacteria may have associated or simply co-aggregated with the amebocytes. While similar rates of phagocytosis have been recorded for other invertebrate hemocytes, such as *Acanthoscurria gomesiana* (Fukuzawa et al., 2008) and *Penaeus monodon* (Xian et al., 2010), a 9% rate of phagocytosis is generally quite low among invertebrates (Table 4.1). Despite the low percentage of phagocytically active amebocytes *in vitro*, they nonetheless appear capable of functioning as efficiently as other invertebrate phagocytic cells; phagocytic indices displayed by HSC amebocytes here (1.2 to 1.7) are comparable to other phagocytic cells. *G. mellonella* hemocytes show a similar response to fungi with a phagocytic index for *Candida albicans* of ~ 1.18 (Bergin et al., 2005) (~ 1.3 for HSC amebocytes in the presence of *S. cerevisiae* and *B. bassiana*), while *Litopenaeus vannamei* exhibits a phagocytic index between 1.2 and 2 for bacteria, dependent on the species (Pope et al., 2011) (~ 1.7 for HSC amebocytes in the presence

of *B. megaterium*). Interestingly, amebocytes and mammalian neutrophils appear to ingest similar levels of fungi *in vitro*, ~ 1.26 and ~ 1.25, respectively (Bergin et al., 2005).

Using a protease cocktail and a high concentration of EDTA, Zhu et al., (2005) recorded a large decrease in *C. rotundicauda* amebocytes either associating with or phagocytosing bacteria. Data presented here depicts a 4-fold reduction in the percentage of amebocytes phagocytosing bacteria or fungi, in the absence of hemolymph plasma or in the presence of heat-treated plasma (Fig. 4.12). These preliminary data suggest that HSC proteins analogous to complement-like proteins or other humoral components (E.g. opsonins) may co-facilitate the recognition and subsequent ingestion of pathogens by amebocytes *in vivo* (similar to such processes in mammals).

The mechanisms of pathogen internalisation and subsequent termination are well characterised in mammals and many arthropod species (crustaceans, insects; Table 4.1) but not in HSC amebocytes. Amebocyte pseudopod formation, cytoskeletal rearrangements (polymerisation of G-actin into F-actin) and intracellular Camp levels during phagocytosis (Gupta and Campenot, 1996, Gupta, 1997) and exocytosis (Conrad et al., 2004) all share a high degree of similarity with mammalian macrophages, platelets and neutrophils. Furthermore, during immune challenge *L. polyphemus* amebocytes are known to produce nitric oxide (via nitric oxide synthase) (Radomski et al., 1991) and to up-regulate the expression of amine oxidase which generates H₂O₂ (Ding et al., 2005). Respiratory burst associated with phagocytosis is ubiquitous among vertebrate neutrophils and invertebrate hemocytes studied so far (chapter 1.2.5), and may be conserved in HSCs.

Table 4.1 Phagocytic properties of selected immune cells

Species	Phagocytic cells [†]	Phagocytic Index*	Targets	Reference
<i>Aedes aegypti</i>	41.8 %	-	carboxylate-latex microspheres (1µm)	[1]
<i>Acanthoscurria gomesiana</i>	< 10 %	-	<i>S. cerevisiae</i>	[2]
<i>Amblyomma americanum</i>	20.7 %	-	carboxylate-latex microspheres (1µm)	[1]
<i>Carcinus maenas</i>	~ 2.5 -15%	~ 2 - 3	<i>B. cereus</i> , <i>G. homari</i> and <i>Moraxella</i> sp.	[3]
<i>Dermacentor variabilis</i>	14.1 %	-	carboxylate-latex microspheres (1µm)	[1]
<i>Galleria mellonella</i>	~ 60 %	1.18	<i>Candida albicans</i>	[4]
<i>Ixodes scapularis</i>	26.2 %	-	carboxylate-latex microspheres (1µm)	[1]
<i>Limulus polyphemus</i>	~ 15- 55%	-	1 µm latex microspheres, chicken erythrocytes	[5]
<i>Litopenaeus vannamei</i>	7.5 %	-	carboxylate-latex microspheres (1µm)	[1]
<i>Litopenaeus vannamei</i>	-	1.2 – 2	<i>Bacillus subtilis</i> and <i>Vibrio</i> spp.	[6]
<i>Macrobrachium rosenbergii</i>	~ 18 %	-	<i>Aeromonas hydrophila</i> , <i>Enterococcus faecium</i> and <i>Debaryomyces hansenii</i>	[7]
<i>Manduca sexta</i>	9.1 %	-	carboxylate-latex microspheres (1µm)	[1]
Mammalian neutrophil	-	1.25	<i>Candida albicans</i>	[4]
<i>Penaeus monodon</i>	9.5 %	-	1 µm latex microspheres	[8]
<i>Polistes dominulus</i>	15 %	-	latex microspheres	[9]
<i>Rhodnius prolixus</i>	60 %	-	0.3 µm latex microspheres, <i>E. coli</i> and <i>S. aureus</i>	[10]

References; 1) Oliver et al., (2011), 2) Fukuzawa et al., (2008), 3) Smith and Ratcliffe (1978), 4) Bergin et al., (2005), 5) Gupta & Campenot, (1996), 6) Pope et al., 2011, 7) Hsu et al., (2005), 8) Xian et al., (2010), 9) Manfredini et al., (2010), 10) Borges et al., (2008). *Phagocytic index values are expressed as the mean number of internalised target per phagocyte. †Phagocytic cells represent the proportion of active cells in a population.

4.6 Conclusion

The method developed in this study, preserved viability and importantly, functionality of HSC amebocytes *in vitro*. The phagocytic capacity of amebocytes in the presence of microbes and synthetic microspheres was monitored successfully using membrane probes and quenching of fluorescence. This methodology may be applied to further characterise the phagocytic capacity of HSC amebocytes, and other invertebrate immune cells (hemocytes, coelomocytes).

4.7 Acknowledgements

Special thanks to Alex Mühlhölzl, Managing Director, Marine Biotech Limited, for providing horseshoe crabs and to Bill Jamieson (BES Cartographer, University of Stirling) for guidance with image preparation. Thanks are also due to Kate Howie (C&MS, University of Stirling) for helpful comments on data analysis.

Chapter 5:

Phagocytosis-induced cell death of amebocytes: A potential mechanism for the activation of hemocyanin-derived phenoloxidase, *in vivo*

A version of this chapter is in preparation for publication;

Christopher J. Coates and Jacqueline Nairn. 2013. A putative link between phagocytosis-induced cell death and hemocyanin-derived phenoloxidase activation in *Limulus polyphemus*. Intended submission to *Innate Immunity*.

5.1 Abstract

Cell death is an essential process required for developmental and immunological homeostasis in flora and fauna. Properties of cell death in mammalian leukocytes and to a lesser extent in arthropod hemocytes have been well documented. Conversely, such processes have received little attention in horseshoe crab amebocytes. This chapter explores the cell death characteristics displayed by amebocytes upon phagocytosis of microbial targets *in vitro*. The observed cellular modifications associated with phagocytosis-induced cell death of amebocytes are reminiscent of apoptosis-related processes. Phagocytosis-induced cell death was accompanied by extracellularisation of phosphatidylserine, the fragmentation of nuclear DNA and increases in caspase-3 activity. Interestingly, an increase in hemocyanin-derived phenoloxidase activity, coinciding with cell death patterns of phagocytically active amebocytes, has been detected. These findings not only provide further evidence to suggest that properties of programmed cell death are conserved amongst eukaryotes, but identify a potentially novel mechanism which may contribute to the activation of hemocyanin into an immune-enzyme, *in vivo*.

5.2 Introduction

Cell death processes are widely considered to be conserved amongst vertebrates and invertebrates, involved in essential processes for shaping development (phagoptosis), disposal of compromised/defective cells (apoptosis), recycling cellular components (autophagy) and deterring microbial infections (Brown and Neher, 2012; Kroemer et al., 2009; Wang et al., 2006). Cell death phenomena, particularly apoptosis, have been studied in great detail in mammalian (Elmore, 2007), insect (Cooper and Mitchell-Foster, 2011), crustacean (Menze et al., 2010) and mollusc (Sokolova, 2009) systems. When cells undergo apoptosis, a tightly regulated sequence of events eventually leads to the formation of microvesicles (apoptotic bodies) containing processed cytosolic components. The dying cell advertises its defective condition via the extracellularisation of phosphatidylserine (PS) and the release of “eat me” chemo-attractants; patrolling phagocytes recognise these signals and subsequently ingest the apoptotic corpse in a process known as efferocytosis (Martin et al., 2012; Wu et al., 2006; Grimsley and Ravichandran, 2003). Dysfunctional apoptotic regulation can lead to oncosis and numerous other degenerative disorders, both in mammals and arthropods (Hanahan and Weinberg, 2000).

Phagocytosis-induced cell death (PICD) is a process that occurs when immune cells ingest microbes and subsequently undergo apoptosis. In neutrophils and mollusc hemocytes, evidence suggests that ROS generation is the main inducer of PICD (Sokolova, 2009; Zhang et al., 2003). It is thought that PICD deters the systemic spread of pathogens while alerting other leukocytes to its compromised state (i.e. the presence of an internalised pathogen). In data presented here, horseshoe crab amebocytes display a number of apoptotic signals after ingesting *B. bassiana* spores, *in vitro*. PICD of amebocytes was monitored using a series of fluorescence microscopy techniques:

Annexin V-FITC/propidium iodide, TUNEL and MitoTracker Orange CMTMRos staining. Caspase-3 activity of phagocytic and non-phagocytic amebocytes was also recorded.

Upon exposure of amebocytes to microbes, an increase in PO activity derived from Hc was observed. Hc-d PO activity broadly correlated with apoptotic patterns of phagocytically active amebocytes. Hc can be activated into a PO-like enzyme upon exposure to PS (Chapter 2) and other amebocyte-derived components (Nagai et al., 2001; Nagai and Kawabata, 2000; Nellaiappan and Sugumaran, 1996). Results from a series of experiments suggest that Hc may interact with redistributed PS (or some other unknown membrane structure) present on dying amebocytes, and be converted into an immune enzyme. This chapter describes, for the first time, cell death characteristics of horseshoe crab amebocytes, and provides evidence to further support PS as a putative activator of Hc-d PO, *in vivo*.

5.3 Materials and methods

5.3.1 Chemicals, reagents and detection kits

All chemicals and reagents used in this chapter were purchased from Sigma Aldrich chemical company (Dorset, UK), unless otherwise stated. Annexin-V FITC/propidium iodide apoptosis detection reagents were purchased from Calbiochem. Caspase-3 and TUNEL assay components were purchased from Invitrogen and Milipore, respectively. Courmarin (AMCA-X, SE) and MitoTracker Orange CMTMRos were purchased from Molecular probes, Invitrogen, A6118 and M7510, respectively. Vectashield Mounting Medium containing DAPI was supplied by Vector Laboratories (H-1200).

5.3.2 Maintenance of *Limulus polyphemus*

L. polyphemus were maintained as outlined in *chapter 4, section 4.3.2*. Briefly, animals were housed in a closed circulation tank (at ~ 14°C) and fed on mussels/shrimp every second day. Approximately 35 % of water was exchanged weekly, in addition to using external filters, siphoning of particulates and regular assessments of water quality (Appendix C).

5.3.3 Hemolymph extraction and amebocyte properties

Hemolymph was removed via the arthroidal sinus, as described in section 4.3.5. No more than 500 µL of hemolymph was removed per HSC per extraction. Amebocytes were pelleted, 200 x g for 5 min, and subsequently washed in 3% NaCl-20 mM HEPES, pH 7.5. Washed amebocytes (~ 1 x10⁵) were then seeded into each well of a sterile 24-well culture plate containing NaHEP (3 % NaCl- 20 mM HEPES, pH 7.5, 10 mM CaCl₂, 10 mM MgCl₂, 5 mM KCl₂, and 10 mM NaHCO₃), supplemented with 5 % v/v HSC plasma to a final volume of 500 µL per well.

Viability of amebocytes *in vitro* was assessed using the trypan-blue method (section 3.3.3, and a number of fluorescence microscopy techniques. Amebocyte degranulation, in the absence of endotoxin, was monitored both in the presence and absence of coumarin labelled spores.

5.3.4 Microbial cultures and preparation of fluorescent targets

Beauveria bassiana, *Bascillus megaterium* and *Saccharomyces cerevisiae* were cultured, enumerated and labelled fluorescently with FITC and/or Rhodamine B as stated previously (sections 4.3.3/4.3.4). Dried *B. bassiana* spores (10 mg mL^{-1}) and 1 mL each of *B. megaterium* and *S. cerevisiae* cultures were pelleted ($10,000 \times g$ for 5 min), washed four times in 100 mM NaHCO_3 , pH 9, and re-suspended in the same buffer containing coumarin (AMCA-X, SE; 0.1 mg mL^{-1}). Spores and cultured cells were incubated in coumarin for 2 h at room temperature, in the dark. Subsequently, labelled-microbes were pelleted and washed in 100 mM NaHCO_3 , pH 9 until a clear supernatant was observed. The final pellet was re-suspended in 1 mL PBS, pH 7.3 and stored at 4°C for no more than a week. $2 \mu\text{m}$ blue-fluorescent latex microspheres, purchased pre-labelled from Sigma (L0280), were also used in phagocytosis assays (conditions similar to those outlined in sections 4.3.4 and 4.3.8)

5.3.5 Phagocytosis assays

Extracted amebocytes (1×10^5 per well) were added to pre-prepared culture wells containing fluorescent-labelled targets (amebocyte : target ratio, 1:20)(quantitative methods are outlined in sections 4.3.3 and 4.3.5). Amebocytes were allowed to settle for 30 min to promote monolayer formation. Assays were monitored over a 1 h period and stopped by the addition of 2.5% neutral formaldehyde. Confirmation of target

internalisation was achieved using crystal violet quenching of fluorescence (chapter 4, section 4.3.8). Cells were viewed and quantified using the appropriate filters (DAPI/Coumarin were detected with a blue-filter set; excitation 365-395 nm and emission 420-460 nm) on an Axiovert 135 epifluorescence inverted microscope. Randomly chosen fields of view were selected until ~ 300 individual cells had been assessed per well (this method of analysis was used for sections 5.3.6 to 5.3.8, also).

5.3.6 Staining amebocyte mitochondria, *in vitro*

Viability of amebocytes *in vitro*, in the absence and presence of microbes, was assessed using MitoTracker Orange CMTMRos (MT-Orange). Amebocytes maintained in NaHEP, for 4 h, were assessed for intact mitochondrial membrane potential (viable cells) by labelling with 0.1 μM MT-Orange for 30 min at room temperature. Labelled cells were washed using LPS-free saline and subsequently fixed in 3.7% neutral-formaldehyde (in PBS, pH 7.3) for 10 min. Fixed amebocytes were washed and counterstained using DAPI (1 μM) to locate the nucleus. Negative controls consisted of amebocytes incubated at 40°C for 1.5 h, in the absence and presence of labelled targets.

5.3.7 Annexin V-FITC and propidium iodide staining of amebocytes

Amebocytes in the absence and presence of microbes (phagocytosis assays) were assessed for signs of cell death, *in vitro*. NaHEP was removed from the culture wells, via aspiration, and replaced with 3% NaCl-20 mM HEPES, pH 7.5 supplemented with 10 mM CaCl_2 (final volume; 500 μL). Media binding reagent³ (10 μL) and 0.5 μg Annexin V-FITC were added to each well and incubated at room temperature for 30 min, in the dark. Culture plates were centrifuged at 500 x g for 5 min; supernatant was removed by aspiration and replaced with pre-chilled 1X binding buffer³ (final volume; 500 μL) containing 0.3 μg propidium iodide. Samples were immediately placed on ice and

analysed using fluorescence microscopy. Positive controls consisted of amebocytes incubated at 40°C for 1.5 h, in the absence and presence of labelled targets.

5.3.8 TUNEL staining of amebocytes

Amebocytes in the absence and presence of microbes (phagocytosis assays), *in situ*, were assessed for signs of nuclear DNA fragmentation. NaHEP was removed from the culture wells; amebocytes were washed twice in PBS, pH 7.3 and then fixed in 100 mM NaH₂PO₄, pH 7.4 containing 4% paraformaldehyde⁴, for 25 min at room temperature. After fixing, amebocytes were washed twice in PBS, pH 7.3 (200 x g for 2 min) and incubated in 0.5% Tween[®]-20/0.2% BSA (in PBS) for 30 min. Again, amebocytes were washed twice in PBS, pH 7.3 and incubated with terminal deoxynucleotidyl transferase (TdT) end-labelling cocktail (containing ~ 12.5 μM biotin-dUTP; purchased pre-prepared from Milipore) for 1 hr. TdT end-labelling was stopped by removal of TdT cocktail and incubation of amebocytes in 1X termination buffer (TB)³ for 10 min. TB was removed and washed amebocytes were covered with blocking buffer (BB)³ for 30 min. BB was then removed and amebocytes were labelled with avidin-FITC (0.25 μg mL⁻¹) solution, for 45 min in the dark. Finally, amebocytes were washed and analysed using fluorescence microscopy. All incubation steps were performed at room temperature unless stated otherwise. A positive control consisted of fixed-amebocytes treated with 5 μg mL⁻¹ DNase, at 37°C for 1 hr, in the absence and presence of labelled targets, and subsequently processed as stated above. A negative control (monitoring non-specific binding of avidin-FITC) consisted of the above protocol, omitting TdT end-labelling.

In some cases, samples were counterstained by incubation in PBS, pH 7.3 containing ~ 240 mM Eriochrome Blue-Black for 10 min at room temperature. Counter-stained samples were washed and analysed.

Footnote 3; All buffers marked are purchased fully prepared from their respective manufacturers, section 5.3.1.

Footnote 4; Fixative was prepared by adding the appropriate amount of paraformaldehyde to a heated (60°C) solution of 100 mM NaH₂PO₄ and adding drops of 2 M NaOH until clear. A final pH of 7.2 was achieved using HCL. Store at 4°C (Ausubel et al., 2002).

5.3.9 Caspase-3 activity assay

Caspase-3 activity was assessed in amebocytes incubated in the presence and absence of microbes for 4 h, *in vitro*. Amebocytes were dissociated from the substratum of culture wells by trypsinization (0.1 mM trypsin, prepared in PBS, pH 7.3), pelleted (500 x g for 2 min), re-suspended in cell lysis buffer³ and incubated on ice for 15 min. Lysed amebocytes were centrifuged at 10,000 x g for 2 min. The supernatant was removed and stored on ice. Estimates of protein concentrations present in supernatant were performed using a BSA standard curve as previously stated (section 4.3.7).

Photometric determination of caspase-3 activity was carried out at 37°C in a 96-well plate (MDS VERSA max microplate reader). Assays consisted of 100-500 µg mL⁻¹ cytosol extract and 1X reaction buffer³ containing 10 mM DTT and 0.2 mM DEVD-*p*NA (substrate); final assay volume was ~ 100 µL (per well). Activity was monitored by an increase in absorbance at 405 nm, over a period of 2 h. At each time point, potential caspase activity values derived from spores alone were deducted from amebocyte/spore assays. Controls consisted of assays in the absence of amebocyte-lysate.

Positive controls consisted of amebocytes incubated at 40°C for 4 h, in the absence and presence of labelled targets.

5.3.10 Measurements of hemocyanin-derived phenoloxidase activity *in vitro*

A) *In situ* Hc-d PO activity_(total membrane bound and cell-free)

Amebocytes were maintained *in vitro* in the presence and absence of microbes for 4 h. Total *in situ* Hc-d PO activity was assessed by addition of substrate (2 mM dopamine) directly into culture wells. After 10 mins, the supernatant containing HSC

plasma/NaHEP (including Hc) was removed (via aspiration) and centrifuged at 1000 x g for 5 min at room temperature. Supernatant was removed and diluted immediately (1:1) in 100 mM Tris-HCl, pH 7, and the pellet discarded. Hc-d PO activity was assessed by taking measurements of dopamine oxidation at 475 nm using an Ultrospec 2100 pro UV/Visible spectrophotometer.

B) *Ex situ* Hc-d PO assay_(cell-free only)

Amebocytes were maintained as stated above. Supernatant (~ 500 μ L) was removed directly from each culture well, centrifuged and placed in a cuvette with either **1)** 500 μ L 100 mM Tris-HCl, pH 7 containing 2 mM dopamine or **2)** treated with 0.1% SDS (in 100 mM Tris-HCl) for 5 min prior to addition of dopamine. Assays were initiated with the addition of substrate and PO activity was monitored as stated above (over a period of 10 min).

In experiments A and B, cell numbers per well was assessed across the range 1×10^5 to 5×10^5 . Cell maintenance buffer, NaHEP, is supplemented with 5% HSC plasma (section 5.3.3). Protein concentration of HSC hemolymph was calculated at $\sim 40 \text{ mg mL}^{-1}$ (> 90% is Hc; Ding et al., 2005), therefore, each well was supplemented with $\sim 1 \text{ mg}$ of protein (25 μ L HSC plasma plus 475 μ L NaHEP). As the ratio of amebocytes to microbes was maintained at 1: 20, it was technically challenging to conduct assays with amebocyte concentrations above 5×10^5 cells per well, as spore numbers would exceed 1×10^7 . The auto-oxidation of dopamine into dopachrome was deducted from assay values, therefore, data represent activity due to Hc-d PO only. One unit is defined as 1 μ mol of dopachrome formed per minute, with an absorption coefficient for dopachrome at this wavelength (475 nm) of $3600 \text{ M}^{-1} \text{ cm}^{-1}$. Labelled-targets in the absence of amebocytes failed to elicit PO activity in Hc.

5.3.11 Data handling

A total of six horseshoe crabs were used in this study. Four HSCs were bled on four independent occasions and two HSCs were bled on three independent occasions. HSCs were bled no more than once a week. Data were pooled together and values are represented by the mean \pm standard deviation. The Ryan-Joiner normality test and Levene's test for homoscedasticity were applied to all percentage data sets. Data were arcsine transformed successfully. ANOVA (with Bonferroni *post hoc* tests) were applied to assess rates of phagocytosis, degranulation, FITC/propidium iodide staining and caspase activity data. Two sample t-tests were applied to TUNEL and MT-Orange data sets. Analysis was performed using Minitab analytical software version 16.

5.4 Results

5.4.1 Functional properties of amebocytes in the absence and presence of coumarin-labelled microbes

Upon exposure of amebocytes to coumarin-labelled microbes *in vitro*, approximately 8.8% of amebocytes display phagocytic properties, irrespective of the target used (Fig. 5.1A). Furthermore, phagocytic indices of amebocytes determined for each target, *B. bassiana*, *B. megaterium* and *S. cerevisiae*, displayed similar levels of inclusion, between 1.3 and 1.6 (Fig 5.1B). Crystal violet (CV) quenching of microbial fluorescence was successful in distinguishing between phagocytosed and non-internalised amebocyte associated coumarin-labelled spores (Fig. 5.1C). Blue-fluorescent 2 μm latex-microspheres were also used as targets for amebocyte phagocytosis, however, it was difficult to confirm microsphere internalisation due to rapid photo-bleaching.

Previously, amebocytes have been shown to undergo spontaneous degranulation in the absence of endotoxin, *in vitro* (Armstrong 1980; Conrad et al., 2006). The proportions of degranulated amebocytes in the absence and presence of labelled-spores were 13.2% and 16% after 24 h, respectively (Fig. 5.2).

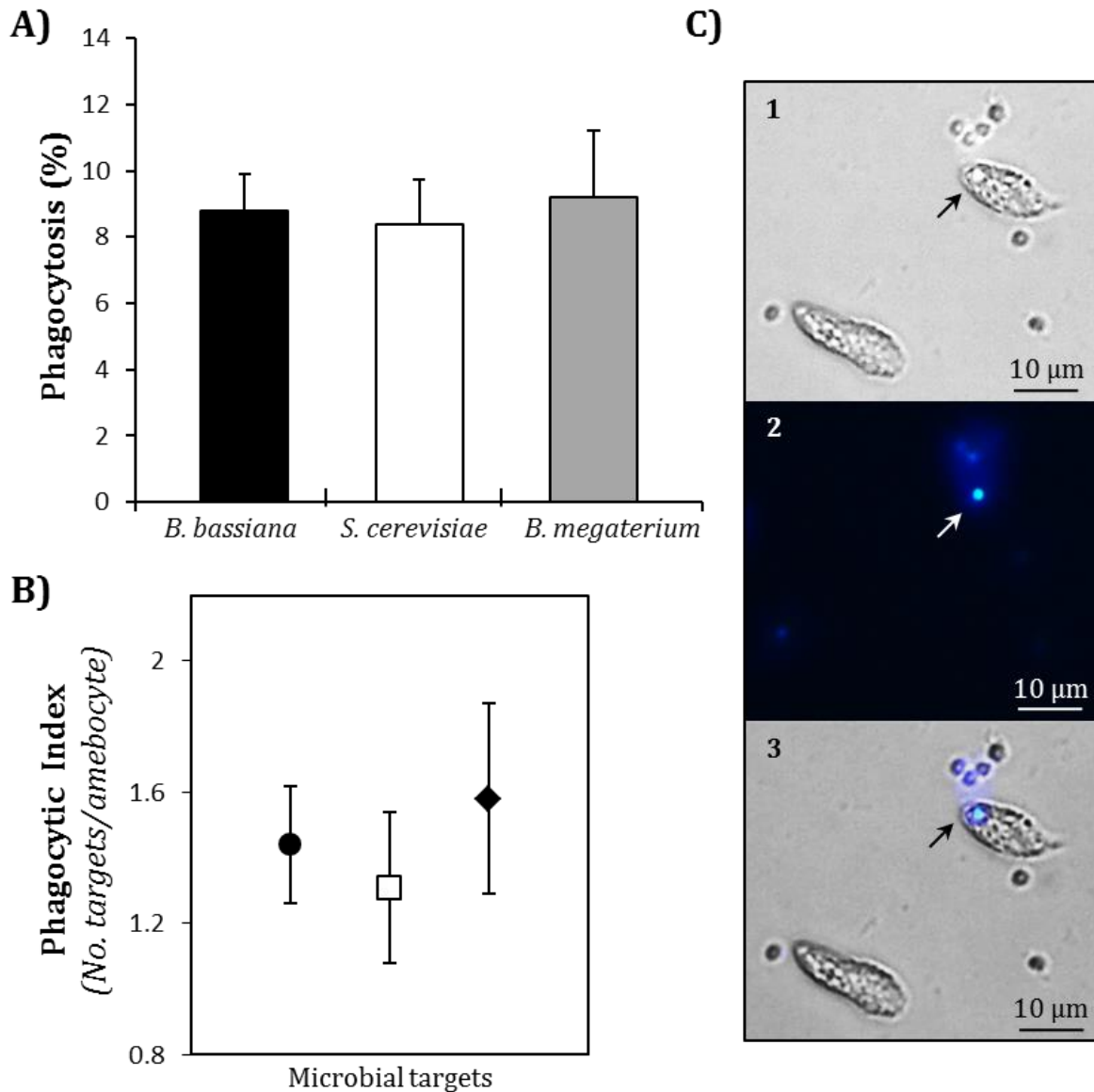


Figure 5.1 Phagocytic properties of amebocytes in the presence of coumarin-labelled microbes. **A)** Proportion of phagocytically active amebocytes. **B)** The number of internalised targets per active amebocyte. Symbols: ● *B. bassiana*, □ *S. cerevisiae*, ◆ *B. megaterium*. **C)** Images depicting an internalised coumarin-labelled *B. bassiana* spore. 1, brightfield view of amebocytes and spores, 2, fluorescent spores post quenching using crystal violet and 3, a merged image showing the location of the internalised spore.. Image J software was used to prepare images. Values are mean \pm SD, n = 5. No significant differences were detected.

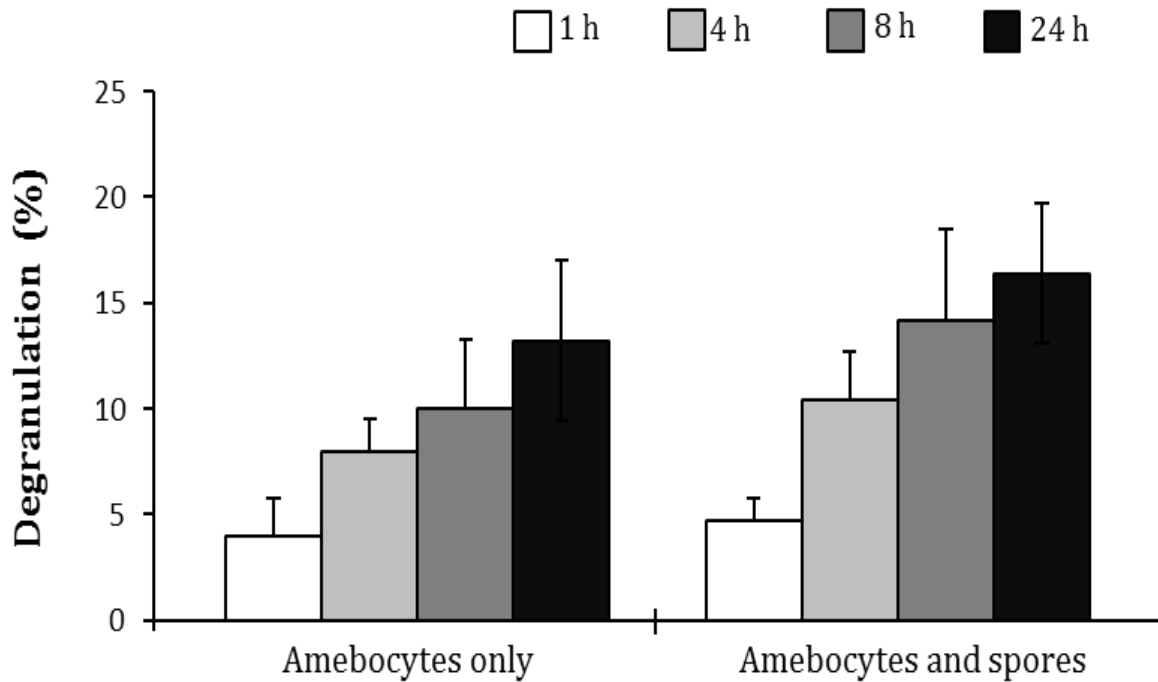


Figure 5.2 Exocytosis of amebocyte cytosolic granules in the absence of endotoxin, *in vitro*. Amebocytes were maintained in NaHEP (supplemented with 5% v/v HSC plasma) and monitored at various time points over a period of 24h. Amebocytes having released >50% of cytosolic content were considered degranulated. Values are mean \pm SD, n = 5. No significant differences in percentage degranulation were detected between amebocytes incubated in the presence of absence of spores.

5.4.2 Apoptotic modalities of amebocytes, *in vitro*

PICD is a phenomenon that occurs when phagocytes internalise pathogens and subsequently 'terminate themselves' in order to prevent pathogen dissemination. Phagocytically active amebocytes studied here, having internalised coumarin-labelled spores, demonstrated a number of morphological and biochemical hallmarks of apoptotic cell death (Fig. 5.3 to Fig. 5.8).

Mitochondrial membrane potential of amebocytes in the presence of coumarin-labelled spores was significantly reduced ($p \leq 0.05$) in comparison to amebocytes maintained without spores (Fig. 5.3). PS extracellularisation (Annexin V-FITC +; Fig. 5.4), loss of plasma membrane integrity (Annexin V-FITC +/propidium iodide +; Fig. 5.5), nuclear DNA fragmentation (TUNEL +; Fig. 5.6 and Fig. 5.7) and an increase in caspase-3 activity were observed in amebocytes. Caspase activity detected was proportional to the amount of protein used (Fig. 5.7). In all experiments, amebocytes in the absence of spores demonstrated significantly lower rates of cell death compared to those exposed to spores. The proportions of apoptotic/dying amebocytes in the absence of spores and non-phagocytic amebocytes in the presence of spores were highly comparable, between 4.5 % and 6.5 %.

Annexin V-FITC and propidium iodide staining of amebocytes at 1, 2, 3 and 4 h post incubation with spores, suggested a significant increase in PS extracellularisation and concurrent loss of plasma membrane potential of phagocytically active amebocytes (Fig. 5.4 and Fig. 5.5). By subtracting the percentage of FITC/propidium iodide positive amebocytes in the absence of spores from those in the presence of spores, the average difference is 8.97 % for the duration of the experiment. Results indicate that all phagocytic cells (8.8 %; Fig. 5.1) exposed PS within 2 h of ingesting spores (Fig. 5.4), *in*

vitro. Cell death rates in non-phagocytic amoebocytes are in agreement with previously recorded rates of amoebocyte mortality when maintained in NaHEP (chapter 4; Fig. 4.1, $\leq 6\%$ at 4 h).

Positive controls for all assays consisted of incubating amoebocytes at or above 37°C for 1.5 to 4 h. Between 85% and 95% of control amoebocytes stained positive for all apoptotic signals measured, with no differences detected between amoebocyte populations incubated with, or without spores (Fig. 5.4B, Fig. 5.6B and Fig. 5.8B). Other markers of apoptotic cell death were recorded in amoebocytes maintained *in vitro*, including, cytosol vacuolisation and membrane blebbing. However, due to the changeable and highly motile nature of amoebocytes and the appearance of multiple vacuoles post exocytosis, these features were not used as quantitative markers of cell death.

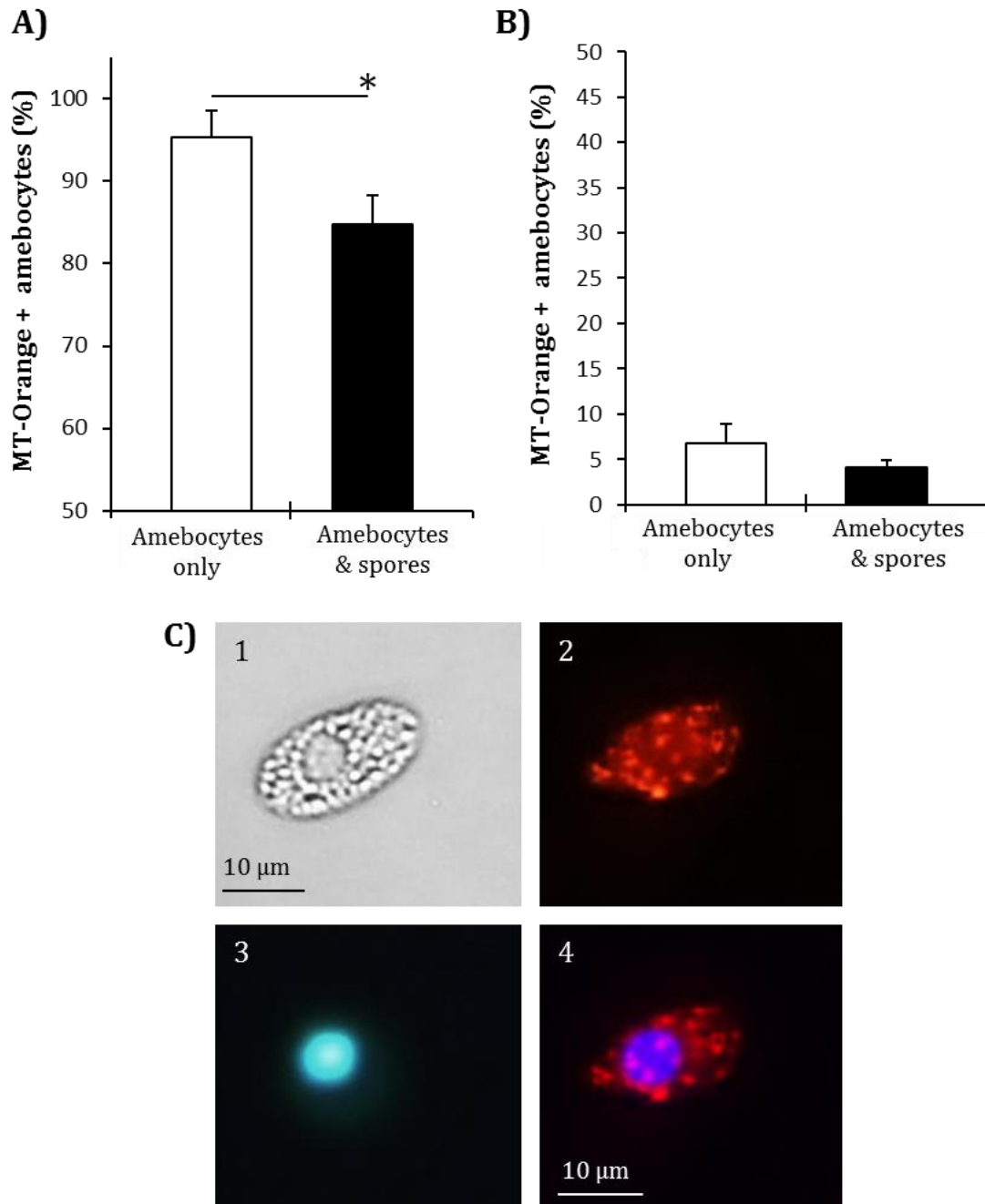


Figure 5.3 MitoTracker Orange CMTMRos staining of mitochondria present in *Limulus polyphemus* amebocytes. **A)** Amebocytes in the presence and absence of labelled spores (for 4 h) were assessed for mitochondrial potential. **B)** Negative controls (loss of function) consisted of amebocytes incubated at 40°C for 1.5 h, in the absence and presence of labelled targets. **C)** Viable amebocytes, *in vitro*, were stained successfully. MitoTracker Orange CMTMRos only fluoresces in the presence of functioning mitochondria. Images; **1)** Brightfield view of an amebocyte *in vitro*, **2)** positively stained mitochondria dispersed throughout the cytosol, **3)** DAPI staining of an intact nucleus and **4)** merged images 3 and 4. Scale bar represents 10 μm. Images were prepared using Image J software. A significant decrease in amebocyte mitochondrial membrane potential at $p \leq 0.05$ is represented by *. Values are mean \pm SD, n = 5.

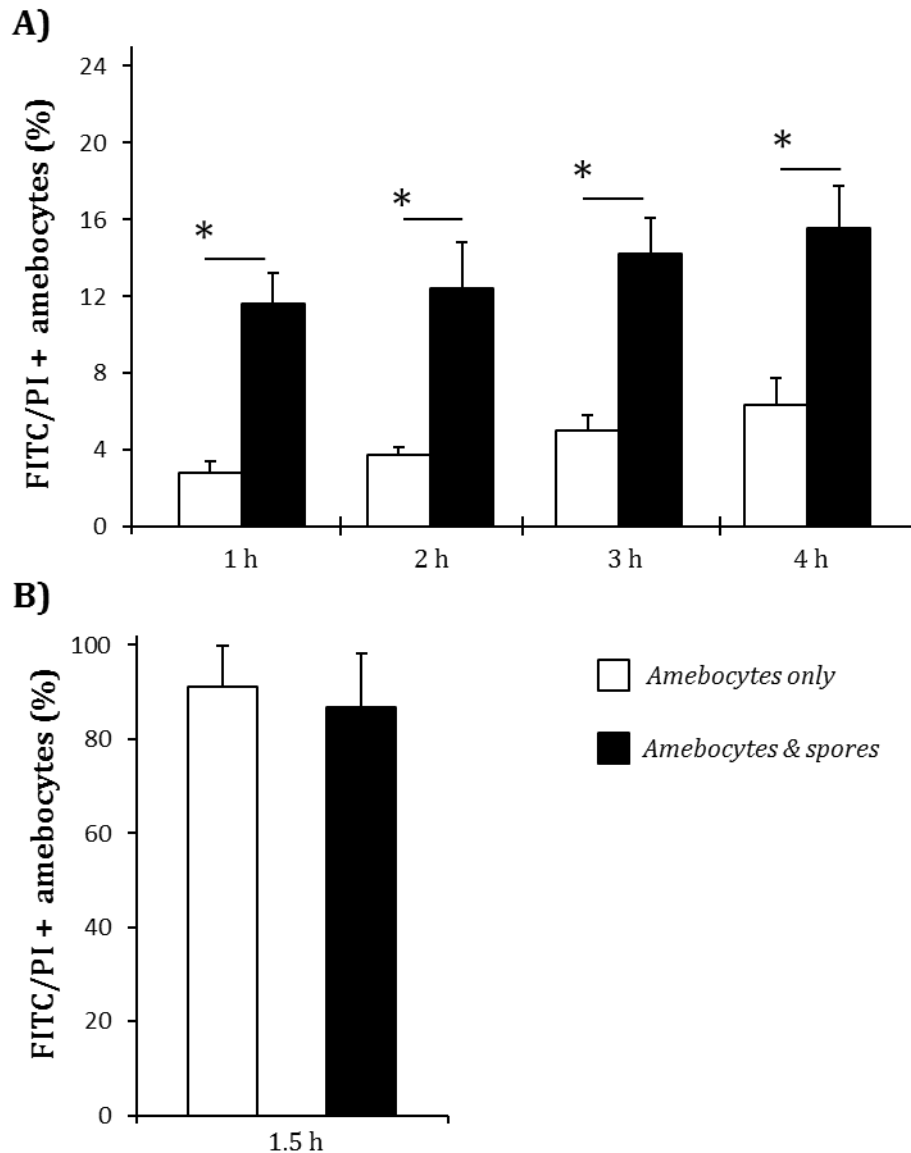


Figure 5.4 Using Annexin V-FITC and propidium iodide staining to monitor amebocyte cell death, *in vitro*. **A)** amebocytes maintained in NaHEP for 24h at 18°C in the presence or absence of labelled-spores were assessed for signs of phosphatidylserine (PS) extracellularisation (Annexin V-FITC positive) and loss of plasma membrane potential (propidium iodide positive). **B)** Positive controls consisted of incubating amebocytes in the presence or absence of labelled-spores at 40°C for 1.5 hours. A significant increase in proportions of FITC/propidium iodide positive amebocytes at $p \leq 0.05$ is represented by *. Values are mean \pm SD, n = 5.

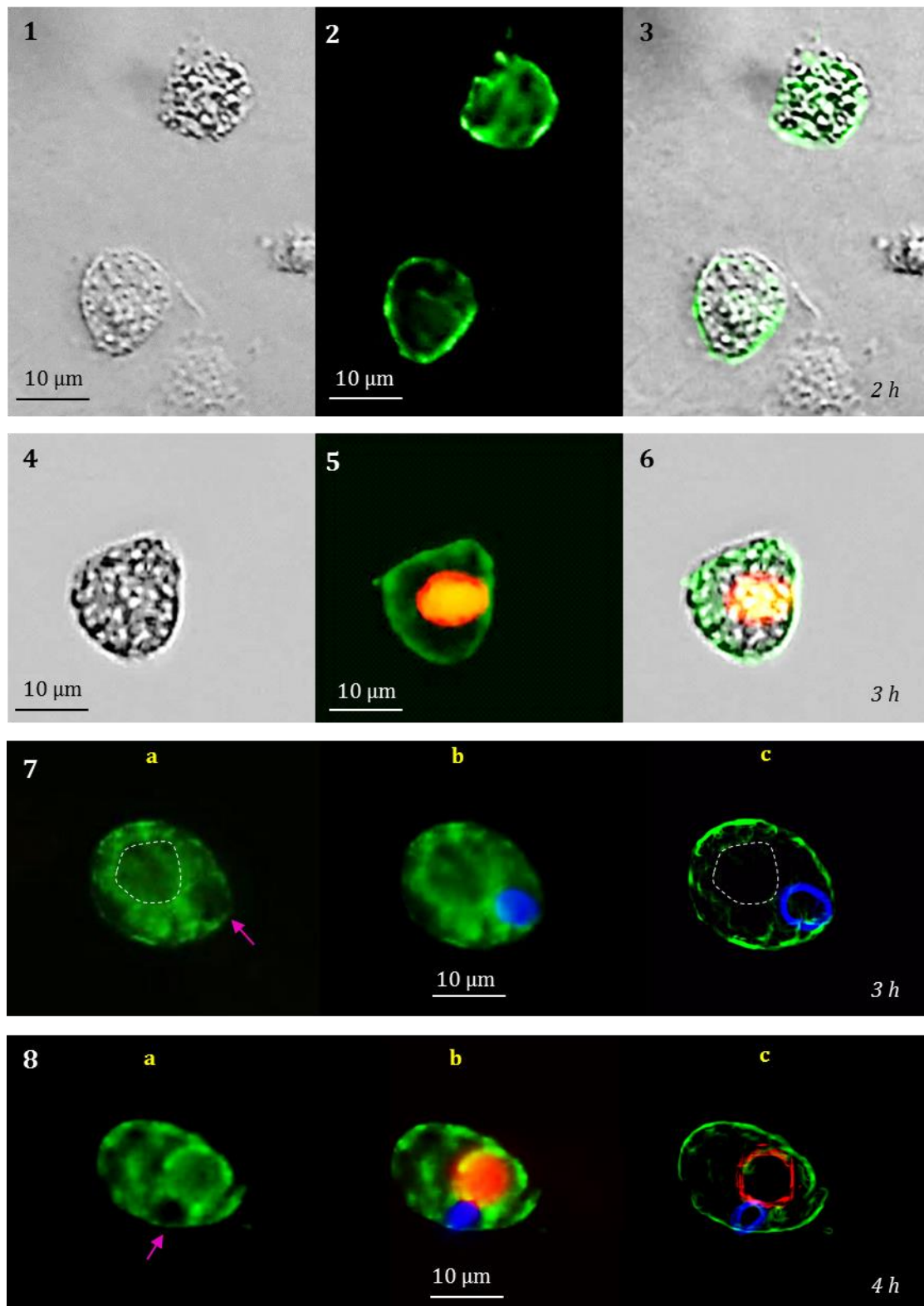


Figure 5.5 A series of images depicting phosphatidylserine exposure and loss of plasma membrane integrity of dying amebocytes. Annexin V-FITC positive/propidium iodide negative detection of PS: 1, 2 and 3 (early apoptotic). Annexin V-FITC positive and propidium iodide positive amebocytes: 4, 5 and 6 (late apoptotic or necrotic). 7a-c) Annexin-V/FITC positive amebocyte with an internalised coumarin-labelled spore. 8a-c) Annexin-V/FITC and propidium iodide positive amebocyte with a coumarin-labelled spore. Pink arrows indicate the location of phagosomes and the broken white line in images 7a and 7b highlight the location of the nucleus. The time scale is depicted in each set of images. Images were prepared using Image J software.

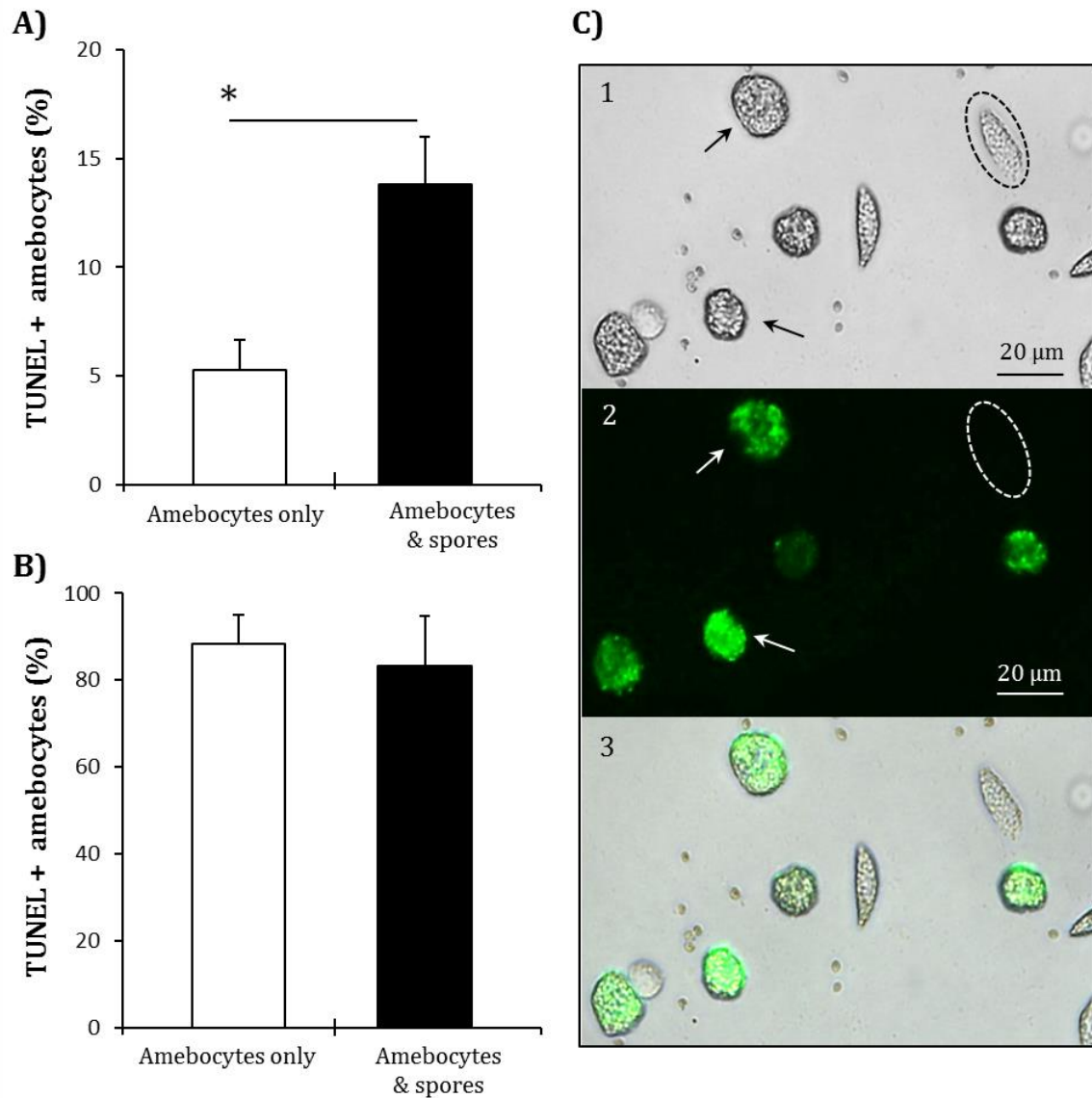


Figure 5.6 Using TUNEL staining to monitor amebocyte cell death, *in vitro*. **A)** Amebocytes maintained in NaHEP for 4 h at 18°C in the presence or absence of labelled-spores were assessed for signs of nuclear DNA fragmentation (TUNEL positive). **B)** Positive controls consisted of treating amebocytes in the presence or absence of labelled-spores with DNase for 1 h at 37°C. **C)** Images demonstrating TUNEL staining of amebocytes. 1) Bright field view of amebocytes, 2) TUNEL-positive amebocytes (biotin-dUTP is transferred to cleaved DNA and visualised using avidin-FITC) and 3) a merging of images 2 and 3. Blue arrows indicate TUNEL positive amebocytes and broken lines highlight a TUNEL negative amebocyte. A significant increase in proportions of TUNEL positive amebocytes at $p \leq 0.05$ is represented by *. Values are mean \pm SD, n = 5.

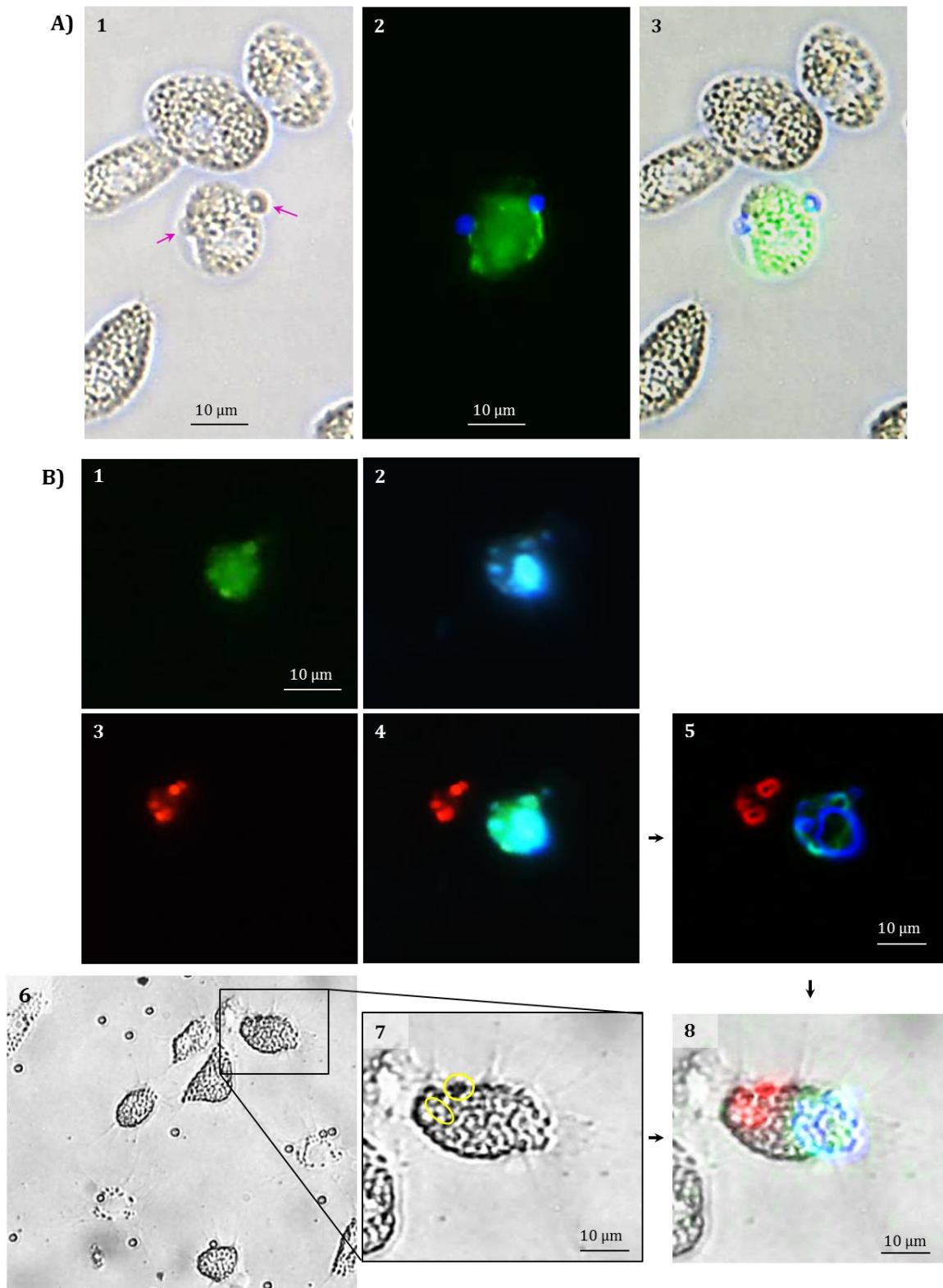


Figure 5.7 TUNEL staining of phagocytically active amebocytes, *in vitro*. **A)** A series of images depicting a TUNEL positive (green) amebocyte having internalised or associated with coumarin- labelled *B. bassiana* spores (pink arrows). **B)** A TUNEL positive amebocyte after ingesting two Rhodamine B-labelled spores (red). 1) TUNEL stained nuclear DNA, 2) DAPI staining of the nucleus, 3) Rhodamine B-labelled spores, 4) images 1-3 merged, 5) the edges of the labelled cellular components, 6) & 7) brightfield views of amebocytes and 8) An image consisting of 5 and 7 merged. Yellow circles highlight the location of the internalised spores.

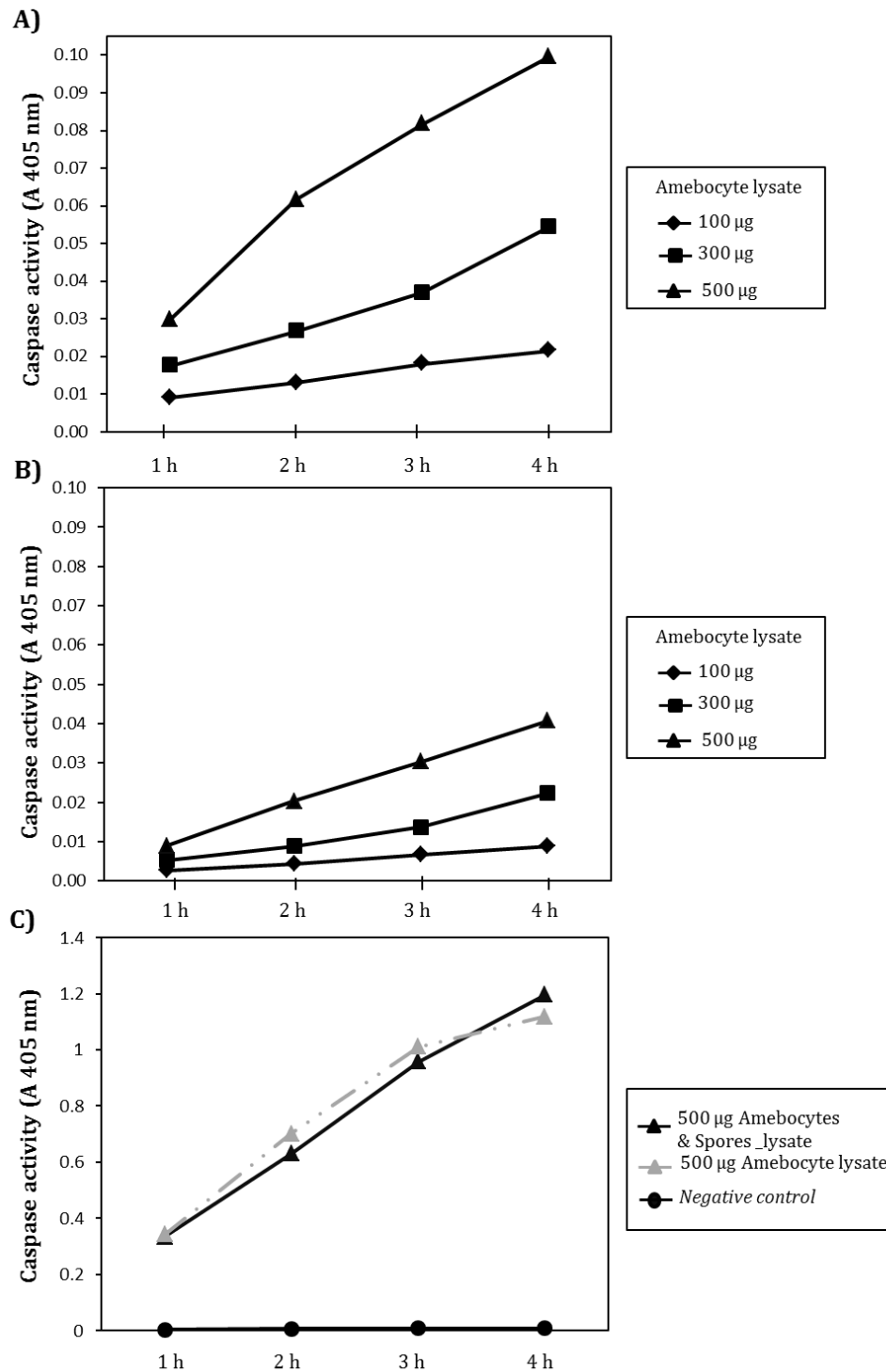


Figure 5.8 Caspase-3 activities of amebocytes in the presence and absence of spores, *in vitro*. Assays consisted of 100-500 $\mu\text{g mL}^{-1}$ cytosol extract (from 1×10^5 cells), 1X reaction buffer³ containing 10 mM DTT and 0.2 mM DEVD-*p*NA (substrate); final assay volume was $\sim 100 \mu\text{L}$ (per well). Activity was monitored by an increase in absorbance at 405 nm, over a period of 2 h at 37°C. **A)** Amebocytes in the presence of labelled spores, *in vitro*. **B)** Amebocytes only. **C)** Positive controls consisted of incubating amebocytes in the absence or presence of spores, over a period of 4 h at 40°C. The negative control consisted of substrate (0.2 mM DEVD-*p*NA) in the absence of amebocytes. Assays were performed in triplicate on three independent occasions ($n = 3$) and are represented as mean values.

5.4.3 Hemocyanin activation in the presence of phagocytically active amebocytes

Previously, it has been demonstrated that membrane phospholipids, especially PS, are potent activators of PO activity in Hc (chapter 2; Coates et al., 2011). After documenting a substantial increase in PS exposure on phagocytic amebocytes undergoing apoptosis (Fig 5.4), PO activity of Hc was subsequently monitored in culture wells (Fig. 5.9). Hc-d PO activity was detected in wells containing amebocytes that had been maintained in the presence and absence of spores for 4h (Fig. 5.9). Total Hc-d PO activity (*in situ*) was recorded at ~ 0.73 U in the presence of 5×10^5 amebocytes per well, including spores (Fig. 5.9A). In contrast, Hc-d PO activity in wells containing amebocytes (5×10^5) in the absence of spores was significantly less ($p < 0.05$), with ~ 0.25 U observed.

Soluble (acellular) Hc-d PO activity was investigated by removing supernatant and adding substrate (*ex situ*) in the absence of amebocytes. Activity was recorded as ~ 0.17 U from wells containing both amebocytes and spores, and 0.051 U with amebocytes only (Fig. 5.9B). Total potential PO activity of soluble Hc (*ex situ*) was assessed by treatment with SDS micelles for 5 min prior to addition of substrate. 3.5 U and 3.96 U of dopachrome formation were observed in samples taken from culture wells containing amebocytes with and without spores, respectively (Fig. 5.9C).

Furthermore, inducible PO activity of purified Hc, and Hc present in hemolymph were highly comparable. Hc present in hemolymph displayed 92% and 93% of PO activity levels detected for purified Hc in the presence of PS and SDS, respectively (Fig. 5.10). Microbial proteases have been shown previously to induce PO activity of *C. rotundicauda* Hc (Jiang et al., 2007). Control experiments conducted here indicate that no measureable induction of PO activity derived from *L. polyphemus* Hc in the presence of *B. bassiana* spores. In the absence of amebocytes, PS and/or SDS, no Hc-d PO activity could be detected.

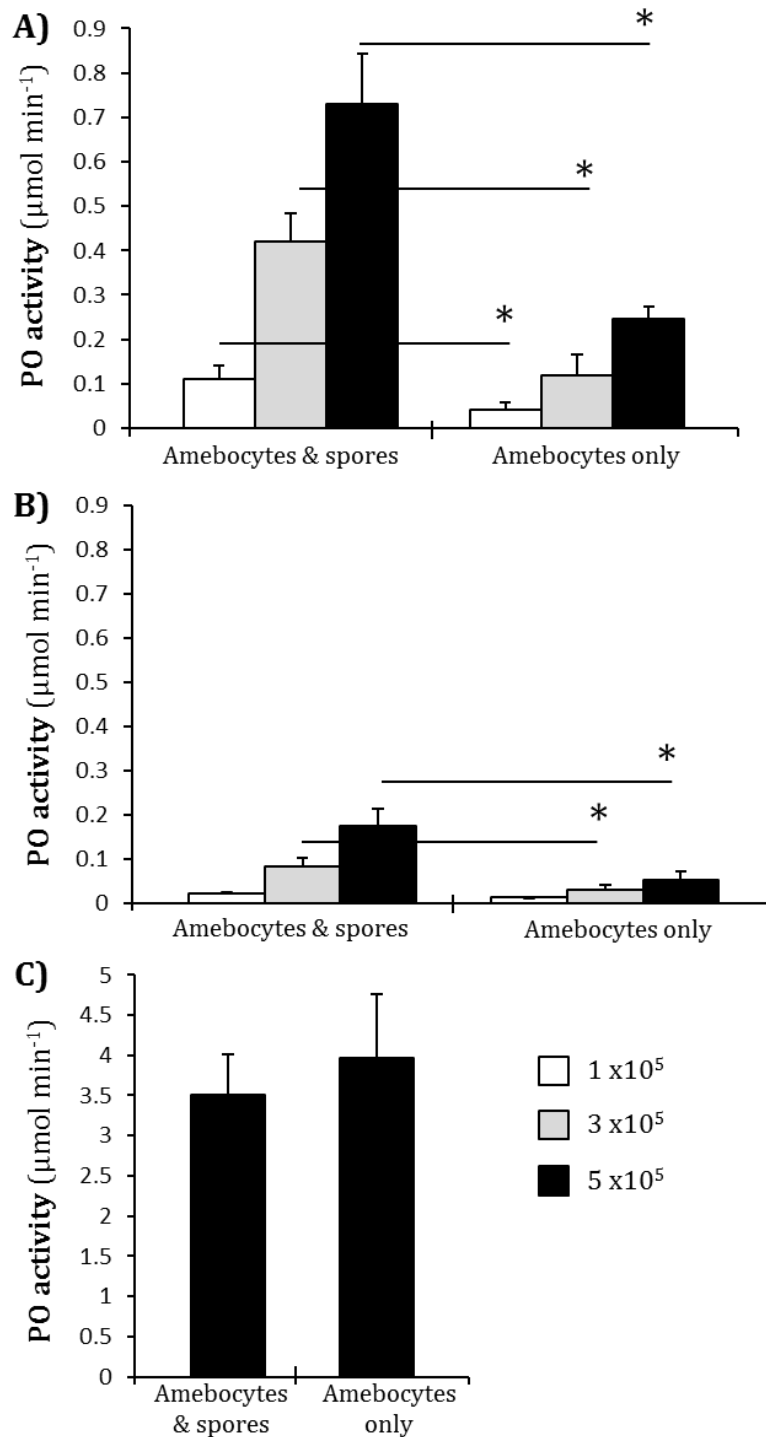


Figure 5.9 Inducible phenoloxidase activity of hemocyanin in the presence of dying amebocytes. Amebocytes were maintained (in NaHEP) in the presence and absence of coumarin-labelled spores for 4 h. PO activity, derived from hemocyanin was measured **A) *in situ*** (culture wells) by addition of substrate (2 mM dopamine) and **B) *ex situ***, by removal of supernatant and addition of substrate. **C)** Potential PO activity of hemocyanin (positive control) was measured by treating *ex situ* supernatant with 0.1% SDS for 5 min prior to addition of substrate. Hc-d PO activity was detected by an increase in absorbance at 475 nm, due to dopamine oxidation. A significant difference in Hc-d PO activity at $p \leq 0.05$ is represented by *. Values are mean \pm SD, n = 5.

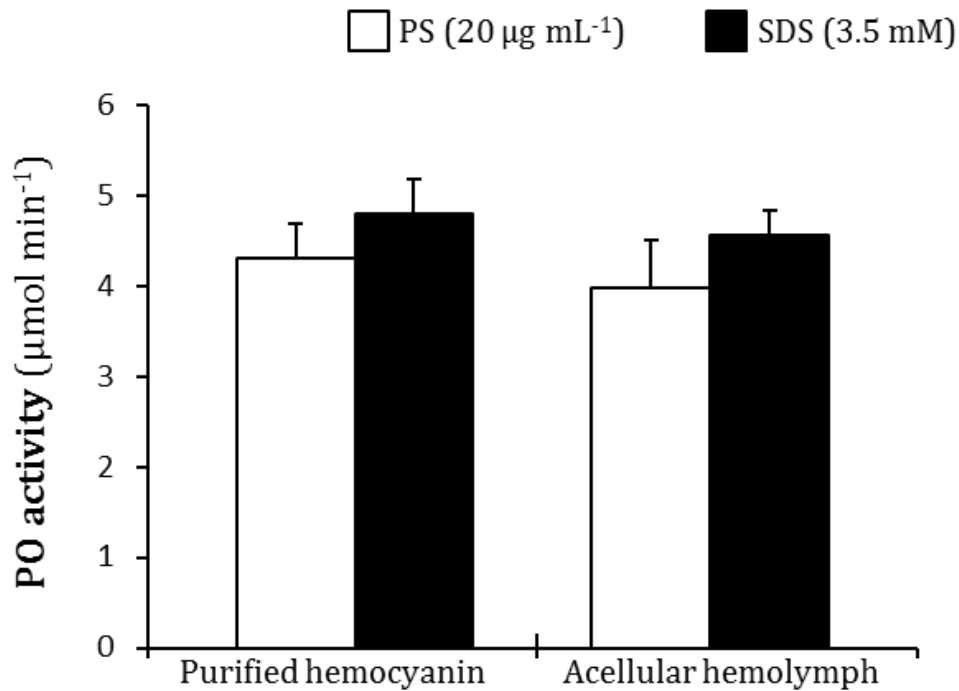


Figure 5.10 Inducible phenoloxidase activity of *Limulus polyphemus* hemocyanin. Assays included 2 mM dopamine and 1 mg mL⁻¹ purified hemocyanin or 1 mg mL⁻¹ hemolymph protein. Assays were carried out in 100 mM Tris-HCl, pH 7.5. Samples were pre-incubated for 10 min with either phosphatidylserine or SDS. Phenoloxidase activity was initiated by the addition of substrate (dopamine). The histogram illustrates an increase in absorbance at 475 nm resulting from the formation of dopachrome and its derivatives, over a period of 10 minutes. Assays were conducted in triplicate on three independent occasions (n = 3). Values represent mean ± SD.

5.5 Discussion

5.5.1 Phagocytosis-induced cell death in invertebrates

Type 1 programmed cell death, also known as apoptosis, is a crucial process required for development, immunomodulation and pathogen deterrence (Sokolova, 2009). Using mammalian and selected invertebrate model organisms (*D. melanogaster* and *Caenorhabditis elegans*), phagocytes have been shown to undergo apoptosis after pathogen internalisation, notably viruses (Menze et al., 2010; Franc, 2002). It is suggested that apoptosis is an essential innate immune mechanism required to block the replication and subsequent systemic dissemination of hazardous microorganisms (Cooper and Mitchell-Foster, 2011). The importance of apoptosis in antimicrobial immunity is evident from the number of apoptotic modulating strategies employed by obligate intracellular pathogens (Menze et al., 2010; De Leo, 2004). Many pathogens are known to secrete a battery of anti-apoptotic molecules in order to avoid detection *in vivo*, including, preventing PS relocation by disabling flippases and interfering with p53, mitochondrial and caspase activities (McLean et al., 2008; Hilleman, 2004). On the other hand, certain bacteria are known to promote apoptosis in vertebrate macrophages in order to suppress pro-inflammatory signalling (De Leo, 2004; Frankenberg et al., 2008). Over the last decade, research has focussed predominantly on characterising proteolytic cascades and apoptotic machinery present in invertebrates, and their similarities with mammalian counterparts (Menze et al., 2010; Sokolova, 2009), however, relatively few studies have investigated episodes of PICD.

M. rosenbergii hemocytes displayed PICD after internalising bacteria and yeast, however, phagocytosis of latex microspheres did not lead to apoptosis (Hsu et al., 2005). Hemocyte apoptosis was identified by TUNEL staining and membrane blebbing

depicted in electron micrographs. Similarly, phagocytically active amebocytes observed here in the presence of fungal spores (Fig. 5.6) shared comparable levels of TUNEL staining with *M. rosenbergii* hemocytes. Whether PICD in *M. rosenbergii* was self-induced for host protection or pathogen induced for immune-suppression purposes remains unclear. The complex relationships between crustacean hemocyte PICD and apoptosis avoidance strategies used by viruses have gained substantial attention due to the economic importance of shellfish. However, opinion is divided on whether PICD during viremia in crustaceans is beneficial or detrimental to the host, as convincing evidence exists for both arguments (Smith, 2010; Menze et al., 2010).

Phagocytosis rates of *L. polyphemus* amebocytes in the presence of coumarin-labelled spores were comparable to rates observed previously with FITC and/or Rhodamine-B labelled targets (chapter 4, Fig. 4.10 and Fig. 5.1). Internalisation of coumarin-labelled spores by amebocytes *in vitro* induces morphological and biochemical changes consistent with apoptosis. Hallmarks of apoptosis recorded for phagocytic amebocytes included: loss of mitochondrial and plasma membrane integrity (Fig. 5.3 and Fig. 5.5), redistribution of PS (Fig. 5.4 and Fig. 5.5), nuclear DNA fragmentation (Fig. 5.6 and Fig. 5.7) and an increase in caspase-3 activity. The substrate used for caspase-3 activity assays, DEVD-pNA, can be processed by a number of different caspases, notably caspase-7 (Krzyzowska et al., 2002), therefore, DEVDase activity detected here may be due to a number of activated caspase-like proteins present in amebocytes. In all instances, levels of amebocyte cell death were highest in the presence of spores, with the majority of these amebocytes being confirmed as phagocytically active. The remaining proportion of dying cells (non-phagocytic) in the presence of spores shared

great similarities with the proportion of non-viable amebocytes in the absence of spores, over the duration of the experiment (4 h).

During sepsis by *P. aeruginosa*, 13 apoptosis-related ESTs, including cytochrome c-oxidase (COX) and sensitive to apoptosis gene (SAG) were identified in the chelicerate, *Carcinoscorpius rotundicauda* (Ding et al., 2005). Such apoptosis-related ESTs were recorded at higher levels 3 h post infection. Likewise, all phagocytically active amebocytes recorded here for *L. polyphemus*, stained positive for extracellular PS (Fig. 5.4) and demonstrate a 10- fold increase in caspase activity (Fig. 5.8) within 3 h of exposure to fungal spores. Additionally, nuclear DNA fragmentation (Fig. 5.7) was noted in phagocytic amebocytes at 4 h post incubation. COX subunits have been identified in *L. polyphemus* and are known to be involved in apoptosis (Lavrov et al., 2000). The presence of amine oxidase (AOx) was also observed in challenged *C. rotundicauda*. AOx, like COX proteins, is involved in ROS production and apoptosis (Ding et al., 2005). Zhang et al., (2003) determined ROS production to be the main cause of PICD in murine and human neutrophils. Whether ROS generation in HSC amebocytes also influences PICD remains to be confirmed.

5.5.2 Activation of hemocyanin into a phenoloxidase *in vivo*

Exposure of PS onto the external leaflet of plasma membrane is the most commonly observed feature of apoptotic cells (across all phyla) and is mediated by ATP-dependent aminophospholipid translocases (i.e. flippases) (Wu et al., 2006). Interestingly, recent work carried out by Lee et al., (2012) demonstrated that cell shrinkage during apoptosis of human Jurkat cells leads to the redirection of cytosolic plasma membrane derived vesicles back to the plasma membrane, whereby they fuse and expose more PS. In *L. polyphemus*, PS exposure by phagocytic amebocytes (amongst other markers of cell

death) was recorded concurrently with Hc-d PO activity (Fig. 5.4 and Fig. 5.9). Levels of Hc-d PO were significantly higher in culture wells containing both amebocytes and spores. Importantly, control experiments indicated that spores alone did not lead to detectable Hc-d PO activity.

PS has been shown to interact with *L. polyphemus* Hc and induce a conformational change leading to PO activity (chapter 2/Coates et al., 2011). Evidence suggests that PS is also involved in the activation of *D. melanogaster* proPO into PO, during injury (Bilda et al., 2009). It is postulated that PICD of amebocytes during immune challenge could potentially provide Hc with a mode of activation via the presentation of redistributed PS. Purified Hc (1 mg mL⁻¹) displayed ~ 4 U of activity in the presence of 20 µg mL⁻¹ liposomal PS (Fig. 5.10). While such an amount of PS is unlikely to be available in HSC hemolymph, total Hc-d PO in the presence of ~ 50,000 apoptotic amebocytes was recorded at ~ 0.7 U (Fig. 5.3 to Fig. 5.8). It is possible that Hc could interact with other membrane components, together with PS. For example, phosphatidylethanolamine (PE) is known to be relocated to the external side of plasma membrane during apoptosis (Lee et al., 2012). Although not as effective as PS or SDS, PE has been shown to induce PO activity in Hc (Nagai and Kawabata, 2000; Nellaiappan and Sugumaran, 1996). PO activity of Hc associated with apoptotic amebocytes made up 78% of the of total PO activity recorded, while soluble Hc-d PO (in the absence of amebocytes), accounted for the remaining 22% (Fig. 5.9). Even though no differences were detected in the degranulation rates of amebocytes in either the presence or absence of spores (Fig. 5.2), the release of immune effectors such as clotting factors and anti-microbial peptides by amebocytes (Nagai et al., 2001; Nagai and Kawabata, 2000; Nellaiappan and

Sugumaran, 1996) may be responsible for the activation of soluble (acellular) Hc-d PO recorded here.

Across all phyla, cell death events are broadly correlated with the progression of many debilitating diseases, influencing both hypersensitive and suppressive immune mechanisms. Although present in an archaic species, *L. polyphemus* amebocytes share many functional and mechanistic properties with mammalian and arthropod immune cells, including, phagocytosis, release of eicosanoids, diapedesis and AMP synthesis (Kawabata et al., 2009; MacPherson et al., 1998; Armstrong and Levin, 1979). Now, evidence presented here suggests that PICD is also conserved.

PS is a potent immune effector: 'branding' defective cells for phagocytosis (Martin et al., 2012), activating clotting proteins in mammals (Zwaal et al., 1998; Stace and Ktistakis, 2006) and inducing PO activity in fruit flies (Bilda et al., 2009). The concept of Hc being converted into an immune enzyme via an interaction with PS or by some other unknown plasma membrane component on apoptotic amebocytes is intriguing. Evidence provided here suggests the need to further explore PS as a likely putative activator of Hc-d PO *in vivo*.

5.6 Conclusion

Amebocytes that have phagocytosed microbial targets, *in vitro*, appear to undergo cell death, characterised by traditional hallmarks of type-1 programmed cell death, apoptosis. The extracellularisation of PS onto the plasma membrane during PICD could potentially activate Hc-d PO activity, *in vivo*, providing an alternative function for infected amebocytes.

Chapter 6:

Monitoring the Effect of Temperature on the Health Status of Captive *Limulus polyphemus*; Biochemical and Cellular Properties of Hemolymph

A version of this chapter has been published;

Christopher J. Coates, Emma L. Bradford^a, Carsten A. Krome^b and Jacqueline Nairn. 2012. Effect of temperature on biochemical and cellular properties of captive *Limulus polyphemus*. *Aquaculture*. 334-337, 30-38.

^a E. L. Bradford aided quantitative analysis of hemolymph properties.

^b C.A. Krome set-up tanks and weighed the horseshoe crabs on two sampling days.

6.1 Abstract

The maintenance of horseshoe crabs in culture is being explored to address the recent decline of the species. While a number of indicators have been used to monitor the health status of the horseshoe crabs, the limited success of culture methods suggests that an alternative approach is required. In this chapter, the effect of temperature on physiological, biochemical and cellular characteristics of hemolymph were used to assess the health status of the Atlantic horseshoe crab, *Limulus polyphemus*. *L. polyphemus* were maintained across the temperature range, 8 °C to 23 °C, for a period of 56 days. Mean body weight, hemocyanin concentration and function, amebocyte numbers and morphology were monitored. Results showed a general decrease in hemocyanin concentration and amebocyte numbers across the temperature range. The decreased amebocyte numbers was accompanied by a shift in amebocyte morphology with increasing temperature. The percentage of hemocyanin with bound dioxygen and the specific activity of phenoloxidase, derived from hemocyanin, changed little during the experiment and these data are corroborated with *in vitro* analysis of purified Hc exposed to similar temperature conditions. The immune-competence of horseshoe crabs appeared to be adversely affected by captivity induced stress and this was exacerbated by higher temperatures.

6.2 Introduction

The Atlantic horseshoe crab *Limulus polyphemus* (Linnaeus, 1758) is one of four extant species of horseshoe crab (HSC) and the only one to inhabit the east coast of the U.S.A. The remaining three species; *Tachypleus tridentatus* (Leach, 1819), *Tachypleus gigas* (Müller, 1785) and *Carcinoscorpius rotundicauda* (Latreille, 1802) inhabit distinct coastal waters of southern Asia (Walls et al., 2002) (Fig. 6.1). For over a century, *L. polyphemus* has been utilised by the fishing industry as bait (for eel and whelk) and by the farming industry as fertiliser for soil (Berkson and Shuster, 1999 and Walls et al., 2002). For example, 165,000 individual HSCs are taken as bait to support the local whelk industry in the state of Massachusetts alone. In addition, biomedical companies harvest HSCs from natural populations and bleed them for the production of LAL. LAL is derived from the proteins stored in the cytoplasmic granules of *L. polyphemus* blood cells, enabling the detection of picogram levels of endotoxins present in biopharmaceuticals. It is estimated that LAL production is worth approximately 50 million dollars worldwide, equating to bleeding and processing ~ 250,000 animals annually. Mortality rates are estimated to be between 10 to 15%, i.e. 20,000 to 37,500 HSCs (Anon, 2013; <http://www.horseshoecrab.org/info/conservation.html>).

HSCs possess a primitive yet highly effective biological defence system; including, the multi-functional protein hemocyanin (Hc) and the granular amebocyte. Hc is a type three copper protein which functions primarily as a carrier of molecular oxygen in arthropods and molluscs. Over the last decade, it has become evident that Hc plays multiple roles in invertebrate immunity (Cerenius et al., 2010 and Coates et al., 2011]). For example, the conversion of Hc from a respiratory protein into an enzyme displaying phenoloxidase (PO) activity in crustaceans, chelicerates and molluscs has been well

documented (Decker and Jaenicke, 2004). Amebocytes comprise approximately 99% of circulating blood cells present in the hemolymph of *L. polyphemus* (Suhr-Jessen et al., 1989). Amebocytes are highly refractile cells containing an abundance of large and small cytoplasmic granules. These granules are released in response to the presence of microbial ligands, especially lipopolysaccharide (LPS) found in the cell wall of pathogens (basis of the LAL test), thus releasing a battery of immune molecules into the surrounding milieu (Iwanaga and Lee, 2005). A primary function of the amebocyte appears to be the exocytosis of immune effectors, however, amebocytes also exhibit phagocytic properties and are involved in hemostasis (Armstrong and Levin, 1979 and Zhu et al., 2005; chapter 4). *L. polyphemus* amebocytes appear to exist in a number of morphological states in culture. Spherical contracted cells are the most viable in culture and this morphological state may represent most closely the state of healthy amebocytes *in vivo* (Chen et al., 1986, Chen et al., 1989 and Hurton et al., 2005).

Exposure of invertebrates to a variety of stressors, including temperature, can have deleterious impacts on health; affecting fecundity, immune competence, metabolite homeostasis and survival (Le Moullac and Haffner, 2000). Recent studies indicate that temperature is an important effector of development in the native habitats of HSCs (Faurby et al., 2010, Lee and Morton, 2009 and Tzafrir-Prag et al., 2010). Temperature is also an important factor in *L. polyphemus* aquaculture (Schreibman and Zarnoch, 2009). Temperature shock (acute increase or decrease) can lead to up-regulation of the immune response in decapods (Truscott and White, 1990), however, prolonged or chronic exposure can lead to a reduction in immune cell numbers, phagocytic ability and alterations in PO activity (Pascual et al., 2003, Paterson and Stewart, 1973 and Vargas-Albores et al., 1998). The aim of this study was to establish the effects of temperature on *L. polyphemus* Hc concentration and function as well as changes in amebocyte numbers and morphology with a view to optimising aquaculture conditions and evaluating captivity induced stress.

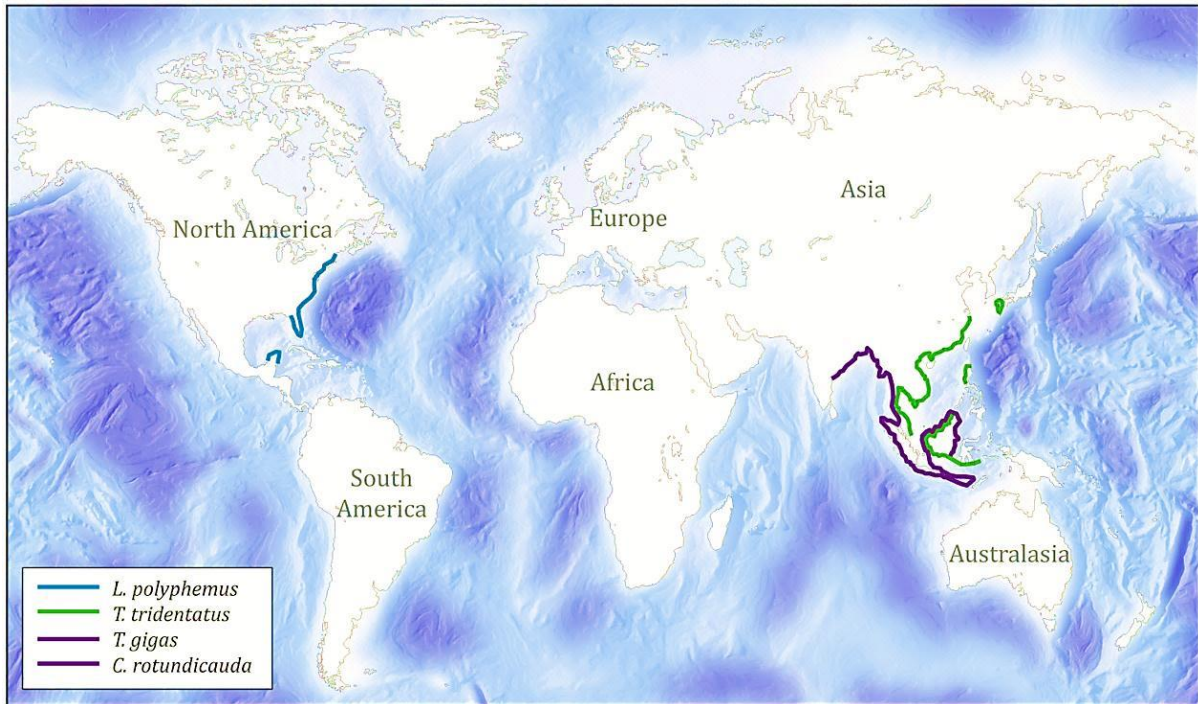


Figure 6.1 Geographical distributions of the four extant species of horseshoe crabs.

6.3 Materials and Methods

All chemicals and reagents used were of the highest quality and purity, purchased from Sigma Aldrich Chemical Company (Dorset, UK) unless otherwise stated.

6.3.1 *L. polyphemus* and culture conditions

Fifty intermolt male horseshoe crabs were used in total. 48 HSCs were used for the temperature trials - 12 per trial; 8 °C, 13 °C, 18 °C and 23 °C (with 3 crabs per temperature acting as controls) (Fig. 6.2). All trial values represent the mean (n = 9, 3 HSCs per replicate) ± standard deviation. The remaining 2 HSCs were used to purify hemocyanin from. HSCs were weighed, tagged (with a Parkside PFBS 9.6 etching drill, using numerical nomenclature) and inspected thoroughly for any signs of external physical damage (Fig. 6.2). HSC hemolymph samples and swabs from the gill flaps were tested for the presence of pathogenic bacteria by incubation on sterile Tryptic Soy Agar-2% NaCl at 20 °C for 48 h. HSCs were housed in closed circulation tanks (at 15 °C) containing prepared sea water (3%-Red Sea salt) at a stocking density of no more than three crabs per 1 m² floor space and fed approximately 2% of their body weight in mussels, 2 to 3 times per week. Approximately 25% to 35% of seawater was exchanged per week, in addition to using internal submerged filter pumps (Fluval U2 and Hailea HL-BT1000) and siphoning of faeces, to maintain water quality. Assessments of salinity, nitrite/nitrate, ammonia/ammonium and pH levels were performed routinely (Tropic Marin, Expert test kit). HSCs were placed in their experimental tanks (3 animals per tank, 200 L) and acclimated to their treatment temperatures over a period of 48 h, with the water temperature increasing/decreasing gradually. HSCs were housed across the temperature range 8 °C to 23 °C for the duration of the experiment (56 days). External water chillers (D-D Refrigerant cooler DC750) and internal heaters (Eheim Jager 3616

(150w) and Hagen Elite (200w)) were placed in their respective tanks in order to maintain the various experimental temperatures.

6.3.2 Bleeding regime

Before extraction of hemolymph, HSCs were weighed and a physical inspection was carried out to note any damage or signs of infection/disease (Fig. 6.2). Experimental HSCs were bled on day 0 and subsequently bled every fortnight for the duration of the experiment. A total of 5 mL of hemolymph was extracted per HSC on each day: 0, 14, 28, 42, 56 and collected into pre-chilled sterile 15 mL falcon tubes. The arthroidal membrane was cleaned with 70% ethanol prior to and post bleeding in order to avoid sepsis. Half of the extracted hemolymph was used for protein analysis and the remaining half was used for cellular analysis. Approximately 20 μ L of hemolymph was retained per HSC (inclusive of controls), on each bleeding occasion, and tested for microbial growth. Control HSCs were cultured under the same conditions as the experimental animals but were bled on day 0 and day 56 only, to determine the effects of the bleeding process.

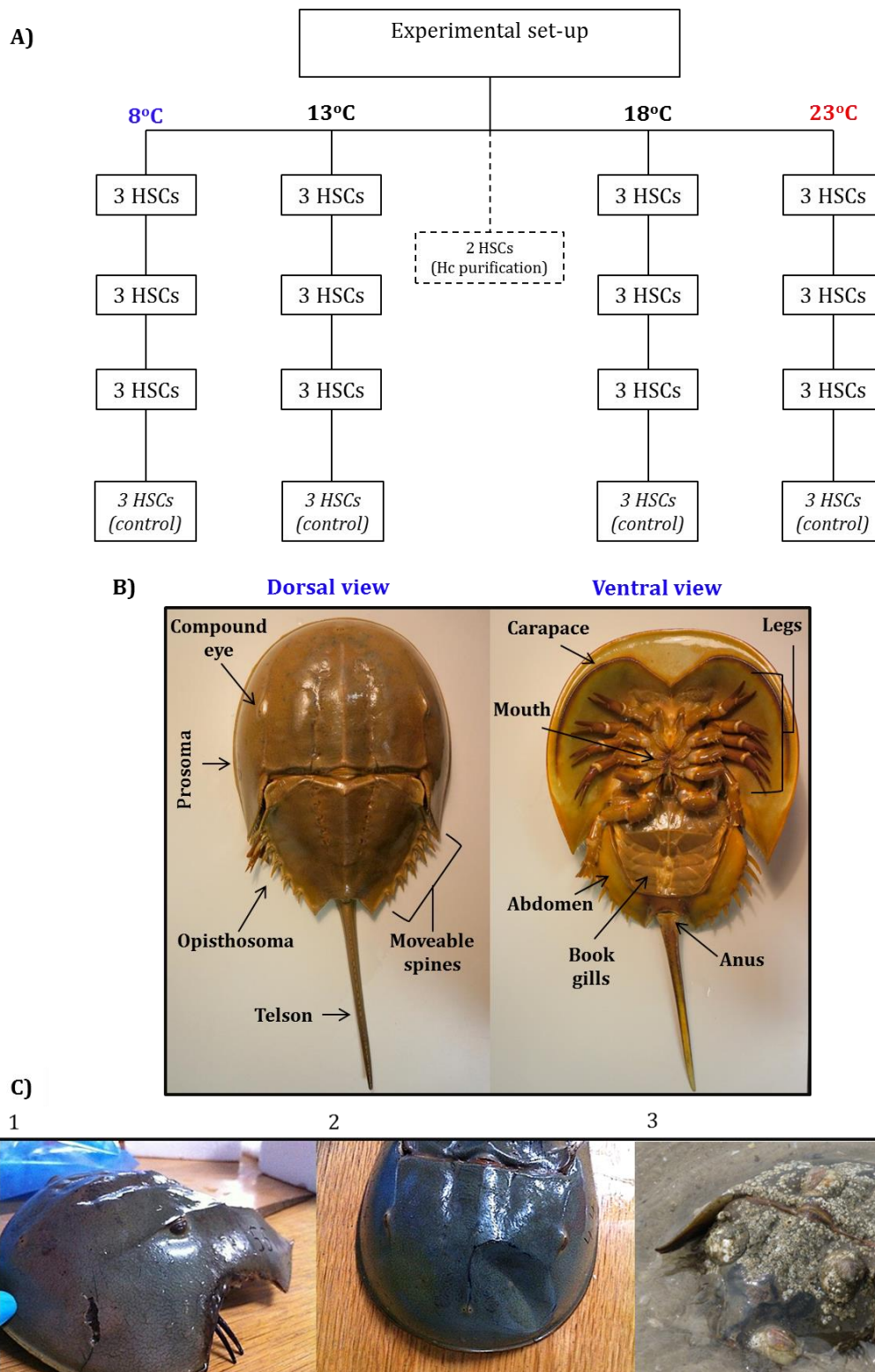


Figure 6.2 **A)** Experimental set-up of horseshoe crabs (50 in total). Each box (containing HSCs) represents an individual tank. **B);** 1) and 2) Anatomy of intermoult-adult female *L. polyphemus*; damage/signs of deterioration of external body segments were monitored throughout the period of research. **C)** *L. polyphemus* specimens with severe fractures (1 and 2) and aggressive colonisation of the carapace by barnacles and other epibionts (3). Image 3 was sourced, and modified, from <http://matthewwills.com/tag/horseshoe-crab/> on 4th August 2012).

6.3.3 Estimation of hemocyanin concentration and the percentage of hemocyanin with dioxygen bound

Half of the extracted hemolymph (2.5 mL) was centrifuged immediately at $500 \times g$ for 5 min at 4 °C; the pellet was discarded and the acellular fraction was decanted and stored on ice until analysis. Cell-free hemolymph was diluted in 100 mM Tris-HCl buffer, pH 7.5 and protein concentration estimates were performed using an Ultrospec 2100 pro spectrophotometer. UV absorbance measurements were taken at 280 nm; using the value of 1.39 for the absorbance of a 1 mg mL^{-1} Hc solution from *L. polyphemus* in a quartz cuvette of 1 cm pathlength. The absorbance at 350 nm (indicative of type 3 copper proteins with dioxygen bound) was used to calculate the percentage of Hc with dioxygen bound, with an absorption coefficient at this wavelength of $20,000 \text{ M}^{-1} \text{ cm}^{-1}$.

6.3.4 Purification of *Limulus polyphemus* hemocyanin

Hemocyanin was purified from *L. polyphemus* hemolymph according to the protocol outlined in 2.3.1 (Coates et al., 2011). Hemolymph was processed from two individual horseshoe crabs housed separately from the trial animals (48 HSCs).

6.3.5 Phenoloxidase assay measurements

Spectrophotometric analysis of hemocyanin-derived phenoloxidase (Hc-d PO) activity was performed at various temperatures, in a 96 well plate (MDS VERSA max microplate reader).

- I. Whole hemolymph Hc-d PO assays were performed at 20°C, in 100 mM Tris-HCl, pH 7.5. Samples were pre-incubated with SDS for 10 min, before assays were initiated by addition of substrate.

- II. Hc purified from *L. polyphemus* was pre-incubated across the temperature range, 5°C – 50°C, for 10 mins, in the presence of SDS. PO assays were performed in 100 mM NaPi, pH 7.5.

Each assay (100 μ L volume) assay consisted of Hc at a concentration of 1 mg mL⁻¹, 2 mM dopamine hydrochloride and 0.1% (3.5 mM) SDS. PO activity was monitored as outlined in section 2.3.4. Values for the auto-oxidation of dopamine into dopachrome were subtracted from the final Hc-d PO values, thus, values presented here represent PO activity attributed to Hc-d PO only. PO assays were performed in triplicate.

6.3.6 Circular dichroism

CD spectra were recorded on a Jasco J-810 spectropolarimeter, previously calibrated with 1S-(+)-10-camphorsulphonic acid. Spectral measurements were carried out in 100 mM NaPi buffer, pH 7.5. In all near and far UV measurements, each spectrum recorded was corrected by the subtraction of a spectrum of buffer alone.

Spectra in the far UV region (180 nm to 260 nm) were recorded in a quartz cylindrical cell of pathlength 0.02 cm at a protein concentration of 0.3 mg mL⁻¹. Hc was pre-incubated for 10 min at each temperature (5°C to 25°C) prior to spectral analysis. In each case, 4 scans were recorded (and averaged) at a scan rate of 50 nm min⁻¹ with a time constant of 0.5 s.

Spectra in the near UV region (250nm to 400 nm) were recorded in a quartz rectangular cell of pathlength 1 cm at a protein concentration of 0.4 mg mL⁻¹. Hc was pre-incubated for 10 min at each temperature (5°C to 25°C) prior to spectral analysis. In each case, 1 scan was recorded at a scan rate of 10 nm min⁻¹ with a time constant of 2 s.

6.3.7 Fluorescence spectroscopy

All experiments were recorded on a Perkin Elmer LS50 spectrofluorimeter. Intrinsic tryptophan fluorescence and histidine fluorescence were recorded using a quartz cuvette of 1 cm pathlength at a protein concentration of 0.1 mg mL⁻¹ in 100 mM NaPi buffer, pH 7.5. The excitation wavelengths used for tryptophan and histidine residues were 290 nm and 330 nm respectively, with a 5 nm bandwidth for the excitation and emission. Hc was incubated at various temperatures (5°C to 25°C) for 10 min prior to measurements. All scans were recorded at a scan rate of 50 nm min⁻¹ and were corrected by subtraction of a spectrum of buffer alone.

6.3.8 Absorption spectroscopy

Absorption spectra of Hc samples were recorded on an Ultrospec 2100 pro UV/Visible spectrophotometer over the range 240 nm to 380 nm. Properties of the di-copper active site of Hc were monitored via the absorption peak at 350 nm (indicative of type three copper enzymes). The effects of various temperatures on the di-copper active site were determined by pre- incubating 0.3 mg mL⁻¹ Hc for 10 min in 100 mM NaPi buffer, pH 7.5, across the temperature range 5°C to 50°C, prior to spectral measurements

6.3.9 Determination of *L. polyphemus* amebocyte numbers and morphology

All glassware and salts were baked for a period no less than 4 h at 180 °C to deter endotoxin contamination. Extracted hemolymph (2.5 mL) was diluted immediately in pre-chilled marine anticoagulant (see section 4.3.5) and supplemented with 2.5% neutral formaldehyde. This method retained the morphological state of amebocytes assumed to be representative of cells *in vivo* (Armstrong, 1979). Amebocytes were stored at 4 °C until analysis. Serial dilutions were carried out in LPS-free saline (3% NaCl, 10 mM NaHCO₃, pH 7.5) and amebocyte concentration was estimated using an

improved Neubauer haemocytometer. Amebocyte morphology was examined using brightfield optics of an Olympus M081 inverted microscope. Amebocyte morphologies were identified using the categories outlined by Hurton et al. (2005) (also described in 5.3.6).

6.3.10 Statistical analysis

Fifty male horseshoe crabs were used in total. It should be noted that between sample day 28 and day 42, 2 mortalities occurred at 23 °C (n = 7, for day 42 and day 56). Phenoloxidase assays, amebocyte number and amebocyte morphology studies were all performed in duplicate. Repeated measure analysis of variance (ANOVA) was utilised for measurements made over time (e.g. Hc concentration and amebocyte numbers). This was followed by Tukey post-hoc tests for multiple comparisons when necessary. Hc concentration, percentage dioxygen bound and granular-spherical amebocyte data sets were transformed using Natural log, Exponential square root and Square root functions, respectively. Unpaired 2-sample t-tests were used to assess differences between trial and control data sets. Statistical analysis was carried out using Minitab analytical software version 16. Differences were considered significant at $p \leq 0.05$.

All PO assays of purified hemocyanin were performed in triplicate on two independent occasions. Values are represented by the mean \pm standard deviation.

6.4 Results

6.4.1 Physical evaluation; mortality and weight

Thorough physical examinations of HSCs were carried out prior to each sampling session, encompassing: the carapace (prosoma, opisthosoma and telson), the gills (including gill flaps) and appendages (Fig. 6.2). No signs of parasites and/or epibionts were found. All HSC hemolymph and gill flap swabs were devoid of detectable microbial growth. Cosmetic damages noted on day 0 were monitored throughout the experiment and were found to remain unchanged.

Hemolymph clotting was observed in the gills of two individuals on sample day 28; HSC 46 and HSC 48 (23 °C). HSC 46 subsequently died before day 42 sampling, however, HSC 48 appeared to recover and had no noticeable ailments for the remainder of the experiment. A second HSC (23 °C) died between sampling days 28 and 42, however, all previous physical examinations of this organism showed no signs of damage and/or infection. In total, two mortalities were recorded over the 56-day period, both occurring at 23 °C. No deaths and/or signs of physical damage were recorded in the control HSCs.

Overall, a subtle decrease in HSC body weight was recorded over the 56-day period (Fig. 6.3), with HSCs housed at 23 °C suffering the largest decrease, - 8.2%. Repeated measure analysis of variance revealed time to have a significant effect, whereas temperature did not (Time; $F_{(4,124)} = 62.81$, $p < 0.001$, Temp; $F_{(3,32)} = 0.28$, $p = 0.84$, Temp*Time; $F_{(12,124)} = 2.76$, $p = 0.002$). Control HSC mean body weight demonstrated almost identical trends to experimental HSCs.

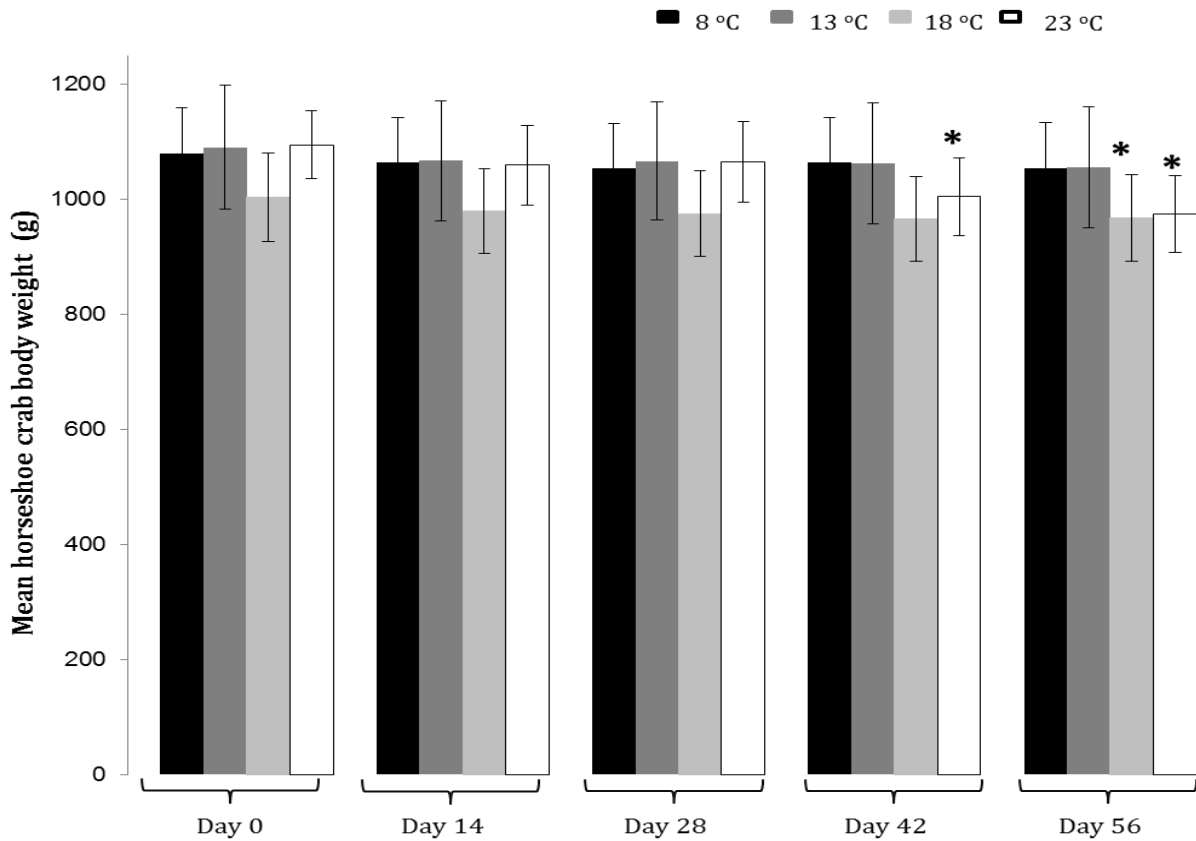


Figure 6.3 Effect of temperature on mean body weight of captive horseshoe crabs. **A)** Average horseshoe crab weights (g) are represented by the mean \pm standard deviation for different temperatures (8 °C, 13 °C, 18 °C, 23 °C) over a trial period of 56 days with hemolymph extractions on days 0, 14, 28, 42 and 56. Significant ($p \leq 0.05$) time effect compared to day 0 weights are indicated by * ($n = 9$ per trial; total 36).

6.4.2 Quantitative analysis of hemocyanin across the temperature range 8°C to 23°C

Hc concentration decreased continually across the temperature range for the duration of the experiment (Fig. 6.4). Temperature and time were both found to have a significant effect on Hc concentration (Temp; $F_{(3,32)} = 88.95$, $p < 0.001$, Time; $F_{(4,124)} = 106.09$, $p < 0.001$, Temp*Time; $F_{(12,124)} = 13.33$, $p < 0.001$). Tukey post hoc analysis revealed significant differences between the lower experimental temperatures, 8 °C and 13 °C and the higher temperatures, 18°C and 23°C, at day 56 (Fig. 6.4). Over the duration of the experiment, the largest decreases in Hc concentration, with a decrease of 43.9% and 69.3%, occurred at 18 °C and 23 °C, respectively (Table 6.1). Hc concentrations recorded for the control HSCs decreased throughout the experimental period, in all temperature treatments, with no significant differences detected between trial and control data (Table 6.1), indicating that additional hemolymph extractions had no measureable effect on Hc concentrations.

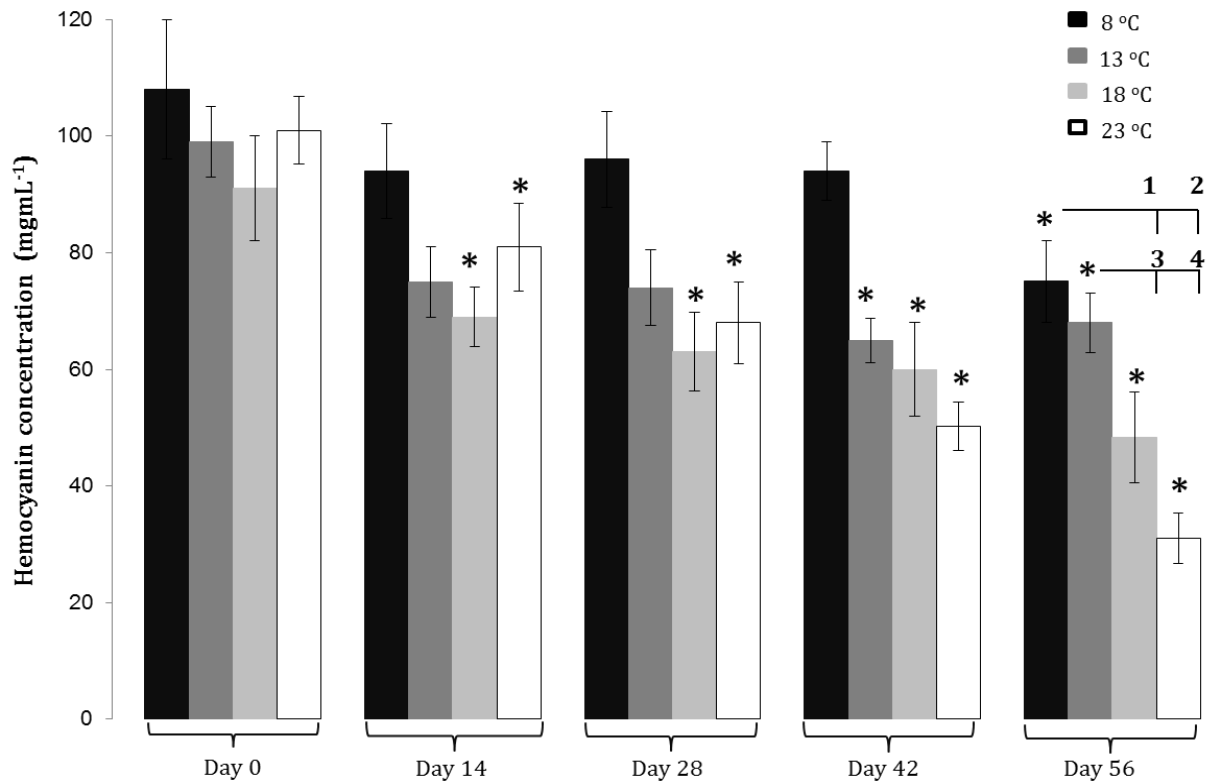


Figure 6.4 Effect of temperature on hemocyanin concentrations (mg mL^{-1}) present in the hemolymph of *L. polyphemus*. The concentration of hemocyanin from horseshoe crabs maintained across the temperature range 8°C to 23°C for a period of 56 days was deduced from UV absorbance measurements at 280 nm following dilution of hemolymph into 100 mM Tris-HCl buffer, pH 7.5. Values represent the mean \pm standard deviation. A significant decrease in Hc concentration compared to sample day 0 (at $p \leq 0.05$) is indicated by * ($n = 9$ per trial; total 36). Tukey post hoc comparisons are represented by 1 (8°C and 18°C), 2 (8°C and 23°C), 3 (13°C and 18°C) and 4 (13°C and 23°C) are significant, $p < 0.001$.

Table 6.1 Biochemical, immunological and cellular measurements of control and trial horseshoe crabs. Hemocyanin concentration, Hc-d PO activity and amebocyte numbers were determined as outlined in section 6.3.

Temperature	Experimental	Day 0	Day 56	Decrease (%)	Trial vs. control
<i>Hemocyanin (mg mL⁻¹)</i>					
8 °C	Trial	108 ± 14.2	71 ± 4.2	34.3	<i>p</i> = 0.239
	Control	135 ± 27	90 ± 14.9	33.3	
13 °C	Trial	99 ± 7.1	68 ± 5.9	31.3	<i>p</i> = 0.787
	Control	95 ± 5.8	69 ± 10	27.4	
18 °C	Trial	91 ± 10.9	51 ± 9.2	43.9	<i>p</i> = 0.488
	Control	80 ± 13.7	41 ± 10	48.8	
23 °C	Trial	101 ± 6.6	31 ± 4.5	69.3	<i>p</i> = 0.396
	Control	80 ± 24	28 ± 4.1	65	
<i>Hc-d PO activity (μmol min⁻¹)</i>					
8 °C	Trial	4 ± 1	2.6 ± 0.52	35	<i>p</i> = 0.286
	Control	2.5 ± 0.34	1.6 ± 0.35	36	
13 °C	Trial	3.4 ± 0.9	2.6 ± 0.52	23.5	<i>p</i> = 0.278
	Control	2.6 ± 0.52	1.9 ± 0.17	26.9	
18 °C	Trial	4.4 ± 1	2.4 ± 0.35	45.5	<i>p</i> = 0.967
	Control	2.6 ± 0.17	1.4 ± 0.35	46.2	
23 °C	Trial	5 ± 0.69	2.1 ± 0.28	58	<i>p</i> = 0.968
	Control	2.5 ± 0.69	1.1 ± 0.28	56	
<i>Amebocytes (× 10⁷ mL⁻¹)</i>					
8 °C	Trial	3.5 ± 0.69	2.4 ± 0.51	31.4	<i>p</i> = 0.963
	Control	3.7 ± 1.7	2.4 ± 0.9	35.1	
13 °C	Trial	3.8 ± 0.86	2.5 ± 0.76	34.2	<i>p</i> = 0.058
	Control	2.6 ± 0.35	1.6 ± 0.35	34.6	
18 °C	Trial	3.3 ± 1.4	1.7 ± 0.35	48.5	<i>p</i> = 0.242
	Control	3.8 ± 0.52	1.8 ± 0.35	52.6	
23 °C	Trial	4.6 ± 1.8	1.3 ± 0.28	71.7	<i>p</i> = 0.507
	Control	2.9 ± 0.17	1 ± 0.14	65.5	

All values are expressed as the mean ± standard deviation. 2 sample t-tests were carried out on trial and control data sets. No significant differences were detected as *p* > 0.05 in all cases (n = 48).

6.4.3 Hemocyanin with dioxygen bound and inducible phenoloxidase activity

The proportion of Hc with dioxygen bound and the level of Hc-d PO activity were used to infer the functionality of Hc present in HSC hemolymph. With the exception of day 14 samples, the percentage of Hc with dioxygen bound appeared to be > 90% across the temperature range (Fig. 6.5). Overall, temperature did not have an effect ($F_{(3,32)} = 2.68, p = 0.063$) on the percentage of dioxygen bound. Analysis revealed a marginal significant difference between sample day 14 and day 28 at 8 °C ($p = 0.046$) (Fig. 6.5).

Hc-d PO assays were standardised (activity determined per mg protein) in order to infer the immune functionality of Hc. Overall, temperature and time appeared to have a significant effect on Hc-d PO activity ($F_{(3,32)} = 294, p = 0.036, F_{(4,124)} = 24.19, p < 0.001$, respectively) (Fig. 6.6). HSCs incubated at 8 °C and 13 °C demonstrated a small decrease in Hc-d PO activity over time (Fig. 6.6), however, no significant differences were detected between day 0 and day 56 measurements for the 8 °C or 13 °C treatments ($p = 0.126, p = 0.962$, respectively). Conversely, a more pronounced decrease was observed for HSCs at 18 °C and 23 °C (Fig. 6.6), with significant differences detected between day 0 and day 56 measurements ($p = 0.002, p < 0.001$, respectively). The most dramatic decrease in Hc-d PO activity measurements occurred at day 14 (across the entire temperature range), this coincides with the decrease in percentage of Hc with dioxygen bound noted at day 14 (Fig. 6.5). As Hc-d PO activity is an oxygen dependent reaction, a significant reduction in the percentage of Hc with dioxygen bound could affect Hc-d PO activity.

Control samples demonstrated similar trends to experimental samples, inferring that neither the percentage of Hc with dioxygen bound or Hc-d PO activity was affected by additional hemolymph extractions (Table 6.1).

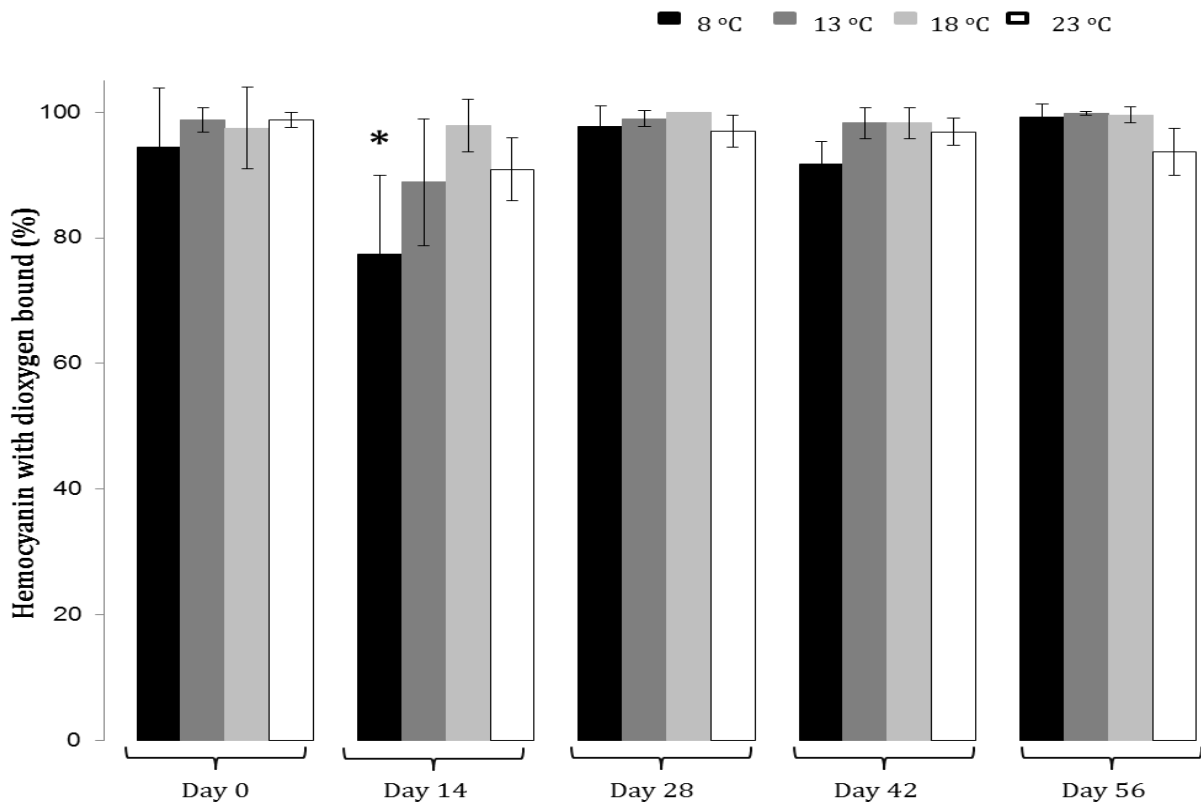


Figure 6.5 Effect of temperature on the percentage of *L. polyphemus* hemocyanin with dioxygen bound. The percentage of hemocyanin with dioxygen bound in the di-copper centre [CuII-O₂²⁻-CuII] was determined using the characteristic absorption peak at 350 nm. **A)** Percentage hemocyanin with dioxygen bound from horseshoe crabs maintained at four different temperatures (8°C, 13°C, 18°C, 23°C) over a trial period of 56 days, with hemolymph extractions on days 0, 14, 28, 42 and 56. **B)** Percentage hemocyanin with dioxygen bound from horseshoe crab control specimens with hemolymph extraction on days 0 and 56 only. Trial and control values represent the mean ± standard deviation. Significant ($p \leq 0.05$) time effect compared to day 0 data are indicated by * ($n = 9$ per trial; total 36).

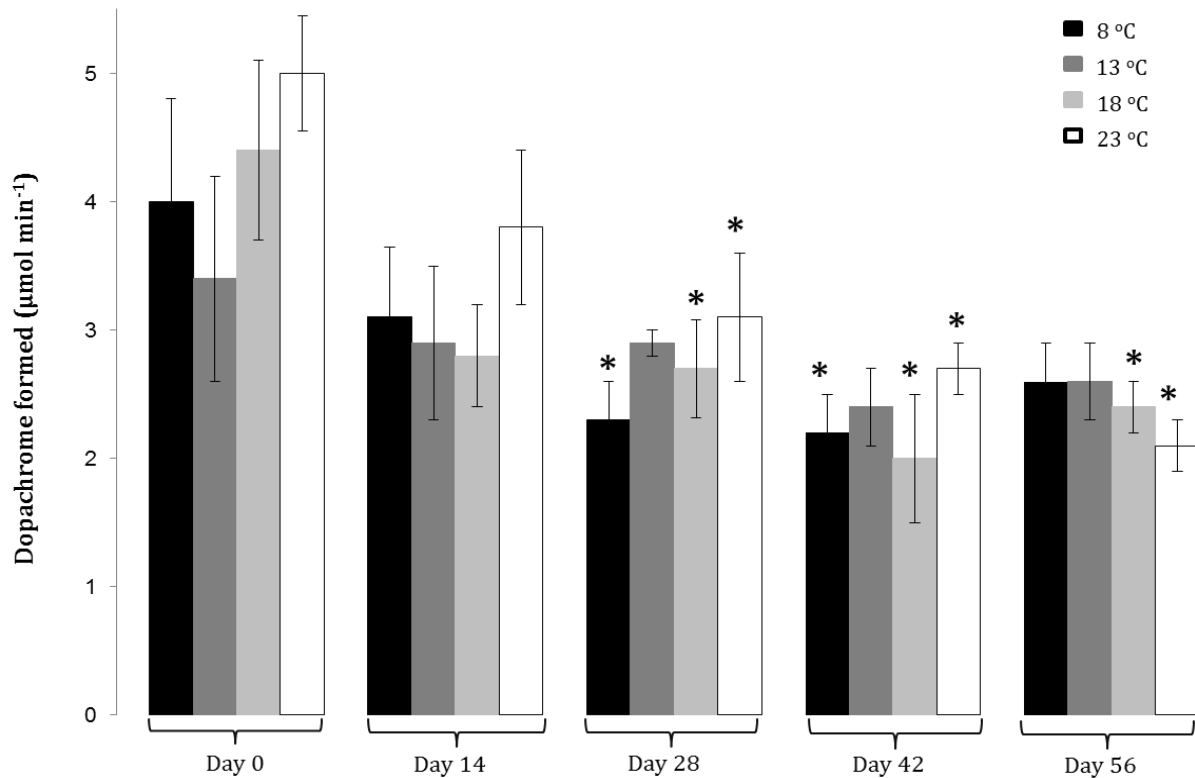


Figure 6.6 Effect of temperature on hemocyanin-derived phenoloxidase activity. Hemocyanin derived phenoloxidase activity from horseshoe crab hemolymph was assessed from crabs maintained across the temperature range 8°C to 23°C. Cell free hemolymph samples were diluted in 100 mM Tris-HCl buffer, pH 7.5 and subsequently incubated with SDS for 10 min prior to spectral readings. The assay was initiated with the addition of substrate. Assays were recorded over a 10 min period. The increase in absorbance at 475 nm is indicative of the formation of dopachrome and its derivatives. Values are represented by the mean \pm standard deviation. Significant ($p \leq 0.05$) time effect compared to day 0 data are indicated by * ($n = 9$ per trial; total 36).

6.4.4 Alterations in amebocyte number and morphology across the temperature range 8°C to 23°C

The number of immune cells in the hemolymph of invertebrates has been used as an indicator of immune status, particularly in insect systems, with a decrease in the cell numbers indicating an unhealthy/stressed organism (Bergin et al., 2003 and Le Moullac and Haffner, 2000). Amebocyte numbers decreased across all temperatures over the experimental period (Fig. 6.7), with the most pronounced decrease of 71.7% occurring at 23 °C (Table 6.1). Overall, both temperature and time were found to have a significant effect on amebocyte number ($F_{(3,32)} = 3.36$, $p = 0.021$, $F_{(4,124)} = 28.71$, $p < 0.001$). Control HSC amebocyte concentrations demonstrated a similar trend to trial HSCs (Table 6.1) with no significant differences found, indicating that additional hemolymph extractions did not influence amebocyte numbers.

It has been observed previously that invertebrate immune cells suffer a loss of functionality caused by prolonged exposure to various environmental stresses (Le Moullac and Haffner, 2000). HSC amebocytes, *in vitro*, demonstrate three distinct morphological states, granular-spherical (GS), granular flattened (GF) and degranulated dendritic-like (D-L) (Fig. 6.8) (Armstrong, 1979 and Hurton et al., 2005). There is evidence to suggest that amebocytes take on these different morphological states *in vivo* (Armstrong, 1979). Temperature and time were both found to affect GS cell numbers (Temp; $F_{(3,32)} = 4.41$, $p = 0.006$, Time; $F_{(4,124)} = 42.91$, $p < 0.001$, Temp*Time; $F_{(12,124)} = 1.86$, $p < 0.045$). The largest decrease in GS cell levels of 54.9% was recorded at 23 °C (Fig. 6.8A). GS cell representation decreased 24.6%, 29.6%, 51.4% and 54.9% at 8 °C, 13 °C, 18 °C and 23 °C, respectively. The proportion of GS amebocytes from HSCs incubated at the lower temperatures, 8 °C and 13 °C, recovered at day 56, whereas the population

of GS amebocytes at 23 °C decreased constantly over time (Fig. 6.8A). As GS levels decreased, GF levels increased by 47.1%, 72.4%, 90.6% and 110.3% at 8 °C, 13 °C, 18 °C and 23 °C, respectively. An increase in the proportion of amebocytes exhibiting D-L morphology was observed at the higher temperatures (18 °C and 23 °C) between days 28 and 56 (Fig. 6.8A). Overall, temperature and time were shown to have a significant effect on D-L cell levels (Temp; $F_{(3,32)} = 7.55$, $p < 0.001$, Time; $F_{(4,124)} = 3.97$, $p = 0.005$, Temp *Time; $F_{(12,124)} = 4.13$, $p < 0.001$). Tukey post hoc analysis revealed that changes in D-L cell numbers were only significant at day 28 and day 56 for HSCs at 23 °C ($p = 0.0448$, $p = 0.0017$, respectively), in comparison to day 0 D-L cell levels. Control samples demonstrated a similar decreasing trend in the proportion of amebocytes with GS morphology coupled with a concomitant increase in GF cell abundance (Fig. 6.8B). Moreover, no differences in the morphological state of the amebocytes (GS, GF and D-L) were detected between trial and control sample sets, suggesting that additional hemolymph extractions in trial experiments had no detectable effects on amebocyte function.

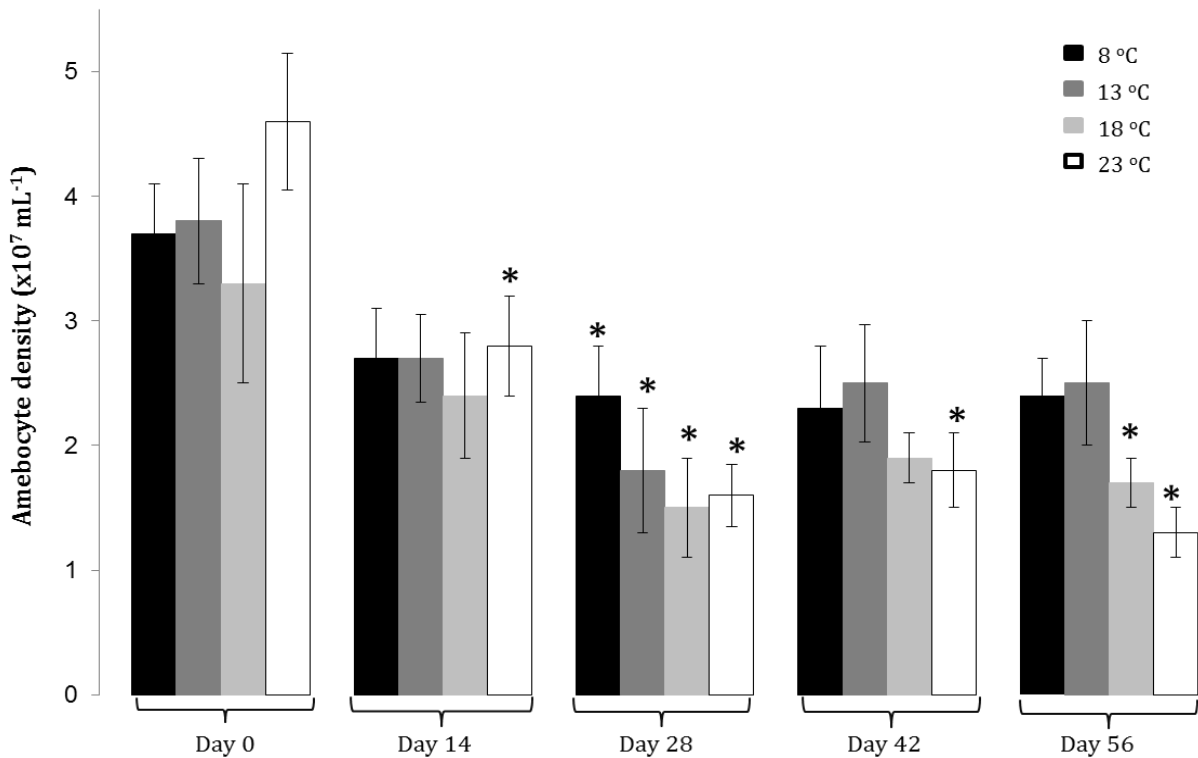


Figure 6.7 Effect of temperature on the numbers of amebocytes from *L. polyphemus* hemolymph. Amebocyte numbers present in hemolymph from horseshoe crabs housed at four different temperatures (8°C, 13°C, 18°C, 23°C) over a trial period of 56 days with hemolymph extractions on days 0, 14, 28, 42 and 56. Values represent the mean \pm standard deviation. Significant ($p \leq 0.05$) time effect compared to day 0 data are indicated by *(n = 9 per trial; total 36).

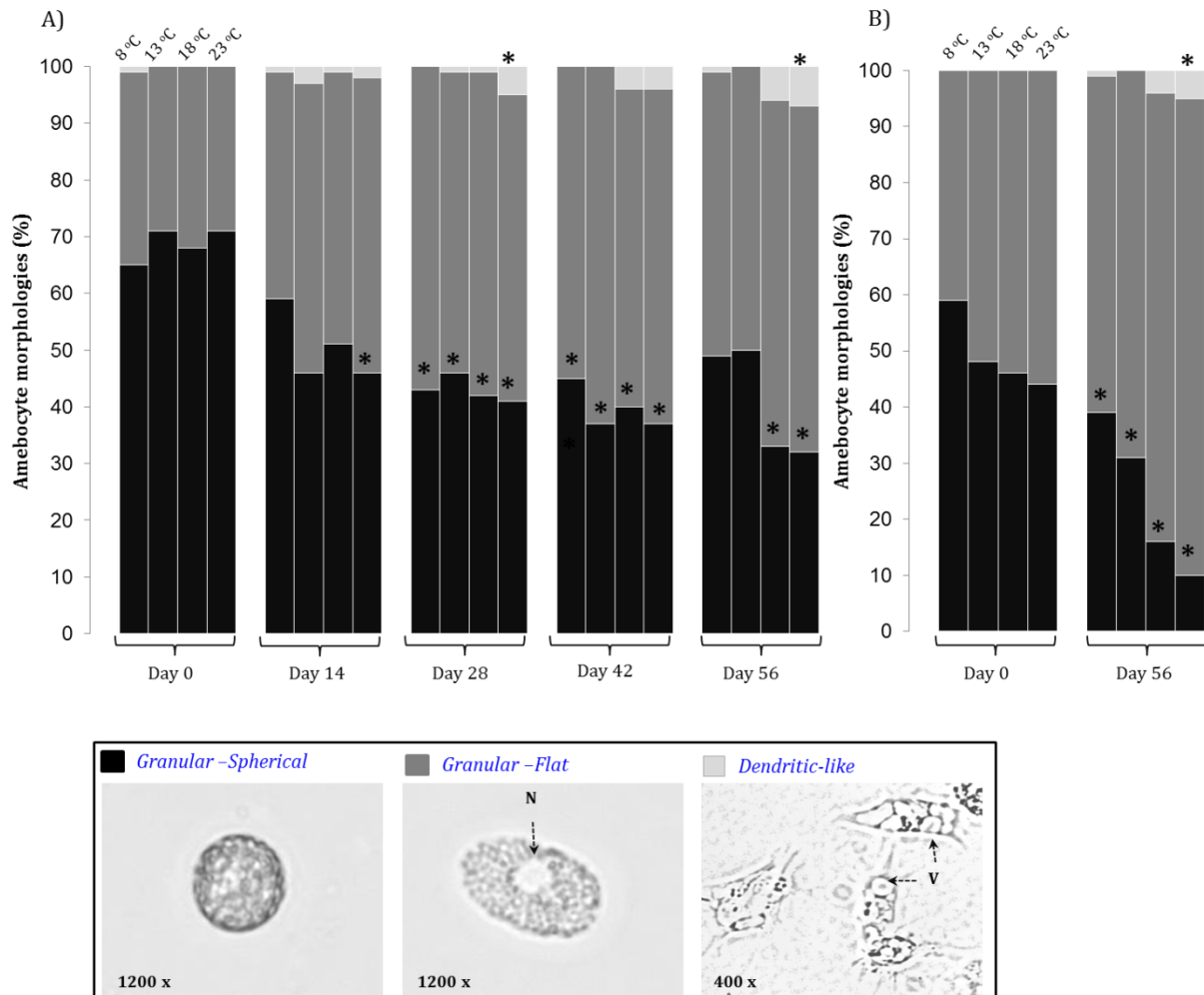


Figure 6.8 Effect of temperature on the morphological status of amebocytes present in *L. polyphemus* hemolymph. **A)** Morphology of amebocytes present in the hemolymph of horseshoe crabs housed at four different temperatures (8 °C, 13 °C, 18 °C, 23 °C) over a trial period of 56 days with hemolymph extractions on days 0, 14, 28, 42 and 56. **B)** Morphology of amebocytes present in the hemolymph of horseshoe crabs housed at four different temperatures (8 °C, 13 °C, 18 °C, 23 °C) over a trial period of 56 days with hemolymph extraction on days 0 and 56 only. Cell morphologies are categorised as (GS) granular spherical cells which are highly retractile, with no visible nucleus (N); (GF) granular flattened cells which lack refractility but have a visible nucleus (N); (DL) dendritic-like cells which appear de-granulated with large vacuoles (V) in the cytoplasm and pseudopodia like projections. Each value is represented by the mean percentage. Significant ($p \leq 0.05$) time effect compared to day 0 data are indicated by * ($n = 9$ per trial and $n = 3$ per control; total 48).

6.4.5 Influence of increasing temperature on inducible phenoloxidase activity of purified hemocyanin

Exposure of Hc to increasing temperatures failed to elicit PO activity in the absence of the exogenous activator SDS (data not shown). In the presence of micellar forms of SDS, PO activity of Hc was detected (Fig. 6.9), with an increase in catalytic activity of Hc concomitant with increasing temperature (8°C to 40°C). For every 10°C increase in temperature, there was an approximate doubling of enzyme activity observed.

6.4.6 Effect of increasing temperature on the secondary structure of purified hemocyanin

Far UV spectra (Fig. 6.10) indicate that temperatures up to 25°C failed to induce any measureable changes in Hc conformation (in the absence of SDS). Analysis of the Hc secondary structural content over the wavelength range (195 nm to 240 nm) using DICHROWEB, suggested that increasing temperature had no detectable effect on Hc (Table 6.2).

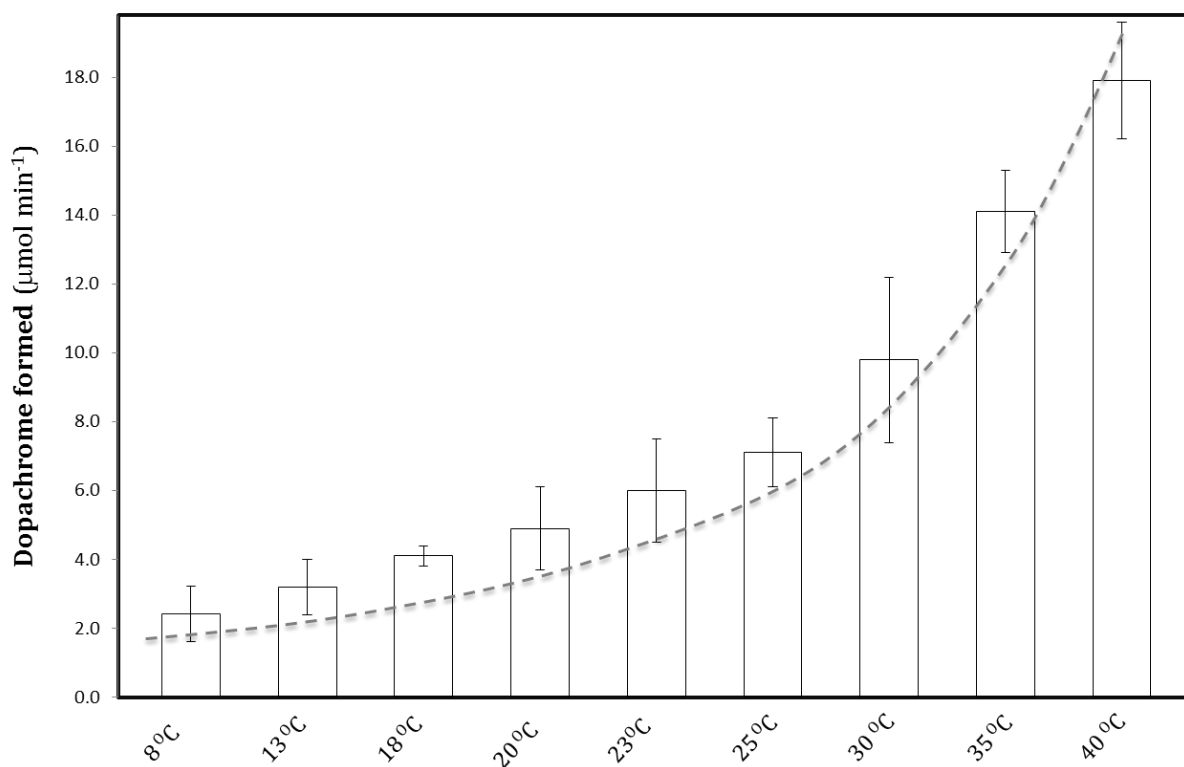


Figure 6.9 Phenoloxidase activity of hemocyanin from *Limulus polyphemus* upon exposure to increasing temperatures. Hemocyanin (1 mg mL⁻¹) in the presence of 3.5 mM SDS was pre-incubated for 10 min across the temperature range, 8°C to 40°C. Assays were carried out in 100 mM sodium phosphate, pH 7.5 and initiated with the addition of substrate (dopamine, 2 mM). The histogram illustrates an increase in absorbance at 475 nm resulting from the formation of dopachrome and its derivatives. Values for the auto-oxidation of dopamine into dopachrome in the absence of hemocyanin were deducted; therefore, data presented here represents phenoloxidase activity derived from hemocyanin only. Values are represented by the mean \pm standard deviation.

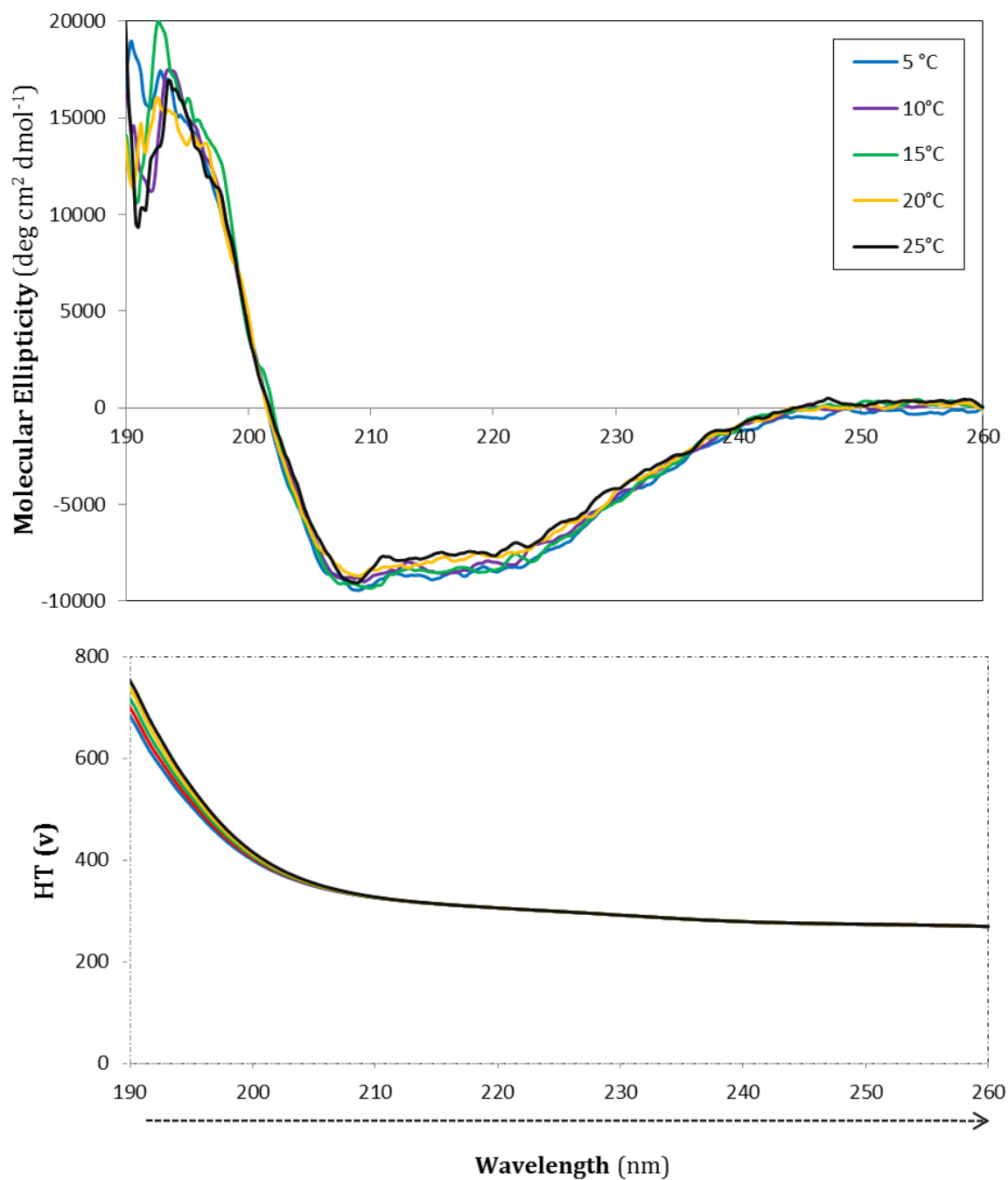


Figure 6.10 Far-UV CD spectra of 0.3 mg mL⁻¹ *Limulus polyphemus* hemocyanin across the temperature range 5 °C to 25°C. Hemocyanin in 100 mM sodium phosphate buffer, pH 7.5, was incubated at each temperature for 10 min prior to the spectral analysis.

Table 6.2 Percentage change in secondary structural content of *L. polyphemus* hemocyanin across the temperature range, 5°C to 25°C

Hemocyanin	Temperature	Experimental conditions*	Helix (%)	Sheet (%)	Turns (%)	Unordered (%)
0.3 mg mL ⁻¹	5°C	10 min	27.01	25.06	19.45	28.46
0.3 mg mL ⁻¹	10°C	10 min	24.68	24.13	21.03	30.13
0.3 mg mL ⁻¹	15°C	10 min	29.08	21.63	21.48	27.78
0.3 mg mL ⁻¹	20°C	10 min	24.52	26.17	20.67	28.62
0.3 mg mL ⁻¹	25°C	10 min	22.33	26.63	19.99	31.43

Secondary structures predictions were conducted using DICHROWEB, using CONTIN and reference set 4. * indicates the amount of time hemocyanin was incubated at each temperature before the spectra were recorded.

6.4.7 Effect of temperature on hemocyanin tertiary structure

Intrinsic tryptophan fluorescence (Fig. 6.11) and near-UV CD (Fig. 6.12) measurements suggest that increasing temperatures have little effect on the tertiary structural integrity of *L. polyphemus* Hc. A minor increase in the fluorescence emission maxima of Hc with increasing temperatures was observed (Fig. 6.11A), however, temperature appeared to have a similar effect on the model compound N-acetyl-L-tryptophan (Fig. 6.11B). This suggests that changes in Hc fluorescence are potentially due to the subtle effect of temperature on exposed tryptophan side chains and not due to a conformational change of the enzyme.

Near UV CD spectra (Fig. 6.12) indicate that temperatures up to 20°C have little effect on Hc structure. A reduction of approximately $19^\circ \text{ cm}^{-1} \text{ dmol}^{-1}$ at the 340 nm absorption band is observed as temperature is increased from 20°C to 25°C. A reduction in the near UV spectrum at $\sim 340 \text{ nm}$ has been previously associated with a conformational change and subsequent induction of PO activity in Hc (Baird et al., 2007; Chapter 2, Fig 2.7). Moreover, Hc did not display any detectable PO activity across the temperature range in the absence of SDS (data not shown). It has been demonstrated previously that removal of copper atoms from Hc or preparation of deoxygenated Hc, displays near UV and absorption spectra absent an absorption peak at 340 nm (Erker et al., 2004).

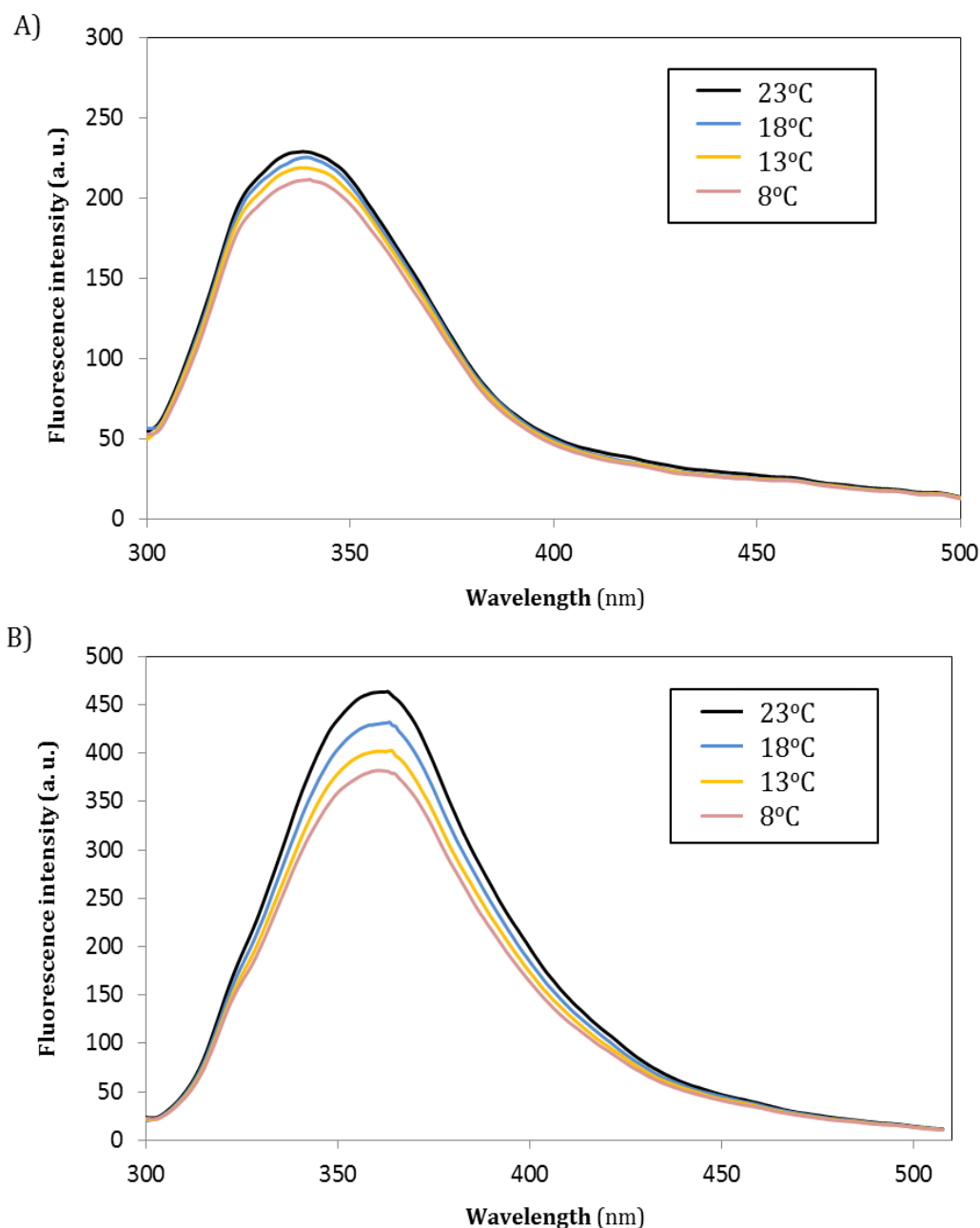


Figure 6.11 Effect of temperature on the tertiary structure of *Limulus polyphemus* hemocyanin. **A)** Fluorescence emission spectra of 0.1 mg mL⁻¹ *L. polyphemus* hemocyanin across the temperature range 5°C to 25°C. Hemocyanin was pre-incubated for 10 min at each temperature prior to spectral readings. Experiments were conducted in 100mM sodium phosphate buffer, pH 7.5. Samples were excited at 290 nm (tryptophan residues) and the subsequent fluorescent spectrum was recorded. **B)** Fluorescence emission spectrum of 2 μM N-acetyl-L-tryptophan, in 100mM sodium phosphate buffer, pH 7.5 across the temperature range 5°C to 25°C.

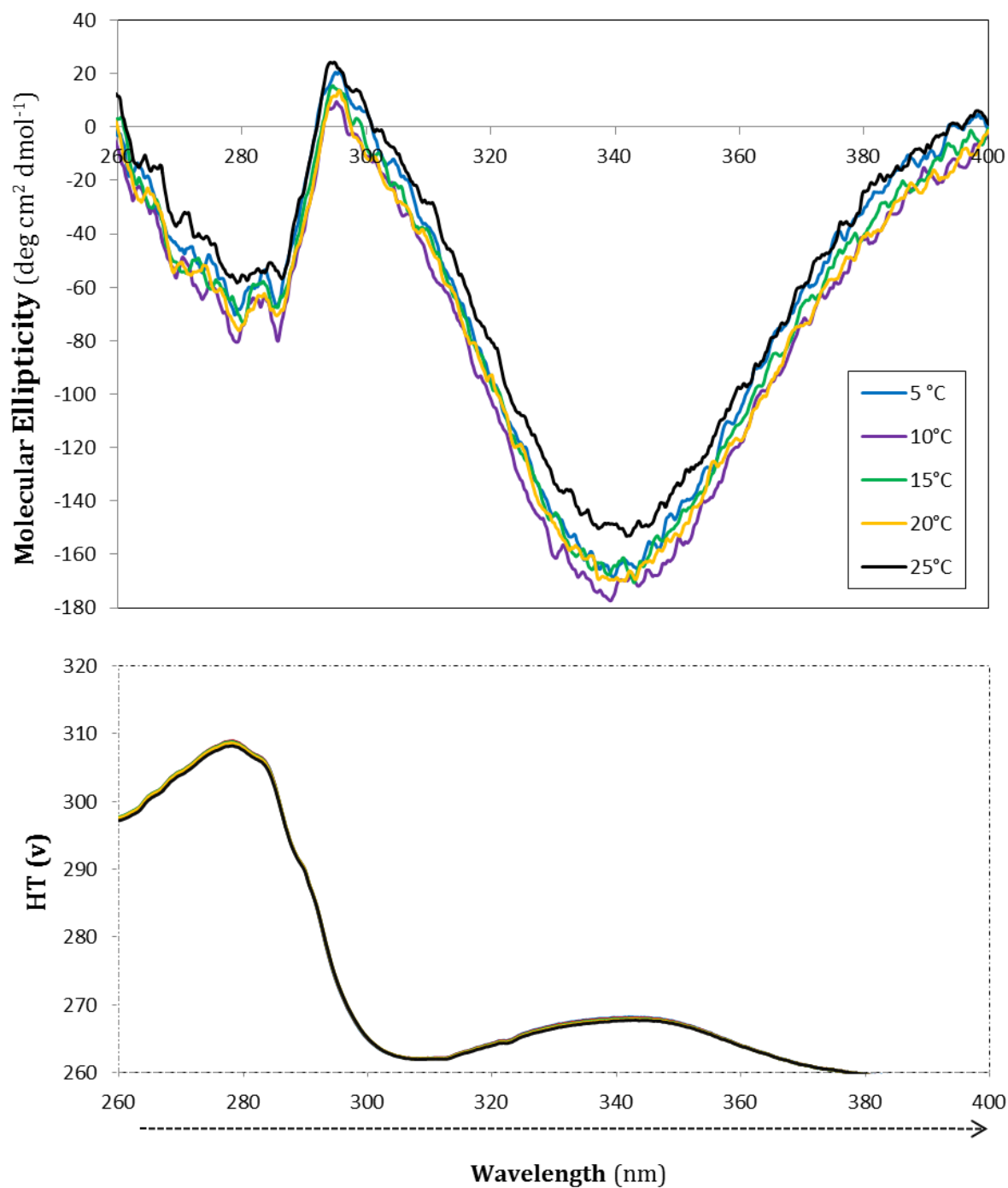


Figure 6.12 Near-UV CD spectra of 0.4 mg mL⁻¹ *Limulus polyphemus* hemocyanin across the temperature range 5 °C to 25°C. Hemocyanin in 100mM sodium phosphate buffer, pH 7.5, was incubated at each temperature for 5 min prior to the spectral analysis.

6.4.8 Effect of temperature on the dicopper active site

The dicopper active sites of type three copper proteins such as Hc and PO possess a characteristic absorption peak at ~ 340 nm ($\epsilon \sim 20,000\text{M}^{-1}\text{cm}^{-1}$) which is also observed in the near UV CD spectrum (Decker et al., 2001). Increasing temperatures up to 50°C had little effect on the absorption band that occurs at ~ 340 nm (Table 7.3). A small reduction of - 9 % in absorption peak intensity between 340 nm and 350 nm was observed.

In addition to the characteristic fluorescence emission peak observed between 340 nm and 350 nm due to aromatic residues, type three copper proteins also exhibit a characteristic fluorescence emission peak between 415 nm to 430 nm caused by the presence of six highly conserved histidine residues that coordinate the copper atoms in the active site. Increasing temperatures up to 25°C did not result in any detectable change in the environment of the dicopper active site (Fig. 6.13). The subtle changes at ~ 340 nm in the absorption spectra and fluorescence intensity at ~ 430 nm suggests that the arrangement around the Cu(II) ions are not altered by increasing temperatures.

Table 6.3 Absorbance peak values for *Limulus polyphemus* hemocyanin across the temperature range 5°C to 50°C

Temperature	Absorbance readings	
	At 280 nm	At 340 nm
5 °C	0.446	0.113
8 °C	0.447	0.113
13 °C	0.445	0.112
18 °C	0.444	0.112
20 °C	0.445	0.11
23 °C	0.446	0.109
25 °C	0.447	0.105
30 °C	0.447	0.103
35 °C	0.446	0.102
40 °C	0.446	0.1
45 °C	0.445	0.099
50 °C	0.445	0.099
Decrease		-12 %

Hemocyanin (0.3 mg mL^{-1}) was pre-incubated for 10 min at each temperature across the range 5°C to 50°C. Values at 280 nm (total protein content) and at 340 nm (copper centre with dioxygen bound) were monitored on the subsequent spectra.

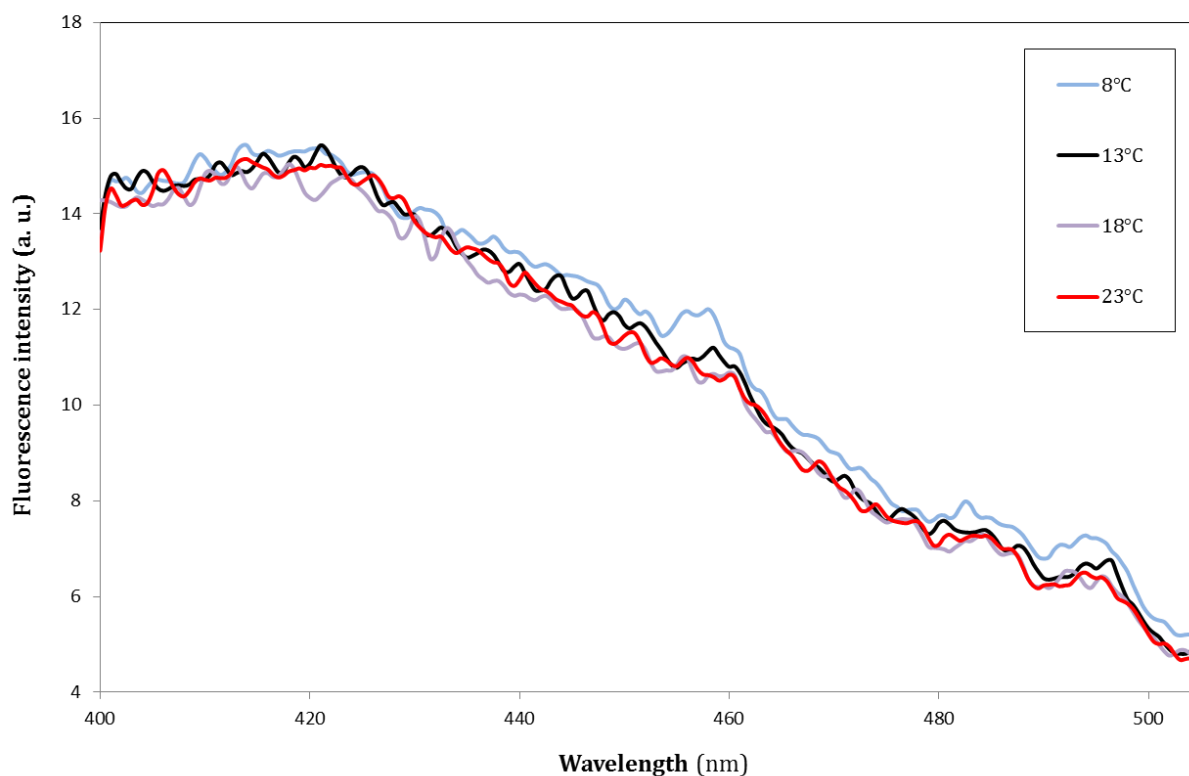


Figure 6.13 Fluorescence emission spectra of 0.1 mg mL^{-1} *Limulus polyphemus* hemocyanin across the temperature range 8°C to 23°C . Hemocyanin was pre-incubated for 10 min at each temperature prior to spectral readings. Experiments were conducted in 100 mM sodium phosphate buffer, pH 7.5. Samples were excited at 330 nm (histidine residues) and the subsequent fluorescent spectrum was recorded.

6.5 Discussion

6.5.1 Health status

Fluctuations in environmental parameters such as temperature, salinity and pH can influence the health status of invertebrates, an effect noted recently in a number of crustaceans (Matozzo et al., 2011 and Mydlarz et al., 2006). In the present study, physiological, cellular, biochemical and immunological indicators are used for the first time in combination to assess the effects of housing the chelicerate *L. polyphemus* at varying temperatures. Exposure of HSCs to increasing temperatures (8 °C, 13 °C, 18 °C and 23 °C) led to an overall decrease in Hc concentration, amebocyte concentration and a change in cell morphology ratios (Fig. 6.4, Fig. 6.7 and Fig. 6.8). Temperature did not appear to affect the viability (95.8%) of the HSCs, indicating that the highest temperatures used were sub-lethal. It should be noted that two mortalities occurred at 23 °C in the trial samples, however, no mortalities were recorded in the control samples. These results are not entirely unexpected given that HSCs have been reported living in native habitats which span the temperature range – 5 °C to 35 °C (Smith and Berkson, 2005). HSCs housed at 23 °C suffered the greatest loss in body weight (– 8.2%). Loss of body weight in crustaceans can be modulated via an influx of water in order to maintain tissue and cellular integrity (Hu et al., 2011). HSCs in this study (in which approximately 0.5% of body weight was collected at each bleeding) could use this mechanism to compensate for the volume of hemolymph extracted throughout the experiment. These observations are in good agreement with results obtained by Novitsky (1984), in which a return to pre-extraction levels of hemolymph was observed within 3–7 days post removal.

6.5.2 Effect of increasing temperature on hemocyanin concentration and functionality

The protein concentration of the hemolymph of invertebrates is routinely used as an indicator of health in crustaceans (Le Moullac and Haffner, 2000). In many invertebrates, Hc is the most abundant protein present in the hemolymph. In the case of *L. polyphemus*, Hc accounts for > 90% of the total hemolymph protein content (Ding et al., 2005), therefore, the protein concentration estimates presented here provide a good measure of the Hc concentration. Aside from its primary function as a respiratory protein, Hcs have demonstrated multiple roles associated with physiological and homeostatic processes in invertebrates, such as, moulting (Adachi et al., 2005a and Adachi et al., 2005b), hormone transport (Jaenicke et al., 1999), protein storage and osmoregulation (Paul and Pirow, 1998). Furthermore, over the last decade it has become evident that Hc plays a role in innate immune defence: conversion of Hc to a PO activity (Decker and Jaenicke, 2004), anti-microbial peptides (AMPs) resulting from proteolytic processing of Hc (Destoumieux-Garzón et al., 2001 and Lee et al., 2003), production of reactive oxygen species (ROS) (Jiang et al., 2007), opsonisation/agglutination of microorganisms (Alpuche et al., 2010, Pan et al., 2008 and Zhang et al., 2006), haemolytic activity (Zhang et al., 2009) and anti-viral defence (Lei et al., 2008 and Zhang et al., 2004). In this study, Hc concentration decreased over the 56-day period in HSCs incubated across all experimental temperatures (8 °C to 23 °C) (Fig. 6.4). Higher temperatures appeared to exacerbate the decline in Hc concentration, with Hc concentration decreasing by 69.3% in HSCs housed at 23 °C compared to a decrease of 31.3% in HSCs housed at 13 °C (Table 6.1). It has been noted previously that HSCs maintained in captivity for an extended period of time (≥ 6 months) suffer from a non-infectious hypoproteinemic disease which has been attributed to a number of factors

including captivity stress (Smith and Berkson, 2005). The multiple physiological and immunological roles of Hc, along with the high proportion of Hc normally present in the hemolymph (Ding et al., 2005) suggest that Hc concentration is a useful biomarker for the health status of cultured HSCs.

The percentage of Hc with dioxygen bound and Hc-d PO activity was also monitored throughout the course of this study. The percentage of Hc with dioxygen bound was high (> 90%) across the temperature range for the duration of the 56-day study (Fig. 6.5), while a continuous decline in Hc concentration was observed (Fig. 6.4). Biophysical assessment of purified Hc exposed to similar temperature regimes indicates that temperature has little effect on the structural conformation of the enzyme. No measureable changes in the far-UV CD spectrum (Fig. 6.10) or the fluorescence emission maximum (Fig. 6.11) were recorded. Both the near-UV CD and absorption spectra displayed a reduction around the 340 nm signal ($\text{CuII-O}_2^2\text{-CuII}$). Previous studies on Hc have detailed a reduction in 340 nm signal in the presence of SDS (Baird et al., 2007; Coates et al., 2011) which is indicative of conformational changes in Hc which coincide with inducible PO activity. However, irrespective of incubation temperature used here, purified Hc failed to display PO activity in the absence of SDS. Further analysis of the dicopper active centre was performed using histidine fluorescence intensities (Fig. 6.13). No changes around the 430 nm signal were detected; the 430 nm signal of Hc is usually quenched due the close proximity of the Cu atoms to the histidine residues, a lack of change in this region suggests that the copper atoms are not lost with increasing temperature and the subtle changes observed in the near UV CD data (Fig. 6.12) and the absorption spectra (Table 7.3) are possibly due to a reduction in oxygen concentration of the solvent, with increasing temperature.

Crustacean and chelicerate Hcs have demonstrated a high resistance to thermal denaturing *in vitro*, with tarantula Hc retaining structural integrity up to 90 °C (Sterner et al., 1995). *L. polyphemus* Hc exists as an octamer of hexameric subunits (Decker et al., 2007), which retains structural integrity across extreme temperatures (0 °C to 68 °C) and pH shifts due to the complex structural oligomerization of the protein. Our indicators of Hc structure and function across the temperature range 8 °C to 23 °C reflect these earlier findings and imply similar stability *in vivo*. The percentage of Hc with di-oxygen bound presents a useful indicator of environmental stress in aquaculture and this has been used to assess successfully the effects of nitrites in aquaculture (Cheng and Chen, 1999): as oxygen will be displaced at the active site. The percentage of Hc with dioxygen bound remained consistently high across the temperature range 8 °C to 23 °C (Fig. 6.5) suggesting that HSCs were not in the presence of deleterious levels of nitrites for the duration of the experiment.

PO enzymes and the associated proPO activation cascade in invertebrates play an essential part in innate immune defence (Cerenius et al., 2010). In HSCs, no true PO enzyme has been characterised (Terwilliger, 2007), therefore, any PO activity observed is assumed to be hemocyanin-derived PO (Hc-d PO) activity. In this study incubation of HSCs at higher temperatures (18 °C and 23 °C) yielded significant decreases in Hc-d PO activity (Fig. 6.6). In contrast to Hc concentration and amebocyte numbers, Hc-d PO activity varied little across the temperature range, mirroring the limited effect of temperature on the percentage of Hc with dioxygen bound. Hc-d PO activity measurements using hemolymph extracts and purified Hc (Fig. 6.9) exhibited similar specific Hc-d PO activity to previous studies (~ 3 U/mg) (Baird et al., 2007); an observation which supports the assumption that Hc accounts for > 90% of HSC

hemolymph protein. An increase in PO activity is often used to gauge stress responses in invertebrates (Cheng and Chen, 2000, Goimier et al., 2006 and Le Moullac and Haffner, 2000). The limited change in Hc-d PO levels across the temperature range in this study is indicative of the absence of severe stress, however, the subtle decrease over time suggests that other factors such as captivity stress may be influencing Hc-d PO activity and this response is exacerbated by the highest experimental temperature, 23 °C.

6.5.3 Effect of temperature on amebocyte number and morphology

In the present study, a significant decrease in amebocyte numbers were recorded in *L. polyphemus* maintained across the temperature range, 8°C to 23°C. Higher temperatures appeared to exacerbate the trend in decreasing amebocyte numbers (Fig. 6.7). According to Levin and Bang (1968), a healthy HSC should contain between 2 to 6 ×10⁷ amebocytes mL⁻¹ of hemolymph. Although a reduction in amebocyte numbers was observed across all temperatures in this study, amebocyte concentrations never went below 2 ×10⁷ cells mL⁻¹ in HSCs incubated at 8 °C and 13 °C. In contrast, amebocyte concentrations recorded for HSCs incubated at 23 °C were lower than 2 ×10⁷ cells mL⁻¹ at day 28 and continued to decrease for the remainder of the experiment (Fig. 6.7). Exposure of invertebrates to stressors, especially temperature, can lead to a decrease in immune cell numbers (Le Moullac and Haffner, 2000). Matozzo et al. (2011) observed a significant decrease in total hemocyte numbers in *Carcinus aestuarii* hemolymph in response to an increase in temperature, likewise, reductions in hemocyte numbers have been recorded in *Macrobrachium rosenbergii*, *Litopenaeus vannamei* and *Litopenaeus setiferus* as a result of thermal stress (Cheng and Chen, 2000, Cheng et al., 2003, Cheng et al., 2005 and Pascual et al., 2003).

HSC amebocytes display a number of morphological states in culture. A spherical-granular state appears to be the most common cell morphology, with studies from Hurton et al. (2005) indicating this cellular state as the most viable *in vitro*. Furthermore, work carried out by Chen et al., (1986), Chen et al., (1989) and Armstrong (1979) indicated that spherical constricted states of amebocytes in culture may represent the morphology of amebocytes *in vivo*. We observed a change in the ratio of amebocyte morphologies (from granular-spherical to granular-flattened) in the hemolymph of HSCs crabs housed across the temperature range 8 °C to 23 °C (Fig. 6.8A and B). This change in amebocyte morphology may represent a change in cell functionality or membrane fluidity. It has been well documented that invertebrate immune cells display compromised functionality including reduced phagocytic performance, anti-bacterial activity and alterations in the proPO activation cascade, in response to thermal stress (Cheng and Chen, 2000, Cheng et al., 2003, Cheng et al., 2005 and Vargas-Albores et al., 1998).

Overall, the cellular properties measured in this study altered more than the biochemical properties monitored (Fig. 6.14). As amebocyte numbers decreased, the remaining amebocytes present in the hemolymph displayed a shift in morphology. Interestingly, as Hc levels declined, the proportion of bound dioxygen and Hc-d PO activity units remained relatively stable.

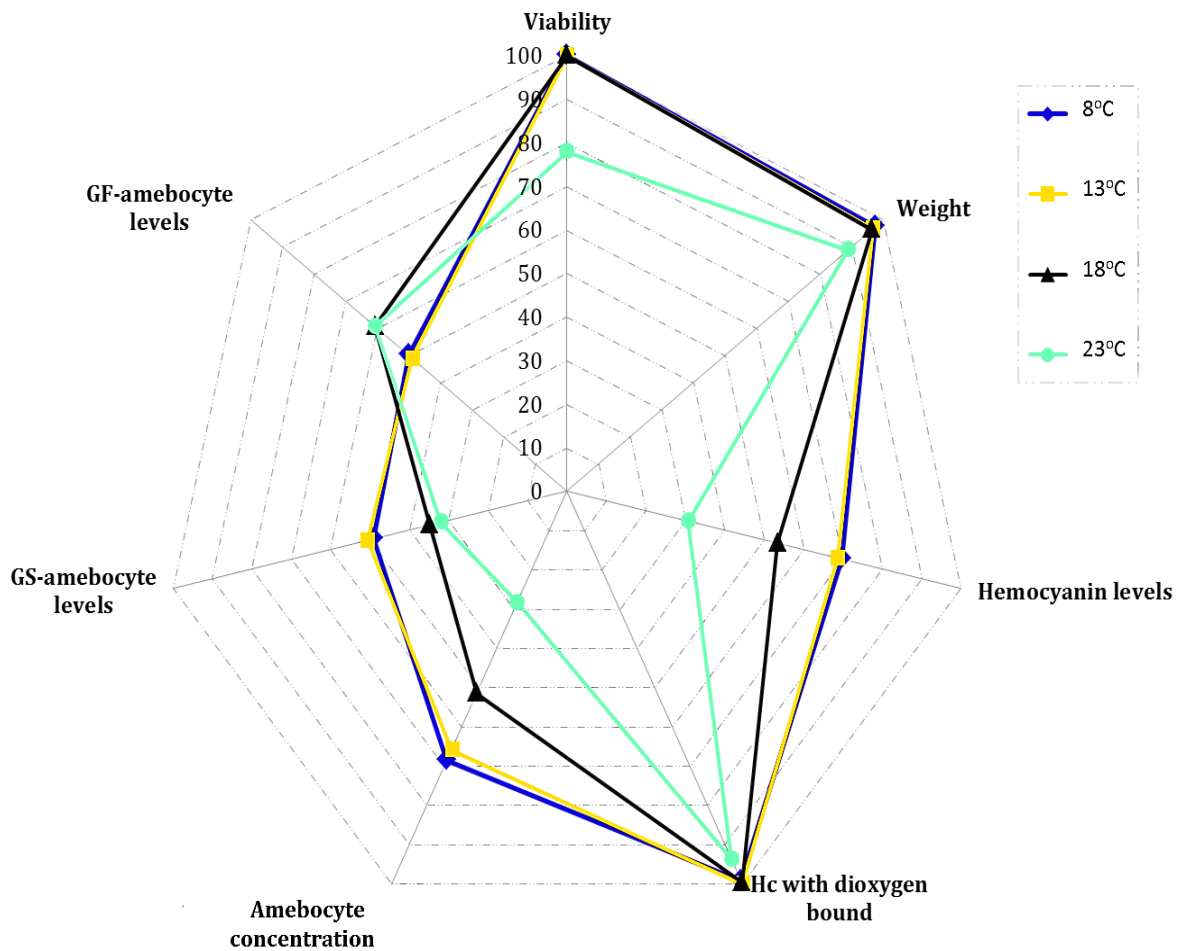


Figure 6.14 Direct comparison of the biochemical and cellular properties of captive *Limulus polyphemus* across the temperature range, 8°C to 23°C. The radar-graph represents the % change between Day 0 and Day 56 recordings. *Hc-d PO* data were omitted as units of activity per mg of Hc were very similar across the temperature range at Day 56 (2.1 to 2.6 U: 8°C to 23°C).

6.6 Conclusion

Results suggest that HSCs maintained in captivity are sensitive to the highest temperature (23 °C) in this study. Increasing temperatures led to a decrease in Hc concentration, amebocyte number and a change in the ratio of amebocyte morphological states. Temperature had little effect on the level of Hc with dioxygen bound and the associated Hc-d PO activity levels. The combination of cellular, biochemical and immunological indicators used in this study could be used to assess the health status of HSCs in captivity and in natural populations, and their response to environmental pressures. These findings suggest that an increase in temperature results in a reduction in the concentration of hemolymph Hc while Hc functionality is retained. Furthermore, an increased rate of PO Hc-d PO activity is observed with increasing temperatures, however, Hc structural conformation remains intact at the highest temperature used in this study.

6.7 Acknowledgements

Special thanks to Alex Mühlhölzl, Managing Director, Marine Biotech Limited for providing access to *L. polyphemus*. Many thanks to Kate Howie (C&MS, University of Stirling) for guidance through statistical analysis, Brain Craig for his technical assistance and Dr. Tim Whalley (BES, University of Stirling) for his helpful discussions on the cellular aspects of this study. Also, to James Weir and Ronald Balfour (BES, School of Natural Sciences) for their advice on experimental set-up and to Bill Jamieson (BES Cartography Unit) for preparation of Fig. 6.1. With thanks to Liam Cavin for his assistance with photography (Fig. 6.2).

Chapter 7:

Overall Summary and General Discussion

The purpose of this chapter is to contextualise the research findings discussed within all previous chapters.

7.1 A pro-Hemocyanin activation cascade?

Unlike the proPO activation cascade in arthropods (Fig. 1.8), the induction of PO activity in Hc *in vivo* has received little attention; therefore, the overall aim of this research was to characterise the physiological circumstances in which hemocyanin is converted into an immune enzyme. Research presented in chapters 2, 4 and 5 have addressed successfully a number of key objectives:

1. to test the ability of natural phospholipids to induce PO activity in Hc
2. to characterise the structural changes associated with the induction of PO activity in Hc by natural activator(s)
3. to isolate invertebrate immune cells and maintain them *in vitro*
4. to monitor phagocytic activity and apoptosis of invertebrate immune cells during microbial challenge
5. to monitor Hc-derived PO activity in the presence of quiescent and active immune cells

In chapter 2 it was demonstrated that the acidic phospholipid, PS, can induce PO activity in Hc, through subtle secondary and tertiary structural changes which appear more stable when compared to those observed in the presence of the exogenous lipid mimic, SDS. Exposure of Hc to 20 $\mu\text{g mL}^{-1}$ liposomal PS achieved >90% of the activity observed in the presence of micellar SDS. Even though solubility issues with higher concentrations of PS hindered further investigation, attempts to characterise the PS-Hc interactions suggested that electrostatics play a role in the protein-phospholipid complex. Incubation of Hc/PS with increasing concentrations of NaCl appeared to interfere with the structural conformation of activated Hc and this was accompanied by a reduction in enzyme activity (Fig. 2.15 and Fig. 2.16). Interestingly, work carried out by Li et al., (2009) highlighted also, the importance of changes in electrostatic surface potential of *M. sexta* proPO, pre and post activation. Additional optimisation of phospholipid liposome composition/structure would permit further investigation on putative phospholipid binding sites present on *L. polyphemus* Hc.

In order to monitor the behaviour of *L. polyphemus* amebocytes during immune challenge, it was necessary to optimise their maintenance *in vitro*. Historically, attempts to culture and/or maintain arthropod hemocytes *ex vivo*, particularly crustaceans, have proven relatively ineffective (Rinkevich, 2011). While insect cell lines are readily maintained in laboratories, significant investment is required to develop cell lines from marine arthropods. Reports focussing on the maintenance of HSC amebocytes *in vitro* are contradictory. Such reports cite cell viability rather than functionality as a measure of success for the maintenance of HSC amebocytes. In chapter 4, the short term maintenance of *L. polyphemus* amebocytes *in vitro* was achieved using media which is assumed to imitate most closely, the physiological properties of HSC hemolymph

(NaHEP). Viability of the amebocytes was ~84% after 24h *in vitro*. Amebocyte morphology and LPS-induced exocytosis were used favourably as markers of retained functionality. Although 24 h is not an extensive period of time, these data nevertheless provide a method to investigate amebocyte functionality, and may assist in the design of future systems for the maintenance of cells from other marine organisms. Consequently, the phagocytic properties of *L. polyphemus* amebocytes were determined, *in vitro*. Employing a number of membrane probes and quenchers of fluorescence (enabling the visualisation of internalised targets), rates of phagocytosis and phagocytic indices of active amebocytes were recorded using fungal, bacterial and synthetic targets.

Building on data presented in chapter 4, the nature of amebocyte phagocytosis would benefit from subsequent investigations focussing on modes of pathogen killing, once internalisation has occurred. The uptake of microspheres by amebocytes enables phagosomes to be isolated (using differential centrifugation) and studied in greater detail. Monitoring differences in protein expression profiles of phagocytically active amebocytes versus non-phagocytic amebocytes would provide insight into phagosome biogenesis and pathogen clearance abilities in invertebrates. It should be noted that the task of maintaining marine arthropod immune cells *in vitro* for extended periods of time (> 14 days) is on-going, with current efforts focussing on characterising hematopoietic tissues.

Data presented in chapter 5 further supports PS as an endogenous activator of Hc-d PO in *L. polyphemus*. Phagocytosis of spores by amebocytes was accompanied by a series of cell death characteristics, associated conventionally with apoptosis. PICD is a phenomenon that has been characterised in a number of species previously, but this is the first demonstration of PICD in a chelicerate. In the presence of apoptotic

amebocytes, a measureable increase in Hc-d PO was observed. The majority of Hc-d PO activity was detected in Hc that was most likely associated with extracellular amebocyte-derived components. While data attests to a feasible PS-Hc activation complex, it cannot be ruled out that other unidentified membrane components may be involved in the conversion of Hc into an immune-enzyme.

Hc purified from the HSCs, *T. tridentatus* and *C. rotundicauda*, can be converted into a PO-like enzyme upon incubation with amphiphilic molecules similar to PS and SDS: microbial proteases (Jiang et al., 2007), amebocyte-derived clotting components (Nagai and Kawabata, 2000) and chitin-binding antimicrobial peptides (tachyplexins) (Nagai et al., 2001). The authors proposed that upon infection, microbial proteases cleave Hc in a manner that initiates PO activity and the accompanying generation of ROS. Additionally, when microbial ligands are detected by amebocytes, the release of immune-bioactives, including tachyplexins, could induce PO activity in Hc while anchoring the protein to exposed chitin within the proximity of the wound that facilitated the microbial invasion. Using Hc in such a manner provides the host with a pro-clotting and simultaneous anti-microbial response.

Based on data gathered in chapters 2 and 5, a third mode of Hc activation is proposed. During an infection, patrolling amebocytes present in *L. polyphemus* hemolymph could recognise opsonised-microbes and ingest them. Following the redistribution of PS caused by PICD, Hc could interact with exposed PS, thus resulting in its conversion into a PO-like enzyme. As Hcs are known to display a high level of cooperativity, it is possible that upon binding of Hc to the amebocyte plasma membrane, structural changes induced by such interactions may promote further Hc recruitment, leading to enhanced PO activity. The activation of Hc upon association with amebocytes undergoing

apoptosis also provides a mechanism to switch-off and/or limit such activity. Apoptotic cells are eventually phagocytosed by other leukocytes/hemocytes in mammal/insect systems, and in theory, *L. polyphemus* amebocytes would ingest activated Hc in the same process. This mode of immune-silencing would deter unwanted/excess PO activity.

In mammals, the expression of PS on activated platelet membranes is vital to the conversion of the prothrombin zymogen into thrombin, a central molecule in blood clotting (Vance and Steenbergen, 2005). PS is known also to possess a high affinity for the LPS-sensitive Factor C protease, involved in complement, microbe recognition, hemostasis and endogenous feedback that stimulates degranulation in HSC amebocytes during sepsis and mycosis (Kawabata et al., 2009, Kurata et al., 2006). Interestingly, apoptosis in mammalian leukocytes is known to induce the expression of the clotting protein, transglutaminase (Volokhina et al., 2003). Transglutaminases are also conserved in HSCs and an increase in the expression of its substrate has been recorded in apoptotic amebocytes during bacterial infection (Ding et al., 2005). Furthermore, the concept of a PO-like enzyme interacting with cell membrane components to necessitate activation is not unheard of, as membrane bound POs are known to exist in a number of plant species, and play a role in immune defence (Zaini et al., 2013).

Although data presented in chapters 2 and 5 suggest a role for apoptotic cells in the activation of Hc into a PO-like enzyme, further work involving the use of synthetic peptides and/or site directed mutagenesis to inhibit/interfere with the PS-Hc association is required. SDS-PAGE and western blot analysis can be applied to assess whether alternative cell-derived compounds (such as tachyplesin) are being released *in vitro*, and potentially activating Hc-d PO in co-operation with PS. Also, the endogenous phenolic substrate that would be essential for Hc-d PO activity, *in vivo*, remains

unknown and requires investigation. Additional factors, similar to those associated with the proPO activation complex, may also be required for optimal activation of Hc.

Considering many factors, such as the abundance of Hc in invertebrate hemolymph, the lack of a true-PO in chelicerates (Terwilliger and Ryan, 2006), the many immune-functions of Hc (Table 1.2) and findings from research undertaken here, it is suggested that Hc is an integral component of innate immunity.

7.2 Applications of research

7.2.1 Pigmentation and commercially important invertebrates

In general, the study of type-3 copper proteins is important for biomedical and economic reasons, including: vaccine design, food sustainability, cosmetics and bio-fuel production. PO enzymes (both tyrosinases and catecholoxidases) present in flora and fauna, catalyse the initial reactions involved in the biogenesis of melanin (Cerenius and Soderhall, 2004). Melanin, aside from immune defence, plays an essential role in the integumentary system by ameliorating the effects of solar radiation on skin, but, has been linked to many disorders. Melasma is a facial discolouration disorder associated with the overproduction of eumelanin caused by tyrosinases (Jones et al., 2002). Equally, an autoimmune disease in humans known as vitiligo, involves the destruction of melanocytes by oxidative stress and the abnormal expression of tyrosinase caused by auto-antibodies, leading to chronic de-pigmentation (Trouba et al., 2002). The congenital disorder, albinism, is directly associated with defective tyrosinases. Oculocutaneous Albinism type 1 can be caused by any one of the 100 currently identified mutations found on the human tyrosinase gene (Wang et al., 2012).

The over- accumulation of melanin, known as hyperpigmentation, is an undesirable and costly occurrence in fruit crops, shellfish and mushrooms during storage. Hyperpigmentation in farmed and fresh caught shellfish (notably shrimp) is a non-infectious condition that causes cuticular darkening, resulting in reduced market value and large accumulation of waste (Fig. 3.1). Traditionally, sulfiting compounds have been used to inhibit hyperpigmentation, however, such compounds display allergenic properties and are linked to occupational illness (Steiner et al., 2008). Therefore, the development of safe and effective alternatives to sulphiting compounds is needed in order to alleviate FDA concerns and importantly, retain the nutritional integrity of farmed and fresh-caught shellfish. Although a number of inhibitors are currently used to prevent hyperpigmentation, the true target remains poorly characterised. Using *N. norvegicus*, experiments detailed in chapter 3 tackled the final objective of this thesis;

'to explore the role of Hc-d PO in shellfish hyperpigmentation'

Upon exposure of cellular-PO and Hc-d PO to freezing and thawing conditions that mimic *in situ* handling of shrimp, almost all cellular-PO activity was eliminated. Conversely, Hc-d PO not only retained activity but demonstrated an increase after 72 h. Overall, Hc is a more stable protein, is more abundant in shrimp hemolymph than PO and can be inhibited by commonly used PO inhibitors (Wright et al., 2012). 4-HR proved to be the most appropriate compound for reducing the unwanted PO activity of shrimp Hc, and fortunately, is FDA approved.

Future studies employing both inhibition and structural data will enable the development of specific inhibitors of Hc-d PO which may prevent hyperpigmentation. Immunohistochemistry and scanning electron microscopy may be used to correlate pigmentation patterns of the carapace with the location of Hc/PO within tissues. The

inhibition of all sources of shellfish hyperpigmentation, including PO and Hc-d PO, is vital for the enhancement of shellfish sustainability and the food security agenda.

7.2.2 Biomedical applications

The HSC, *L. polyphemus*, is a multi-resource species, having existed for over 250 million years in a microbiologically harsh environment. Initially used in the study of vision, *L. polyphemus* is most famously known for the cell-derived pyrogen detection assay kit, LAL. A number of anthropogenic practices currently threaten the existence of the four remaining extant species of HSC, habitat loss due to pollution and the biannual bleeding of over 250,000 HSCs for the production of biopharmaceuticals (Anon, 2012). For example, Hc purified from *L. polyphemus* and the keyhole limpet (KL) are used in biomedicine due to their extraordinary immunostimulatory properties. KL-Hc is commonly used as a vaccine adjuvant, for the generation of antibodies against hapten molecules and as an immunotherapeutic/prophylactic agent in patients suffering from a range of cancers (Arancibia et al., 2012). Little success has been achieved in rearing HSCs in captivity and a synthetic alternative for pyrogen detection has only been developed recently (Ding and Ho, 2010).

In chapter 6, the health status of captive-HSCs across the temperature range, 8°C to 23°C, was investigated with a view to improving success in maintaining HSCs in captivity. By monitoring a number of biochemical and cellular properties, HSC deterioration was found to correlate directly with increasing temperatures. While a decrease in Hc concentration was observed, the structural and functional integrity of the protein remained intact. Amebocyte numbers also decreased, with the remaining amebocyte populations changing morphology.

Amebocytes are the sole immune cell type present in HSC hemolymph, impairment in amebocyte effectiveness would almost certainly result in an enhanced susceptibility to disease. The changes observed in amebocytes will require subsequent work to establish the functional differences between the three distinct morphologies observed. Optimising the temperature at which captive HSCs are housed is one of many conditions that need to be evaluated further. Exposing amebocytes, *in vitro*, to similar temperature regimes and monitoring protein expression profiles, may provide insight into the response of HSCs to environmental stressors (such as pollution, temperature and pH shifts), both in captivity and *in situ* natural populations. Conservation of HSCs is not only important for species diversity but for the biomedical properties of its hemolymph. For future work, it may be judicious to make adjustments to the experimental design detailed in chapter 6:

- to enhance statistical robustness, equal sample numbers for both the experimental and control groups could be used
- increasing the period of acclimation >48 hours for those organisms at temperature extremes may avoid additional stress, and
- using longer periods of incubation time for detecting microbial pathogens on gill swabs and screening for viruses would ensure the inclusion of healthy HSCs only

Cumulatively, the study of type-three copper proteins, their structure-function relationships and their activities influencing host immunity have many applications, ranging from anti-cancer therapeutics to species conservation. Importantly, investment and research in these areas can be translated for the benefit of society.

BIBLIOGRAPHY

A

- Adachi, K., Endo, H., Watanabe, T., Nishioka, T., Hirata, T. 2005a. Hemocyanin in the exoskeleton of crustaceans: enzymatic properties and immunolocalization. *Pigment Cell Research*. 18, 136–143.
- Adachi, K., Hirata, T., Nagai, K., Fujisawa, S., Kinoshita, M., Sakaguchi, M. 1999. Purification and characterisation of prophenoloxidase from Kuruma prawn, *Penaeus japonicus*. *Fisheries Science*. 65, 919-925.
- Adachi, K., Hirata, T., Nagai, K., Sakaguchi, M. 2001. Hemocyanin: a most likely inducer of black spots in Kuruma prawns *Penaeus japonicus* during storage. *JFS Food Chemistry and Toxicology*. 66, 1130-1136.
- Adachi, K., Hirata, T., Nishioka, T., Sakaguchi, M. 2003. Hemocyte components in crustaceans convert hemocyanin into a phenoloxidase-like enzyme. *Comparative Biochemistry and Physiology Part B*. 134, 135-141.
- Adachi, K., Wakamatsu, K., Ito, S., Miyamoto, N., Kokubo, T., Hirata, T. 2005b. An oxygen transporter hemocyanin can act on the late pathway of melanin synthesis. *Pigment Cell Research*. 19, 214–219.
- Adams, M.D., Celniker, S.E., and others. 2000. The genome sequence of *Drosophila melanogaster*. *Science*. 287, (5461) 2185-2195.
- Agaisse, H., Perrimon, N. 2004. The role of the JAK/STAT signalling in *Drosophila* immune response. *Immunology Reviews*. 196, 72-82.
- Akbar-John, B., Jalal, K.C.A., Kamaruzzaman, Y.B., Zaleha, K. 2010. Mechanism in the clot formation of horseshoe crab blood during bacterial endotoxin invasion. *Journal of Applied Sciences*. 10, 1930–1936.
- Aladaileh, S., Nair, S., Raftos, D.A. 2007. Induction of phenoloxidase and other immunological activities in Sydney rock oysters challenged with microbial pathogen-associated molecular patterns. *Fish and Shellfish Immunology* 23, 1196-1208.
- Alpuche, J., Pereyra, A., Mendoza-Hernandez, G., Agundis, C. 2010. Purification and partial characterisation of an agglutinin from *Octopus maya* serum. *Comparative Biochemistry and Physiology Part B*. 156, 1–5.
- Alpuche, J., Rosas, C., Vazquez, L., Guevara, J., Pereyra, A., Agundis, C., Pascual, C., Zenteno, E. 2009. Activation of immunological responses in *Litopenaeus setiferus* hemocytes by a hemocyanin like lectin. *Aquaculture*. 292, 11-15.
- Altman, S.A., Randers, L., Rao, G. 1993. Comparison of trypan blue dye exclusion and fluorometric assays for mammalian cell viability determinants. *Biotechnology Progress*. 9, 671–674.
- Amore, V., Belardinelli, M., Guerra, L., Buonocore, A.M., Ubero-Pascal, N., Fochetti, R. 2009. Do all stoneflies nymphs have respiratory proteins? Further data on the

presence of hemocyanin in the larval stages of plecoptera species. *Insect Molecular Biology*. 18, 203-211.

- Amore, V., Fochetti, R. 2009. Present knowledge on the presence of hemocyanin in stoneflies (Insecta: Plecoptera). *Aquatic Insects*. 31, 577-583.
- Anon. 2012. <http://www.horseshoecrab.org/info/conservation.html>.
- Arancibia, S., Salazar, F., Becker, M.I. 2012. Hemocyanins in the Immunotherapy of Superficial Bladder Cancer. In; A. Canda (Ed). Bladder Cancer - From Basic Science to Robotic Surgery. Chapter 11, pp 221-242. *In Tech*.
- Ariki, S., Koori, K., Osaki, T., Motoyama, K., Inamori, K., Kawabata, S. 2004. A serine protease zymogen functions as a pattern-recognition receptor for lipopolysaccharides. *Proceedings of the National Academy of Sciences, USA*. 101, 953-958.
- Ariki, S., Takahara S., Shibata, T., Fukuoka, T, Ozaki A., Endo, Y., Fujita, T., Koshiba, T., Kawabata, S. 2008. Factor C acts as a lipopolysaccharide-responsive C3 convertase in horseshoe crab complement activation. *Journal of Immunology*. 181, 7994-8001.
- Armstrong, P. 1979. Motility of the *Limulus* blood cell. *Journal of Cell Science*. 37, 169-180.
- Armstrong, P.B. 1980. Adhesion and spreading of *Limulus* blood cells on artificial surfaces. *Journal of Cell Science*. 44, 243-262.
- Armstrong, P. 1985. Adhesion and motility of the blood cells of *Limulus*. In: Cohen, E. (Ed.), *Blood Cells of Marine Invertebrates: Experimental Systems in Cell Biology and Comparative Physiology*. Alan R. Liss, Inc., New York, pp. 77-124.
- Armstrong, P., Levin, J. 1979. *In vitro* phagocytosis by *Limulus* blood cells. *Journal of Invertebrate Pathology*. 34, 145-151.
- Armstrong, P., Rickles, F.R., 1982. Endotoxin-induced degranulation of the *Limulus* amoebocyte. *Experimental Cell Research*. 140, 15-24.
- Ausubel, M.F., Brent, R., Kingston, R.E., Moore, D.D., Seidman, J.G., Smith, J.A., Struhl, K (Eds.). 2002. Short protocols in molecular biology: A compendium of methods from current protocols in molecular biology. John Wiley & Sons, Inc. USA, pp A1-21.

B

- Bacci, M., Baldecchi, M.G., Fabeni, P., Linari, R. and Pazzi, G.P. 1983. Emission spectra from copper proteins containing type-3 centres. *Biophysical Chemistry* 17, 125-130.
- Baird, S. 2007. PhD thesis; a study of type-3 copper proteins in arthropods. <https://dspace.stir.ac.uk/bitstream/1893/266/1/Miss%20Sharon%20Baird%20Final%20Thesis%20Version.pdf>
- Baird, S., Kelly, S.M., Price, N.C., Jaenicke, E., Meesters, C., Nillius, D., Decker, H., Nairn, J. 2007. Hemocyanin conformational changes associated with SDS-induced phenoloxidase activation. *Biochimica et Biophysica Acta*. 1774, 1380 - 1394.

- Bang, F.B. 1956. A bacterial disease of *Limulus polyphemus*. *Bulletin of the Johns Hopkins Hospital*. 98, 325-351.
- Banville, N., Fallon, J., McLoughlin, K., Kavanagh, K. 2011. Disruption of haemocyte function by exposure to cytochalasin b or nocodazole increases the susceptibility of *Galleria mellonella* larvae to infection. *Microbes and infections*. 13, 1191-1198.
- Bao, Y., Wang, Q., Lin Z. 2011. Hemoglobin of the bloody clam *Tegillarca granosa* (Tg-HbI) is involved in the immune response against bacterial infection. *Fish and Shellfish Immunology*. 31, 517-523.
- Bergin, D., Brennan, M., Kavanagh, K. 2003. Fluctuations in haemocyte density and microbial load may be used as indicators of fungal pathogenicity in larvae of *Galleria mellonella*. *Microbes and Infection*. 5, 1389–1395.
- Bergin, D., Reeves, E.P., Renwick, J., Wientjes, M., Kavanagh, K. 2005. Superoxide production in hemocytes of *Galleria mellonella*, identification of proteins homologous to the NADPH oxidase complex of human neutrophils. *Infection and Immunity*. 73, 4161–4173.
- Berkson, J.M., Shuster, C.N. 1999. The horseshoe crab: the battle over a true multiple use resource. *Fisheries*. 24, 6–10.
- Bhagvat, K., Richter, D. 1938. Animal phenolases and adrenaline. *Biochemical Journal*. 32, 1397-1406.
- Bilda, A., Dushay, M.S., Theopold, U. 2007. Crystal rupture after injury in *Drosophila* requires JNK pathway, small GTPases and the TNF homolog Eiger. *Journal of Cell Sciences*. 120, 1209 – 1215.
- Bilda, A., Hauling, T., Dushay, M.S., Theopold, U. 2009. Activation of insect phenoloxidase after injury: endogenous versus foreign elicitors. *Journal of Innate Immunity*. 1, 301-308.
- Billingsley, P.E., Lehane, M.J. 1996. Biology of the insect midgut. *Chapman and Hall*. New York.
- Bogdan, C. 2007. Oxidative burst without phagocytes: the role of respiratory proteins. *Nature Immunology*. 8, 1029-1031.
- Borges, A.R., Santos, P.N., Furtado, A.F., Figueiredo, R.C.B.Q. 2008. Phagocytosis of latex beads and bacteria by hemocytes of the triatomine bug *Rhodnius prolixus* (Hemiptera: Reduviidae). *Micron*. 39, 486–494.
- Bourchookarn, A., Havanapan, P-O., Thongboonkerd, V., Krittanai, C. 2008. Proteomic analysis of altered proteins in lymphoid organ of yellow head virus infected *Penaeus monodon*. *Biochimica et Biophysica Acta*. 1784, 504-511.
- Brogden, K.A. 2005. Anti-microbial peptides: pore formers or metabolic inhibitors in bacteria. *Nature Reviews Microbiology*. 3, 238-250.
- Brouwer, M., Whaling, P., Engel, D.W. 1986. Copper-metallothioneins in the American lobster, *Homarus americanus*: potential role as Cu(I) donors to apohemocyanin. *Environmental Health Perspectives* 65. 93-100.
- Brown, G.C., Neher, J.J. 2012. Eaten alive! Cell death by primary phagocytosis: 'phagoptosis'. *Trends in Biochemical Sciences*. 37, 325-332.

- Brinkmann, V., Reichard, U., Goosmann, C., Fauler, B., Uhlemann, Y., Weiss, D.S., Weinrauch, Y., Zychlinsky, A. 2004. Neutrophil extracellular traps kill bacteria. *Science*. 303, 1532–1535.
- Burmester, T. 1999. Evolution and function of insect hexamerins. *European Journal of Entomology*. 96, 213-225.
- Burmester, T. 2001. Molecular evolution of the arthropod hemocyanin superfamily. *Molecular Biology and Evolution*. 18, 184-195.
- Burmester, T., Hankeln, T. 2007. The respiratory proteins of insects. *Journal of Insect Physiology*. 53, 285-294.

C

- Campello, S., Beltramini, M., Giordano, G., Di Muro, P., Marino, S.M., Bubacco, L. 2008. Role of the tertiary structure in the diphenol oxidase activity of *Octopus vulgaris* hemocyanin. *Archives of Biochemistry and Biophysics*. 471, 159-167.
- Cerenius, L., Lee, B.L., Söderhäll, K. 2008. The pro-PO system: pros and cons for its role in invertebrate immunity. *Trends in Immunology*. 29, 263 – 271.
- Cerenius, L., Kawabata, S.-I., Lee, B.L., Nonaka, M., Söderhäll, K. 2010. Proteolytic cascades and their involvement in invertebrate immunity. *Trends in Biochemical Science*. 35, 575–583.
- Cerenius, L., Soderhall, K. 2004. The prophenoloxidase-activating system in invertebrates. *Immunological Reviews*. 198, 72-82.
- Chang, T-S. 2009. An updated review of tyrosinase inhibitors. *International Journal of Molecular Sciences*. 10, 2440-2475.
- Chaurio, R.A., Janko, C., Munoz, L.E., Frey, B., Herrmann, M., Gaipf, U.S. 2009. Phospholipids: key players in apoptosis and immune regulation. *Molecules*. 14, 4892 – 4914.
- Chen, I.-J., Chen, Y.-M., Hong, S.J., Chiang, L.-C. 1986. Morphological changes of horseshoe crab amebocytes during *in vitro* cultivation. *Kaohsiung Journal of Medical Science*. 2, 769–773.
- Chen, I.-J., Hong, S.-J., Chen, Y.-M., Yang, Y.-C. 1989. Cultivation of horseshoe crab amebocytes. *The Kaohsiung Journal of Medical Sciences*. 5, 515–521.
- Chen, F.-j., Yan, F., Yang, P. 2009. Studies on phenoloxidase activity of hemocyanin in *Scylla serrata*. *Journal of South China Agricultural University*, 01-013.
- Cheng, W., Chen, J.-C. 1999. Hemocyanin oxygen affinity and the fractionation of oxyhemocyanin and deoxyhemocyanin for *Penaeus monodon* exposed to elevated nitrite. *Aquatic Toxicology*. 45, 35–46.
- Cheng, W., Chen, J.-C. 2000. Effects of pH, temperature and salinity on immune parameters of the freshwater prawn *Macrobrachium rosenbergii*. *Fish and Shellfish Immunology*. 10, 387–391.
- Cheng, W., Chen, S.-M., Wang, F.-I., Hsu, P.-I., Liu, C.-H., Chen, J.-C. 2003. Effects of temperature, pH, salinity and ammonia on the phagocytic activity and clearance efficiency of the giant freshwater prawn *Macrobrachium rosenbergii* to *Lactococcus garvieae*. *Aquaculture*. 219, 111–121.

- Cheng, W., Wang, C.-U., Chen, J.-C. 2005. Effect of water temperature on the immune response of white shrimp *Litopenaeus vannamei* to *Vibrio alginolyticus*. *Aquaculture*. 250, 592–601.
- Coates, C.J., Bradford, E.L., Krome, C.A., Nairn, J. 2012. Effect of temperature on biochemical and cellular properties of captive *Limulus polyphemus*. *Aquaculture*. 334–337, 30–38.
- Coates, C.J., Kelly, S.M., Nairn, J. 2011. Possible role of phosphatidylserine-hemocyanin interaction in the innate immune response of *Limulus polyphemus*. *Developmental and Comparative Immunology*. 35, 155–163.
- Coates, C.J., Whalley, T., Nairn, J. 2012. Phagocytic activity of *Limulus polyphemus* amebocytes *in vitro*. *Journal of Invertebrate Pathology*. 111, 205–210.
- Cochilla, A.J., Angleson, J.K., Betz, W.J. 1999. Monitoring secretory membrane with FM1-43 fluorescence. *Annual Review of Neuroscience*. 22, 1–10.
- Cong, R., Sun, W., Liu, G., Fan, T., Meng, X., Yang, L., Zhu, L. 2005. Purification and characterization of phenoloxidase from clam *Ruditapes philippinarum*. *Fish and Shellfish Immunology*. 18, 61–70.
- Conrad, M., Denobile, J., Chaikhoutdinov, I., Escribano, D., Lee, K.-G., Cohen, W.D. 2004. Cytoskeletal organization of *Limulus* amebocytes pre- and post-activation: comparative aspects. *Biological Bulletin*. 207, 56–66.
- Conrad M.L., Pardy R.L., Wainwright N., Child A., Armstrong P.B. 2006. Response of the blood clotting system of the American horseshoe crab, *Limulus polyphemus*, to a novel form of lipopolysaccharide from a green alga. *Comparative Biochemistry and Physiology Part A*. 144, 423–428.
- Cooper, D.M., Mitchell-Foster, K. 2011. Death for survival: what do we know about innate immunity and cell death in insects? *Invertebrate Survival Journal*. 8, 162–172.
- Copeland, D.E., Levin, J. 1985. The fine structure of the amebocyte in the blood of *Limulus polyphemus*. I. Morphology of the normal cell. *Biological Bulletin*. 169, 449–457.
- Coursey, Y., Ahmad, N., McGee, B.M., Steimel, N., Kimble, M. 2003. Amebocyte production begins at stage 18 during embryogenesis in *Limulus polyphemus*, the American horseshoe crab. *Biological Bulletin*. 204, 21–27.
- Cuff, M., Miller, K., Hendrickson, W. 1998. Crystal structure of a function unit form *Octopus* hemocyanin. *Journal of Molecular Biology*. 278, 855–70.

D

- Date, M.S., Dominy, B.N. 2013. Modelling the influence of salt on the hydrophobic effect and protein fold stability. *Communications in Computational Physics*. 13, 90–106.
- Dean, P., Potter, U., Edwards, J.P., Charnley, K.A., Reynolds, S.E. 2004a. Hyperphagocytic hemocytes in *Manduca sexta*. *Journal of Insect Physiology*. 50, 1027–1036.

- Dean, P., Richards, E. H., Edwards, J.P., Reynolds, S.E., Charnley, K. 2004b. Microbial infection causes the appearance of hemocytes with extreme spreading ability in monolayers of the tobacco hornworm *Manduca sexta*. *Developmental and Comparative Immunology*. 28, 689-700.
- Decker, H., Hellmann, N., Jaenicke, E., Lieb, B., Meissner, U., Markl, J. 2007a. Recent progress in hemocyanin research. *Integrative and Comparative Biology*. 47, 631 – 644.
- Decker, H., Jaenicke, E. 2004. Recent findings on phenoloxidase activity and antimicrobial activity of hemocyanins. *Developmental and Comparative Immunology*. 28, 673 – 687.
- Decker, H., Rimke, T. 1998. Tarantula hemocyanin shows phenoloxidase activity. *Journal of Biological Chemistry*. 273, 25889-25892.
- Decker, H., Ryan, M., Jaenicke, E. 2001. SDS-induced phenoloxidase activity in hemocyanins from *Limulus polyphemus*, *Eurypelma californicum* and *Cancer magister*. *Journal of Biological Chemistry*. 276, 17796 – 17799.
- Decker, H., Schweikardt, T., Nillius, D., Salzbrunn, U., Jaenicke, E., Tuczec, F. 2007b. Similar enzyme activation and catalysis in hemocyanins and tyrosinases. *GENE*. 398, 183 – 191.
- Decker, H., Tuczec, F. 2000. Tyrosinase/catecholoxidase activity of hemocyanins: structural basis and molecular mechanisms. *Trends in Biochemical Sciences*. 25, 392 – 397.
- Decker, H., van-Holde, K.E. 2010. Oxygen and the Evolution of Life. Springer. New York.
- De Gregorio, E., Spellman, P.T., Rubin, G.M., Lemaitre, B. 2001. Genome wide analysis of the *Drosophila* immune response by oligonucleotide microarrays. *Proceedings of the National Academy of Sciences U.S.A.* 98, 12590-12595.
- DeLeo, F.R. 2004. Modulation of phagocyte apoptosis by bacterial pathogens. *Apoptosis*. 9, 399-413.
- Desbois, A.P., Coote, P.J. 2011. Wax moth larva *Galleria mellonella*: A new *in vivo* model for evaluating the efficacy of anti-staphylococcal agents. *Journal of Antimicrobial Chemotherapy*. 66, 1785-1790.
- Destoumieux, D., Bulet, P., Loew, D., Van Dorsselaer, A., Rodriguez, J., Bachere, E. 1997. Penaeidins, a new family of antimicrobial peptides isolated from the shrimp *Penaeus vannamei* (Decapoda). *Journal of Biological Chemistry*. 272, 28398-28406.
- Destoumieux-Garzón, D., Saulnier, D., Garnier, J., Jouffrey, C., Bulet, P., Bachère, E. 2001. Crustacean immunity-antifungal peptides are generated from the C-terminus of shrimp hemocyanin in response to microbial challenge. *Journal of Biological Chemistry*. 276, 47070 – 47077.
- Ding, J.L., Ho, B. 2001. A new era in pyrogen testing. *Trends in Biotechnology*. 19, 227-281.

- Ding, J.L., Ho, B. 2010. Endotoxin detection-from *Limulus* amebocyte lysate to recombinant factor C. In: Wang, X., Quinn, P.J. (Eds.), Endotoxins: structure, function and recognition. Springer, pp. 187-208.
- Ding, J.L., Thangamani, S., Kusuma, N., Seow, W.K., Bui, T.H.H., Wang, J., Ho, B. 2005. Spatial and temporal coordination of expression of immune genes during *Pseudomonas* infection of horseshoe crab, *Carcinoscorpius rotundicauda*. *Genes and Immunity*. 6, 557-574.
- Dolashka-Angelova, P., Lieb, B., Velkova, L., Heilen, N., Sandra, K., Nikolaeva-Glomb, L., Dolashki, A., Galabov, A.S., Van Beeumen, J., Stevanovic, S., Voelter, W., Devreese, B. 2009. Identification of glycosylated sites in *Rapana* Hemocyanin by mass spectrometry and gene sequence, and their antiviral effect. *Bioconjugate Chemistry*. 20, 1315-1322.
- Dolashka, P., Velkova, L., Shishkov, S., Kostova, K., Dolashki, A., Dimitrov, I., Atanasov, B., Devreese, B., Voelter, W., Van Beeumen, J. 2010. Glycan structures and their antiviral effect of the structural subunit RvH2 of *Rapana* hemocyanin.
- Dolashki, A., Voelter, W., Dolashka, P. 2011. Phenoloxidase activity of intact and chemically modified functional unit RvH1-A from molluscan *Rapana venosa* hemocyanin. *Comparative Biochemistry and Physiology Part B*. 160, 1-7.
- Dostert, C., Jouanguy, E., Irving, P., Troxler, L., Galiana-Arnoux, D., Hetru, C., Hoffmann, J.A., Imler, J-L. 2005. The Jak-STAT signalling pathway is required but not sufficient for the antiviral response of *Drosophila*. *Nature Immunology*. 6, 946-953.

E

- El-Benna, J., My-Chan Dang, P., Gougerot-Pocidallo, M-A. 2008. Priming of the neutrophil NADPH oxidase activation: role of p47phos phosphorylation and NOX2 mobilization to the plasma membrane. *Seminars in Immunopathology*. 30, 279-289.
- Elmore, S. 2007. Apoptosis: a review of programmed cell death. *Toxicologic Pathology*. 35, 495-516.
- Emmendörffer, A., Hecht, M., Lohmann-Matthes, M-L., Roesler, J., 1990. A fast and easy method to determine the production of reactive oxygen intermediates by human and murine phagocytes using dihydrorhodamine 123. *Journal of Immunological Methods*. 131, 269-275.
- Erker, W., Schoen, A., Basche, T., Decker, H. 2004. Fluorescence labels as sensors for oxygen binding of arthropod hemocyanins. *Biochemical and Biophysical Research Communications*. 342, 893-900.

F

- Fahrenbach, W.H. 1970. The cyanoblast: hemocyanin formation in *Limulus polyphemus*. *Journal of Cell Biology*. 44, 445-453.

- Fan, T., Zhang, Y., Yang, L., Yang, X., Jiang, G., Yu, M., Cong, R. 2009. Identification and characterisation of a hemocyanin-derived phenoloxidase from the crab *Charybdis japonica*. *Comparative Biochemistry and Physiology Part B*. 152, 144-149.
- Faulhaber, L.M., Karp, R.D. 1992. A diphasic immune response against bacteria in the American cockroach. *Immunology*. 75, 378-381.
- Faurby, S., King, T.L., Obst, M., Hallerman, E.M., Pertoldi, C., Funch, P. 2010. Population dynamics of American horseshoe crabs-historic climatic events and recent anthropogenic pressures. *Molecular Ecology*. 19, 3088-3100.
- Feig, C., Peter, M.E. 2007. How apoptosis got the immune system in shape. *European Journal of Immunology*. 37, S61-70.
- Fenoll, L., Rodriguez-Lopez, J., Varon, R., Garcia-Ruiz, P., Garcia-Canovas, F., Tudela, J. 2002. Kinetic characterization of reaction mechanism of mushroom-tyrosinase on tyramine/dopamine and L-tyrosine methyl ester/L-dopa methyl ester. *International Journal of Biochemistry and Cell Biology*. 34, 1594-1607.
- Ferrandon, D., Imler, J-L., Hertu, C., Hoffmann, J.A. 2007. The *Drosophila* systemic immune response; sensing and signalling during bacterial and fungal infections. *Nature Reviews Immunology*. 7, 862-874.
- Fochetti, R., Belardinelli, M., Geurra, L., Buonocore, F., Fausto, A.M., Caporale, C. 2006. Cloning and analysis of a hemocyanin from the stonefly *Perla grandis*. *Protein Journal*. 25, 443-454.
- Fontana, R., Mendes, M.A., de Souza, B.M., Konno, K., César, L.M.M., Malaspina, O., Palma, M.S. 2004. Jelleines: a family of antimicrobial peptides from the Royal Jelly of honeybees (*Apis mellifera*). *Peptides*. 25, 919-928.
- Franc, N.C. 2002. Phagocytosis of apoptotic cells in mammals, *Caenorhabditis elegans* and *Drosophila melanogaster*: molecular mechanisms and physiological consequences. *Frontiers in Biosciences*. 7, 1298-1313.
- Frankenberg, T., Kirschnek, S., Hacker, H., Hacker, G. Phagocytosis-induced apoptosis of macrophages is linked to uptake, killing and degradation of bacteria. *European Journal of Immunology*. 38, 204-215.
- Fujieda, N., Yakiyama, A., Itoh, S. 2010a. Five monomeric hemocyanin subunits from *Portunus trituberculatus*: purification, spectroscopic characterization, and quantitative evaluation of monooxygenase activity. *Biochimica et Biophysica Acta*. 1804, 2128-2135.
- Fujieda, N., Yakiyama, A., Itoh, S. 2010b. Catalytic oxygenation of phenols by arthropod hemocyanin, an oxygen carrier protein, from *Portunus trituberculatus*. *Dalton Transactions*. 39, 3083-3092.
- Fukuzawa, A.H., Vellutini, B.C., Lorenzini, D.M., Silva Jr., P.I., Mortara, R.A., da Silva, J.M.C., Daffre, S. 2008. The role of hemocytes in the immunity of the spider *Acanthoscurria gomesiana*. *Developmental and Comparative Immunology*. 32, 716-725.

G

- Garcia-Carreño, F.L., Cote, K., Navarrete Del Toro, M.A. 2008. Phenoloxidase activity of hemocyanin in whiteleg-shrimp *Penaeus vannamei*: conversion, characterisation of catalytic properties, and role in post mortem melanosis. *Journal of Agricultural and Food Chemistry*. 56, 6454-6549.
- Garcia-García, E., Prado-Alvarez, M., Novoa, B., Figueras, A., Rosales, C. 2008. Immune response of mussel hemocyte subpopulations are differentially regulated by enzymes of the PI 3-K, PKC and ERK kinase families. *Developmental and Comparative Immunology*. 32, 637-653.
- Garin, J., Diez, R., Kieffer, S., Dermine, J.-F., Duclos, S., Gagnon, E., Sadoul, R., Rondeau, C., Desjardins, M., 2001. The phagosome proteome: insight into phagosome functions. *Journal of Cell Biology*. 152 (1), 165–180.
- Georgieva, D.N., Stoeva, S., Abid Ali, S., Abbasi, A., Genov, N., Voelter, W. 1998. Circular dichroism study of hemocyanin thermostability. *Spectrochimica Acta Part A*. 54, 765–771.
- Gillespie, J.P., Kanost, M.R., Trenczek, T. 1997. Biological mediators of insect immunity. *Annual Review of Entomology*. 42, 611-643.
- Gimenez, B., Martínez-Alvarez, O., Montero, P., Gómez-Guillén, M.C. 2010. Characterisation of phenoloxidase activity of carapace and viscera from cephalothorax of Norway lobster (*Nephrops norvegicus*). *LWT-Food Science and Technology*. 43, 1240-1245.
- Goimier, Y., Pascual, C., Sánchez, A., Gaxiola, G., Sánchez, A., Rosas, C. 2006. Relation between reproductive, physiological, and immunological condition of *Litopenaeus setiferus* pre-adult males fed different dietary protein levels (Crustacea; Penaeidae). *Animal Reproduction Science*. 92, 193–208.
- Goyette, G., Boulais, J., Carruthers, N.J., Landry, C.R., Jutras, I., Duclos, S., Dermine, J.-F., Michnick, S.W., and others. 2012. Proteomic characterisation of the phagosomal membrane microdomains during phagolysosome biogenesis and evolution. *Molecular and Cellular Proteomics*. In press.
- Grimsley, C., Ravichandran, K.S. 2003. Cues for apoptotic cell engulfment: eat me, don't eat me and come get me signals. *Trends in Cell Biology*. 13, 648-656.
- Guo, D., Zhang, Y., Zeng, D., Wang, H., Li, X., Li, Y., Fan, X. 2009. Functional properties of hemocyanin from *Oncomelania hupensis* the intermediate host of *Schistosoma japonicum*. *Experimental Parasitology*. 123, 277-281.
- Gupta, A.P. 1997. Plasma membrane specialisations in resting, stimulated and phagocytosing arthropod (*Limulus Polyphemus*, *Gromphadorhina portentosa* and *Blattella germanica*) immunocytes: structural and functional analogies with those of vertebrate macrophages and neutrophils. *Tissue and Cell*. 29, 365–373.
- Gupta, A.P., Campenot, E.S. 1996. Cytoskeletal F-actin polymerization from cytosolic G-actin occurs in phagocytosing immunocytes of arthropods (*Limulus polyphemus* and *Gromphadorhina portentosa*): does [cAMP]_i play any role? *Journal of Invertebrate Pathology*. 68, 118–130.
- Gupta, A.P., Orenberg, S.D., Das, Y.T., Chattopadhyay, S.K. 1991. Lectin- binding receptors, Na⁺ and K⁺-ATPase, and acetylcholinesterase on immunocytes plasma membrane of *Limulus polyphemus*. *Experimental Cell Research*. 194, 83–89.

H

- Hagner-Holler, S., Schoen, A., Erker, W., Marden, J.H., Rupprecht, R., Decker, H., Burmester, T. 2004. A respiratory hemocyanin in insects. *Proceedings of the National Academy of Sciences, USA*. 101, 871-874.
- Haine, H.R., Moret, Y., Siva-jothy, M.T., Rolff, J. 2008. Anti-microbial peptide defence and persistent infection in insects. *Science*. 322, 1257-1559.
- Hanahan, D., Weinberg, R.A. 2000. The hallmarks of cancer. *Cell*. 100, 57-70.
- Harrington, J.M., Leippe, M., Armstrong, P.B. 2008. Epithelial immunity in a marine invertebrate: a cytolytic activity from cuticular secretion of the American horseshoe crab, *Limulus polyphemus*. *Marine Biology*. 153, 1165-1171.
- Harris, R.W., Sims, P.J., Tweten, R.K. 1991. Evidence that *Clostridium perfringens* theta-toxin induces colloid-osmotic lysis of erythrocytes. *Infection and Immunity*. 59, 2499-2501.
- Harvard, S., Doury, G., Ravallec, M., Brehelin, M., Prevost, G., Eslin, P. 2012. Structural and functional characterization of pseudopodocyte, a shaggy immune cell produced by two *Drosophila* species of the *obscura* group. *Developmental and Comparative Immunology*. 36, 323-331.
- Havanapan, P., Kanlaya, R., Bourchookarn, A., Krittanai, C., Thongboonkerd, V. 2009. C-terminal hemocyanin from hemocytes of *Penaeus vannamei* interacts with ERK 1/2 and undergoes serine phosphorylation. *Journal of Proteome Research*. 8, 2476-2483.
- Hazes, B., Magnus, K., Bonaventura, C., Bonaventura, J., Dauter, Z., Kall, K., Hol, W. 1993. Crystal structure of deoxygenated *Limulus polyphemus* subunit two hemocyanin at 2.18 Å resolution, clues for a mechanism of allosteric regulation. *Protein Science*. 2, 597-619.
- Hengartner, M.O. 1996. Programmed cell death in invertebrates. *Current Opinion in Genetics and Development*. 6, 34-38.
- Hengartner, M.O. 2000. The biochemistry of apoptosis. *Nature*. 407, 770-776.
- Hillman, M.R. 2004. Strategies and mechanisms for host and pathogen survival in acute and persistent viral infections. *Proceedings of the National Academy of Sciences, USA*. 101, 14560-14566.
- Hoffmann, J.A. 2003. The immune response of *Drosophila*. *Nature*. 426, 33-38.
- Hong, L., Dearolf, C.R. 2001. The JAK-STAT pathway and *Drosophila* development. *Bioessays*. 23, 1138-1147.
- Hristova, R., Dolashki, A., Voelter, W., Stevanovic, S., Dolashka-Angelova, P. 2008. o-Diphenol oxidase activity of molluscan hemocyanins. *Comparative Biochemistry and Physiology Part B*. 149, 439-446.
- Hsu, J.-P., Huang, C., Liao, C.-M., Hsuan, S.-L., Hung, H.-H., Chien, M.-S. 2005. Engulfed pathogen-induced apoptosis in haemocytes of giant freshwater prawn, *Macrobrachium rosenbergii*. *Journal of Fish Diseases*. 28, 729-735.
- Hu, M., Youji, W., Tsang, S.T., Cheung, S.G., Shin, P.K.S. 2011. Effect of starvation on the energy budget of two Asian horseshoe crab species: *Tachypleus*

tridentatus and *Carcinoscorpius rotundicauda* (Chelicerata: Xiphosura). *Marine Biology*. 158, 1591–1600.

- Hurton, L.V., Berkson, J.M., Smith, S.A. 2005. Selection of a standard culture medium for primary culture of *Limulus polyphemus* amebocytes. *In Vitro Cellular & Developmental Biology-Animal*. 41, 325–329.

I

- Idakieva, K., Islam-Siddiqui, N., Meersman, F., De Maeyer, M., Chakarska, I., Gielena, C. 2009. Influence of limited proteolysis, detergent treatment and lyophilisation on the phenoloxidase activity of *Rapana thomasiana* hemocyanin. *International Journal of Biological Macromolecule*. 45, 181-187.
- Idakieva, K., Raynova, Y., Meersman, F., Gielens, C. 2013. Phenoloxidase activity and thermostability of *Cancer pagarus* and *Limulus polyphemus* hemocyanin. *Comparative Biochemistry and Physiology Part B*. 164, 201-209.
- Ikonomou, L., Schneider, Y.J., Agathos, S.N. 2003. Insect cell culture for industrial production of recombinant proteins. *Applied Microbiology and Biotechnology*. 62, 1–20.
- Inamori, K., Ariki, S., Kawabata, S. 2004. A Toll-like receptor in horseshoe crabs. *Immunological Reviews*. 198, 106-115.
- Ismaya, W.T., Rozeboom, H.J., Weijn, A., Mes, J.J., Fusetti, F., Wichers, H.J., Dijkstra, B.W. 2011. Crystal Structure of *Agaricus bisporus* Mushroom Tyrosinase: Identity of the Tetramer Subunits and Interaction with tropolone. *Biochemistry*. 50, 5477-5486.
- Iwanaga, S. 2002. The molecular basis of innate immunity in the horseshoe crab. *Current Opinion in Immunology*. 14, 87–95.
- Iwanaga, S., Lee, B.L. 2005. Recent advances in the innate immunity of invertebrate animals. *Journal of Biochemistry and Molecular Biology*. 38, 128–150.

J

- Jakobsen, P.P., Suhr-Jessen, P. 1990. The horseshoe crab *Tachypleus tridentatus* has two kinds of hemocytes: granulocytes and plasmatocytes. *Biological Bulletin*. 178, 55-64
- Jaenicke, E., Büchler, K., Markl, J., Decker, H., Barends, T. 2010. The cupredoxin-like domains in hemocyanins ***Biochemical Journal*. 426, 373-378**
- Jaenicke, E., Decker, H. 2003. Tyrosinases from crustaceans form hexamers. *Biochemical Journal*. 371, 515-523.
- Jaenicke, E., Decker, H. 2004. Conversion of crustacean hemocyanin to catechol-oxidase. *Micron*. 35, 89-90.

- Jaenicke, E., Decker, H. 2008. Kinetic properties of catecholoxidase activity of tarantula hemocyanin. *FEBS Journal*. 275, 1518-1528.
- Jaenicke, E., Foll, R., Decker, H. 1999. Spider hemocyanin binds ecdysone and 20-OH-ecdysone. *Journal of Biological Chemistry*. 274, 34,267–34,271.
- Jaenicke, E., Fraune, S., May, S., Irmak, P., Augustin, R., Meesters, C., Decker, H., Zimmer, M. 2009. Is activated hemocyanin instead of phenoloxidase involved in the immune response in woodlice? *Developmental and Comparative Immunology*. 33, 1055-1063.
- Jiang, N., Tan, N.S., Ho, B., Ding, J.L. 2007. Respiratory protein generated reactive oxygen species as an antimicrobial strategy. *Nature Immunology*. 8, 1114 – 1122.
- Jiravanichpaisal, P., Lee, B.L., Soderhall, K. 2006. Cell-mediated immunity in arthropods: Hemoatopoiesis, coagulation, melanisation and opsonisation. *Immunobiology*. 211, 213-236.
- Jones, K. Hughes, J., Hong, M., Jia, Q., Orndorff, S. 2002. Modulation of melanogenesis by Aloesin: a competitive inhibitor of tyrosinase. *Pigment Cell Research*. 15, 335-340.

K

- Kanduc, D., Mittelman, A., Serpico, R., Sinigaglia, E., Sinha, A.A., Natale, C., Santacroce, R., Grazia Di Corcia, M., Lucchese, A., Dini, L., Pani, P., Santacroce, S., Simone, S., Bucci, R., Farber, E. 2002. Cell death: apoptosis versus necrosis. *International Journal of Oncology*. 21, 165-170.
- Kanost, M.R., Jiang, H., Yu, X-Q. 2004. Innate immune response of a lepidopteran insect, *Manduca sexta*. *Immunology Reviews*. 198, 97-105.
- Kavanagh, K., Reeves, E.P. 2004. Exploiting the potential of insects for in vivo pathogenicity testing of microbial pathogens. *FEMS Microbiology Reviews*. 28, 101-112.
- Kawabata, S., Koshiha, T., Shibata, T. 2009. The lipopolysaccharide-activated innate immune response network of the horseshoe crab. *Invertebrate Survival Journal*. 6, 59–77.
- Kerr, J.F., Wylie, A.H., Currie, A.R. 1972. Apoptosis: a basic biological phenomenon with wide-ranging implications in tissue kinetics. *British Journal of Cancer*. 26, 239-257.
- Khan, M.T.H. 2012. Novel tyrosinase inhibitors from natural resources-their computational studies. *Current Medicinal Chemistry*. 19, 2262-2272.
- Kim, S.G., Jung, B.W., Kim, H.H. 2011. Hemocyanin-derived phenoloxidase activity with broad temperature stability extending into the cold environment in hemocytes of the hair crab *Erimacrus isenbeckii*. *Comparative Biochemistry and Physiology Part B*. 159, 103-108.
- Kim, J., Marshall, M.R., Wei, C. 2000a. Polyphenoloxidase. In F. Norman and K. Benjamin (Eds.), *Seafood Enzymes. Utilization and influence on post-harvest seafood quality* (pp. 271-315). New York: Marcel Decker.

- Kim, S.K., Hebrok, M., Li, E., Oh, S.P., Schrewe, H., Harmon, E.B., Lee, J.S. and Melton, D.A. 2000b. Activin receptor patterning of fore-gut organogenesis. *Genes and Development*. 14, 1866-1871.
- Koizumi, N., Imai, Y., Morozumi, A., Imamura, M., Kadotani, T., Yaoi, K., Iwahana, H., Sato, R. 1999. Lipopolysaccharide binding of *B. mori* participates in hemocytic defence reaction against gram-negative bacteria. *Journal of Insect Physiology*. 45, 853-859.
- Koshiba, T., Hashii, T., Kawabata, S. 2007. A structural perspective on the interaction between lipopolysaccharide and Factor C, a receptor involved in recognition of Gram-negative bacteria. *Journal of Biological Chemistry*. 282, 3962-3967.
- Kroemer, G., Galluzzi, L., Vandenabeele, P., Abrams, J., Alnemri, E.S., Baehrecke, E.H., Blagosklonny, M.V., El-Deiry, W.S., Golstein, P. and others. 2009. Classification of cell death: recommendations of the nomenclature committee on cell death 2009. *Cell Death and Differentiation*. 16, 3-11.
- Krzyzowska, M., Schollenberger, A., Skierski, J., Niemiałowski, M. 2002. Apoptosis during *ectromelia orthopoxvirus* infection is DEVDase dependent: *in vitro* and *in vivo* studies *Microbes and Infection*. 4, 599-611.
- Kurata, S., Ariki, S., Kawabata, S. 2006. Recognition of pathogens and activation of immune responses in *Drosophila* and horseshoe crab innate immunity. *Immunobiology*. 211, 237-249.

L

- Lavine, M.D., Strand, M.R. 2002. Insect hemocytes and their role in immunity. *Insect Biochemistry and Molecular Biology*. 32, 1295-1309.
- Lavrov D.V., Boore, J.L., Brown W.M. 2000. The complete mitochondrial DNA sequence of the horseshoe crab *Limulus polyphemus*. *Molecular Biology and Evolution*. 17, 813-824.
- Le Moullac, G., Haffner, P. 2000. Environmental factors affecting immune responses in Crustacea. *Aquaculture*. 191, 121-131.
- Lee, C.N., Morton, B. 2009. Emergence behaviour of *Tachypleus tridentatus* under simulated tidal conditions in the laboratory and at two different sediment temperatures. In: Tanacredi, J.T., Botton, M.L., Smith, D.R. (Eds.), *Biology and Conservation of Horseshoe Crabs*. Springer, New York, pp. 275-283.
- Lee, S.H., Meng, X.W., Flatten, K.S., Loegering, D.A., Kaufmann, S.H. 2012. Phosphatidylserine exposure during apoptosis reflects bidirectional trafficking between plasma membrane and cytoplasm. *Cell Death and Differentiation*. 1-13.
- Lee, S.Y., Lee, B.L., Söderhäll, K. 2003. Processing of an antimicrobial peptide from hemocyanin of the freshwater crayfish *Pacifastacus leniusculus*. *Journal of Biological Chemistry*. 278, 7927 - 7933.

- Lee, S.Y, Lee, B.L., Soderhall, K. 2004. Processing of crayfish hemocyanin subunits into phenoloxidase. *Biochemical and Biophysical Research Communications*. 322, 490-496.
- Lei, K., Li, F., Zhang, M., Yang, H., Luo, T., Xu, X. 2008. Difference between hemocyanin subunits from shrimp *Penaeus japonicus* in anti-WSSV defence. *Developmental and Comparative Immunology*. 32, 808 – 813.
- Lemaitre, B., Hoffmann, J. 2007. The host defence of *Drosophila melanogaster*. *Annual Review of Immunology*. 25, 697-743.
- Lemaitre, B., Nicolas, E., Michaut, L., Reichhart, J-M., Hoffmann, J.A. 1996. The dorsoventral regulatory gene cassette *spätzle/Toll/cactus* controls the potent antifungal response in *Drosophila* Adults. *Cell*. 86, 973-983.
- Lemaitre, B., Reichhart, J.M., Hoffmann, J.A. 1997. *Drosophila* host defence, differential induction of AMP genes after infection by various classes of microorganisms. *Proceedings of the National Academy of Science, U.S.A.* 94, 14614-14619.
- Leulier, F., Rodriguez, A., Khush, R.M., Abrams, J.M., Lemaitre, B. 2000. The *Drosophila* caspase DREDD is required to resist gram-negative bacterial infection. *EMBO Reports*. 4, 353-358.
- Levin, J., Bang, F.B. 1968. Clottable protein in *Limulus*: its localization and kinetics of its coagulation by endotoxin. *Thrombosis et Diathesis Haemorrhagica*. 19, 186–197.
- Levin, J. 1988. The horseshoe crab: a model for Gram-negative infection in marine organisms and humans. *Progress in Clinical and Biological Research*. 272, 3-15.
- Li, D., Scherfer, C., Korayem, A.M., Zhao, Z., Schmidt, O., Theopold, U. 2002. Insect hemolymph clotting, evidence for interaction between the coagulation system and the pro-phenoloxidase activating cascade. *Insect Biochemistry and Molecular Biology*. 32, 919-928.
- Li, F., Xiang, J. 2012. Signalling pathways regulating innate immune responses in shrimp. *Fish and Shellfish Immunology*. <http://dx.org/10.1016/j.fsi.2012.08.023>.
- Li, Y., Wang, Y., Jiang, H., Deng, J. 2009. Crystal structure of *Manduca sexta* prophenoloxidase provides insights into the mechanism of type-3 copper enzymes. *Proceedings of the National Academy of Sciences, USA*. 106, 17002 – 17006.
- Lieb, B., Altenhein, B., Markl, J. 2000. The Sequence of a Gastropod Hemocyanin (HtH1 from *Haliotis tuberculata*). *Journal of Biological Chemistry*. 275, 5675-5681.
- Liu, G., Yang, L., Fan, T., Cong, R., Tang, Z., Sun, W., Meng, X., & Zhu, L. 2006. Purification and characterization of phenoloxidase from crab *Charybdis japonica*. *Fish and Shellfish Immunology*. 20, 47-57.

M

- MacPherson, J.C., Pavlovich, J.G., Jacobs, R.S. 1998. Phospholipid composition of the granular amebocyte from the horseshoe crab, *Limulus polyphemus*. *Lipids*. 33, 931 – 940.
- McLean, J.E., Ruck, A., Shirazian, S., Pooyaei-Mehr, F., Zakeri, Z.F. 2008. Viral manipulation of cell death. *Current Pharmaceutical Design*. 14, 198-220.
- Magnus, K., Hazes, B., Ton-That, H., Bonaventura, C., Bonaventura, J., Hol, W. 1994. Crystallographic analysis of oxygenated and deoxygenated states of arthropod hemocyanin shows unusual differences. *Proteins*. 19, 302-309.
- Manfredini, F., Benati, D., Beani, L. 2010. The strepsipteran endoparasite *Xenos vesparum* alters the immunocompetence of its host, the paper wasp *Polistes dominulus*. *Journal Insect Physiology*. 56, 253–259.
- Mangum, C.P., Ricci, J. 1989. The influence of temperature on O₂ uptake and transport in the horseshoe crab *Limulus polyphemus* L. *Journal of Experimental Marine Biology and Ecology*. 129, 243–250.
- Martin, C.J. Booty, M.G., Rosebrock, T.R., Nunes-Alves, C., Desjardins, D.M., Keren, I., Fortune, S.M., Remold, H.G., Behar, S.M. 2012. Efferocytosis is an innate antibacterial mechanism. *Cell Host and Microbe*. 12, 289-300.
- Martinez-Alvarez, O., Gomez-Guillen, C., Montero, P. 2008. Presence of hemocyanin with diphenoloxidase activity in deepwater pink-shrimp (*Parapenaeus longirostris*) post mortem. *Food Chemistry*. 107, 1450-1460.
- Matozzo, V., Gallo, C., Marin, M.G. 2011. Effects of temperature on cellular and biochemical parameters in the crab, *Carcinus aestuarii* (Crustacea, Decapoda). *Marine Environmental Research*. 71, 351–356.
- Meister, M. 2004. Blood cells of *Drosophila*: cell lineage and role in host defence. *Current Opinion in Immunology*. 16, 10-15.
- Menze, M.A., Fortner, G., Nag, S., Hand, S.C. 2010. Mechanisms of apoptosis in crustacea: what conditions induce versus suppress cell death? *Apoptosis*. 15, 293-312.
- Miller, J.S., Nguyen, T., Stanley-Samuels, D.W. 1994. Eicosanoids mediate insect nodulation in response to bacterial infection. *Proceedings of the National Academy of Science, U.S.A.* 91, 12418-12422.
- Montero, P., Avalos, A., Perez-Mateos, M. 2001. Characterization of Polyphenoloxidase of prawns (*Penaeus japonicus*). Alternatives to inhibition: additives and high pressure-treatment. *Food Chemistry*. 75, 317-324.
- Mora, C., Tittensor, D.P., Adl, S., Simpson, A.G.B., Worm, B. 2011. How many species are there on earth and in the ocean? *Plos Biology*. 9 (e1001127), 1-8.
- Moret, Y., Siva-Jothy, M.T. 2003. Adaptive innate immunity? Responsive mode prophylaxis in the mealworm beetle, *Tenebrio molitor*. *Proceedings of the Royal Society B*. 270(1532), 2475-2480.
- Morioka, C., Tachi, Y., Suzuki, S., Itoh, S. 2006. Significant enhancement of monooxygenase activity of oxygen carrier protein hemocyanin by Urea. *Journal of the American Chemical Society*. 128, 6788-6789.

- Mowlds, P., Coates, C., Renwick, J., Kavanagh, K. 2010. Dose dependent cellular and humoral responses in *Galleria mellonella* larvae following β -glucan inoculation. *Microbes and Infection*. 12, 146-153.
- Mydlarz, L.D., Jones, L.E., Harvell, C.D. 2006. Innate immunity, environmental drivers, and disease ecology of marine and freshwater invertebrates. *Annual Reviews Ecology Evolution and Systematics*. 37, 251–288.

N

- Nagai, T., Kawabata, S. 2000. A link between blood coagulation and prophenoloxidase activation in the arthropod host defence. *Journal of Biological Chemistry*. 275, 29264 – 29267.
- Nagai, T., Osaki, T., Kawabata, S. 2001. Functional conversion of hemocyanin to phenoloxidase by horseshoe crab antimicrobial peptides. *Journal of Biological Chemistry*. 276, 27166 – 27170.
- Nakahara, A., Suzuki, S., Kino, J. 1983. Tyrosinase activity of squid hemocyanin. *Life Chemistry Reports*. 1, 319-322.
- Nehme, N.T., Liegeois, S., Kele, B., Giammarinaro, P., Pradel, E., Hoffmann, J.A., Ewbank, J.J., Ferrandon, D. 2007. A model of bacterial intestinal infection in *Drosophila melanogaster*. *PLOS Pathogens*. 3, 1694-1709.
- Nelliappan, K., Sugumaran, M. 1996. On the presence of prophenoloxidase in the hemolymph of the horseshoe crab, *Limulus*. *Comparative Biochemistry and Physiology Part B*. 113, 163-168.
- Nillius, D., Jaenicke, E., Decker, H. 2008. Switch between tyrosinase and catecholoxidase activity of scorpion hemocyanin. *FEBS Letters*. 582, 749–754.
- Nirmal, N.P., Benjakul, S. 2009. Melanosis and quality changes of Pacific white shrimp (*Litopenaeus vannamei*) treated with catechin during iced storage. *Journal of Agricultural and Food Chemistry*. 57, 3578-3586.
- Nonaka, M. 2011. The complement C3 protein family in invertebrates. *Invertebrate Survival Journal*. 8, 21-32.
- Noonin, C., Lin, X., Jiravanichpaisal P., Soderhall, K., Soderhall, I. 2012. Invertebrate hemoatopoiesis: an anterior proliferation center as a link between the hematopoietic tissue and the brain. *Stem Cells and Development*. doi:10.1089/scd.2012.0077.
- Novitsky, T.J. 1984. Discovery to commercialisation: the blood of the horseshoe crab. *Oceanus*. 27, 13–18.

O

- Ohta, M., Ito, H., Masuda, K., Tanaka, S., Arakawa, Y., Wacharotayankun, R., Kato, N. 1992. Mechanisms of antibacterial action of tachyplexins and polyphemusins, a group of antimicrobial peptides isolated from horseshoe crab hemocytes. *Antimicrobial Agents and Chemotherapy*. 36(7), 1460-1465.

- Oliver, J.D., Loy, J.D., Parikh, G., Bartholomay, L. 2011. Comparative analysis of hemocyte phagocytosis between six species of arthropods as measured by flow cytometry. *Journal of Invertebrate Pathology*. 108, 126–130.

P

- Pan, D., He, N., Yang, Z., Haipeng, L., Xun, X. 2005. Differential gene expression profile of WSSV resistant shrimp (*Penaeus japonicus*) by suppression subtraction hybridisation. *Developmental and Comparative Immunology*. 29, 103-112
- Pan, J.-Y., Zhang, Y.-L., Wang, S.-Y., Peng, X.-X. 2008. Dodecamer is required for agglutination of *Litopenaeus vannamei* hemocyanin with bacterial cells and red blood cells. *Marine Biotechnology*. 10, 645–652.
- Pascual, C., Sánchez, A., Sánchez, A., Vargas-Albores, F., Le Moullac, G., Rosas, C. 2003. Haemolymph metabolic variables and immune response in *Litopenaeus setiferus* adult males: an effect of an extreme temperature. *Aquaculture*. 218, 637–650.
- Paterson, W.D., Stewart, J.E. 1973. *In vitro* phagocytosis by hemocytes of the American lobster (*Homarus americanus*). *Journal of the Fisheries Research Board of Canada*. 31, 1051–1056.
- Paul, R.J., Pirow, R. 1998. The physiological significance of respiratory proteins in invertebrates. *Zoology*. 100, 298–306.
- Peng, W., Jiang, J., Wang, J., Ding, X. 2010. Effect of physiochemical factors on phenoloxidase activity of hemocyanin from abalone *Haliotis diversicolor*. *South China Fisheries Science*. DOI; CNKI:SUN:NFSC.02010-02-001.
- Perdomo-Morales, R., Montero-Alejo, V., Perera, E., Pardo-Ruiz, Z., Alonso-Jimenez, E. 2008. Hemocyanin-derived phenoloxidase activity in the spiny lobster *Panulirus argus* (Latreille, 1804). *Biochimica et Biophysica Acta* 1780, 652-658.
- Pick, C., Hagner-Holler, S., Burmester, T. 2008. Molecular characterization of hemocyanin and hexamerin from the firebrat *Thermobia domestica* (Zygentoma). *Insect Biochemistry and Molecular Biology*. 38, 977- 983.
- Pick, C., Schneuer, M., Burmester, T. 2009. The occurrence of hemocyanin in hexapoda. *FEBS Journal*. 276, 1930-1941.
- Pick, C., Schneuer, M., Burmester, T. 2010. Ontogeny of hemocyanin in the ovoviviparous cockroach *Blaptica dubia* suggests an embryo specific role in oxygen supply. *Journal of Insect Physiology*. 56, 455-460.
- Pless, D.D., Aguilar, M.B., Falcon, A., Lozano-Alvarez, E., Heimer de la Cotera, E.P. 2003. Latent phenoloxidase activity and N-terminal amino acid sequence of hemocyanin from *Bathynomus giganteus*, a primitive crustacean. *Archives of Biochemistry and Biophysics*. 409, 402-410.
- Pope, E.C., Powell, A., Roberts, E.C., Shields, R.J., Wardle, R., Rowley, A.F. 2011. Enhanced cellular immunity in shrimp (*Litopenaeus vannamei*) after vaccination. *Plos one*. 6, 1–7.

- Price, C.D., Ratcliffe, N.A. 1974. A reappraisal of insect hemocyte classification by examination of the blood from fifteen insect orders. *Z Zellforsch.* 147, 537-549.

Q

R

- Radomski, M.W., Martin, J.F., Moncada, S. 1991. Synthesis of nitric oxide by haemocytes of the American horseshoe crab (*Limulus polyphemus*). *Philosophical Transactions of the Royal Society; Biological Sciences.* 334, 129-133.
- Ratner, S., Vinson, S.B. 1983. Phagocytosis and encapsulation: cellular immune responses in Arthropoda. *American Zoologist.* 23, 185-194.
- Rattanarojpong, T., Wang, H-C., Lo, C-F., Flegel, T.W. 2007. Analysis of differentially expressed proteins and transcripts in gills of *Penaeus vannamei* after yellow head virus infection. *Proteomics.* 7, 3809-3814.
- Ravi, M., Nazeer Basha, A., Taju, G., Ram Kumar, R., Sahul Hameed, A.S. 2010. Clearance of *Macrobrachium rosenbergii* nodavirus (MrNV) and extra small virus (XSV) and immunological changes in experimentally injected *Macrobrachium rosenbergii*. *Fish and Shellfish immunology.* 28, 428-433.
- Remijnen, Q., Kuijpers, T.W., Wirawan, E., Lippens, S., Vandenabeele, P., Vanden Berghe, T. 2011. *Cell Death and Differentiation.* 18, 581-588.
- Renwick, J., Reeves, E.P., Wientjes, F.B., Kavanagh, K. 2007. Translocation of proteins homologous to human neutrophil p47phox and p67phox to the cell membrane in activated hemocytes of *Galleria mellonella*. *Developmental and Comparative Immunology.* 27, 661-672.
- Ricklin, D., Hajishengallis, G., Yang, K., Lambris, J.D. 2010. Complement: A key system for immune surveillance and homeostasis. *Nature Immunology,* 11, 785-797.
- Rinkevich, B. 2005. Marine invertebrate cell cultures: new millennium trends. *Marine Biotechnology.* 7, 429-439.
- Rinkevich, B. 2011. Cell cultures from marine invertebrates; new insights for capturing endless stemness. *Marine Biotechnology.* 13, 345-354.
- Robb, C.T., Dyrzynda, E.A., Rossi, A.G., Smith, V.J. 2012. Extracellular chromatin traps are an ancient eukaryotic cellular defence strategy. *Oral presentation at 12th International Society of Developmental and Comparative Immunology conference, Fukuoka, Japan.*
- Robertson, J.D., 1970. Osmotic and ionic regulation in the horseshoe crab, *Limulus polyphemus* (Linnaeus). *Biological Bulletin.* 138, 157-183.
- Rosales, C. 2011. Phagocytosis, a cellular immune response in insects. *Invertebrate Survival Journal.* 8, 109- 131.

- Roulston, C., Smith, V.J. 2011. Isolation and *in vitro* characterisation of prohaemocytes from the spider crab, *Hyas araneus*. *Developmental and Comparative Immunology*. 35, 537-544.
- Rowley, A.F., Powell, A. 2007. Invertebrate immune systems—specific, quasi-specific or nonspecific? *Journal of Immunology*. 179, 7209-7214.
- Roxström-Lindquist, K., Terenius, O., Faye, I. 2004. Parasite specific immune responses in *Drosophila melanogaster*, a genomic study. *EMBO Reports*. 5, 207-212.
- Ruediger, R.F., Davis, D.J. 1907. Phagocytosis and opsonins in lower animals. *Journal of Infectious Diseases*. 4, 333–336.

S

- Salvato, B., Jori, G., Piazzese, A., Ghiretti, F., Beltramini, M., Lerch, K. 1983. Enzymatic activities of type 3 copper pair in *Octopus vulgaris* hemocyanin. *Life Chemistry Reports*. 1, 313-317.
- Salvato, B., Santamaria, M., Beltramini, M., Alzuet, G., Casella, L. 1998. The enzymatic properties of Octopus Vulgaris hemocyanin, o-diphenol oxidase activity. *Biochemistry*. 347, 14065-14077.
- Sanchez, D., Ganfornina, M.D., Gutierrez, G., Bastiani, M.J. 1998. Molecular characterisation and phylogenetic relationships of protein with potential oxygen-binding capabilities in the grasshopper embryo. A hemocyanin in insects? *Molecular Biology and Evolution*. 15, 415-426.
- Schreibman, M.P., Zarnoch, C.B. 2009. Aquaculture methods and early growth of juvenile horseshoe crabs (*Limulus polyphemus*). In: Tanacredi, J.T., Botton, M.L., Smith, D.R. (Eds.), *Biology and Conservation of Horseshoe Crabs*. Springer, New York, pp. 501–511.
- Sedmak, J.J., Grossberg, S.E. 1977. A rapid, sensitive and versatile assay for protein using coomassie brilliant blue G250. *Analytical Biochemistry*. 79, 544-552.
- Sendovski, M., Kanteev, M., Ben-Yosef, V.S., Adir, N., Fishman, A. 2011. First Structures of an Active Bacterial Tyrosinase Reveal Copper Plasticity. *Journal of Molecular Biology*. 405, 227-237.
- Serda, R.E., Gu, J., Burks, J.K., Ferrari, K., Ferrari, C., Ferrari, M. 2009. Quantitative mechanics of endothelial phagocytosis of silicon microparticles. *Cytometry. Part A*. 75A, 752-760.
- Sherman, R.G. 1981. Chelicerates. In: Ratcliffe, N.A., Rowley, A.F. (Eds.), *Invertebrate Blood Cells*. Academic Press, New York, pp. 335–384.
- Shi, X-Z., Li, X-C., Wang, S., Zhao, X-F., Wang, J-X. 2010. Transcriptome analysis of hemocytes and hepatopancreas in red swamp crayfish, *Procambarus clarkii*, challenged with white spot syndrome virus. *Invertebrate Survival Journal*. 7, 119-131.

- Siddiqui, N.I., Akosung, R.F., Gielens, C. Location of intrinsic and inducible phenoloxidase activity in molluscan hemocyanin. *Biochemical and Biophysical Research Communications*. 348, 1138-1144.
- Silverman, N., Paquette, N., Aggarwal, K. 2009. Specificity and signalling in the *Drosophila* immune response. *Invertebrate Survival Journal*. 6, 163-174.
- Smagghe, G., Goodman, C.L., Stanley, D. 2009. Insect cell culture and applications to research and pest management. *In vitro Cell and Developmental Biology, Animal*. 45, 93-105.
- Smith, V.J. 2010. Immunology of invertebrates: cellular. *Encyclopedia of life sciences*. John Wiley and Sons, Ltd: Chicester.
- Smith, V.J., Desbois, A.P., Dyrzynda, E.A. 2010. Conventional and unconventional antimicrobials from fish: marine invertebrates and microalgae. *Marine Drugs*. 8, 1213-1262.
- Smith, V.J., Ratcliffe, N.A. 1978. Host defence reactions of the shore crab, *Carcinus maenas* (L.), *in vitro*. *Journal of the marine biological association of the U.K.* 58, 367- 379.
- Smith, S.A., Berkson, J. 2005. Laboratory culture and maintenance of the horseshoe crab (*Limulus polyphemus*). *Laboratory Animal*. 34, 27-34.
- Söderhäll, K., Cerenius L. 1998. Role of phenoloxidase activating system in invertebrate immunity. *Current Opinion in Immunology*. 10, 23-28.
- Söderhäll, K., Smith, V.J. 1983. Separation of the haemocyte populations of *Carcinus maenas* and other marine decapods, and prophenoloxidase distribution. *Developmental and Comparative Immunology*. 7, 229-239.
- Sokolova, I.M. 2009. Apoptosis in molluscan immune defense. *Invertebrate Survival Journal*. 6, 49-58.
- Stace, C.L., Ktistakis, N.T. 2006. Phosphatidic acid-and phosphatidylserine-binding proteins. *Biochimica et Biophysica Acta*. 1761, 913 - 926.
- Stagner, J.I., Redmond, J.R., 1975. The immunological mechanism of the horseshoe crab, *Limulus polyphemus*. *Marine Fisheries Review*. 37, 11-19.
- Stanley-Samuelson, D.W., Jensen, E., Nickerson, K.W., Tiebel, K., Ogg, C.L., Howard, R.W. 1991. Insect immune response to bacterial infection is mediated by eicosanoids. *Proceedings of the National Academy of Science, U.S.A.* 88, 1064-1068.
- Steiner, M., Scaife, A., Semple, S., Hulks, G., Ayres, J.G. 2008. Sodium metabisulphite induced airways disease in the fishing and fish-processing industry. *Occupational medicine-Oxford*. 58, 545-550.
- Sterner, R., Vogl, T., Hinz, H.-J., Penz, F., Hoff, R., Föll, R., Decker, H. 1995. Extreme thermostability of tarantula hemocyanin. *FEBS Letters*. 364, 9-12.
- Strand, M.R. 2008. The insect cellular immune response. *Insect Science*. 15, 1-14.
- Strand, M.R., Clark, K.D. 1999. Plasmatocyte spreading peptide induces spreading of plasmatocytes but represses spreading of granulocytes. *Archives of Insect Biochemistry and Physiology*. 42, 213-223.

- Sugumaran, M., Nellaiappan, K. 1990. On the latency and nature of phenoloxidase present in the left colleterial gland of the cockroach *Periplaneta americana*. *Archives of Insect Biochemistry and Physiology*. 15, 165 – 181.
- Sugumaran, M., Nellaiappan, K. 1991. Lysolecithin - a potent activator of prophenoloxidase from the hemolymph of the lobster, *Homarus americanus*. *Biochemical and Biophysical Research Communications*. 176, 1371 – 1376.
- Suhr-Jessen, P., Baek, L., Jakobsen, P.P. 1989. Microscopical, biochemical and immunological studies of the immune defense system of the horseshoe crab, *Limulus polyphemus*. *Biological Bulletin*. 176, 290–300.
- Suzuki, K., Shimokawa, C., Morioka, C., Itoh, S. 2008. Monooxygenase activity of *Octopus vulgaris* hemocyanin. *Biochemistry*. 47, 7108-7115.

T

- Tagawa, K., Yoshihara, T., Shibata, T., Kitazaki, K., Endo, Y., Fujita, T., Koshiba, T., Kawabata, S. 2012. Microbes specific C3b deposition in horseshoe crab complement system in a C2/Factor B-dependent or independent manner. *Plos one*. 7 (e36783), 1–9. <http://dx.doi.org/10.1371/journal.pone.0036783>.
- Tanji, T., Tony-Ip, Y. 2005. Regulation of the Toll and Imd pathways in the *Drosophila* innate immune response. *Trends in Immunology*. 26, 193-198.
- Terwilliger, N.B. 2007. Hemocyanin and immune response: defence against the dark arts. *Integrative and Comparative Biology*. 47, 662–665.
- Terwilliger, N.B., Dangott, L., Ryan, M. 1999. Cryptocyanin, a crustacean moulting protein: evolutionary link with arthropod hemocyanins and insect hexamerins. *Proceedings of the National Academy of Sciences, USA*. 96, 2013-2018.
- Terwilliger, N.B., Ryan, M.C. 2006. Functional and phylogenetic analyses of phenoloxidase from the brachyuran (*Cancer magister*) and branchiopod (*Artemia franciscana*, *Triops longicaudatus*) crustaceans. *Biological Bulletin*. 210, 38 – 50.
- Theopold, U., Li, D., Fabbri, M., Scherfer, C., Schmidt, O. 2002. The coagulation of insect hemolymph. *Cellular and Molecular Life Sciences*. 59, 363-372.
- Trouba, K.J., Hamadeh, H.K., Amin, R.P., Germolec, D.R. 2002. Oxidative stress and its role in skin disease. *Antioxidants and Redox Signalling*, 4, 665-673.
- Truscott, R., White, K.N. 1990. The influence of metal and temperature stress on the immune system of crabs. *Functional Ecology*. 4, 455–461.
- Tzafirir-Prag, T., Schreiberman, M.P., Lupatsch, I., Zarnoch, C.B. 2010. Preliminary studies of energy and protein requirements of Atlantic horseshoe crabs, *Limulus polyphemus*, grown in captivity. *Journal of the World Aquaculture Society*. 41, 874–883.
- Tzou, P., De Gregorio, E., Lemaitre, B. 2002. How *Drosophila* combats microbial infection: a model to study innate immunity and host pathogen interactions. *Current Opinion in Microbiology*. 5, 102-110.

U

- Uvell, H., Engstrom, Y. 2007. A multi-layered defence against infection; combinatorial control of insect immune genes. *Trends in Genetics*. 23, 342-349.

V

- Van Amersfoort, E.S., Van Strijp, J.A.G. 1994. Evaluation of flow cytometric fluorescence quenching assay of phagocytosis of sensitized sheep erythrocytes by polymorphonuclear leukocytes. *Cytometry*. 17, 294-301.
- Vance, J.E., Steenbergen, R. 2005. Metabolism and functions of phosphatidylserine. *Progress in Lipid Research*. 44, 207-234.
- Van-Holde, K.E., Miller, K.I., Decker, H. 2001. Hemocyanins and invertebrate evolution. *Journal of Biological Chemistry*. 276, 15563-15566.
- Vargas-Albores, F., Baltazar, P.H., Clark, G.P., Barajas, F.M. 1998. Influence of temperature and salinity on the yellowlegs shrimp *Penaeus californiensis* Holmes, prophenoloxidase system. *Aquaculture Research*. 29, 549-553.
- Vazquez, L., Alpuche, J., Maldonado, G., Agundis, C., Peretra-Morales, A., Zenteno, E. 2009. Immunity mechanisms in crustaceans. *Innate Immunity*. 15, 179-188.
- Vilmos, P., Kurucz, E. 1998. Insect immunity, evolutionary roots of the mammalian immune system. *Immunology Letters*. 62, 59-66.
- Voit, R., Feldmaier-Fuchs, G., Schweikardt, T., Decker, H., Burmester, T. 2000. Complete Sequence of the 24-mer Hemocyanin of the Tarantula *Eurypelma californicum*: structure and intramolecular evolution of the subunits. *Journal of Biological Chemistry*. 275, 39339- 39344.
- Volbeda, A., Hol, W. J. G. 1989. Crystal structure of hexameric hemocyanin from *Panulirus interruptus* refined at 3.2 Å resolution. *Journal of Molecular Biology*. 209,249-279.
- Volokhina, E.B., Hulshof, R., Haanen, C., Vermes, I. 2003. Tissue transglutaminase mRNA expression in apoptotic cell death. *Apoptosis*. 8, 673-679.

W

- Walls, E.L., Berkson, J., Smith, S.A. 2002. The Horseshoe Crab, *Limulus polyphemus*: 200 million years of existence, 100 years of study. *Review Fisheries Sciences*. 10, 39-73.
- Walton, A., Smith, V.J. 1999. Primary culture of the hyaline haemocytes from marine decapods. *Fish and Shellfish Immunology*. 9, 181-194.
- Wang, S.F., Oh, S., Si, Y-X., Wang, Z-J., Han, H-Y., Lee, J., Qian, G.Y. 2012. Computational predictions of protein-protein interactions of human tyrosinase. *Enzyme Research*. Doi:10.1155/2012/192867.
- Wang, X.W., Tan, N.S., Ho, B., Ding, J.L. 2006. Evidence for the ancient origin of the NF-κB/IκB cascade: its archaic role in pathogen infection and immunity. *Proceedings of the National Academy of Sciences USA*. 103, 4204-4209.

- Wang, Z., Wilhelmsson, C., Hyrsi, P., Loof, G.F., Dobes, P., Klupp, M., Loseva, O., Mörgelin, M., Ikle, J., Cripps, R.M., Herwald, H.M., Theopold, U. 2010. Pathogen entrapment by transglutaminase — a conserved early innate immune mechanism. *Plos Pathogens*. 6(2), 1-9.
- Whalley, T., Terasaki, M., Cho, M-S., Vogel, S.S. 1995. Direct membrane retrieval into large vesicles after exocytosis in sea urchin eggs. *Journal of Cell Biology*. 131, 1183-1192.
- Wright, J., McCaskill Clark, W., Cain, J.A., Patterson, A., Coates, C.J., Nairn, J. 2012. Effects of known phenoloxidase inhibitors on hemocyanin-derived phenoloxidase from *Limulus polyphemus*. *Comparative Biochemistry and Physiology Part B*. 163, 303-308.
- Wu, Y., Tibrewal, N., Birge, R.B. 2006. Phosphatidylserine recognition by phagocytes: a view to a kill. *Trends in Cell Biology*. 16, 189-197.

X

- Xian, J-A., Wang, A-L., Ye, C-X., Chen, X-D., Wang, W.-N. 2010. Phagocytic activity, respiratory burst, cytoplasmic free-Ca²⁺ concentration and apoptotic cell ratio of hemocytes from the black tiger shrimp, *Penaeus monodon* under acute copper stress. *Comparative Biochemistry and Physiology Part C*. 152, 182–188.
- Xue, Q-G., Renault, T., Chilmonczyk, S. 2001. Flow cytometric assessments of haemocyte sub-populations in the European flat oyster, *Ostrea edulis*, haemolymph. *Fish and Shellfish Immunology*. 11, 557-567.

Y

- Yan, F., Zhang, Y., Jiang, R., Zhong, M., Hu, Z., Du, H., Lun, J., Chen, J., Li, Y. 2011. Identification and agglutination properties of hemocyanin from the mud crab (*Scylla serrata*). *Fish and Shellfish Immunology*. 30, 354-360.
- Yan, F., Zhang, Y., Luo, H., Hu, Z., Huang, T., Ye, X. 2008. The phenoloxidase activity of hemocyanin from white leg shrimp *Litopenaeus vannamei*. *Fisheries Science*. DOI: CNKI:SUN:CHAN.0.2008-01-001.
- Yeung, T., Terebiznik, M., Yu, L., Silvius, J., Abidi, W.M., Philips, M., Levine, T., Kapus, A., Grinstein, S. 2006. Receptor activation alters inner surface potential during phagocytosis. *Science*. 313, 347-351.
- Yon-Chin, L., Baskaralingam, V., Chen, J.C. 2008. Identification of the copper-zinc superoxide dismutase (ecCuZnSOD) gene of the mud crab *Scylla serrata* and its expression following β -glucan and peptidoglycan injections. *Molecular Immunology*. 45, 1346-1355.
- Young, N.S., Levin, J., Prendergast, R.A. 1972. An invertebrate coagulation system activated by endotoxin: evidence for enzymatic mediation. *Journal of Clinical Investigation*. 51, 1790-1797.

Z

- Zaini, N.A.M., Osman, A., Hamid, A.A., Ebrahimpour, A., Saari, N. 2013. Purification and characterisation of membrane-bound Polyphenoloxidase (mPPO) from snake fruit [*Salacca zalacca* (Gaertn.) Voss]. *Food Chemistry*. 136, 407-414.
- Zhang, B., Hirahashi, J., Cullere, X., Mayadas, T.N. 2003. Elucidation of molecular events leading to neutrophil apoptosis following phagocytosis. *Journal of Biological Chemistry*. 278, 28443-28454.
- Zhang, X., Huang, C., Qin, Q. 2004a. Anti-viral properties of hemocyanin isolated from shrimp *Penaeus monodon*. *Antiviral Research*. 61, 93 – 99.
- Zhang, Y., Wang, S., Peng, X. 2004b. Identification of a type of human IgG-like protein in shrimp *Penaeus vannamei* by mass spectrometry. *Journal of Experimental Marine Biology and Ecology*. 301, 39-54.
- Zhang, Y., Chen, J., Lin, B., Huang, T., Liu, G., Zou, X. 2005. An attempt to study the agglutinative activity of hemocyanin from shrimp *Penaeus vannamei* with several kinds of erythrocyte. *Journal of Shantou University*. DOI: 1001-4217.0.2005-03-007.
- Zhang, Y., Wang, S., Xu, A., Chen, J., Lin, B., Peng, X. 2006. Affinity proteomic approach for identification of an IgA like protein in *Litopenaeus vannamei* and study on its agglutination characterization. *Journal of Proteome Research*. 5, 815 – 821.
- Zhang, Y., Lin, B., Chen, J., Hu, Z., Huang, T., Yan, F. 2006. Bacterial agglutinative activity of hemocyanin in shrimp *Litopenaeus vannamei*. *Journal of Fishery Sciences of China*. DOI; CNKI:SUN:ZSCK:0.2006.-06-020.
- Zhang, Y., Yan, F., Hu, Z., Zhao, X., Min, S., Du, Z., Zhao, S., Ye, X., Li, Y. 2009. Hemocyanin from shrimp *Litopenaeus vannamei* shows hemolytic activity. *Fish and Shellfish Immunology*. 27, 330 – 335.
- Zhang, Y., Ye, X., Chen, J., Huang, T., Hu, Z., Li, Y. 2008. A new fragment with 28.5 kDa degraded from hemocyanin in shrimp *Litopenaeus vannamei*. *Journal of Fishery Sciences of China*. DOI; CNKI:SUN:ZSCK.0.2008-03-008.
- Zhao, X., Guo, L., Zhang, Y., Liu, Y., Zhang, X., Lun, J., Chen, J., Li, Y. 2012. SNPs of hemocyanin C-terminal fragment in shrimp *Litopenaeus vannamei*. *FEBS Letters*. 586, 403-410.
- Zhou, Q., Kapoor, M., Guo, M., Belani, R., Xu, X., Kiosses, W.B., Hanan, M., Park, C., Armour, E., Do, M-H., Nangle, L.A., Schimmel, P. and Yang, X-L. 2009. Orthogonal use of human tRNA synthetase active site to achieve multifunctionality. *Nature Structural and Molecular Biology*. 17, 57-61.
- Zhu, Y., Thangamani, S., Ho, B., Ding, J.L. 2005. The ancient origin of the complement system. *EMBO Journal*. 24, 382–394.
- Zlateva, T., Di Muro, P., Salvato, B., Beltramini, M. 1996. The o-diphenol oxidase activity of arthropod hemocyanin. *FEBS Letters*. 384, 251 – 254.
- Zwaal, R.F.A., Comfurius, P., Bevers, E.M. 1998. Lipid-protein interactions in blood coagulation. *Biochimica et Biophysica Acta*. 1376, 433 – 453.

APPENDICES

Appendix A-Mass spectrometry

Table A1 Data from peptide mass fingerprint analysis of proteins purified from *Limulus polyphemus* and *Nephrops norvegicus*

A) *Limulus polyphemus* hemocyanin (Fig. 2.1B)

Accession No.	MW	Sequence	Protein name	Taxonomy	score	e-value
gi/122696646	73.2 kDa	R.FIDNMFQ Y EYKA	Hemocyanin subunit IV	<i>L. polyphemus</i>	74	0.00044
		R.FIDNMFQ Y EYKA	Hemocyanin subunit IV	<i>L. polyphemus</i>	57	0.018
		R.DLNDVSLQ E MER.W	Hemocyanin subunit IV	<i>L. polyphemus</i>	56	0.03
		R.DLNDVSLQ E MER.W	Hemocyanin subunit IV	<i>L. polyphemus</i>	58	0.018
		R.DLNDVSLQ E MER.W	Hemocyanin subunit IV	<i>L. polyphemus</i>	56	0.028
		R.ILVLF E HLSLTK.H	Hemocyanin subunit IV	<i>L. polyphemus</i>	57	0.011
		K.GLAV P PIQEIFPDR.F	Hemocyanin subunit IV	<i>L. polyphemus</i>	55	0.055
gi/122696648	74.2 kDa	K.YDELGN E LDTK.N	Hemocyanin subunit VI	<i>L. polyphemus</i>	63	0.0067
		R.VLPL F EYASIP T K.E	Hemocyanin subunit VI	<i>L. polyphemus</i>	64	0.0052
gi/71738535	73.2 kDa	K.YDELGN L LTPEQQR.R	Hemocyanin subunit IIIb	<i>C. rotundicauda</i>	61	0.02
		K.YDELGN L LTPEQQR.R	Hemocyanin subunit IIIb	<i>C. rotundicauda</i>	82	0.00016
gi/71738533	73.4 kDa	R.TLDN L FQ E YK.E	Hemocyanin subunit IIIa	<i>C. rotundicauda</i> / <i>L. polyphemus</i>	65	0.0071
		R.TLDN L FQ E YK.E	Hemocyanin subunit IIIa	<i>C. rotundicauda</i> / <i>L. polyphemus</i>	74	0.00078
gi/122791	73.1 kDa	R.DLG D IEISEMVR.M	Hemocyanin subunit II	<i>L. polyphemus</i>	58	0.036
		R.DLG D IEISE M VVR.M	Hemocyanin subunit II	<i>L. polyphemus</i>	53	0.099
		R.DLG D IEISE M VVR.M	Hemocyanin subunit II	<i>L. polyphemus</i>	58	0.03
gi/28569688	71.8 kDa	R.FIDN I FQDYK.Q	Hemocyanin subunit E	<i>N. inaurata-madagascariensis</i> *	58	0.031

Notes; Underlined amino acids indicate oxidation. **Nephila inaurata-madagascariensis*.

B) *Limulus polyphemus* C-reactive protein (Fig. 2.1B)

Accession No.	MW	Sequence	Protein name	Taxonomy	score	e-value
UniRef100_P06205	27.2 kDa	R.HIYGNIQWDK.T	C-reactive protein	<i>L. polyphemus</i>	41	3.3
		K.VKFPPSSSPFPR.L	C-reactive protein	<i>L. polyphemus</i>	41	4.3
		K.VKFPPSSSPFPR.L	C-reactive protein	<i>L. polyphemus</i>	48	0.92
		K.VKFPPSSSPFPR.L	C-reactive protein	<i>L. polyphemus</i>	70	0.0053
		K.VKFPPSSSPFPR.L	C-reactive protein	<i>L. polyphemus</i>	40	5
		K.VKFPPSSSPFPR.L	C-reactive protein	<i>L. polyphemus</i>	47	1
		K.VKFPPSSSPFPR.L	C-reactive protein	<i>L. polyphemus</i>	43	2.8
		K.VKFPPSSSPFPR.L	C-reactive protein	<i>L. polyphemus</i>	45	1.9
		K.AYDGVVLSPEICA.-	C-reactive protein	<i>L. polyphemus</i>	44	1.2
		K.AYDGVVLSPEICA.-	C-reactive protein	<i>L. polyphemus</i>	43	1.5
UniRef100_P02744	9.6 kDa	-.LEEGETSK.V	Limulin (C-reactive protein)	<i>L. polyphemus</i>	55	0.18
		-.LEEGETSK.V	Limulin (C-reactive protein)	<i>L. polyphemus</i>	48	0.8
		-.LEEGETSK.V + <i>acetyl</i>	Limulin (C-reactive protein)	<i>L. polyphemus</i>	46	0.98
		K.VKFPPSSSPFPR.L	Limulin (C-reactive protein)	<i>L. polyphemus</i>	41	4.3
		K.VKFPPSSSPFPR.L	Limulin (C-reactive protein)	<i>L. polyphemus</i>	48	0.92
		K.VKFPPSSSPFPR.L	Limulin (C-reactive protein)	<i>L. polyphemus</i>	70	0.0053
		K.VKFPPSSSPFPR.L	Limulin (C-reactive protein)	<i>L. polyphemus</i>	40	5
		K.VKFPPSSSPFPR.L	Limulin (C-reactive protein)	<i>L. polyphemus</i>	47	1
		K.VKFPPSSSPFPR.L	Limulin (C-reactive protein)	<i>L. polyphemus</i>	43	2.8
		K.VKFPPSSSPFPR.L	Limulin (C-reactive protein)	<i>L. polyphemus</i>	45	1.9

C) *Nephrops norvegicus* hemocyanin (Fig. 3.3B)

Accession No.	MW	Sequence	Protein name	Taxonomy	score	e-value		
gi/7105883	77.5 kDa	R.IIHEGFAPHTSYK.Y	Hemocyanin α -subunit	<i>H. americanus</i>	58	0.073		
		K.SWECFVDNAAFFR.E	Hemocyanin α -subunit	<i>H. americanus</i>	58	0.021		
		K.SWECFVDNAAFFR.E	Hemocyanin α -subunit	<i>H. americanus</i>	79	0.00017		
		R.EEALMLFDVLMHCK.S	Hemocyanin α -subunit	<i>H. americanus</i>	76	0.00087		
		R.EEALMLFDVLMHCK.S	Hemocyanin α -subunit	<i>H. americanus</i>	68	0.005		
		K.FNMPPGVMEHFETATR.D	Hemocyanin α -subunit	<i>H. americanus</i>	68	0.0047		
		K.FNMPPGVMEHFETATR.D	Hemocyanin α -subunit	<i>H. americanus</i>	70	0.0025		
		R.QREEALMLFDVLMHCK.S	Hemocyanin α -subunit	<i>H. americanus</i>	63	0.021		
		R.QREEALMLFDVLMHCK.S	Hemocyanin α -subunit	<i>H. americanus</i>	64	0.016		
		R.QREEALMLFDVLMHCK.S	Hemocyanin α -subunit	<i>H. americanus</i>	70	0.0049		
		R.VAYFGEDIGLNIHHVTWHMDFPFWWK.D	Hemocyanin α -subunit	<i>H. americanus</i>	60	0.04		
		gi/119487825	76.5 kDa	K.SWECFVDNAAFFR.E	Hemocyanin β -subunit	<i>H. americanus</i>	58	0.021
				K.SWECFVDNAAFFR.E	Hemocyanin β -subunit	<i>H. americanus</i>	79	0.00017
R.EEALMLFDVLMHCK.S	Hemocyanin β -subunit			<i>H. americanus</i>	76	0.00087		
R.EEALMLFDVLMHCK.S	Hemocyanin β -subunit			<i>H. americanus</i>	68	0.005		
R.LLEQHHWFSLFNPR.Q	Hemocyanin β -subunit			<i>H. americanus</i>	60	0.06		
R.LLEQHHWFSLFNPR.Q	Hemocyanin β -subunit			<i>H. americanus</i>	64	0.024		
R.LLEQHHWFSLFNPR.Q	Hemocyanin β -subunit			<i>H. americanus</i>	81	0.0005		
R.LLEQHHWFSLFNPR.Q	Hemocyanin β -subunit			<i>H. americanus</i>	75	0.0017		
R.LLEQHHWFSLFNPR.Q	Hemocyanin β -subunit			<i>H. americanus</i>	58	0.092		
R.LLEQHHWFSLFNPR.Q	Hemocyanin β -subunit			<i>H. americanus</i>	60	0.06		
R.LLEQHHWFSLFNPR.Q + acetyl	Hemocyanin β -subunit			<i>H. americanus</i>	58	0.09		
R.QREEALMLFDVLMHCK.S	Hemocyanin β -subunit			<i>H. americanus</i>	63	0.021		
R.QREEALMLFDVLMHCK.S	Hemocyanin β -subunit			<i>H. americanus</i>	64	0.016		
R.QREEALMLFDVLMHCK.S	Hemocyanin β -subunit			<i>H. americanus</i>	70	0.0049		
R.VAYFGEDIGLNIHHVTWHMDFPFWWK.D	Hemocyanin β -subunit	<i>H. americanus</i>	60	0.04				
gi/6118551	70.8 kDa	R.IIHEGFAPHTSYK.Y	Hemocyanin I, partial	<i>N. norvegicus</i>	58	0.073		
		R.LSNYLDPVDELHWER.I	Hemocyanin I, partial	<i>N. norvegicus</i>	62	0.03		
		R.LSNYLDPVDELHWER.I + acetyl	Hemocyanin I, partial	<i>N. norvegicus</i>	58	0.07		
		R.LSNYLDPVDELHWER.I + acetyl	Hemocyanin I, partial	<i>N. norvegicus</i>	87	0.000089		
		R.IRDAIAHGYVTDTEGHHINIR.N	Hemocyanin I, partial	<i>N. norvegicus</i>	59	0.077		
		R.VAYFGEDIGLNIHHVTWHMDFPFWWK.D	Hemocyanin I, partial	<i>N. norvegicus</i>	60	0.04		

Table A1 C) continued

gi/15528531 ^A	78.8 kDa	K.GELFFWVHHQLTAR.F	Hemocyanin subunit III	<i>P. vulgaris</i>	63	0.028
		K.GELFFWVHHQLTAR.F	Hemocyanin subunit III	<i>P. vulgaris</i>	61	0.04
		K.FNMPPGVMEHFETATR.D	Hemocyanin subunit III	<i>P. vulgaris</i>	68	0.0047
		K.FN <u>M</u> PPGVMEHFETATR.D	Hemocyanin subunit III	<i>P. vulgaris</i>	70	0.0025
gi/262072532	79.4 kDa	K.YGTPPGVMEHFETATR.D + acetyl	Hemocyanin subunit I (precursor)	<i>S. tulumensis</i>	62	0.018
		K.YALPPGVLEHFETATR.D + acetyl	Hemocyanin	<i>L. vannamei</i>	58	0.088

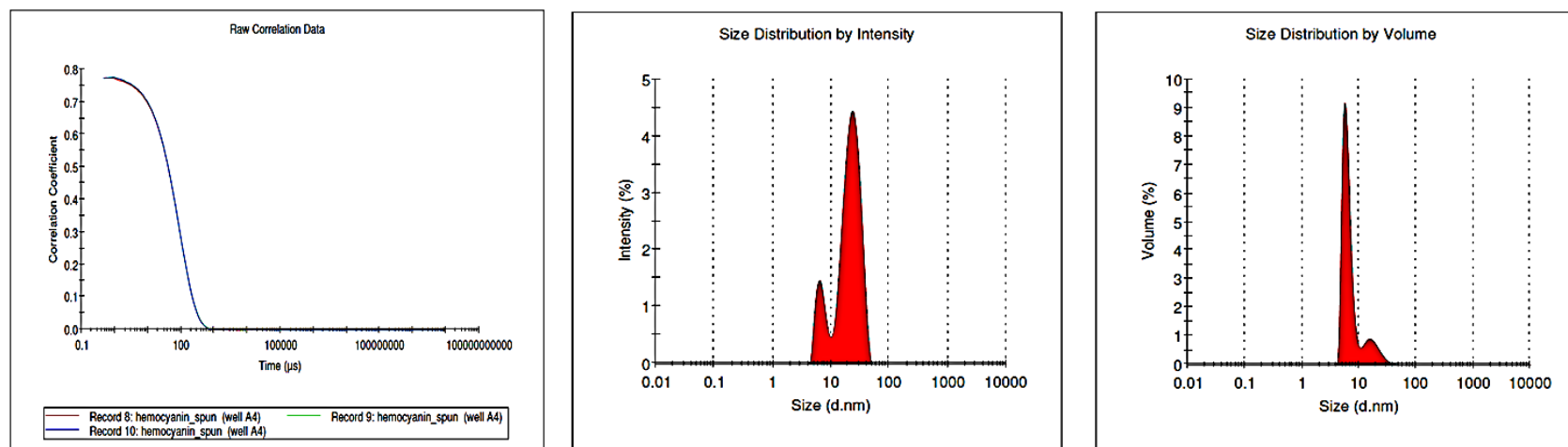
Notes; Underlined amino acids indicate oxidation. Sequences highlighted in blue are unique. *Homarus americanus*, *Nephrops norvegicus*, *Palinurus vulgaris*, *Litopenaeus vannamei*, *Speleonectes tulumensis*.

^A Protein matching same set of peptides; gi/32363480; Mass: 75912 Score: 132 Matches: 4(4) Sequences: 2(2); Full=Hemocyanin.

^B Protein matching same set of peptides; gi/222476500 ; Mass: 77595 Score: 58 Matches: 1(0) Sequences: 1(0); Hemocyanin [*Fenneropenaeus chinensis*]

Appendix B- Dynamic light scattering

A) Hemocyanin



B) Filtered PS liposomes

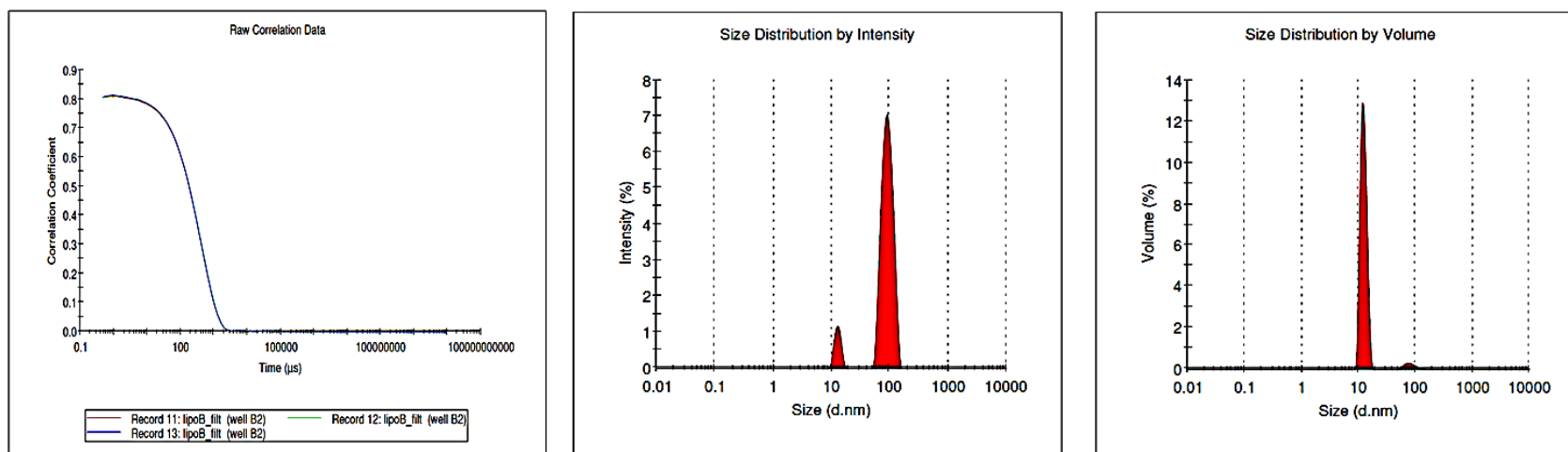


Figure B1 Dynamic light scattering measurements of *Limulus polyphemus* hemocyanin and phospholipid liposomes. Calculating the radius of gyration for **A)** Hemocyanin (1 mg mL^{-1}) and **B)** Phosphatidylserine liposomes ($10 \text{ } \mu\text{g mL}^{-1}$) in 100 mM Tris-HCl, pH 7.5.

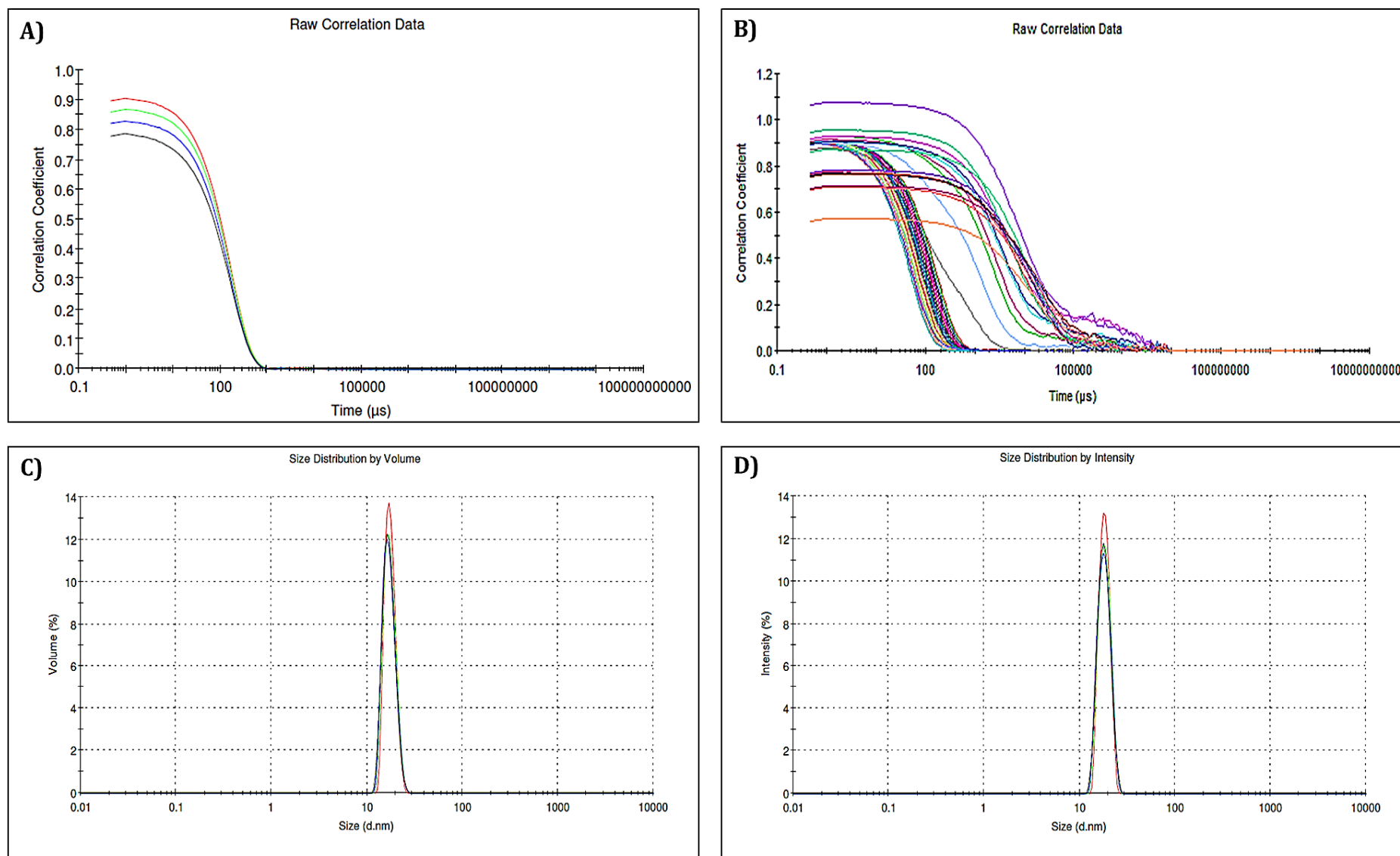


Figure B2 Dynamic light scattering measurements of *Nephrops norvegicus* hemocyanin. A) Raw correlation data, B) correlation data of hemocyanin with temperature melting curves overlaid, C) and D) represent the average size distribution by volume and density, respectively. Measurements were carried out in 100 mM Tris-HCl, pH 7.5.

Appendix C- Water quality properties

Table C1 Assessment of water quality

Water quality parameters	Measurements	Recommendations
Ammonia (NH ₃)	~ 0- 0.1 mg L ⁻¹	*
Calcium (Ca)	~ 420 mg L ⁻¹	400-500 mg L ⁻¹
Carbonate hardness (KH)	~ 162 mg L ⁻¹	150-190 mg L ⁻¹
Iron (Fe) <i>_Non chelated</i>	0 mg L ⁻¹	< 3 mg L ⁻¹
Iron (Fe) <i>_Chelated</i>	0 mg L ⁻¹	*
Nitrate (NO ₃ ⁻)	~ 5 mg L ⁻¹	< 20 mg L ⁻¹
Nitrite (NO ₂)	~ 0.1 mg L ⁻¹	≤ 0.3 mg L ⁻¹
pH	8.1 ± 0.19	~ 8.1 – 8.3
Phosphate (PO ₄)	0 – 0.25 mg L ⁻¹	≤ 1mg L ⁻¹
Salinity (NaCl)	33.4 ± 1.5 ppm	33 – 35 ppm†

*Levels should not be detectable in saltwater. † Horseshoe crabs live in water bodies with varying salinities, the presented value is a recommendation for saltwater aquariums, in general. Measurements are representative of the period February 2011 to August 2012.

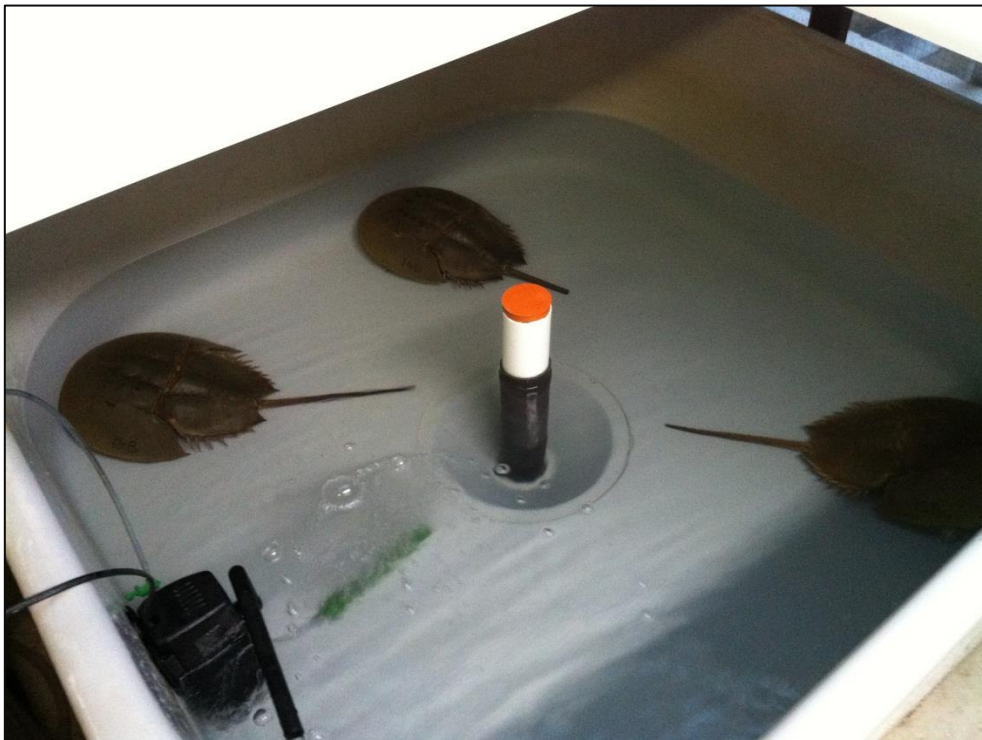


Figure C1 Typical tank set-up for housing horseshoe crabs, *Limulus polyphemus*.